



The University of
Nottingham

UNITED KINGDOM • CHINA • MALAYSIA

Polymer from pyrolysis liquid: Pyrolymer

John Ryan, MSc

Thesis submitted to the University of Nottingham for the degree of Doctor of
Philosophy

March 2021



The world that you created

Is not mightier

Than our means to remake it.

Acknowledgements

I would firstly like to thank the EPSRC CDT in Sustainable Chemistry for giving me the opportunity to undertake this PhD specifically to Perislava Williams, Prof Peter Licence and Prof Christopher Moody for the opportunity, Dr Yonas Chebude and Dr Nigist Asfaw for perspective and my fellow students for providing me with an inundation of opportunities for growth.

I am forever grateful to my supervisory team, Dr John Robinson, Dr Eleanor Binner and Prof. Derek Irvine for their unwavering support, guidance and positivity throughout my PhD. I am particularly grateful also to collaborators in the wider faculty of engineering, Dr Davide De Focatiis and Matthew Elsmore who undertook all mechanical testing of pyrolymer samples and generously shared that data so that it could be presented in this thesis. I am grateful also to Dr Mick Cooper, Dr Kevin Butler and Shazad Aslam for finding the time to help me with some analysis in this thesis.

Great thanks are also due to my colleague's Dr William Meredith, Dr Emily Kostas, Dr Benjamin Shepherd, Dr Daniel Beneroso and Dr Mohamed Adam who guided me in so many ways throughout this project. Thanks also to Clive Dixon and Connor Howell-Bennett for persevering with some pretty niche glassblowing. Additional thanks to Prof Ross Denton, Dr James Dowden and Prof Steven Howdle for generously and occasionally unknowingly giving me access to equipment.

Thanks also to the Process development unit at the Biorenewables Development Centre, Dr Mark Gronnow, Darren Phillips, John Angus and Dr Andrew Danby. To the Green Chemistry Centre of Excellence, Prof James Clark, Dr James Comerford and Dr Fergal Byrne. Biome bioplastics Dr Krisztina Kovacs-Schreiner Dr Paul Law and Paul Mines for giving me the opportunity to put the skills learned over the course of the last four years into practice.

A big thank you to my other colleagues, friends and technicians who offered help and support along the way.

Finally, I would like to thank my Mum, Dad and Grandparents for their genes, sister for her constant support and Frankie for holding me and everything together.

Abstract

An estimated 8.3 billion tonnes of plastic waste has been generated globally since the 1950s of which approximately 80% remains in landfill or loose in the environment.¹ Global greenhouse gas emissions from the production and disposal of plastics is more than double that of air travel.² In line with current demand, oil-based plastics are produced at a rate of ~350mtpa.

While useful, fossil-derived plastics have been developed focusing on function rather than end-of-life performance and their environmental impact. Recycling alone is not the complete answer to the "plastics problem". These include cost, food contamination, polymer degradation and environmental leakage. Bio-based plastics are an important part of the solution.

This work demonstrates a novel approach to going some way towards solving the "plastic problem" by adding value to biomass pyrolysis liquids through transesterification of the diverse range of alcohol functional groups within the mixture to give rise to polymerizable monomers from biomass, without requiring extensive separation. Previous studies have worked on using highly reactive acyl chlorides/acid anhydrides on model compounds to achieve similar results. Using transesterification, production of the monomer is achieved in one reaction step and without separation or the use of toxic reagents. Strategies to tune the process to vary glass transition temperature (T_g) and M_p are discussed. A scheme of future work to exploit this in applications is included.

Table of contents

Acknowledgements	iii
Abstract	iv
Table of contents	v
List of abbreviations and nomenclature	ix
Chapter 1. Introduction	11
1.1 Background	11
1.1.1 Plastics	11
1.1.2 Routes to more sustainable polymers	13
1.1.3 Which biomass source?	17
1.2 What is pyrolysis?	17
1.2.1 Pyrolysis reaction conditions and mechanisms	19
1.2.2 Measuring differences in composition of pyrolysis liquid	24
1.2.3 Reactor design for fast pyrolysis	26
1.3 Microwave heating	32
1.3.1 Background	32
1.3.2 The future of microwave pyrolysis	35
1.3.3 General points to note on previous microwave pyrolysis studies	37
1.4 Use of pyrolysis liquid in polymers	39
1.4.1 Radical polymerisation and analysis	42
1.5 Principle thesis hypotheses and aims	45
1.5.1 Final hypotheses	45
1.5.2 Aims	45
Chapter 2. Experimental methods and materials	47

2.1 Materials	47
2.1.1 Biomass moisture content.....	48
2.1.2 Biomass dielectric properties.....	49
2.1.3 Biomass density	49
2.2 Pyrolysis methods.....	50
2.2.1 Gas inerted fixed bed conventional pyrolysis.....	50
2.2.2 Microwave tuning.....	51
2.2.3 Gas inerted fixed bed microwave pyrolysis.....	52
2.2.4 Liquid inerted fixed bed microwave pyrolysis	53
2.3 Pyrolysis calculations	55
2.3.1 Specific absorbed energy	55
2.4 Pyrolysis liquid analysis	56
2.4.1 Gas-liquid chromatography mass spectrometry	56
2.4.2 Magnetic resonance spectroscopy	58
2.4.3 Karl Fischer titration.....	59
2.5 General method of producing polymer from pyrolysis liquid	60
2.5.1 Experimental setup and method for pyrolysis liquid drying	60
2.5.2 Experimental setup at T_o and T_f and method for pyrolysis transesterification.....	61
2.5.3 Experimental method for functionalised pyrolysis liquid polymerisation.	61
2.6 Characterisation of pyrolysis liquid polymer.....	62
2.6.1 Thermogravimetric analysis (TGA)	62
2.6.2 Differential scanning calorimetry (DSC).....	62
2.6.3 Size exclusion chromatography	62
2.7 Polymerisation calculations	62
2.7.1 Transesterification yield	62

2.7.2 Polymerisation yield.....	62
Chapter 3. Upgrading pyrolysis liquid with polymerisation <i>via</i> transesterification.....	64
3.1 Setting the scene.....	64
3.2 Transesterification of pyrolysis liquid.....	65
3.2.1 Preliminary pyrolysis liquid transesterification.....	67
3.2.2 Cause of polymerisation during preliminary transesterification.....	70
3.2.3 Inhibitor addition to transesterification	73
3.2.4 Water Effects.....	76
3.2.5 Temperature Reduction	78
3.2.6 Catalyst screening	82
3.3 Polymerisation of functionalised pyrolysis liquid	83
3.3.1 Initiator concentration	84
3.3.2 “Wax” polymerisation effects	88
3.4 Pyrolysis liquid Transesterification and polymerisation developed method	90
3.5 Conclusions	93
Chapter 4. Effect of pyrolysis liquid composition on polymer properties	94
4.1 Setting the Scene	94
4.2 Pyrolysis liquid composition effects	95
4.2.1 Pyrolysis reaction temperature control	97
4.2.2 Pyrolysis method effect on liquid composition	108
4.2.3 Origins of distinct pyrolysis liquid compositions.....	116
4.2.4 Summary	119
4.3 Pyrolysis liquid composition effects on transesterification	121
4.4 Pyrolysis liquid composition effects on polymer properties	126
4.4.1 Pyrolysis liquid effect on molecular weight and yield	129

4.4.2 Wax effect on polymerisation.....	133
4.4.3 Thermal properties.....	135
4.4.4 Summary	136
4.5 Preliminary Application specific testing	137
4.5.1 Preliminary Adhesive testing.....	139
4.5.2 Tuning Polymer Properties through copolymerisation	139
4.5.3 Thermal and rheological properties of pyrolysis polymer and p(BMA).....	143
4.5.4 Thermal instability.....	145
4.5.5 Bitumen binder	145
4.6 Conclusions	146
Chapter 5. Conclusions, future work and recommendations.....	148
5.1 Conclusions	148
5.2 General Future work.....	150
5.2.1 Pyrolysis analysis	150
5.2.2 Further transesterification and polymerisation method development	150
5.2.3 Liquid microwave pyrolysis and transesterification optimisation	152
5.2.4 Condensation polymerisation	153
5.2.5 Polymer identification	154
5.2.6 End of use, biodegradability and biocompatibility	154
5.2.7 Regulatory concerns	155
Chapter 6. References	156
Chapter 7. Appendix	I

List of abbreviations and nomenclature

Abbreviations

ABCN	1,1'-Azo-bis(cyclohexanecarbonitrile)
AIBN	Azo-bis(isobutyronitrile)
BFB	Bubbling fluidised bed
BMA	Butyl methacrylate
CFB	Circulating fluidised bed
CHP	Combined heat and power
DCM	Dichloromethane
DDM	Dodecyl mercaptan
DSC	Differential scanning calorimetry
EG	Ethylene glycol
FC	Fixed carbon
FDCA	Furan dicarboxylic acid
FRP	Free radical polymerisation
FT-IR	Fourier transform infrared-red spectroscopy
GC	Gas chromatography
HCl	Hydrochloric acid
HMA	Hot melt adhesive
HMF	Hydroxymethyl furfural
MAA	Methacrylic acid
MMA	Methyl methacrylate
MS	Mass spectroscopy
MWH	Microwave heating
PET	Polyethylene terephthalate
PSA	Pressure sensitive adhesive
RBF	Round bottomed flask
TA	Terephthalic acid
TCR	Thermo-catalytic reforming
THF	Tetrahydrofuran
TGA	Thermogravimetric analysis
TMDP	2-chloro-4,4,5,5-tetramethyl-1,3,2-dioxaphospholane
TNBT	Titanium butoxide
TPPO	Triphenyl phosphine oxide
V-70	2,2'-Azobis(2,4-dimethyl-4-meth-oxy-valeronitrile)

Nomenclature

$J_1^2(x_{1,m})$	Second order of the first kind root of the Bessel function
\bar{D}	Polydispersity $\frac{M_w}{M_n}$
d_n/d_c	Refractive index increment
d_t	Time differential (s)
δ	Dielectric constant
E_s	Specific energy (kJ·g ⁻¹)
f_0	Resonant frequency of the empty cavity
f_s	Resonant frequency of the cavity with the sample present
λ	Loss tangent
M	Mass (g)
M_n	Number averaged molecular mass
M_p	Peak molecular mass
M_w	Molecular weight averaged molar mass
P	Absorbed power (kW)
Q_o	Quality factor of the empty cavity
Q_s	Quality factor of the cavity with the sample present
T_{deg}	Thermal Degradation Temperature
T_g	Glass Transition Temperature
T_m	Melting Temperature
V_0	Volume of the cavity
V_s	Volume of the sample

n.b. the terms “bio-oil”, “pyrolysis oil”, “pyrolysis condensate” and “pyrolysis liquid” are used interchangeably to describe liquid phase products of pyrolysis. For the sake of consistency this work has used “pyrolysis liquid” where applicable. There is also potential to confuse “pyrolysis liquid” with “pyrolytic lignin” in the abbreviation “PL” and for this reason this is not used.

Chapter 1. Introduction

1.1 Background

1.1.1 Plastics

Plastics are everywhere, we use them every day for all kinds of things, and there have been recent leaps and bounds in the field of recycling plastics.³ This extends their useful lifetime though traditionally recycled plastics move down the value chain with high performance polymer becoming cups becoming bags becoming fuel.⁴ Ultimately, the carbon atoms that come from crude oil used to make plastics may end up in the atmosphere as CO₂. The impacts of this release of CO₂ have been widely studied, especially in the context of the negative impact through a change to the global climate on the current and future generations around the globe.⁵ In order to mitigate the impacts of humanity's use of fossil fuels for plastics and hence the release of CO₂, it is proposed that by using carbon atoms that have been fixed by photosynthesis into biomass to make plastics that the amount of carbon from crude oil entering the polymer life cycle, and hence ultimately the atmosphere, can be reduced without reducing the volume of plastic generate. Though this logic, when applied to the competition of renewable energy with fossil fuels, suggests this may not be a simple question of displacement.⁶

Firstly, what are polymers?

The word polymer comes from the Greek words for “many parts.” Each of those parts is a monomer. A polymer is a chain, with each of its links, or repeat units, a monomer. Those monomers can be simple — just an atom or two or three — or they might be complicated ring-shaped structures containing a dozen or more atoms.⁷ Broadly, polymers are classified based on their chemical origin, with condensation polymers formed using condensation chemistry to eliminate small molecule by-products where addition polymers are formed from the propagation of unsaturated compounds so there are usually not reaction by-products.

Condensation polymers

One of the most well-known polymers is polyethylene terephthalate (PET). This is made from terephthalic acid (TA) and ethylene glycol (EG), see Figure 1.

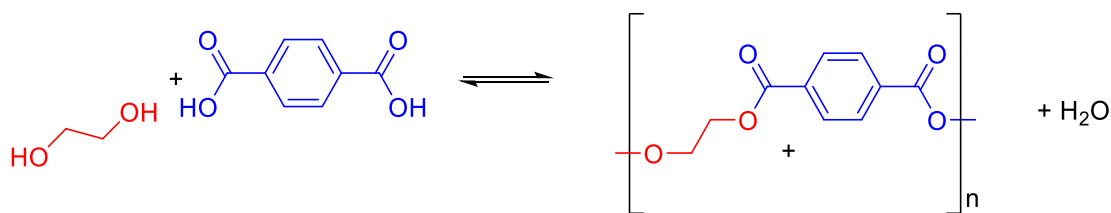


Figure 1 Outline of formation of PET from TA and EG, n is the number of repeat units and is typically 80+ giving high molecular weight polymer as a product. Note that this is an equilibrium reaction requiring the distillation of water to drive to completion

The reaction in Figure 1 is an esterification, these types of reaction are equilibria meaning that in order to drive the position of equilibrium to the products the by product, in the case of Figure 1 water, is usually distilled. PET is used in a range of applications from plastic bottles to clothing. There are a wide range of different diacid and diols along with other functional groups such as amines that can give rise to a range of different polymeric products. This type of chemistry can be applied to amines and carboxylic acids to form polyamides and in some systems both amine and acid groups are on the same molecule, the most common example of this is Nylon.

Addition polymers

One of the most common addition polymers is poly-methyl methacrylate (p(MMA)). This is formed by addition of a thermally activated radical initiator to unsaturated monomers. Azobisisobutyronitrile (AIBN) is the most common. The reason for this is that AIBN has a half-life of one hour at 85 °C (five hours at 70 °C).⁸⁻¹⁰ Consequently, it can continuously supply sufficient initiating radicals at moderate temperatures for reactions requiring several hours to reach completion. 1,1'-Azo-bis(cyclohexanecarbonitrile) (ABCN) has a longer half-life than does AIBN and, thus, is better suited for reactions that require higher temperature or extended reaction times.^{11,12} 2,2'-Azobis(2,4-dimethyl-4-meth-oxy-valeronitrile) (V-70), in contrast, reacts rapidly enough in solution that it initiates reactions run at or near room temperature, a drawback to this approach is the increased viscosity.¹³⁻¹⁶ The implications of lower temperature radical initiation could mean a lower temperature process which is ostensibly more sustainable due to the lower thermal energy requirement however if the polymer or monomer is not molten at the initiation temperature then despite the presence of radicals the reaction can be hindered due to the viscosity limiting mass transfer. The propagation of these radicals generates polymer without the elimination of by-product molecules, shown in Figure 2.

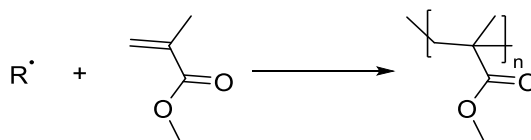


Figure 2 Formation of p(MMA) from MMA, n is the number of repeat units and is typically 80+ giving high molecular weight polymer as a product. Note this is not an equilibrium and no by-product forms.

There are a range of different vinyl, acrylate and methacrylate monomers that react to form polymers in this way. Typically, these are used in applications from resins to adhesives and can be tailored in terms of molecular weight, pendant groups and molecular architecture to fit the needs of an application.

1.1.2 Routes to more sustainable polymers

Recently there has been a general drive toward manufacture of more “sustainable” polymers. There is increasing clarity about to what degree consumers are willing to change their consumption habits to lessen their environmental impact and dynamic legislative pressure to improve the environmental credentials of the plastics industry as a whole.¹⁷ It is important to note that the end users of polymers are more concerned about the properties of polymer and what this allows them to do than the precise chemical structure of the material they use. There are several different approaches and there is lack of consensus around which approach is the most promising due in part to the similar but subtly different terminology;

- Bio-derived

These are structurally identical to existing polymers and have been sourced from “biological” sources in place of the conventional petrochemicals, typically the result of recent advances in biotechnology allowing the production of monomers from renewable feedstock.^{18,19} An example of this is bio derived ethylene glycol (EG) that can be used in the manufacture of a partially “bio-derived” PET with the same molecular structure as petrochemical PET. A breakdown of the bio based content of this is shown in Figure 3. It should be noted that the mass balance is commonly used to assign bio-based content in industrial processes.

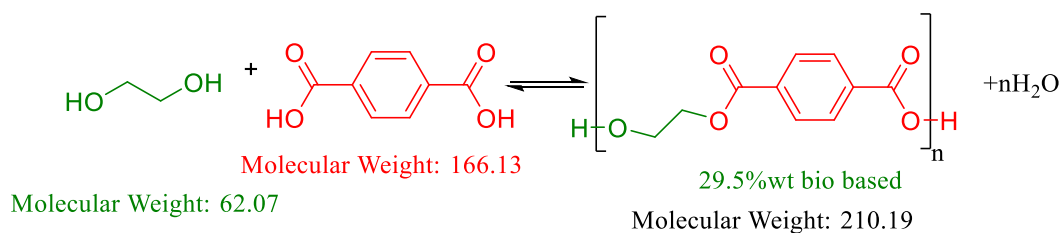


Figure 3 Monomers and molecular masses of bio based/petroleum based PET. This is how partially bioderived polymers can be manufactured - the bio-based content of “bio” PET is 29.5% though one of the two monomers is fully bio based.

- Biopolymer

These are new monomers that can be made, usually more simply, using biotechnology. The most notable of these is furan dicarboxylic acid (FDCA) which can be derived from sugar via hydroxymethyl furfural (HMF) and polymerised into polyethylene furanoate (PEF) which is structurally similar to PET, show in Figure 4.^{20,21} These generally result in structurally distinct polymers from bio sources “biopolymers” and have the potential for new “biomaterials” with different properties from those that currently exist.

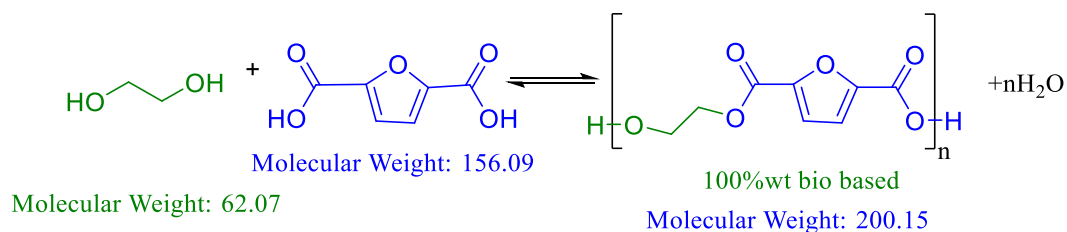


Figure 4 outline of molecular structure of bio-derived FDCA and hence PEF which is purported to be a bio-derived alternative to PET.

- Bio-degradable (or more accurately - compostable)

It is important to note that “bio-derived” and “biopolymer” do not necessarily mean that a polymer will be environmentally degradable. As such, it could be expected that “bioderived” polymers would persist in the environment for just as long as the petrochemical deriver equivalent. There is also a lack of clarity around how much interaction or required conditions are necessary in order for a material to be defined as “biodegradable”. That said, the “ecoflex” film marketed by BASF is reportedly compostable despite its fossil origins, the structure of this is outlined in Figure 5.²² Compostable plastics have a well defined set of parameters in order to be specified as a compostable material.

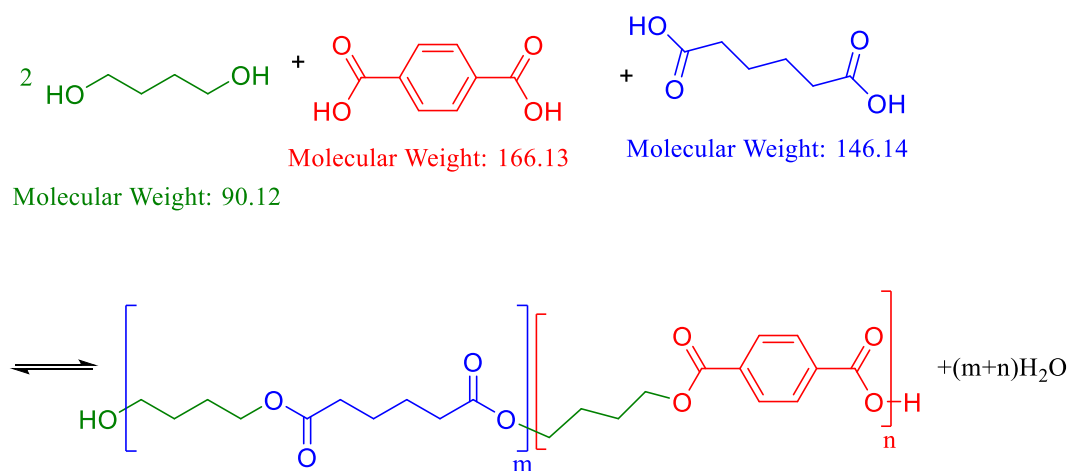


Figure 5 Structure of "ecoflex", this is analogous to PET where butane diol (BD) is used in place of ethylene glycol (EG) and where some portion (m/n) of the terephthalic acid (TA) is replaced with adipic acid. The exact ratios are varied to give different grades of material.

- Recyclable

Recycling is such a broad term for any use of polymer beyond the original intended use. The scale of polymer that is actually recycled vs still ending up in landfill is shown in Figure 6.

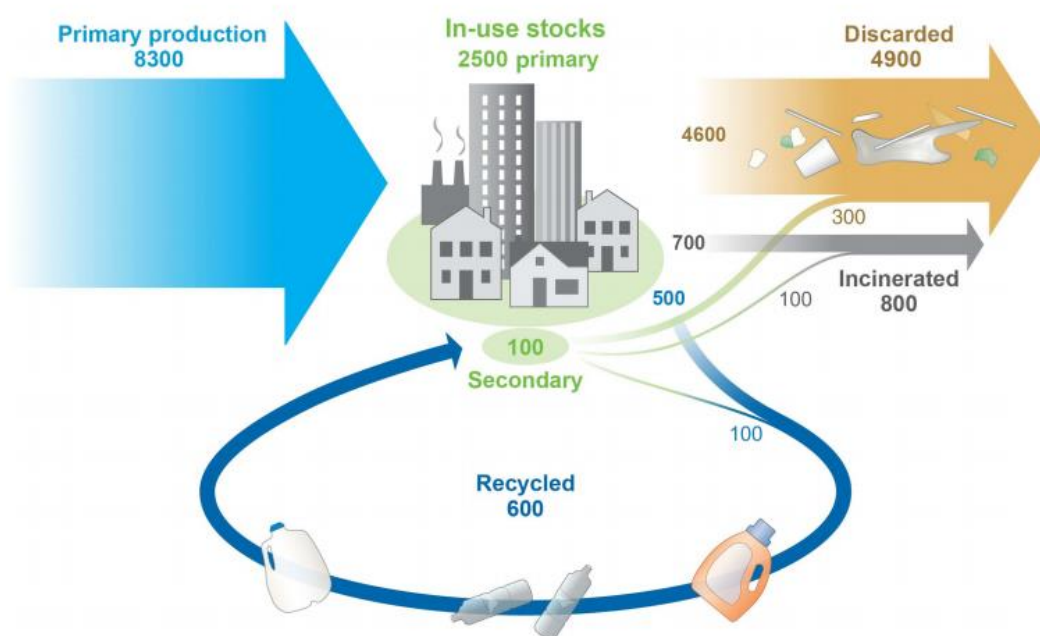


Figure 6 Global production, use, and fate of polymer resins, synthetic fibres, and additives (1950 to 2015; in million metric tons).²³ Showing the disparity between materials produced, recycled, incinerated and ultimately fugitive/landfilled.

This shows that just because a polymer has the technical capability to be recycled does not necessarily mean that in practice it is recycled. For instance, in food packaging where the polymer has become contaminated with organic material, or in multi-layer packaging, sometimes seen in some well-known potato based snacks, separation and cleaning of the material is not technically or economically viable and so the material is often not recycled.²⁴ There are also supply chain issues of collecting, transporting and sorting waste along with consumer barriers if a recyclable product is less desirable or more expensive than corresponding virgin material.

In summary, the next generation of polymeric materials should offer similar or improved performance relative to the current, petrochemical derived, polymers but need to be derived in whole or in part from a non-petrochemical feedstock. Ideally these polymers should also be able to integrate into the existing polymer supply chain. These materials would also ideally be recyclable and for in situations where plastic waste is discarded, biodegradable, in order that there is no further contribution to persistent plastic waste.

1.1.3 Which biomass source?

The largest source of accessible to human, non-petrochemical organic carbon is biomass.²⁵ There are different types of biomass, primary biomass comes from plant material directly, including those used for food production. Using this type of biomass can result in inflated prices of food derived from them and an overall negative impact associated with this. Non-food biomass are therefore preferable to avoid this issue: inedible biomass such as food waste, food and drinks industry co-products and woody biomass such as forestry waste.²⁶ The issue of increased crop production on land use constraints have prompted innovative solutions such as the use of algal feedstock, this presents an opportunity to derive useful products such as fuel or chemicals from biomass without competition with terrestrial farming.^{27–29} Another potential feedstock for biofuels and biochemicals are the so called “terpenes”, these are a family of compounds that can be extracted from natural sources, for instance α -pinene can be extracted from the resin of trees and limonene can be extracted from citrus fruit peel wastes. This could lead to other non-edible food waste streams that can be utilised for biofuel and biochemical production. These represent promising future feedstock opportunities.

1.2 What is pyrolysis?

One promising technology for the conversion of woody and waste biomass into a potential chemical feedstock is pyrolysis. Pyrolysis is an umbrella term for a thermochemical process during which biomass feedstock is heated in an inert atmosphere at 350–700 °C to produce gas, liquid and solid products. Pyrolysis is a mature technology for energy applications but has yet to be fully exploited in other applications such as the production of biochemicals or the recycling of plastics. This technology is widely studied but due to the large number of inherent variables, there can be difficulty in understanding and proving the effects of individual input variations.³⁰ These variables, grouped by physical or chemical, and their implications for any pyrolysis process are included in Table 1.

Table 1 Biomass feedstock physical and chemical properties, including details on potential variability and intrinsic effect on any pyrolysis process.

Physical properties	
Moisture content	Affects feedstock supply and biorefining operations. ^{31,32} High moisture content will increase transportation costs, and moisture above 10% reduces calorific value in thermochemical conversion process. ³³ Moisture above 20% is generally recognized to cause dry matter loss in aerobic storage; ³⁴ while moisture in the 20–40% range causes increased cohesion for poor feeding and handling properties. Moisture also increases dry grinding energy requirements and affects final particle size distributions with dry feeds having more fine particles. For pyrolysis, biomass should be dried to <10% water content as additional water in the bio-oil affects stability, viscosity, pH, and other properties including reduced heating rate and moisture in product. ^{35,36}
Particle morphology/ “grindability”	Practically, all conventional conversion methods require size reduction. Increasing particle size above 3 mm is generally associated with poor feeding and handling properties and sizes below 1 mm with high moisture content are prone to caking. Thermochemical processes typically become increasingly sensitive to particle size as reaction rates increase and residence times decrease. Some conversion processes are generally more tolerant of larger particles, with size and shape requirements set primarily by the engineered systems. ^{37,38} In pyrolysis, char yield increases for many biomass types as size increases larger than 0.5 mm due to reduced heating rates. ^{39,40}
Bulk density	Low bulk density increases transportation and handling costs as well as aggravates performance in gravity-based feeding and handling systems.
Elasticity	Causes increased feeding and handling difficulty because elastic recovery in feed systems affects compressive stresses and material shear strengths at constricted flow points, such as hopper openings/auger feed.
Micro-structure	Open microstructure results in increased access and surface area for biochemical conversion. Rough microstructure results in high inter-particle friction forces with corresponding high shear strengths and poor feeding behaviour. Microstructure also affects adhesion to container walls, reducing cleanout, and live storage volume as well as potentially resulting in spoilage.
Thermal conductivity	Poor heat transfer is a major challenge in thermal processing of biomass. Insufficient heat transfer properties of biomass can cause inhomogeneous heating, affecting the reproducibility of a heating process. These are linked to other material properties such as bulk density and moisture content. Consequently samples with poorer heat transfer properties require further processing, size reduction, moisture removal to compensate.
Chemical properties	
Ash content	Ash content has been shown to negatively affect most conversion processes. Lower ash can increase oil yields by 1–5% for each 1% of ash removed from native biomass. ^{36,41} As such, there have been efforts to reduce ash in biomass. Hydrothermal pretreatment with sodium citrate at a level of 0.25 g/g biomass can reduce structural ash content by 77%. ⁴² The change in ash content from wood (~1% ash) to straw (5–10% ash) can change the deposition rate from 10 to 0.1 g deposit/kg fuel and this can cause reactor fouling. ³³
Volatiles	Generally removing volatiles content decreases acidity and improves energy density. Increased volatiles increases fuel acidity and affect upgradeability and stability. ³⁶
Lignin	Lignin can benefit thermochemical conversion processes by increasing oil yields and improving energy density and requires conversion to be used as a feedstock for biochemical fermentative processes. ⁴¹

Due to the large and multi-faceted impacts of feedstock on a process, a significant amount of research in this field change individual feedstock variables and investigating their effects in isolation. For the purpose of this work feedstock is kept consistent to reduce these as sources of variation. It should be mentioned that the attention paid to each of the variables in Table 1 has been unevenly distributed in the literature, commonly overlooked are the interplay between these variables and their significant impacts on a process. For example, there is significant scope for biomass type materials with typically poor grindability, low bulk density and high elasticity to feed poorly into a gravity feed screw feeder. Hence, as screw speed does not directly control the mass added to reactor (though it is easy to measure by mass difference the amount added) controlling the feed rate is not possible and hence a reproducible (six sigma) type process is unfeasible without significant advances in understanding here. Ash content is essentially a measure of non-volatile materials – commonly salts, metals and silicon. Ash is commonly viewed as a negative characteristic as if there is more ash, there is less biomass available for processing in a given sample, however in combustion applications this ash can help with feedstock feeding in the early stages of co-firing but resulting in greater slag/fly ash build-up.⁴³

1.2.1 Pyrolysis reaction conditions and mechanisms

The liquid product, pyrolysis liquid, is usually the target product of pyrolysis because of its eligibility to be used in applications similar to those of petroleum oil such as heat and power generation. This potential sparked interest in the field, particularly in response to the volatility of the crude oil market. However, it also has potential as a feedstock for chemical production. The gas product is a mixture of mainly CO, H₂, CO₂, and some volatile hydrocarbons. The solid product is a carbonaceous material or char. The fraction and quality of each of the three products are functions of the type of the biomass material used and the processing conditions which include the temperature, the heating rate and the solid and vapour residence time.⁴⁴

Different kinds of lignocellulosic biomass from forestry and agricultural wastes can be used as a feedstock for pyrolysis. This includes, but not limited to, wood, straws, switchgrass, corn stover and bagasse, a number of studies have used seaweed and algae.²⁹ Lignocellulosic biomass is made up of three main constituents: cellulose, hemicellulose and lignin. Both cellulose and hemicellulose are carbohydrate polymers. Cellulose is a linear polymer of β -glucose while hemicellulose is a branched polymer that can contain different monosaccharides of which xylose is the most common especially in hardwoods.⁴⁵ Lignin is a complex highly aromatic non-carbohydrate polymer consisting of three primary monolignols as shown in Figure 7 which also shows the chemical structure of the cellulose and hemicellulose.⁴⁶

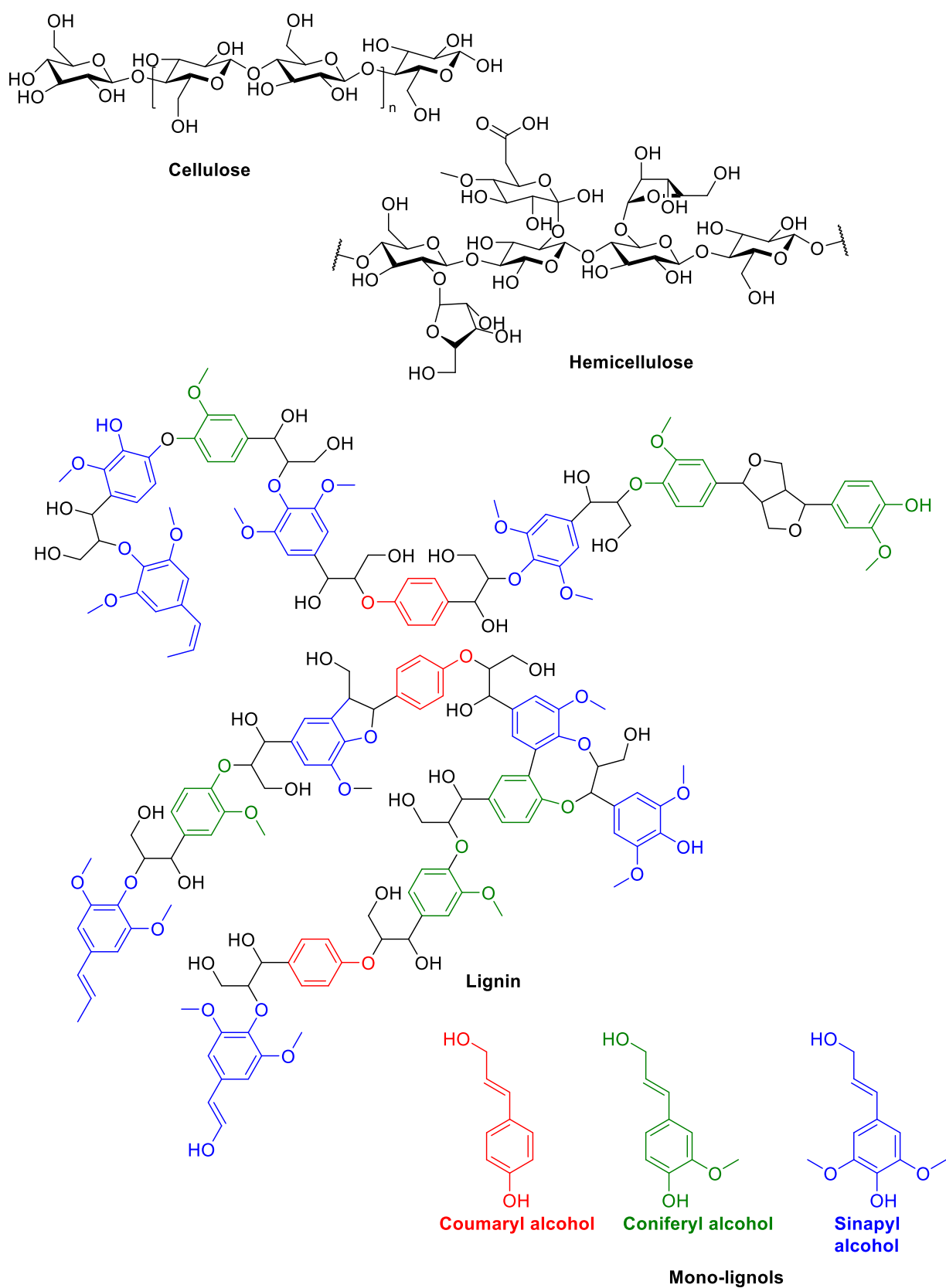


Figure 7 Chemical structure of the main biomass constituents, cellulose, hemicellulose and lignin. With monolignol units within the macro-lignin structure highlighted – note this is a hypothetical version of the lignin macrostructure to outline the types of bonds and chemical structures present. ^{46,47}

Exact mechanism of pyrolysis liquid formation is a complex and promising area for further investigation, in broad terms low reaction temperature with slow heating rate tends to maximise the char yield. Bridgwater *et al.*⁴⁴ identified five pyrolysis modes based on the operating conditions and the products fractions as shown in Table 2. The reason for this difference in product distribution has been established as a combination of the difference in reaction temperatures and sample residence time. It is widely accepted that the primary pyrolysis mechanisms remain similar with respect to temperature though the secondary reactions between the pyrolysis products also affect product distribution. It is thought that the pyrolysis temperature and sample residence time affect the type and duration of the secondary pyrolysis. The secondary pyrolysis reactions at higher temperatures cause the pyrolysis products to undergo pseudo “cracking” reactions into smaller gas molecules which exit the reaction system giving a high gas yield. At lower secondary pyrolysis temperatures secondary pyrolysis tends to combine into higher molecular weight species, hence char forms and a higher solid yield. If a liquid product is desired then these secondary pyrolysis reactions that lead to solid and gas products need to be limited. Among these modes, fast pyrolysis has received great attention as it gives the highest pyrolysis liquid yield.⁴⁴ Many studies have been made on the best approach to the elimination of this phenomena and a promising area for future investigations.⁴⁸

Table 2 Typical product distribution on dry wood basis obtained at different modes of pyrolysis⁴⁴

Mode	Conditions			Product fractions (%)		
	Temperature	Heating rate	Residence time	Solid	Liquid	Gas
Torrefaction	~290 (°C)	Slow	~10-60 mins	0-5	80	15-20
Carbonisation	~400 (°C)	Slow	Hours to days	75	12	13
Intermediate	~500 (°C)	Intermediate	~10-30 s	50	25	25
Fast Pyrolysis	~500 (°C)	Fast	~1 s	30	35	35
Gasification	~750-900 (°C)	V. Fast	<1	5	10	85

The key finding from this work is that pyrolysis temperature and sample heating rate can have an enormous impact of the product spectrum and quality.⁴⁴ This particular reference is chosen over others as it is uncommon for one laboratory to conduct all testing in the same place. The influence of inter-laboratory variability has been shown to be significant in comparing analytical pyrolysis studies.^{49,50} However, despite differences in applied temperature, the fundamental thermodynamics must remain constant. The minimum energy required for pyrolysis is called the enthalpy for pyrolysis. The enthalpy for pyrolysis is the sum of the sensible enthalpy and the enthalpy for

reactions. The former is the energy required to heat the biomass material up to the pyrolysis reaction temperature while the latter is the energy required to drive the pyrolysis reaction.⁵¹ This definition of the enthalpy for pyrolysis does not include any energy losses due to the technology used and the reactor design. Table 3 shows values of enthalpy for pyrolysis for various biomass materials obtained from previous studies.

Table 3 Enthalpy for pyrolysis for various biomass materials from previous studies. These have been grouped by lab conducting experiment to minimise the effect of inter-lab variation. The pine wood entries highlight the difference in experimental methodology can have on results.

Study	Material	Enthalpy of pyrolysis (MJ·kg ⁻¹)	Method
Daugard and Brown ⁵¹	Oak wood	1.46 ± 0.28	Energy balance in a fluidised bed at 500 °C
	Pine wood	1.64 ± 0.33	
	Oat Hulls	0.78 ± 0.20	
	Corn Stover	1.35 ± 0.28	
He <i>et al.</i> ⁵²	Wheat straw	0.558	Differential Scanning Calorimetry (DSC), at 500 °C
	Cotton Stalk	0.465	
	Pine wood	0.600	
	Peanut shell	0.389	
Van de Velden <i>et al.</i> ⁵³	Poplar wood	0.207	Differential Scanning Calorimetry (DSC), at 600 °C
	Sawdust	0.434	
	Straw	0.375	
Yang <i>et al.</i> ⁵⁴	Cedar wood	1.30	Energy balance in a screw conveyer at 600 °C
	Pine wood	1.50	
	Willow wood	1.50	
	Bamboo	1.50	
Chen <i>et al.</i> ⁵⁵	Poplar wood	0.114	Differential Scanning Calorimetry (DSC), at 500 °C
	Pine bark	1.135	
	Corn stalk	0.049	
	Rice straw	0.880	
Atsonios <i>et al.</i> ⁵⁶	Beech wood	1.12 ± 0.17	Energy balance in a fluidised bed at 500 °C

It can be seen from Table 3 that there are large variations in the enthalpy for pyrolysis ranging from 0.049 to 1.64 MJ·kg⁻¹. These large variations can be attributed to the use of different types of biomass material, employing different measurement techniques and reactor design as well as variations in temperature range. Deconvolution of these potential variables to account individually for them is a promising area of future work.

1.2.2 Measuring differences in composition of pyrolysis liquid

The first step in understanding any differences in pyrolysis liquid composition is to understand what it is possible to measure. Readers are referred to the comprehensive reviews in the literature.^{57–60} However some relevant techniques are introduced and discussed here;

Gas chromatography

Gas Chromatography (GC) is the most commonly used analytic technique in identification and quantification of compounds in pyrolysis liquids because it allows for the detection of very low concentration. However, the limit of detection is specific and varied depending on the individual compound(s) of interest.^{61,62} A limitation to this technique is that pyrolysis liquids samples are not always thermally stable so this analysis may induce some change in the sample during analysis. Pyrolysis liquid is not completely volatile so some compounds may not enter the elution column for analysis.

GC involves a mobile and a stationary phase. The mobile phase is a gas typically; helium, argon, hydrogen or nitrogen. Most GC machines use capillary columns, where the stationary phase coats the walls of a small-diameter tube directly (*i.e.*, 0.25 μm film in a 0.32 mm tube). The separation of compounds is based on the different relative strength of the interaction of the compounds with the stationary phase as opposed to the gas phase. The stronger the interaction, the longer the compound interacts with the stationary phase, and the longer the retention time. There are other factors that can affect sample retention time.

Liquid chromatography

LC methods are, unlike GC, not limited by sample volatility, and avoid the thermal degradation of samples resulting in data over- or underestimating.⁶³ However, they are limited by the solubility of the compound/pyrolysis liquid. Most common solvent systems Acetonitrile/water will not full dissolve all pyrolysis liquid. LC allows analysis of a different fraction of the pyrolysis liquid - including volatile, less volatile and the most problematic nonvolatile, high-molecular-weight compounds that are not detectable using GC. On the other hand, the separation ability of the LC methods is worse in comparison with GC. Also, the current detectors applicable for the connection with the LC have a much lower sensitivity for the direct identification of the individual bio-oil compounds than the electron ionization mass spectrometers typically applied in GC-MS. Considering quantitative analysis, LC detectors typically require calibration for each single component separately. All these factors result in a much lower number of identifiable and quantifiable pyrolysis liquid compounds by LC when compared with GC – however the analysis may be more useful if there are only a handful of target compounds of interest.⁶⁰

The main advantages of chromatographic analysis as opposed to more standard analysis (FTIR/NMR) is that the pyrolysis liquid sample is separated by polarity/volatility and then each fraction analysed separately by MS. Without some kind of fractionation, the analysis is too broad to draw conclusions specific enough to be meaningful, as it is difficult to quantify and hence deconvolute what is causing a change in an IR/NMR spectra. One way to overcome this is to introduce functionalisation to the pyrolysis liquid to aid in analysis.³¹P-NMR Phosphorous (³¹P) NMR was first used, in the context of coal derived pyrolysis liquids, in the late 1980's by Wroblewski *et al.*⁶⁴ A phosphorylation reagent, 2-Chloro-4,4,5,5-tetramethyl-1,3,2-dioxaphospholane (TMDP), was identified from a crop of potentials as most promising due to the lack of isomeric resolution between “up” and “down” methyl groups on the dioxaphospholane ring in NMR spectra. This reagent works through reaction to form an adduct, outlined in Figure 8.

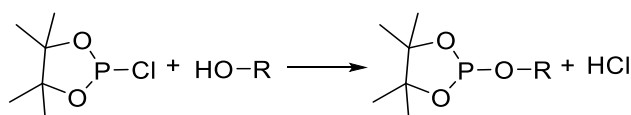


Figure 8 Adduct formation between TMDP and OH functional groups, the change in the chemical shift by NMR is used to quantify tyoes of OH groups in pyrolysis liquid

The method is outlined in the experimental section and involves the addition of several reagents to the sample alongside TMDP.⁶⁵ Deuterated chloroform is used as the main solvent, with the addition of pyridine to quench the HCl and avoid the evolution of toxic gas. Triphenyl phosphine oxide (TPPO) is added in a kmsnown quantity as a phosphorous reference and Chromium(III) acetylacetonate (Cracac) is a relaxation agent added to ensure that in between scans the sample returns to its equilibrium distribution.

It has been observed that the TMDP adducts display different chemical shifts (δ) depending on the chemical environment of the hydroxyl species that has formed the adduct. This phenomenon, after empirical measurement of analytical standards, allows for conclusions to be drawn about composition of pyrolysis liquid using this method.^{66,67} The advantage of this method when compared to chromatographic methods is that there is no need to invest in a library of different analytical compounds to validate any method. However, this means that this method is unsuitable for individual compound identification.^{49,50} The main practical drawback is that this method is quite susceptible to water concentration. Water will preferentially react to form adducts and subsequently dimers, and if the sample water content is too high, then the water dimer adduct precipitates. The published method recommends the addition of pyridine to overcome this, however in the opinion of the author this is not suitable for extremely wet samples. In the case of a sample with high water content, it is best to use less sample. If this is

not possible, react the sample and TMDP in a sealed vessel, and filter this suspension into an NMR tube to remove water dimer precipitate.

Since the focus of this project is in the functionalisation of a wide range of alcohol molecules, with no single compound of interest. This work favours a combination of alcohol content measurement by ^{31}P -NMR and wider characterisation by GC-MS as opposed to individual compound quantification by LC-MS.

1.2.3 Reactor design for fast pyrolysis

Pyrolysis liquid production through pyrolysis is usually achieved in four main steps as explained by Figure 9: (a) feed preparation which includes drying and grinding; (b) reactor system where the pyrolysis reaction takes place; (c) solid separation where the solid is separated from the volatiles; and (d) condensation system in which pyrolysis liquid is condensed and separated from the other incondensable gases.

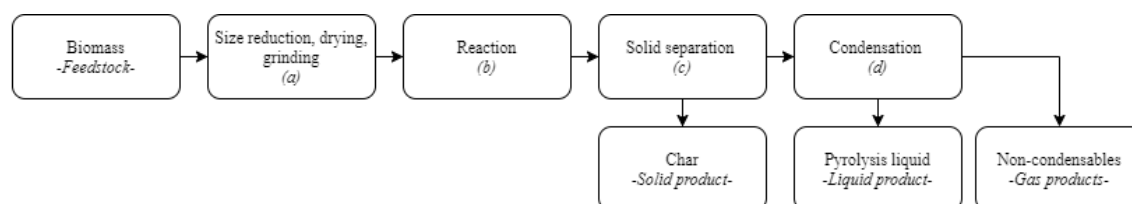


Figure 9 Main process steps of pyrolysis liquid production, showing that there are more process steps than just the reaction and studies should consider all aspects of a process as a whole

The reaction conditions required to achieve high pyrolysis liquid yield as shown in Table 2, limit the choices for the reactor design and the overall process. Several technologies have been introduced as candidates to meet these reactor requirements, each have advantages and limitations. The main existing pyrolysis technologies include bubbling fluidised bed, circulating fluidised bed, rotating cone, ablative pyrolysis, and the auger (screw) system.

Fluidised bed

Fluidised bed (also called bubbling fluidised bed) reactors have been used for decades in petroleum and chemical processes. The main advantage of the fluidised bed process is its ability to provide a high heat transfer rate, due to the large contact area between the fluid and the solid particles.^{44,68,69}

Figure 10 shows a flow diagram for a typical bubbling fluidised bed process for biomass pyrolysis. The biomass material, after preparation, is fed to the fluidised bed column where the pyrolysis reaction takes place. The fluidising gas, which is fed at the bottom of the column, controls the vapour and solid residence times. The pyrolysis products are carried with the fluidising gas and exit at the top of the reactor. This mixture is passed

through a series of cyclones to remove char. The vapours are then fed to a quench cooler where pyrolysis liquid is condensed. Pyrolysis liquid yield from a fluidised bed reactor could be as high as 75%.⁴⁴ The non-condensable gases from the condenser could be recycled and used as a fluidising gas.

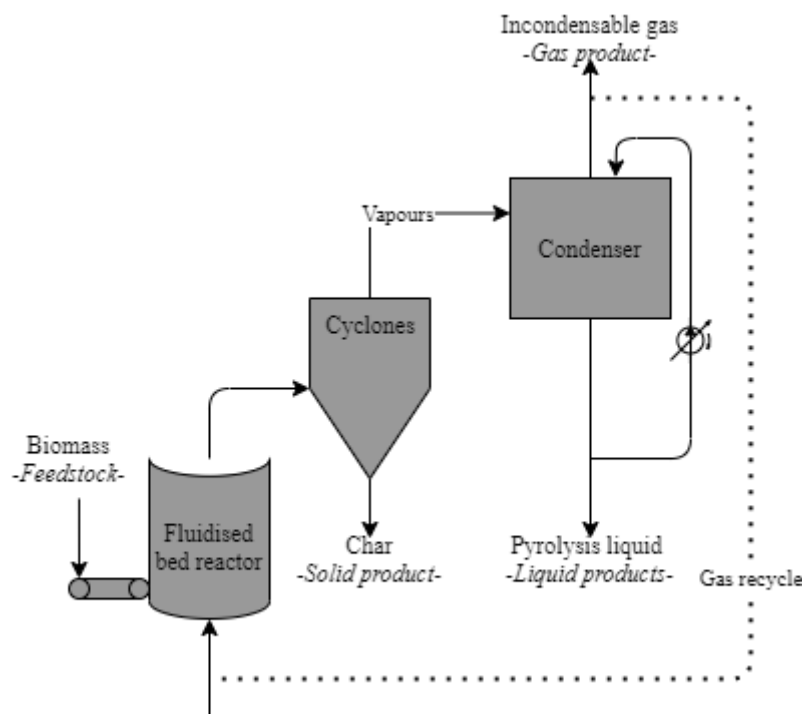


Figure 10 Typical bubbling fluidised bed technology for pyrolysis liquid production through “fast pyrolysis” where sample residence time is low and reaction temperature is higher

The operating temperature for bubbling fluidised bed reactors is around 500 – 550 °C which can be controlled through the temperature and flowrate of the fluidising gas.⁶⁸ The heat required to achieve the pyrolysis reaction can be provided through one or a combination of the following methods.^{44,68}

- Hot fluidising gas
- Heating through the reactor walls
- Immersed heating tubes
- Recycled hot sand

One of the limitations of this technology is that it requires the use of small particle sizes of less than 3 mm in order to achieve high heat transfer – this requires significant size reduction/grinding.⁴⁴ This size reduction step represents a significant energy and capital cost, Grinding costs can add up to \$11/MT of biomass.^{70–72} Also, the high gas flow required for fluidisation decreases the vapour pressure of the pyrolysis vapours, making oil

condensation and recovery more difficult.⁷³ Early research on biomass pyrolysis in fluidised beds was pioneered by the researchers at the University of Waterloo in Canada which led to the development of Research Triangle Institute's pyrolysis process. Based on this, Dynamotive built a 100 tonne per day and 200 tonne per day plants in Canada.^{44,74–77} Recently, Fortum has built and commissioned a commercial-scale 10 tonne per day plant in Finland employing the fluidised bed technology. The pyrolysis liquid plant is integrated with a combined heat and power (CHP) plant.⁷⁸

Circulating Fluidised Bed

Circulating fluidised bed (CFB) is similar to bubbling fluidised bed in many aspects. The main difference is that CFB technology uses much higher gas velocity causing shorter particle and vapour residence times.^{44,69} Hot sand is usually used in CFB (where this is not used in a fluidised bed reactor) to provide the process with the heat required to achieve the pyrolysis reaction. The higher gas velocity acts to lift the biomass and char particles through the reactor. Figure 11 shows a typical CFB process in which the prepared biomass material, is fed to the reaction column where it is rapidly heated upon contact with the hot fluidising gas and sand. The produced vapours together with char and sand are propelled up with the carrier gas which is fed at the bottom of the column. The char and sand are separated from the hot vapours in cyclones and fed to a combustor where the char is burned. The combustion heat is transferred to the sand which is then recycled to the reactor. The hot vapours from the cyclones are fed to a quench cooler to condense and collect the pyrolysis liquid. The incondensable gases are recycled to the column to be used as a carrier.

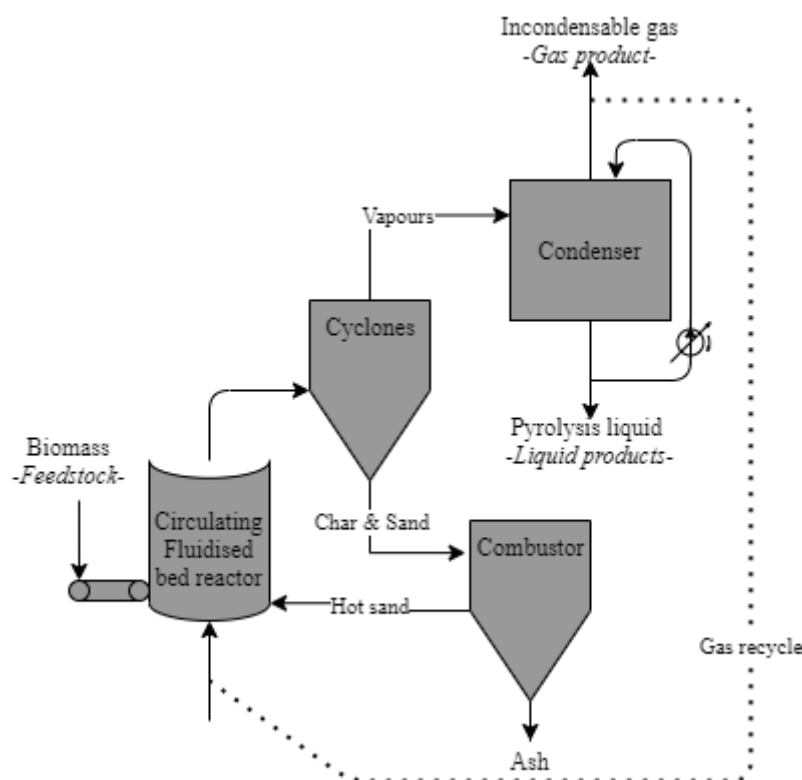


Figure 11 Simplified flow diagram of the circulating fluidised bed process developed by (Ensyn) for pyrolysis liquid production through “fast pyrolysis” where sample residence time is low and reaction temperature is higher

Due to its short vapour and solid residence times the secondary cracking reactions are limited. The solid residence time is usually less than 2 seconds.⁶⁹ Furthermore, CFB reactors are suitable for high throughputs which is ideal for commercial scale operation.⁴⁴ However, the design and operation of the CFB process are more complicated compared to the bubbling fluidised bed process due to the high gas velocity and the recirculation of sand.^{44,68} The sand flowrate is usually 10 to 20 times greater than the biomass feed rate which adds high energy cost.⁶⁸ The developments and commercialisation of the CFB technology have been led by Ensyn who, with partners, have designed and constructed several commercial-scale pyrolysis liquid plants in USA, Canada and Brazil.⁷⁸

Rotating cone

This technology, which was developed by the Biomass Technology Group (BTG), involves mixing the biomass material with hot sand in rotating cone inside a vessel. It does not require using an inert gas which substantially reduces the size of the reactor and the condenser.⁶⁸ As in the CFB technology, the sand and char from the reactor are fed into a combustor where the char is burned and the heat is transferred to the sand which is then recycled to the reactor. Typical flow diagram of the process developed by BTG-BTL is shown in Figure 12. The main disadvantage of the rotating cone process is its complexity, moving parts, a fluidised bed combustor for burning

the char and pneumatic transport of the sand. EMPYRO has recently constructed and opened a 5 tonne per hour demonstration plant in Netherlands. Employing BTG's rotating cone technology, the plant simultaneously produces process steam, electricity and pyrolysis liquid.⁷⁹

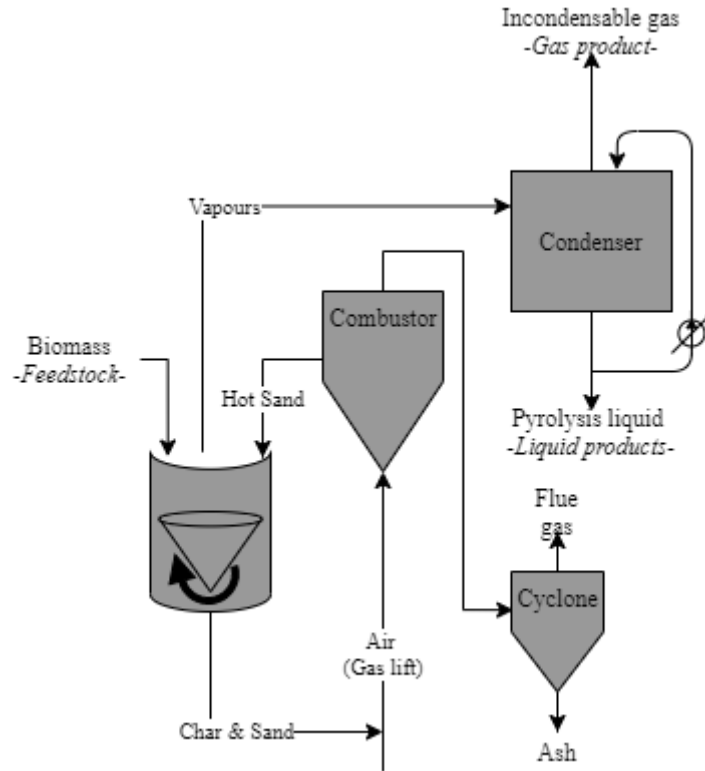


Figure 12 Process flow diagram of the rotating cone technology developed by BTG-BTL for pyrolysis liquid production through “fast pyrolysis” where sample residence time is low and reaction temperature is higher

Ablative pyrolysis

The concept of this technology is different than the others in that instead of using a heat carrier, the biomass particles are contacted with a hot metal surface.^{78,80} The char layer formed on the particle's surface during the reaction is continuously removed as a result of an ablative force applied on the particle through either high gas velocity flowing tangentially to the reactor walls (gas ablation) or mechanically using a rotary disc/blade.^{44,68} The reactor wall temperature is usually kept around 600 °C. The main advantage of this technique is that it can process particles as large as 20mm.⁶⁸ Research on this technology was led by NREL between 1980 and 1996 who employed the gas ablation method.⁶⁸ However, NREL's work on this technology was abandoned in 1997 due to technical issues related to the high gas and particle velocities which resulted in excessive erosion, and also because of uncertainties regarding the scalability of the technology.⁶⁸ Recent activities on this technology have been

focused more on the mechanical ablation such as the 250 kg·h⁻¹ plant constructed by Pytec and the 100 kg·h⁻¹ plant operated by Fraunhofer UMSICHT, both in Germany.^{78,80}

Auger Reactor

The main feature of this technology is that the biomass material is fed to the reactor and moved inside it mechanically through auger or screw. The heat for the reaction is usually provided through hot sand which is mixed with the feed at the entrance. The sand is then separated from the product, reheated and recycled again.⁸¹ The heat could also be provided externally through the wall. The main advantages of the auger reactor are its simplicity and flexibility in terms of feed particle size and shape. However, the solid and vapours residence time inside the reactor for this technology are long compared to the fluid-transported technologies leading to high char and low liquid yields.⁴⁴ This reactor has been refined to include catalytic steps in the so called Thermo-Catalytic Reforming (TCR) system.⁸²

Other Technologies

There are other types of reactor design which have not received as much attention and development towards scaling up as the earlier discussed technologies. One of these is the vacuum reactor which does not require a carrier gas to sweep the vapours out of the reactor. This makes the condensation easier and results in a clean oil with little or no char particles.⁶⁸ Although the vapour residence time is short, vacuum pyrolysis is still considered a slow pyrolysis process with a liquid yield of 35 – 50%. Another technology is the fixed bed reactor which has been used widely in laboratory scale studies but there is no evidence that it could be used in larger scale applications.⁴⁴

Fixed Bed Conventional pyrolysis discussion

A number of technologies have been introduced as possible candidates to meet the requirements for high pyrolysis liquid yield through fast pyrolysis. These requirements include a high heating rate, intermediate temperature and a short vapour residence time. The differences in the reactor design between these technologies can be found in mainly two areas: the method of solid flow/movement and the method of heat transfer to the biomass material. These are the focus of most of the research and development in fast pyrolysis technologies. Biomass materials, in general, are known for their complex flow behaviour and in the above-discussed technologies, there are essentially two methods for feeding and moving the biomass materials inside the reactor. One is using a gas carrier such as in the bubbling and circulating fluid bed reactors and the gas ablative reactors. The other is mechanical such as in the auger reactor and the mechanical ablative reactors. Although the rotating cone reactor uses the gravity force

for feeding the solid into the reactor, it could be considered as a mechanical flow method because the reaction takes place in the rotating cone and the char and sand are transported out of the reaction area using the centrifugal force supplied by the rotating cone. The gas carrier systems have the advantage of their ability to provide shorter vapour residence time which is required for high liquid yield. They can also improve the heat transfer if the gas is preheated. However, a large condenser is required to cope with the high gas flowrate. The heat required to achieve the pyrolysis reaction can be provided to the biomass material through either a heating medium (hot gas or hot sand) which is the most common method or through a hot surface such as in the ablative reactor. Using hot gas alone is usually not sufficient to provide the heat of reaction unless the gas temperature is excessively raised which would degrade the liquid yield and quality.⁴⁴ This is why it is usually used in a combination with hot sand or hot surface. Adding hot sand to the process adds high energy cost for moving the sand around the process.⁶⁸ Providing the energy required to achieve the biomass reaction with high heating rate has been one of the major challenges facing the development of fast pyrolysis technologies.⁴⁴ A promising alternative heating method is microwave heating. Microwave heating is a volumetric heating technique where energy is transferred to molecules instantaneously because of their interaction with the microwave electromagnetic field. It is more akin to an energy transfer and subsequent conversion to heat rather than heat transfer. Microwave is also a selective heating technique, based on the sample's ability to interact with magnetic fields and also the ability to convert this energy into heat, this means that it could be targeted to preferentially heat any good microwave absorbent material where gases, free space, non-polar molecules and quartz are mostly transparent to microwaves.⁸³ With its selective and volumetric heating features, microwaves can provide a rapid heating in a cold environment. In biomass pyrolysis, this could limit secondary degradation reactions preserving product quality. It may also help to reduce the energy consumption as the energy is used to directly heat the biomass material with no need to heat its environment.⁸⁴ Many studies have been published on biomass pyrolysis employing the microwave heating technique. However, before reviewing these studies, some fundamentals of microwave heating will be discussed.

1.3 Microwave heating

1.3.1 Background

What are microwaves? They are a group of electromagnetic “waves” generated in a magnetron using electricity and subsequently directed using waveguides. Microwaves are directed into an enclosed space where the microwave radiation cannot escape – the cavity. Microwaves behave as standing waves and are capable of constructive and destructive interference – this is key to manipulation of them. There are different types of cavity

size and shape affecting how and where the microwaves constructively and destructively interfere.^{85,86} A cavity where there is only one maximum of constructive microwave interference is known as a monomodal cavity, larger cavities with multiple places of constructive interference are referred to as “multi-modal”. To change the location of hot spots in a multimodal cavity a stub tuner vary the electromagnetic wave shape and hence the location of interference.

Materials can be classified according to their interaction with the electromagnetic fields into conductors, insulators, and absorbers. In the case of microwave frequencies (0.3 to 300 GHz) conductors reflect the radiation and they are used as waveguides and walls in microwave cavities, insulators behave as transparent media and they are used as supports and holders in microwave heating applications, and absorbers (also called dielectric materials) absorb the radiation and can be heated by the microwave energy.⁸⁷

The idea with tuning the microwave with the cavity to increase the amount of energy absorbed by the sample and avoid wasting energy. Typically the forward and reflected power are measured through a tuner and in the difference lies the amount absorbed by the sample. Coupling the tuner with forward and reflected power measurements, the amount of power absorbed by the sample is maximised – tuning. It is important to note that the measurement of forward and reflected microwave power and tuning is not possible in conventional kitchen microwaves. How much microwave energy is absorbed by a sample depends on the properties of the sample namely the dielectric constant (δ), the ability of a molecule to interact with microwaves, loosely the polarity of a molecule and the loss tangent (λ) which is the ability of a sample to convert absorbed energy.^{88,89}

Generally, pyrolysis uses conduction and convection as methods to transfer heat from the reactor to sample, for the duration of this work this is described as “conventional” heating. This thesis is an effort to compare this to an alternative method of applying heat to a sample is microwave heating (MWH) in the context of heating biomass for pyrolysis for use as feedstock in the production of monomers and polymers. Microwave heating technique is one of the electrical volumetric heating family which includes also conduction and induction heating (resistive heating), Ohmic heating and, radio frequency (RF) heating.⁸³ The frequency ranges for each of these heating techniques are indicated in Figure 13.

Resistive (Ohmic)		Induction			Radio		Microwave		Frequency (Hz)					
10	10 ²	10 ³	10 ⁴	10 ⁵	10 ⁶	10 ⁷	10 ⁸	10 ⁹	10 ¹⁰	10 ¹¹	10 ¹²	10 ¹³	10 ¹⁴	10 ¹⁵
Power (50/60)		Telephones (audio frequency)		Long wave	Medium wave	Short wave	VHF	TV				Infra-red	Visible light	Ultra violet

Figure 13 Volumetric heating methods in the electromagnetic spectrum. Adopted from Meredith et al.⁸³ Energy inherent in the electromagnetic waves increase from left to right.

Certain frequencies have been specified for domestic, industrial, and medical uses as an international agreement to avoid interference with communication signals.⁸³ However, the most commonly used microwave frequencies for these applications are 2.45 GHz and near 900 MHz (896 MHz in the United Kingdom and 915 MHz in the United States). In the RF region, 6.78 MHz, 13.56 MHz, 27.12 MHz and 40.68 MHz are commonly used.⁹⁰

Dielectric materials are heated electromagnetically *via* polarisation (also referred to as relaxation) or conduction loss effects.⁸⁹ Polarisation loss occurs as a result of the charges displacement from their equilibrium position when the alternating electromagnetic field is applied to them. This is accompanied by a motion as the molecules move to align with the alternating magnetic fields, this leads to heat dissipation. Dipolar loss is more significant in liquids and Conductive loss is the dominant loss mechanism in solids.^{88,91,92} Conductive loss (also called ionic conduction) is related to poor electric conductors which contain charge carriers free to move under the influence of the electric field.⁸³ The applied electric field redistributes the charge carriers forming a conducting path and the material, in this case, is heated due to the electrical resistance (charged particles collision) resulting from the conduction.^{88,93} There are also electronic and atomic polarisation mechanisms, however these have a negligible effect within the microwave and RF frequency ranges and they are effective only in the infrared and visible parts of the electromagnetic spectrum.⁸⁸ Generally the intensity of the electric field strength determines the amount of energy absorbed, however at increased field strengths different interactions between the sample and the field can

exist. For biomass materials, their high moisture content makes dipolar loss the dominant loss mechanism at room temperature. However, during biomass pyrolysis, when char starts to form at high temperature, the conductive loss becomes the dominant loss mechanism.⁹⁴

1.3.2 The future of microwave pyrolysis

Microwave heating has been considered as a promising technique for providing the energy input to biomass pyrolysis due to its volumetric and selective nature which allows for rapid heating in a cold environment. These features can help to preserve the product quality by limiting the unwanted secondary reactions.⁸⁴ They can also help to reduce the energy consumption as the energy is used to directly heat the biomass material with no need to heat its environment.⁸⁴ Many studies have been conducted and there are already several review papers published on microwave pyrolysis of biomass materials.⁹⁵⁻⁹⁹ Different factors have been found to effect the product yield and quality. These include the type and size of the biomass material, the microwave energy input (power and time), the type of the microwave cavity and the reactor design.⁹⁷ Liquid yields as high as 60% have been reported.⁸⁴ One of the early studies that discussed in some details the benefits of the heating in a cold environment during microwave pyrolysis is the work reported by Miura *et al.*¹⁰⁰ They looked at the temperature gradient and the mass transfer for both conventional and microwave heating as shown in Figure 14. In conventional heating, the direction of mass transfer is opposite to the direction of heat transfer which results in that the volatile products pass through areas of higher temperature where secondary reactions can be activated. This is not the case in microwave heating where the centre has usually higher temperature than the outer surface and heat and mass transfer are aligned. This microwave heating benefit should be increased in the liquid inerted microwave pyrolysis system, where the

liquid can act as a much more effective heat transfer medium than traditionally inerted systems, these heating methods for pyrolysis are compared in Figure 14.

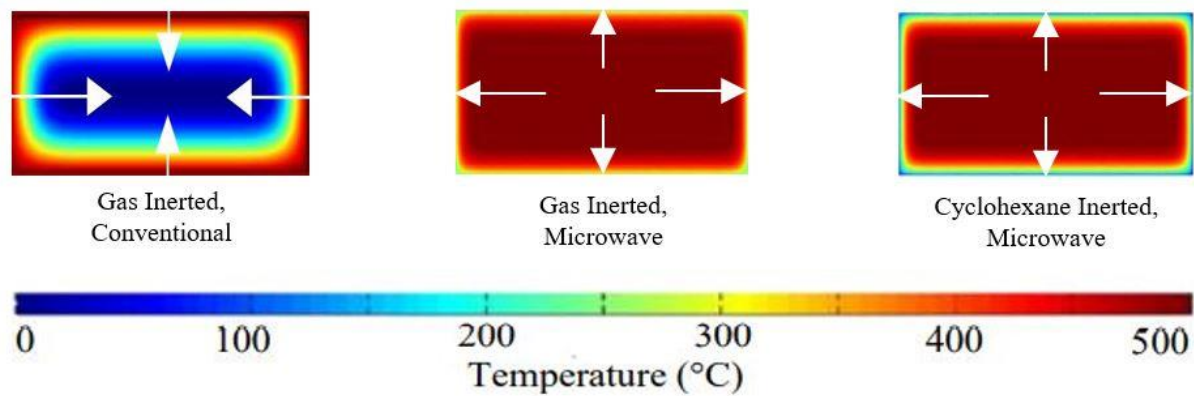


Figure 14 Temperature gradient in conventional, microwave and liquid pyrolysis systems with heat flux shown in white arrow.

Note that in all cases the mass transfer flux is from the core to outside of the particles

Robinson *et al.* studied the effect of microwave pyrolysis on the quality of the produced pyrolysis liquid and compared the results to those obtained using conventional pyrolysis.⁸⁴ They found that the composition of the high molecular weight primary compounds such as levoglucosan in the pyrolysis liquid obtained after microwave pyrolysis was significantly higher than that from conventional pyrolysis. This was attributed to the heating in cold environment advantage that microwave provides which limits the secondary degradations. The model used to predict the temperature in Figure 14 was limited by the assumption of a static dielectric constant, this is known to be not the case, typically the dielectric constant will increase as temperature and char content increase.^{94,96,101–103}

1.3.3 General points to note on previous microwave pyrolysis studies

Microwave heating has been considered as a promising technique for providing the energy input to biomass pyrolysis due to its volumetric and selective nature which allows for rapid heating in a cold environment. These features can help to preserve the product quality by limiting the unwanted secondary reactions.⁸⁴ The following points could be noted with regards previous studies on microwave pyrolysis of biomass material;

- Most published work on microwave pyrolysis of biomass materials is based on lab-scale batch pyrolysis experiments. Many of the experiments were conducted in modified domestic microwave ovens which provide low powers and limited electric field intensity inside the cavity.
- In many of the previous studies, the biomass material was mixed with a microwave susceptor to increase the heating rate and to reach pyrolysis temperature. The use of susceptors eliminate the specific benefits of microwave heating which are the selective and volumetric heating. The biomass material is therefore heated by conduction from the surface of the susceptor which is, in terms of heat transfer, indistinguishable from conventional heating.
- There is, a lack of understanding about the impact of using microwave susceptors (highly microwave absorbent material) on the product yield and quality. There are number of studies which showed that increasing the fraction of the microwave susceptor increases the gas yield at the expense of the liquid, indicating an increase in the secondary cracking reactions. This is often conflated with catalytic effects, for instance the work of Shang *et al* reports that “the addition of potassium carbonate promoted [the activation energy] decreasing due to catalytic effect.” However also reports that “High heating rate shifted the activation energy to higher values; this may be ascribed to high activation energy required for heavy molecular weight hydrocarbons cracking into small molecular materials.” Where an alternate explanation, that doesn’t involve the heating rate changing reaction thermodynamics, is that at high microwave heating rates the critical heat flux of the microwave susceptor has been reached and thus any additional microwave power is not transferred from the susceptor to the sample.¹⁰⁴
- There is also a lack of understanding about the impact of the cavity design and the applied electric field intensity on the performance during microwave heating. The proper design of the microwave heating cavity to provide high electric field intensity eliminates the need for a microwave susceptor.^{29,94,105–107}

- Many pyrolysis methods are analysed with specific applications in mind, this is typically fuel, as such the analysis techniques employed are relevant only to this and are in some cases where different analyses are conducted, the results are not widely comparable.
- Some studies introduce some parameters as “variables” where they do not behave in unexpected ways- the work by Omer *et al.* for instance where high higher heating value (HHV) solvents such as Ethanol and Methanol are blended into pyrolysis liquid and a corresponding increase in HHV is observed.¹⁰⁸
- Some variables are not consistently controlled in studies, this also makes comparison between heating methods more difficult as more than one variable may be changing between studies. It is almost impossible to control for differences within the same feedstock (*i.e.*, seasonality or storage conditions) between ostensibly identical feedstock. This is highlighted in a 2017 round robin study where similar feedstock was used and produced different results in different laboratories and there was inconsistency between feedstock behaviours⁵⁰
- Comparing pyrolysis methods in such a way that the only variable is the heating method is challenging as these are typically run by different operators, in different laboratories, using different equipment, feedstock and analyses and usually there are too many variables changing for reliable and reproducible conclusions to be drawn.
- One of the major challenges facing the microwave pyrolysis of biomass is the heating heterogeneity caused by the nature of the standing waves which creates hot- and cold-spots inside the heating cavity. Due to the high loss factor of the char formed during pyrolysis compared to the raw biomass, the heating heterogeneity can lead to thermal runaway in the hot spots. In single mode cavities, the heating homogeneity can be controlled by processing a small sample size placed at the area of the high electric field intensity however this approach presents challenges in terms of sample handling and preparation.

1.4 Use of pyrolysis liquid in polymers

Addition polymers use a distinct chemistry avoiding the elimination of a small by-product molecule. Methacrylates are among this family of addition polymers. Methacrylate polymers show viability in a wide range of applications, from resins and adhesives to bitumen binders.^{109–114} It has been shown in the literature that these methacrylates from pyrolysis liquid model compounds can be made by the overall mechanism shown in Figure 15.^{109,115–117} Usually the model lignin compounds used are based on the “monolignols” Coumaryl alcohol, Coniferyl alcohol or sinnapyl alcohol (Structures are shown at the bottom of Figure 7), vanillin is also a popular compound as it is structurally similar to both the monolignols and styrene.^{109,116,118}

With R-OH showing the general pyrolysis liquid model compound used.

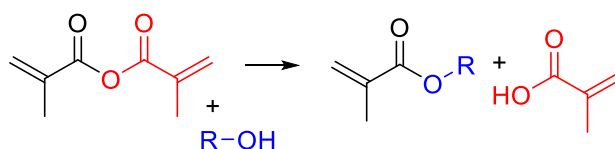


Figure 15 Scheme to show production of pyrolysis liquid monomers from model compounds in the work of Holmberg *et al.*^{109–111,119} With R-OH showing the general pyrolysis liquid model compound used.

This approach showed great potential for pyrolysis liquid to be used in applications beyond fuel. However, this synthetic route requires a very “clean” feedstock and is unsuited to our approach of using unrefined, “crude”, pyrolysis liquids.^{120,121} Recently Bai *et al.*¹²² and Epps *et al.*^{110,111,117,119,123} have shown that similar methacrylate molecules can be produced from less refined (*c.f.* monolignol/model compound) “fractions” of pyrolysis liquid. These were created by dissolving the “crude” pyrolysis liquid in Dichloromethane (DCM). The DCM soluble fraction was not investigated and the insoluble fraction was taken and, through the use of acyl chloride reagents following the general scheme outlined in Figure 16, was methacrylated into a resin type material.

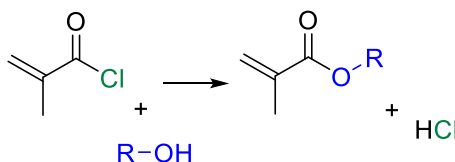


Figure 16 Scheme to show the production of pyrolysis monomers using methacroyl chloride in the work of Bai *et al.*^{124–126} With R-OH showing the general pyrolysis liquid model compound used.

The atom economy of the reaction in Figure 16 is higher than the anhydride mechanism, however this metric does not take into account the environmental cost of acyl chloride production from methacrylic acid which generates a stoichiometric equivalent of thionyl waste or the environmental burden of Hydrochloric acid (HCl) waste produced in reaction. These disadvantages are highlighted in the manuscript of Bai *et al* and a more sustainable esterification route is called for.¹²²

The recent transesterification work of Dundas *et al*¹²⁷ has shown that a wide range of individual alcohols can be transformed into their corresponding methacrylates with commonly used industrial catalyst, Titanium butoxide, (TNBT) and elevated temperatures (160 °C) and butyl methacrylate (BMA) outlined in Figure 17. However, it is necessary to distill the by-product throughout the reaction, in this case butanol, to drive the reaction to completion.

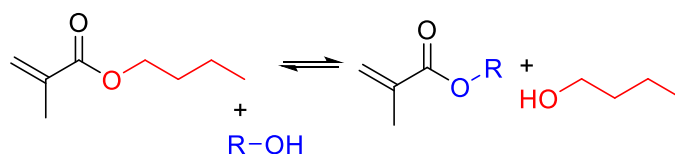


Figure 17 Scheme to outline transesterification reaction. With R-OH showing the general pyrolysis liquid model compound used.

It should then be possible to make these pyrolysis liquid derived monomers *via* transesterification of BMA. BMA has been chosen as the basis for this work, however this is an example and shows potential for more sustainable drop in replacements for butyl, propyl and ethyl methacrylates. BMA itself is produced *via* transesterification from methyl methacrylate on an industrial scale,¹²⁸ but in this case it was chosen as the reagent in favour of the methyl equivalent so that reaction temperatures in the 145–160 °C range could be investigated. Using an excess of methacrylate to improve transesterification yields was proved to be successful in prior work by Dundas *et al*.¹²⁷ The reason for choosing a transesterification as opposed to the direct esterification, from methacrylic acid for example, was due to the difference in a)boiling point of reagent and b) boiling point of reaction by-product c) ease of identification/quantification of by-product (both water and methanol are present and have been shown to be distilled from pyrolysis liquid).^{108,129–132} This is broadly summarised in Table 4.

Table 4 Summary of boiling point differences between methacrylate and reaction by product with energy of vaporisation for comparison. The heat of vaporisation for BuOH is much lower in kJ/kg than water due to a lower density and higher molecular weight – despite similar molar equivalent values.

Reagent	Boiling point (°C)	Reaction By-product	Boiling point (°C)	Heat of vaporisation
Methacrylic acid (MAA)	161	Water	100	2.260 kJ/kg (40.8 kJ/mol)
Methyl Methacrylate (MMA)	101	Methanol	64.7	1.09 kJ/kg (35.21 KJ/mol)
Butyl methacrylate (BMA)	163	Butanol (BuOH)	117.7	0.58 kJ/kg (43.29 kJ/mol)

From Table 4 the boiling points of MAA and BMA are similar and much higher than MMA – this is essentially a ceiling for the reaction as at temperatures above this the reagents will simply distill off, hence the preference from BMA over MMA. In terms of MAA vs BMA, although the boiling point of BuOH is higher than that of water, the heat of vaporisation is much lower, so in a system above the boiling point of both by-products, less energy will be removed from the system to boil off the by-product. A secondary reason for a preference of BuOH waste as opposed to water waste, is that it is much easier to dispose of contaminated BuOH *via* energy recovery than to purify water. For these reasons a transesterification approach was preferred in this study. Upon consideration of the overall process, as BMA is typically made by esterification of MAA/BuOH, by using MAA directly a further process step could be removed which could offset the extra energy and waste disposal considerations.

1.4.1 Radical polymerisation and analysis

Following on from the transesterification, radical polymerisation of the unsaturated monomer through the addition of a radical initiator should be possible. The processes occurring in free radical polymerisation (FRP) can be broken down into: initiation, propagation, chain transfer and termination.

Initiation can be achieved by high energy irradiation or thermal initiation without the addition of initiator. More often free radicals are generated by the addition of molecules that form radicals when heated or irradiated. Most common among these is Azobisisobutyronitrile (AIBN), the thermal initiation of this is shown in Figure 18.

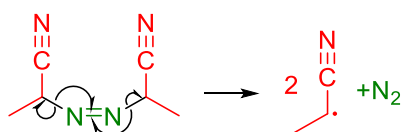


Figure 18 Thermal initiation of AIBN, this is driven by the entropy of producing nitrogen gas.

The generated radical is now free to react with any unsaturated monomer, shown in Figure 19.

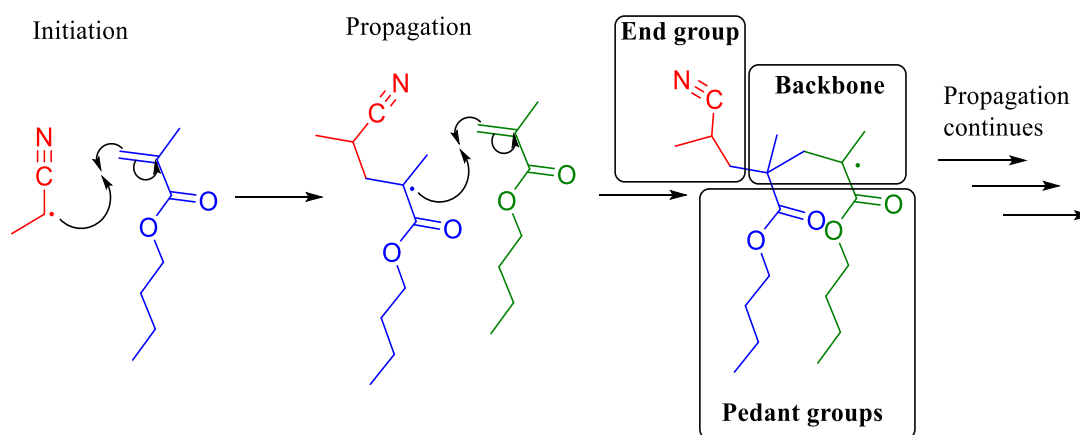


Figure 19 Initiation of FRP polymerisations with AIBN and BMA as examples. The anatomy of a polymer has been highlighted in the initial propagation product to highlight which reagent is likely to constitute the different parts of a polymer

Propagation now proceeds through successive addition of monomers to the growing radical chain. When two radical chains react together this triggers the termination, however this can go in one of two ways, shown in Figure 20.

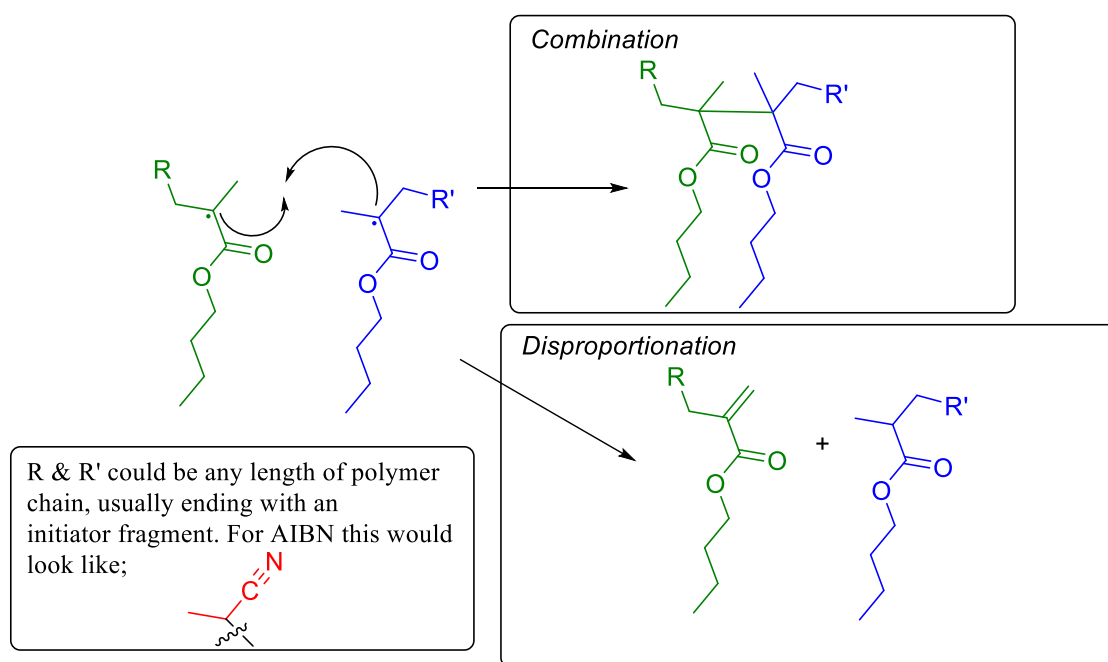


Figure 20 Termination of FRP polymerisations, this outlines the origins of the different possible end groups in a radical polymerisation

The relative proportions of disproportionation and combination depends on the type of monomer and the temperature. In FRP an active site is formed by an initiator and monomer adds very quickly, often in a matter of seconds. The length of the polymer chain depends on the random radical encounters that lead to termination, so there will be a distribution of molecular weights. Unlike step growth polymers, there is no continuous distribution of molecular weights and at any given degree of polymerisation there is a mixture of monomer and polymer chains. The number of chains is determined by the concentration of initiator and therefore the length of the polymer chain will be inversely proportional to the initiator concentration. If we generate a smaller number of initial radicals, the polymer chains will grow longer before they reach another radical and the polymerisation terminates. Chain transfer is where a growing radical chain is terminated and new chain is initiated in its place, a lot of the components in a polymerisation are capable of chain transfer; monomer, solvent, terminated polymer *etc.* Sometimes a chain transfer agent is added to better control the molecular weight by preventing the formation of higher molecular weight species at a faster rate, hence keeping the polydispersity under control. Dodecane thiol/ dodecyl mercaptan (DDM) is a simple chain transfer agent, with a boiling point well above the standard radical polymerisation reaction temperature.^{133–135}

Typically, polymers are analysed using size exclusion chromatography where dissolved polymer is separated by retention time on a column with a variety of pores. This means that smaller polymers take longer to elute down the column as they are more able to interact with the pores.^{133–136}

In a Gaussian SEC polymer curve, shown in Figure 21, peak molecular weight (M_p) is simply the maximum point of the curve. The weight averaged molecular weight (M_w) is usually a bigger value as this is more affected by the longer, heavier polymer chains and the number averaged molecular weight (M_n) is usually smaller as there are usually smaller polymer chains than larger ones. The ratio of M_w/M_n gives a sense of the gradient of the curve, or the polydispersity. The flatter the peak, the bigger is the difference between M_n and M_w and the higher the polydispersity

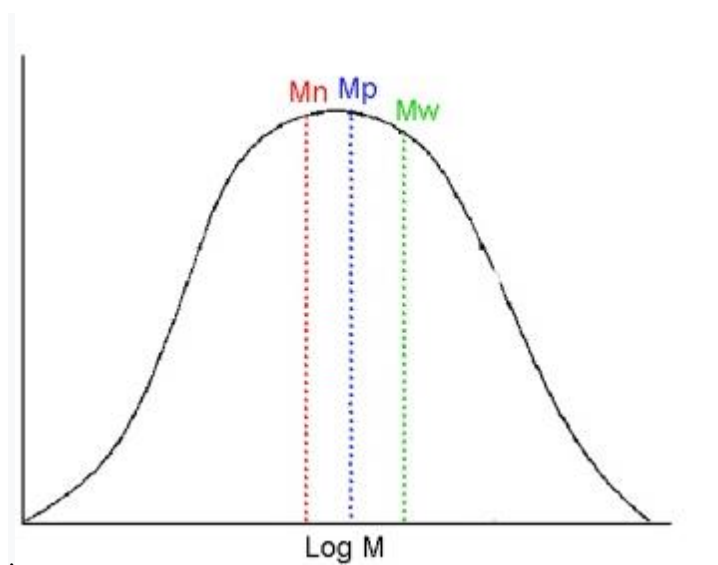


Figure 21 Typical SEC curve and the approximate Molecular weight values M_p , M_n and M_w included with $M_w > M_p > M_n$ being the usual trend in a typical gaussian polymer distribution.

Broadly speaking, in terms of the chemistry, higher molecular weight and a polydispersity close to 1 as possible are most desirable as they indicate good reaction control. However, in some applications such as adhesives, a high polydispersity gives a wide spectrum of polymer chains lengths that affect the interfacial tension, which is key to adhesive performance.¹³⁷ Absolute molecular weight is determined from elution time by comparison with the elution time of known standards.¹³⁸

1.5 Principle thesis hypotheses and aims

It has been shown that chemically it is possible to make methacrylate monomers from refined pyrolysis liquid fractions and model compounds. The aim of this work was to apply the industrially relevant method of transesterification to produce similar monomers from crude pyrolysis liquid. This led to investigations into whether through different pyrolysis heating methods give rise to varied pyrolysis liquid composition and yield. Further to the pyrolysis investigation was the question of whether the pyrolysis liquids could be “improved” by the pyrolysis method such that the transesterification reaction gives higher yields or improved polymer products. These investigations went through a series of refinements and the original hypotheses were narrowed and revised into three hypotheses and subsequent aims outlined below.

1.5.1 Final hypotheses

1. Methacrylate pyrolysis liquid monomer and polymers can be synthesised via transesterification from fractionated and also crude pyrolysis liquid using processes, reagents and conditions that actually exist on an industrial scale.
2. Pyrolysis liquids of comparable yields can be obtained on identical apparatus using different heating/inerting methods - these can be shown on the same piece of analytical equipment to have different compositions.
3. Pyrolysis liquid composition affects transesterification and polymerisation chemistry and the properties of polymer.
4. The properties of the polymer can be influenced by changing pyrolysis conditions.

1.5.2 Aims

1. Identify a suitable method to make polymers from pyrolysis liquid.
2. Understand the effect of heating conditions on the composition of the pyrolysis liquids, along with a comparison of heating methods.
3. Understand how the composition of pyrolysis liquid affects the properties of the produced polymer.

Chapter 2. Experimental methods and materials

Different methods and analytical techniques were used for different purposes in this investigation. In order to give context to the use of experimental methods, their relevance to the process is outlined in Figure 22.

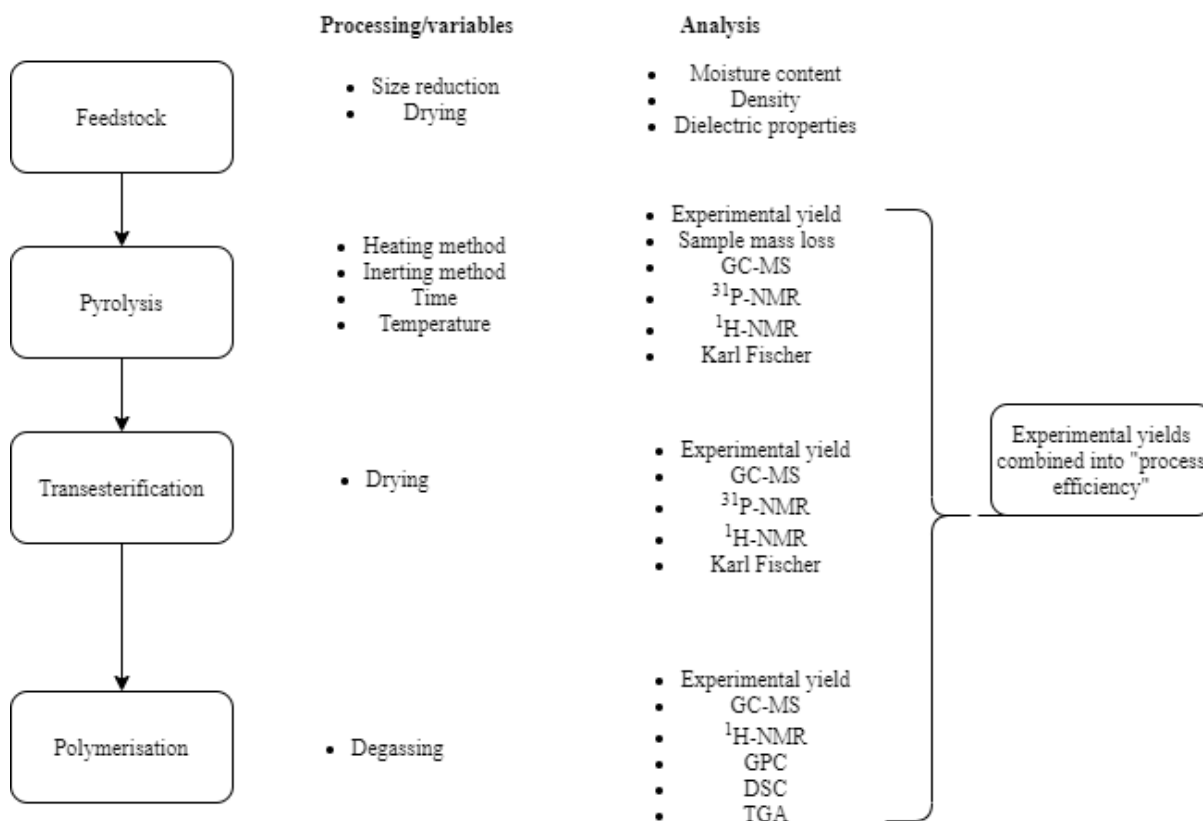


Figure 22 Processing and analytical method outline

2.1 Materials

All reagents were of analytical grade and obtained from Sigma-Aldrich or Fisher Scientific. Pyrolysis liquid was obtained commercially from the Empyro plant (Enschede, Netherlands), stored at 3 °C and used within 2 months of opening. Sycamore *Acer pseudoplatanus* was supplied by Nottinghamshire eco-fuels (UK) and pine *Pinus Sylvestris* by Websters Timber (UK). Biomass samples were cut into 45 × 45 × 15 mm blocks using a stainless-steel saw prior to pyrolysis. Average masses of biomass block moisture content and post-drying density for pine and sycamore respectively are reported in Table 5.

Table 5 Average masses of biomass block moisture content and post-drying density for pine and sycamore

	Pine Wood	Sycamore Wood
Mean Pre-drying mass, g (SD)	20.94 (3.26)	39.56 (4.71)
Mean post-drying mass, g (SD)	18.02 (2.84)	37.15 (4.43)
Moisture content (%)	14%	6%
Post-drying density(g/cm ³)	0.59	1.2

2.1.1 Biomass moisture content

The moisture content was measured by drying a biomass samples for 12 hours in a convection oven at 105 °C (ASTM D4442). The mass of the block was weighed before and after. Results were then used to calculate the yield data on a percentage dry weight basis.

2.1.2 Biomass dielectric properties

The dielectric constant (ϵ') and dielectric loss factor (ϵ'') of biomass samples was determined using the cavity perturbation technique. Measurements were performed at 2470 MHz, from 20 to 600 °C, ramped at 5 °C/min. The resonant cavity consists of a cylindrical copper cavity connected to a vector network analyser, which measures the frequency shift and change in quality factor relative to the empty resonating cavity when a sample is introduced. The sample was loaded into a quartz tube and held in a conventionally heated furnace above the cavity until the temperature set-point was reached. The tube was then moved into the cavity to make the measurement at the required temperature. A detailed description of the equipment is given by Adam and Shepherd.^{86,102} The dielectric constant and loss factor were calculated using the following equations:¹³⁹

$$\text{Equation 1: } \epsilon' = 1 + J_1^2(x_{1,m}) + \left(\frac{f_0 - f_s}{f_s}\right) \frac{V_c}{V_s}$$

$$\text{Equation 2: } \epsilon'' = J_1^2(x_{1,m}) + \left(\frac{1}{Q_s} - \frac{1}{Q_0}\right) \frac{V_c}{V_s}$$

Where;

f_s	Resonant frequency of the cavity with the sample present
f_0	Resonant frequency of the empty cavity
Q_s	Quality factor of the cavity with the sample present
Q_0	Quality factor of the empty cavity
V_s	Volume of the sample
V_c	Volume of the cavity
$J_1^2(x_{1,m})$	Second order of the first kind root of the Bessel function

2.1.3 Biomass density

The overall density of the sycamore blocks used during the study were determined by measuring the exact of dimensions and masses of 35 blocks ranging from sizes 3×3×3 cm to 5×5×5 cm, and using Equation 3 resulting in an average density of 563 ±30 kg·m⁻³.

$$\text{Equation 3: Density, } \rho = \frac{\text{Mass of block (kg)}}{\text{Volume of block (m}^3\text{)}}$$

2.2 Pyrolysis methods

There are a wide range of fast pyrolysis reactor conformations, however the aim of this series of experiments was to minimise all other variables other than the method of providing heat to the sample, for this reason a fixed bed reactor conformation was selected. Since conventional and microwave heating apparatus are very difficult to directly compare, a microwave cavity was designed in the works of Mohamed Adam and Benjamin Shepherd to best mimic that of a fixed bed pyrolysis oven, but allow for the provision of different liquid and gaseous inerting media.^{86,102}

2.2.1 Gas inerted fixed bed conventional pyrolysis

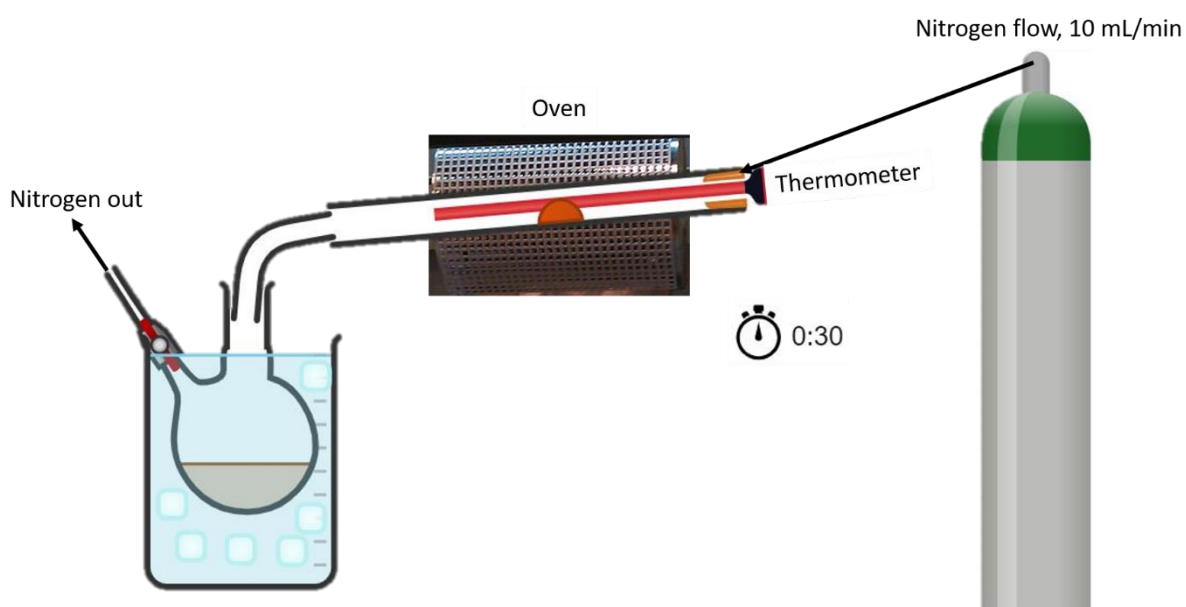


Figure 23 Experimental setup for gas inerted fixed bed conventional pyrolysis for pyrolysis liquid production through “fast pyrolysis” where sample residence time is low and reaction temperature is higher

Gas inerted fixed bed conventional pyrolysis consisted of biomass sample inside inclined (10°) quartz tube insert inside Gray-King tubular furnace at a constant temperature of 1000°C . Nitrogen gas flow throughout the experiments was 5 mL/min and sample was purged for 5 minutes prior to insertion. Insertion of sample tube into furnace was treated as T_0 and pyrolysis continued for 30 seconds, or until internal thermocouple reached 700°C . Tube containing sample was removed and allowed to cool to room temperature under ambient conditions. Pyrolysis liquid was collected *via* cold trap (-5°C). Experimental setup is visualised in Figure 23.

2.2.2 Microwave tuning

Optimal tuner settings were determined before performing any pyrolysis experiments. Cold matching at room temperature was carried out by using a vector network analyser (Rohde & Schwarz ZVL) and adjusting the stub and sliding-short positions to minimise reflected power. The vector network analyser sends signals through the waveguide and measures the magnitude and phase of the reflected signal. For the preliminary pyrolysis tests, the frequency of the generator for 0.5 – 1.8 kW applied power ranged from 2.453 – 2.457 GHz, and so reflected power over that range was minimised, as shown in Figure 24.

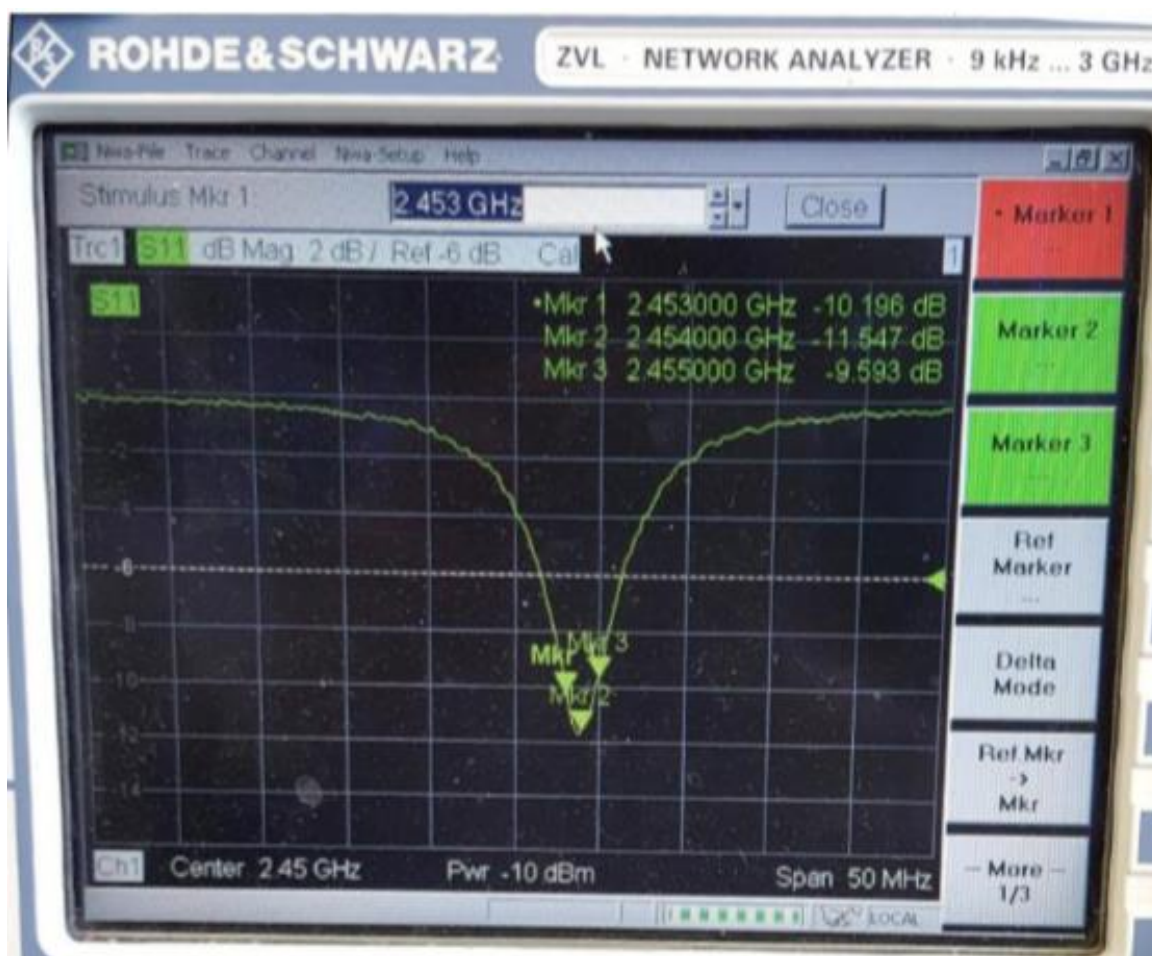


Figure 24 Vector analyser display outlining system microwave absorbance over generator frequency range. The minimum value shown on the display corresponds to sample absorbance maximum. Tuner stubs are adjusted to give symmetrical Gaussian curve at desired frequency. This means the maximum possible microwave energy is absorbed and the minimum amount of energy is wasted, when this is the case, the system is “matched” or “tuned” to the sample .

An automatic three stub tuner (S-TEAM STHD v1.5) was used to maximise the absorbed power and to log forward and reflected power.

2.2.3 Gas inerted fixed bed microwave pyrolysis

Microwave pyrolysis experiments were carried out utilising a 0 – 6 kW microwave generator at 2.45 GHz and a multimode cavity. Optimal tuner settings were determined before pyrolysis experiment. The Biomass block was placed in a 100 mm diameter flanged quartz beaker with a height 250 mm. The beaker was placed in a 240 × 240 × 300 mm reactor cavity. A flanged 100 mm lid was then placed on the beaker and connected within an electromagnetic choke to a condenser with a cooling surface area of 453 cm². The reactor cavity and choke were purged with 10 L/min nitrogen to maintain an inert environment in the event of quartz beaker failure. A schematic of the reactor for the experimental system is shown in Figure 25

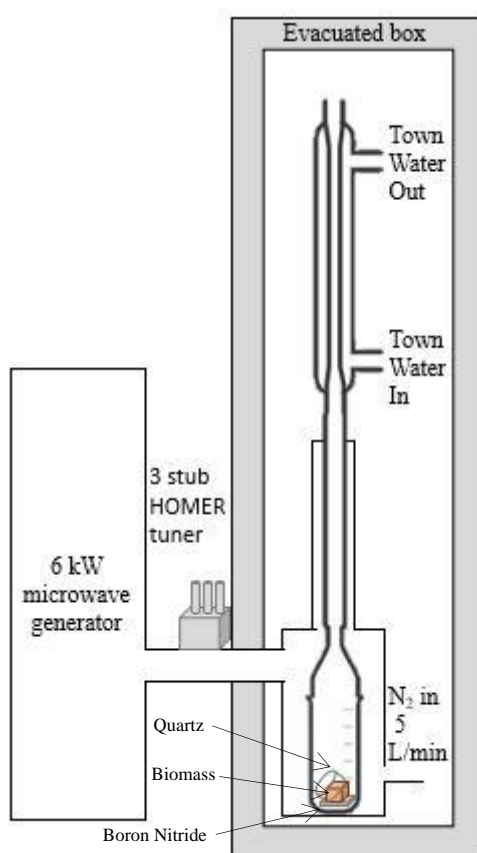


Figure 25 Schematic of fixed bed gas inerted microwave pyrolysis system. The microwaves are generated in the generator and pass along through the waveguide and through the tuner into the cavity. Inside the cavity there is a 5L/min N₂ flow over the sample and through the condenser. A quartz ring is added to prevent sample movement during reaction and provide consistency with liquid inerted experiments. When microwaves are applied to the sample they heat the sample to pyrolysis temperature, the pyrolysis liquid is formed and carried over the condenser by the flow of nitrogen, where it condenses and will eventually reflux back into the cavity.

2.2.4 Liquid inerted fixed bed microwave pyrolysis

Microwave pyrolysis experiments were carried out utilising a 0 – 6 kW microwave generator at 2.45 GHz and a multimode cavity. Optimal tuner settings were determined before pyrolysis experiment. The biomass block was placed in a 100 mm diameter flanged quartz beaker with a height 250 mm and covered with 1000 cm³ solvent (cyclohexane, 2-propanol and water). Biomass is less dense than solvent, to prevent sample floating a quartz ring mass (252.67 g) was added. The beaker was placed in a 240 × 240 × 300 mm reactor cavity. A flanged 100 mm lid was then placed on the beaker and connected within an electromagnetic choke to a condenser with a cooling surface area of 453 cm². The reactor cavity and choke were purged with 10 L/min nitrogen to maintain an inert environment in the event of quartz beaker failure. A schematic of the reactor for the experimental system is shown in Figure 26.

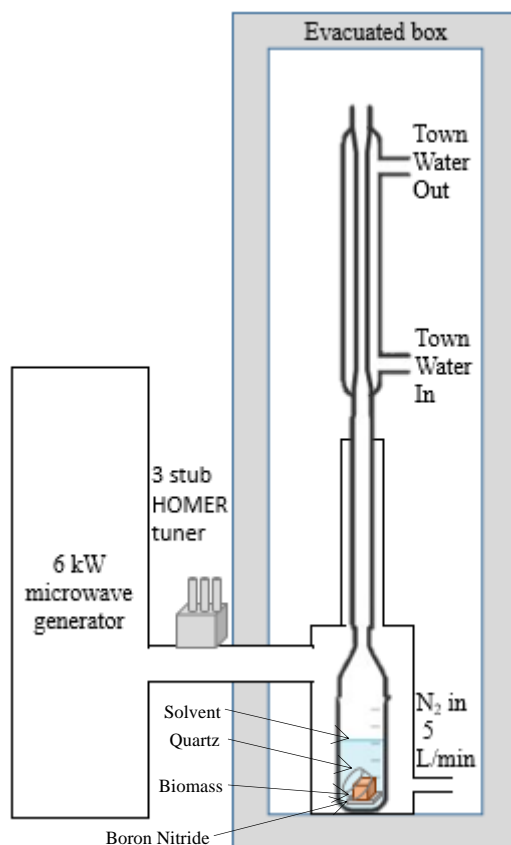


Figure 26 Schematic of Bench scale, Batch, Liquid microwave pyrolysis system. The microwaves are generated in the generator and pass along through the waveguide and through the tuner into the cavity. Inside the cavity there is a 5L/min N_2 flow over the sample/solvent and through the condenser this is to aid mass transfer and to reduce the chance of volatile solvent ignition. The sample is weighed down with a quartz ring to prevent the sample from floating on the surface of the solvent. A heavy, wide cylindrical shape was chosen in order to minimise the surface area of sample insulated from the solvent (for instance if a boron-nitride block is placed on top). The sample was noted to move during the reaction when less heavy quartz is used. When microwaves are applied to the sample they heat the sample to pyrolysis temperature, the pyrolysis liquid is formed and carried over the condenser by the flow of nitrogen and evaporated solvent, where it condenses and will eventually reflux back into the cavity. There is a notable change in colour of the solvent and a phase separation after reaction.

2.3 Pyrolysis calculations

2.3.1 Specific absorbed energy

The absorbed power could be quantified using the applied power and reflected power during pyrolysis (explained further in Sections 3.2.1 and 4.3.1) The specific absorbed energy was determined by numerical integration of the absorbed power:

$$\text{Equation 4: } E_s = \frac{\int P dt}{M}$$

Where;

P	Absorbed power (kW)
E_s	Specific energy (kJ·g ⁻¹)
M	Mass (g)
d_t	Time differential (s)

2.4 Pyrolysis liquid analysis

2.4.1 Gas-liquid chromatography mass spectrometry

Pyrolysis liquid samples were analysed by Gas-Chromatography Mass-Spectrometry (JEOL GCX 215 time-of-flight GC-MS; JEOL Ltd., Tokyo, Japan). Injection port temperature was 200 °C, splitless injection. Column, TG-POLAR (ThermoFisher Scientific, Massachusetts, USA) capillary column (30 m × 0.25 mm, 0.25 µm stationary phase). Helium carrier gas, 1.5 mL min⁻¹. Oven was heated from 40 °C (hold 3 min) to 260 °C at a rate of 5 °C min⁻¹. GC interface, 240 °C, ion source, 280 °C. Eluents ionized at 70 eV and their mass spectra recorded by the TOF-MS. The area percentage method was used for the quantification of the compounds present in the pyrolysis liquid.^{103,140} Identification was performed by comparing experimental mass spectra with those in the NIST Mass Spectral library (NIST14 database; National Institute of Standards and Technology, Maryland, USA). An example peak assignment is shown in Figure 30.

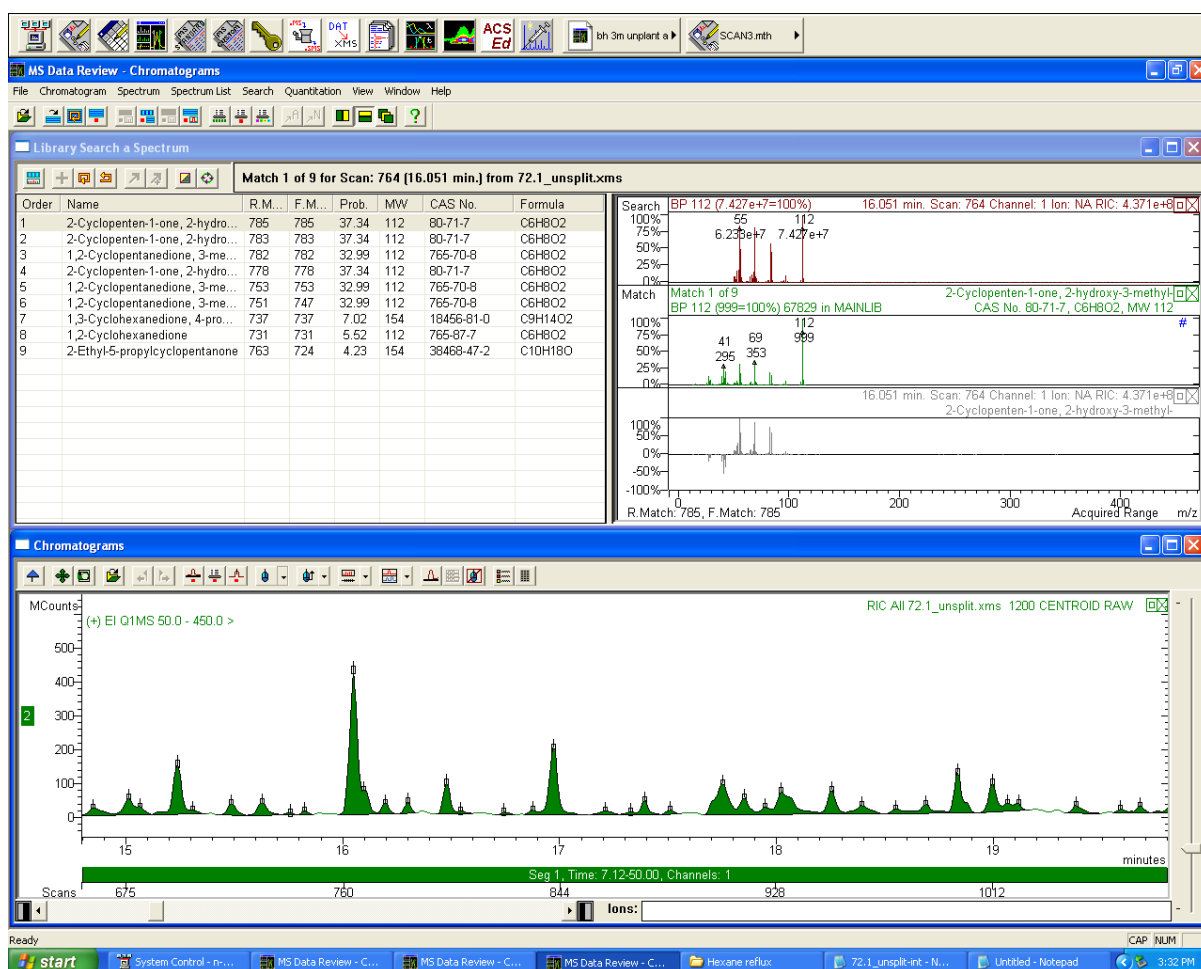


Figure 27 Example of spectra integration/peak assignment software. Zoomed in peak area of focus in the “Chromatogram” window, with mass spectral assignment list in top left and sample (red) NIST standard (green) and difference (grey) mass spectra shown in the top right. Note that the probability (prob) column is a calculation as a function of the overlap between sample/NIST.

In this study, individual GC peaks were integrated and identified following comparison to NIST standard. Individual compounds were grouped by the predominant functional group and this is presented as an area % for the functionalities; Acid, Ester, Alcohol, Aldehyde, Ketone, Furans and Sugars.

2.4.2 Magnetic resonance spectroscopy

The ^{31}P NMR data for the pyrolysis liquid and transesterifications were collected following the method and calculations outlined by NREL.⁶⁵ A stock solution was prepared by dissolving 10.90 mg of $\text{Cr}(\text{acac})_3$ and 72.28 mg of TPPO, internal standard, in 10 mL of a 1.6 : 1 pyridine : CDCl_3 solution. This solution was dried using 4 Å molecular sieves. A 20–30 mg sample of the material was dissolved in 0.4 mL stock solution, before adding 50 μL TMDP. The mixture was left to react for 30 minutes at room temperature before filtering through a 25 μm filter into the NMR tube. ^{31}P -NMR data was acquired, using AV 400 MHz cryoprobe spectrometer. The inverse gated decoupling technique was used with a 10 second delay time and 128 scans. Spectra were referenced in relation to the δ_{TPPO} peak at 27.91 ppm, $\delta_{\text{TMDP}} = 175.5$; $\delta_{\text{Aliphatic OH}} = 152\text{--}145$; $\delta_{\text{Aromatic OH}} = 145\text{--}138$; $\delta_{\text{Carboxylic acid OH}} = 138\text{--}134.6$; $\delta_{\text{Water dimer}} = 133.7\text{--}130$; $\delta_{\text{Water}} = 16.75$; and the comparison integral intensities were used for quantification, with reagent purity accounted for. Example spectra is shown in Figure 28 and example integral regions in Table 6.

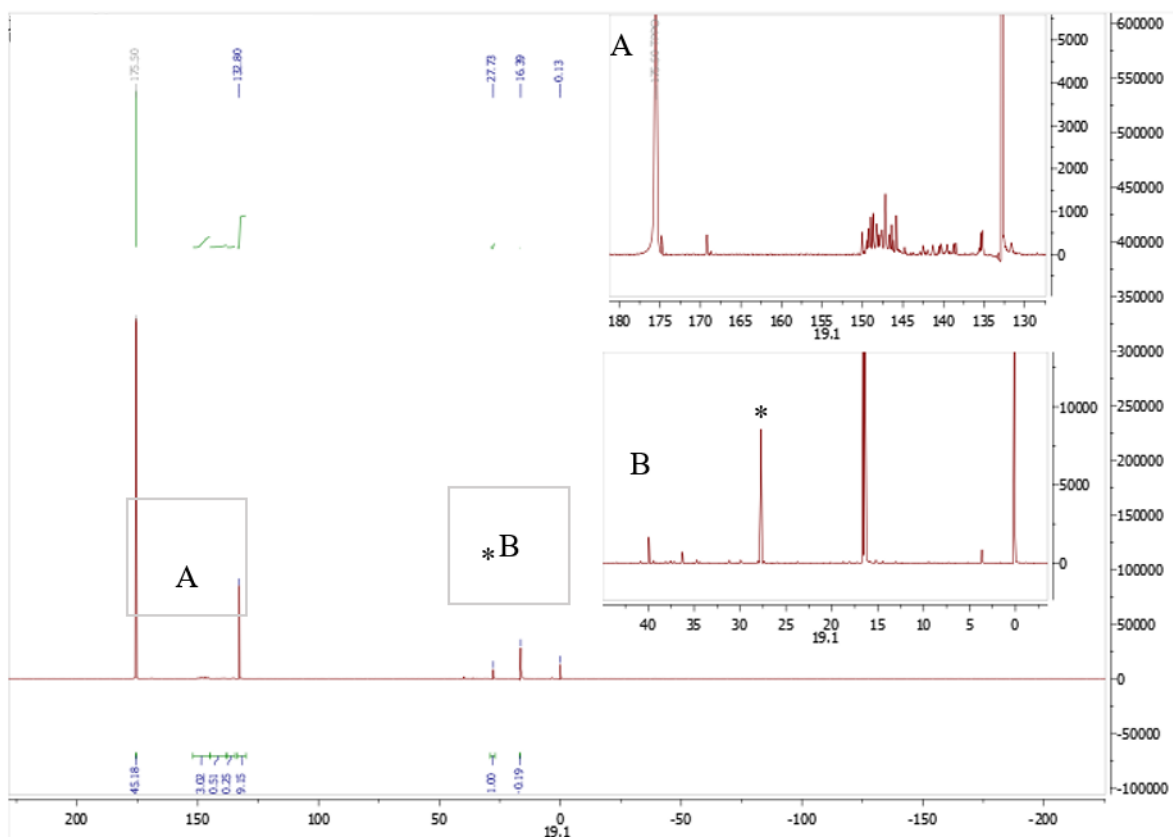


Figure 28 Example ^{31}P -NMR spectra. The peak marked with * is the peak for the TPPO used as integral reference for OH group quantification.

Table 6 Example pyrolysis liquid ^{31}P -NMR OH assignments, taken from empirical measurement.

Integral region (ppm)	Assignment
$\delta = 27.91$	TPPO
$\delta = 175.5$	TMDP
$\delta = 152-145$	Aliphatic OH - TMDP adduct
$\delta = 145-138$	Aromatic OH - TMDP adduct
$\delta = 138-134.6$	Carboxylic acid OH - TMDP adduct
$\delta = 133.7-130$	Water dimer - TMDP adduct
$\delta = 16.75$	Water- TMDP adduct

^1H -NMR of the polymers generated from the pyrolysis oils was conducted using a 400 MHz cryoprobe in acetone- d_6 . Magnetic resonance data analysis was conducted in Mestrelab Mnova 14.1.1.

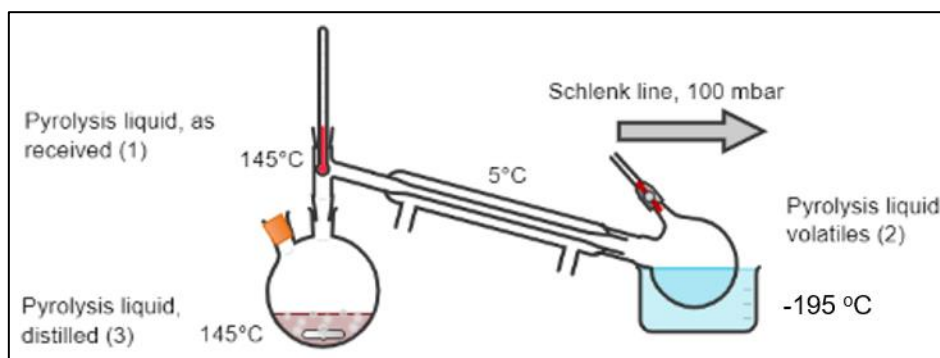
2.4.3 Karl Fischer titration

Moisture content of pyrolysis liquid and product streams were measured using a Mitsubishi CA-200 coulometric moisture meter. Samples above 0.5 wt% water were diluted with THF, with water content calculated as a weight fraction of the initial sample.

2.5 General method of producing polymer from pyrolysis liquid

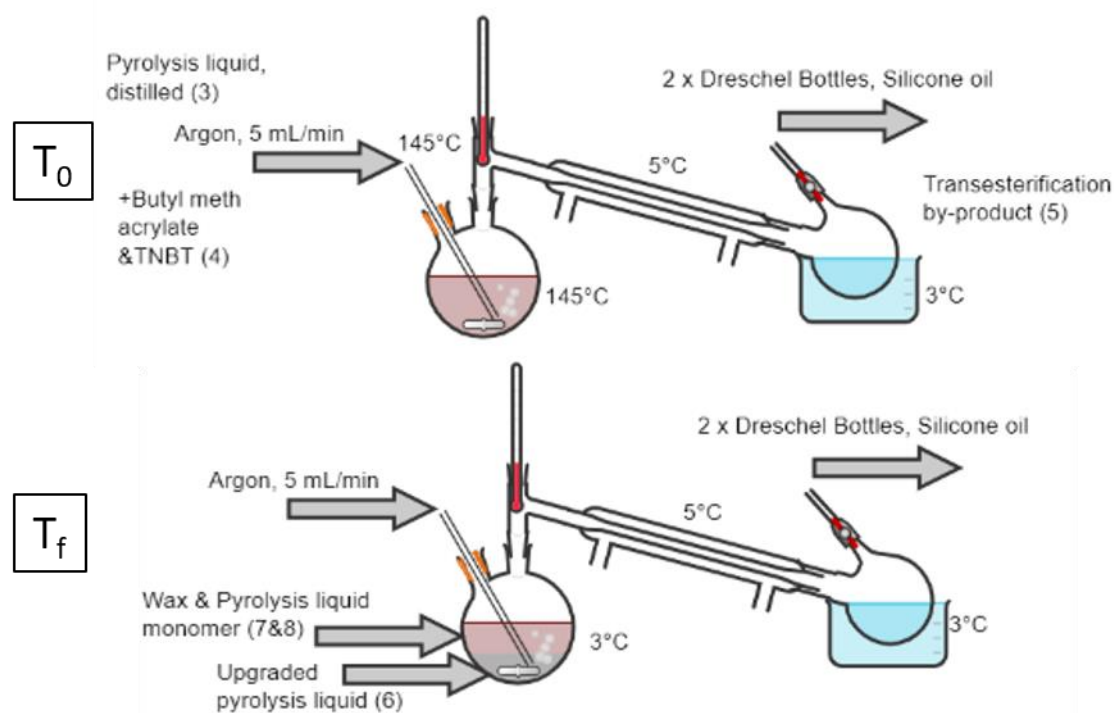
Below are optimised methods for producing methacrylate polymer from pyrolysis liquid, presented for reference, the development of these methods is the subject matter of chapter three.

2.5.1 Experimental setup and method for pyrolysis liquid drying



Pyrolysis liquid as received was added to a round bottom flask (RBF) in a Drysyn heating mantle at 145 °C. This was attached to a vacuum distillation head and trap, which was cooled to -195 °C to condense all vapours. Pressure was reduced to 100 mbar over a period of 20 minutes via a Schlenk line vacuum pump. Temperature was monitored in the Drysyn and still head. Aliquots of this distilled pyrolysis liquid and the distillate were set aside for subsequent analysis. Water content was confirmed by KF analysis prior to transesterification, and the drying step was repeated if more than 0.5% water was detected. Concentration of OH in the distilled pyrolysis liquid, was determined by ^{31}P -NMR, before addition of BMA. Ratios of 0.6, 1.2 and 2.4 were used in this work.

2.5.2 Experimental setup at T_0 and T_f and method for pyrolysis transesterification



The experimental setup, based on that used by Dundas *et al.*¹²⁷ consisted of a two-neck round bottom flask with Suba seal and vacuum distillation head, followed by dreschel bottles, to prevent gas backflow. Stirring and Argon sparge, 5 mL/min were begun 5 minutes prior to temperature increase. Temperature was measured in the oil bath, reaction vessel and still head. Addition of TNBT (0.6 mg, 0.0026 mmol) was treated as reaction start time (T_0). After reaction (T_f), the argon sparge and agitation were stopped and the mixture was then cooled to 3°C for one hour, where $T=145^\circ\text{C}$, phase separation was observed. The upper, clear brown liquid monomer was separated, into a vial, from the lower, highly viscous opaque brown, upgraded pyrolysis liquid.

2.5.3 Experimental method for functionalised pyrolysis liquid polymerisation.

In this study, AIBN (0.2 wt%) was added to the transesterified pyrolysis liquid products (1.78 g, 2 mL) in a sealed vial. The sample was degassed via "freeze pump thaw" three times and backfilled with Argon. The temperature was subsequently raised to 85°C in an oil bath and held for four hours with constant agitation. The reaction mixture was then allowed to cool to room temperature before the crude polymer was dissolved in approximately 5 mL acetone and precipitated into 600 mL of petroleum ether held at 0°C . The precipitation solvent was separated from the polymer by decanting it from the light brown solid, which was the polymer product. The precipitation was repeated and the resulting polymer was then dried under vacuum at 50°C and less than 10 mbar for 7 days.

2.6 Characterisation of pyrolysis liquid polymer

2.6.1 Thermogravimetric analysis (TGA)

TGA experiments were performed on a TA instruments Discovery Q500. 10 mg samples were passed through a 30 - 500 °C, 10 °C·min⁻¹ heating program under 5 mL·min⁻¹ of nitrogen flow.

2.6.2 Differential scanning calorimetry (DSC)

DSC experiments were carried out using a TA instruments DSC2500. 8 mg samples were subjected to a heating rate of 10 °C min⁻¹ from -90 °C to a maximum temperature established by sample decomposition temperature from TGA analysis. Two further cycles of heating and cooling were carried out.

2.6.3 Size exclusion chromatography

Data was generated using an Agilent 1260 Infinity multidetector GPC/SEC system with Agilent PL-gel mixed C column. Wyatt Optilab Multi Angle Light Scattering detector (MALS) and a differential refractometer (dRI) were used for sample detection. Each sample was dissolved to 1 mg·mL⁻¹ in THF and filtered (45 µm) prior to analysis. Where appropriate the d_n/d_c value of 0.087 mL·g⁻¹ was used to calculate molecular weight from light scattering, this is the value for BMA.

2.7 Polymerisation calculations

2.7.1 Transesterification yield

Transesterification yield was calculated by comparison of starting concentration of alcohol in pyrolysis liquid from ³¹P-NMR with experimentally observed moles of butanol distilled.

2.7.2 Polymerisation yield

¹H-NMR of the polymers generated from the pyrolysis oils was conducted using a 400 MHz cryoprobe in acetone-*d*₆. Magnetic resonance data analysis was conducted in Mestrelab Mnova 14.1.1. Example polymer spectra shown in Figure 29.

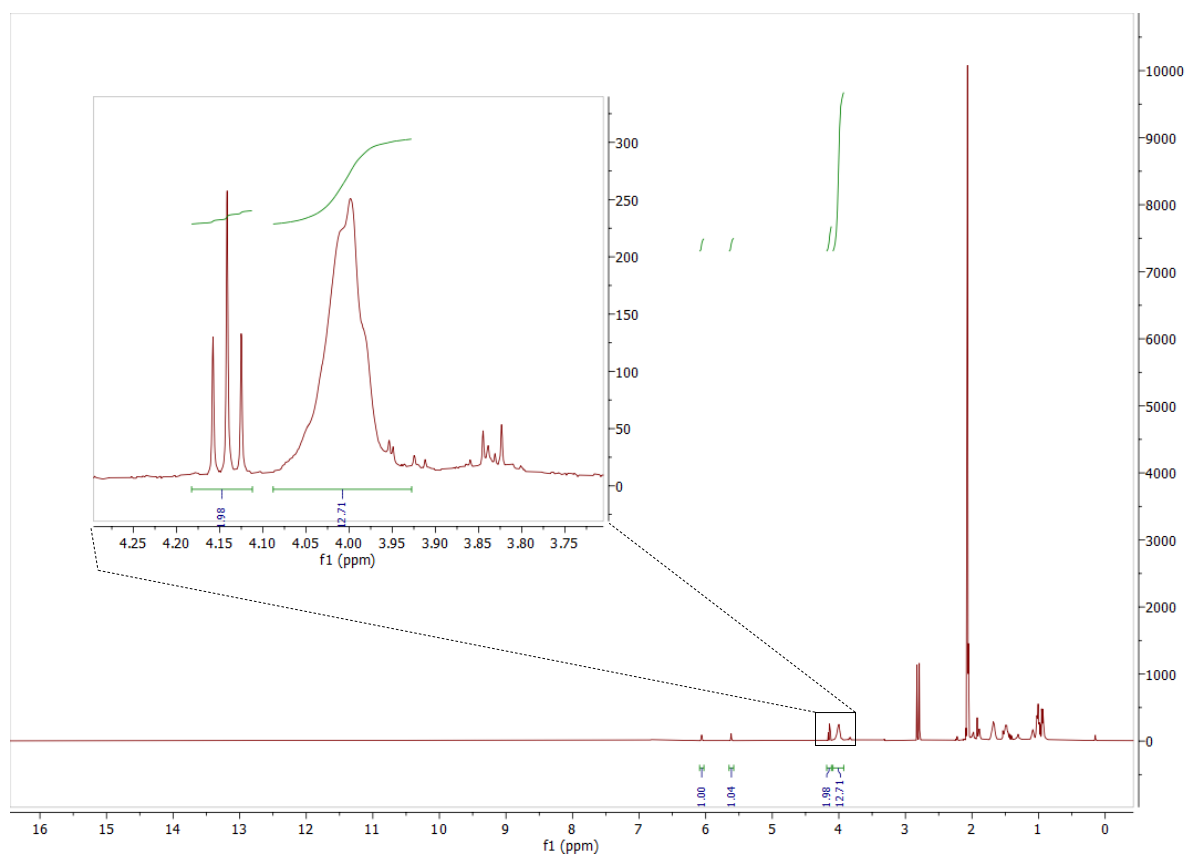


Figure 29 ^1H -NMR polymerisation yield example spectrum

Conversion was calculated by proton peak change in chemical environment. Note that there are 4 CH proton equivalents in the broad peak at 4.00 and two in the triplet at 4.15.¹⁴¹

$$\text{Conversion (\%)} = \frac{[P]}{[M] + [P]} \times 100 = \frac{\left(\frac{12.7}{4}\right)}{\left(\frac{1.98}{2}\right) + \left(\frac{12.7}{4}\right)} \times 100 = \frac{3.175}{4.175} \times 100 = 76\%$$

Chapter 3. Upgrading pyrolysis liquid with polymerisation *via* transesterification

This chapter contains results and discussion also presented in a published article in the RSC Reaction chemistry and engineering journal.¹⁴² Prior to each individual subsection is a mind map outlining the experimental rationale.

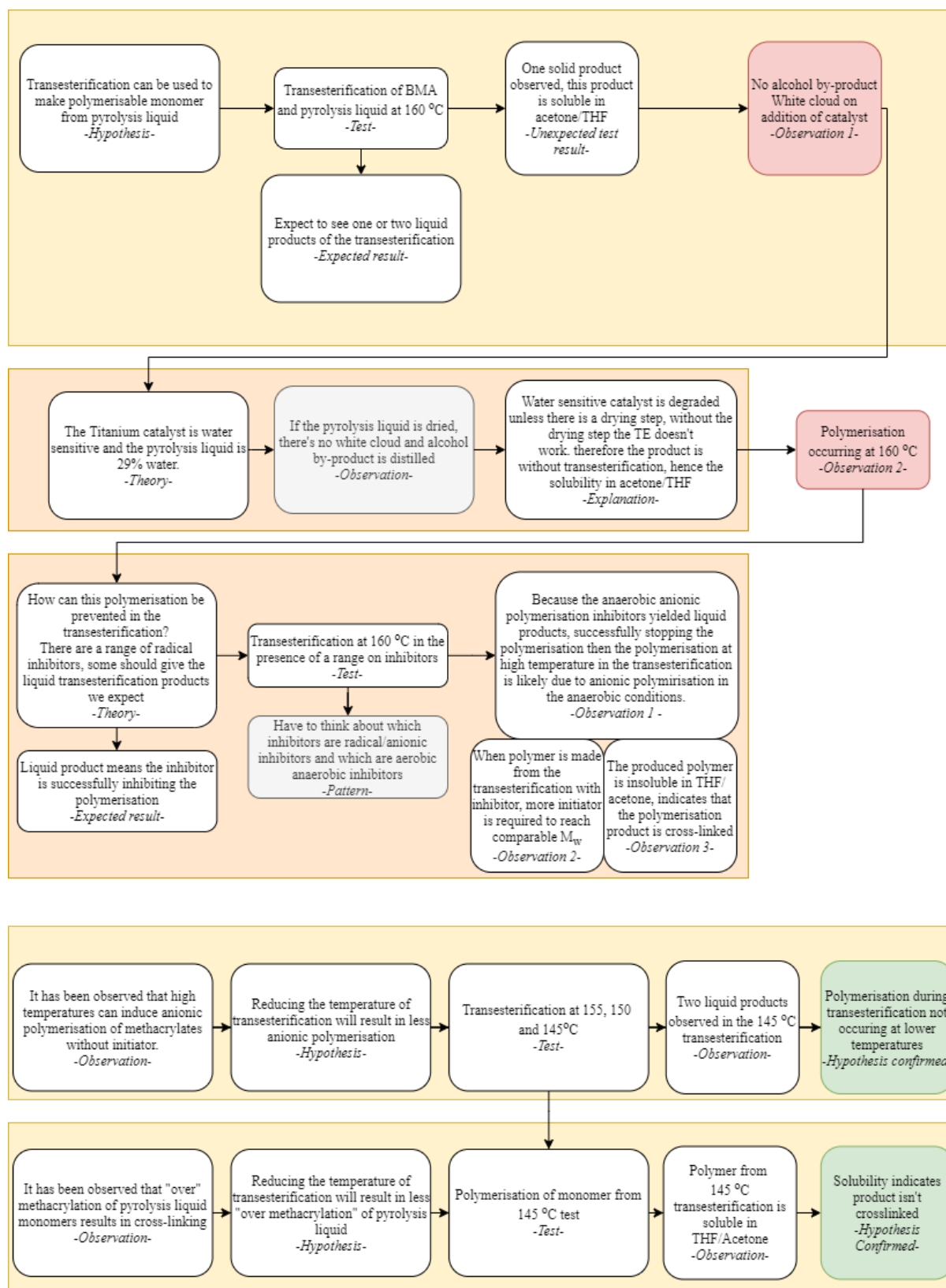
3.1 Setting the scene

Pyrolysis is a technology that has repeatedly sparked interest in response to the volatile crude oil market and rising fuel prices. By heating biomass in the absence of oxygen to temperatures between 350 and 700 °C an alcohol rich liquid can be produced, the temperature and time, along with other variables outlined in the introduction can affect the product distribution. Pyrolysis liquids age over time resulting in: higher molecular weight products, phase separation and decreased pH; all of which are widely considered to be disadvantages for use as a fuel. This chapter proposes that instead of trying to change or work around the properties of pyrolysis liquid, one could take advantage of them to yield interesting new high molecular weight materials. This chapter aims to outline the initial attempts to obtain these materials and is structured in two main parts, as the process involves two distinct but fundamentally linked chemistries; firstly, the transesterification and then the polymerisation.

3.2 Transesterification of pyrolysis liquid

Building on the work by Bai and Epps on the methacrylation of model pyrolysis liquid compounds and purified pyrolysis liquids, the method of transesterification was applied in the hypothesis that it is a more robust and industrially applicable process.^{110,111,122–124}

Below is a brief executive summary of the thought process from hypothesis to test and results rationale for the method development of transesterification process. At this point in the process polymerisation is undesirable, as such different approaches to find the root cause of polymerisation and mitigate were employed. Where expected results are presented, this is an expected result if the original hypothesis was correct. Where “unexpected results” are seen this is where something that challenges the hypothesis were observed – typically followed by a revised hypothesis.



3.2.1 Preliminary pyrolysis liquid transesterification

The experimental setup for the preliminary transesterification of the BMA with crude pyrolysis liquid is outlined in Figure 30. The 500 mL round bottom flask (RBF) is where the reaction takes place, with through flow of N₂ to aid removal of reaction vapours. Vapours rise and are condensed in the still-head, a standard distillation piece as opposed to a Claisen head as this showed no significant advantage. Headspace temperature is monitored with a thermometer in order to verify temperature of distillate, in the drying stage this will rise to 100°C and start to fall as not enough water remains in the sample to regulate the increased temperature, once catalyst is added this will rise a second time to 110 °C as Butanol is distilled

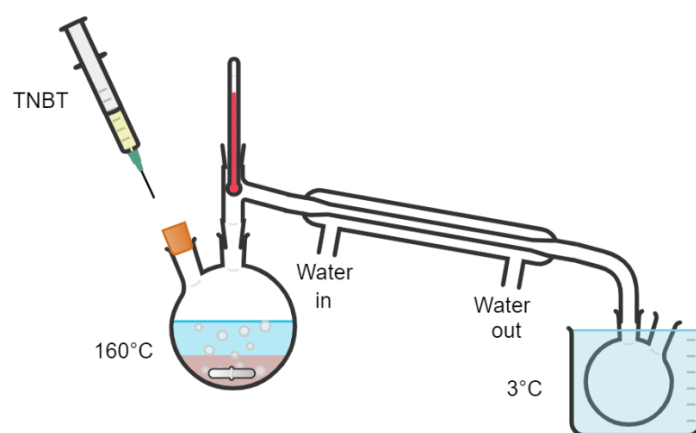


Figure 30 Experimental setup for the preliminary transesterification of the BMA with crude pyrolysis liquid.

BMA/pyrolysis liquid was heated to 160 °C prior to TNBT addition. It was expected that upon addition of the titanium catalyst there would be one or two liquid products left in the reaction vessel as well as one distilled alcohol by-product in the cooled round bottomed flask (RBF). What was initially observed upon addition of TNBT, was a white cloud, slight headspace temperature increase and a single solid product in the reaction vessel and no alcohol distillate determined by GC-MS. The solid product was soluble in acetone and THF and had a M_p of 95.2 kDa ($\pm 5\%$) suggesting that this reaction gave a high molecular weight product. The solubility suggested that this product was not cross-linked, as polymers where the linear polymer chains are bonded together in so called “cross-links” tend to exhibit swelling on contact with solvent as opposed to dissolution.

The results of this preliminary transesterification highlighted some distinct chemical observations:

1. There is no observed alcohol by-product.
2. Polymerisation was occurring spontaneously during transesterification.
3. This product is soluble in acetone.

The first point, the lack of distilled alcohol, can be linked to the initial observation of the white cloud, this was thought to be TiO_2 forming when the TNBT catalyst is exposed to water, later confirmed by XRD measurement to be the case, see Figure 31.

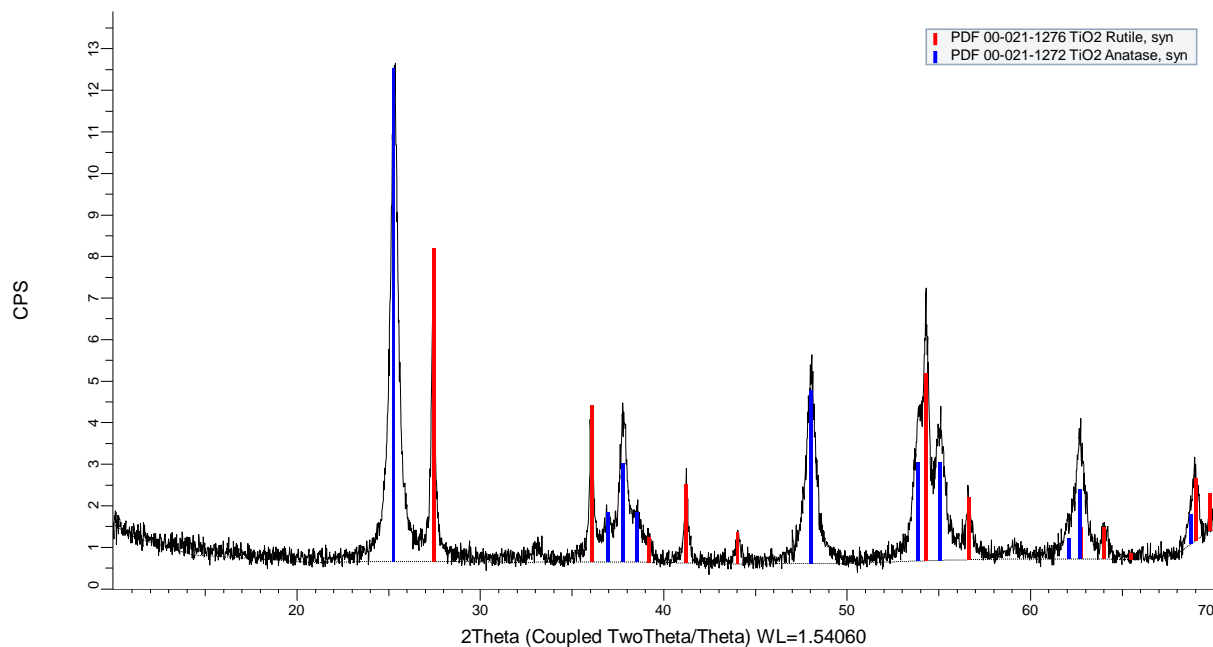


Figure 31 X-ray diffraction (XRD) pattern of the ash residue from the transesterification residue compared to values for Titanium oxide

This observation that the catalyst reacted to form a less active species coupled with the lack of distilled alcohol adds more weight to the conclusion that although a high molecular weight product was formed, the initial transesterification was unsuccessful. This was confirmed by ^1H -NMR when the polymeric product was found to be p(BMA), see Figure 32.

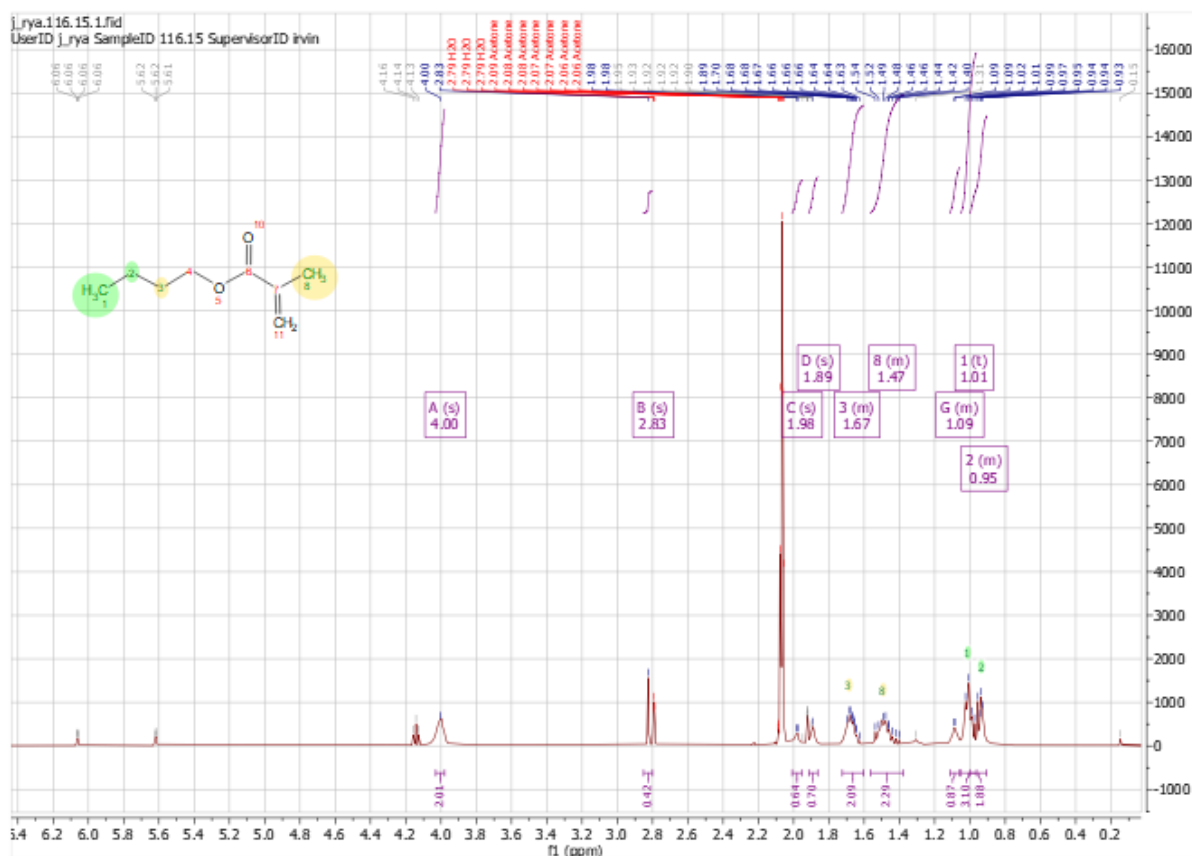


Figure 3 ^1H -NMR spectrum of butyl methacrylate polymerised in the presence of pyrolysis liquid, with carbons 1(1.0ppm 3H),2(0.9ppm 2H),3(1.7ppm 2H) & 8(1.5 ppm 2H) being assigned in the polymer structure, there is evidence of the cis/trans protons on carbon 11 at 5.7 ppm & 6.1 ppm indicating some unreacted BMA and the broad peak at 4.0 ppm is from carbon 4 in the polymer with the triplet at 4.1 ppm from the unreacted BMA .

The second point, spontaneous polymerisation, leads to the speculation that at 160 °C some polymerisation is occurring without the addition of a radical initiator suggesting that at this temperature some initiating radicals spontaneously form and propagate through polymerisation. The high molecular weight found suggested that the concentration of these radicals is quite low. The third observation, about the solubility in acetone, suggests that despite polymerisation occurring at higher temperatures there is no cross-linking as typically crosslinked polymers will “swell” in the presence of solvent and do not dissolve.

These observations allow for preliminary hypotheses to be drawn, that, in the presence of water, despite the elevated temperature, the transesterification does not occur. Without transesterification, polymerisation occurs rapidly and there is no crosslinking of product.

There are two questions immediately raised by the observations above:

1. Can this increase in molecular weight be prevented during the transesterification step?
2. Does water need to be removed? Or are there other water stable transesterification catalysts available?

In order to solve the problem of polymerisation occurring in the transesterification step, two parallel investigations were conducted: an investigation into polymerisation inhibitor addition, and reaction temperature reduction. A preliminary catalyst screening investigation was included to investigate the effect of water.

3.2.2 Cause of polymerisation during preliminary transesterification

In order to understand how the increase in molecular weight during the transesterification can be prevented, we must first understand the root cause. Is the increase in molecular weight due to the addition of methacrylate monomer? Or due to the pyrolysis liquid? It was initially thought that the increase in molecular weight was due to the presence of BMA and the formation of radicals initiating polymerisation at increased temperature. To test this, control reactions of neat BMA and pyrolysis liquid were run under the same conditions as the transesterification, to investigate any increase in molecular weight. Note that this increase in molecular weight is purely due to the increase in temperature in the transesterification step; there is no addition of initiator.

This data, in Table 7, shows that upon reaction temperature increase there is a significant increase in molecular weight for BMA and a similar but smaller increase for the BMA/pyrolysis liquid sample but no increase in the pyrolysis liquid control. If these increases in molecular weight are compared with the GPCs from before and after transesterifications, shown in completeness in Figure 33 a & b and most obvious from Figure 33 c & d, it is clear that there is no high molecular weight peak, labelled peak 3 in Figure 33d, before the increase in temperature and this peak does not appear, even at higher reaction temperatures in the control pyrolysis liquid sample. This suggests that the polymerisation during the transesterification is mainly due to the presence of BMA and therefore most likely follows a radical mechanism.

Table 7 Peak molecular weight and dispersity values for preliminary pyrolysis liquid polymers and neat BMA and PL transesterifications. Note that peaks are numbered in molecular weight order from low to high, peak numbering is outlined in Figure 33 (d). Note that the uncertainty in molecular weight measurement was $\pm 5\%$.

Composition	Number of peaks	Peak 1				Peak 2				Peak 3			
		M _p (kDa)	M _n (kDa)	M _p (kDa)	Dispersity	M _p (kDa)	M _n (kDa)	M _w (kDa)	Dispersity	M _p (kDa)	M _n (kDa)	M _w (kDa)	Dispersity
BMA control (T ₀)	1	<1	<1	<1	1.48	-	-	-	-	-	-	-	-
Pyrolysis liquid control (T ₀)	1	-	-	-	-	5.3	6.3	6.4	1.0	-	-	-	-
BMA & pyrolysis liquid control (T ₀)	2	<1	<1	<1	1.48	5.3	6.3	6.4	1.0	-	-	-	-
BMA control (T ₁₂₀)	1	-	-	-	-	-	-	-	-	22.6	10.0	25.8	2.58
Pyrolysis liquid control (T ₁₂₀)	2	-	-	-	-	5.3	6.3	6.4	1.0	-	-	-	-
BMA & pyrolysis liquid control (T ₁₂₀)	3	<1	<1	<1	1.48	5.3	6.3	6.4	1.0	95.2	55.0	95.0	1.73

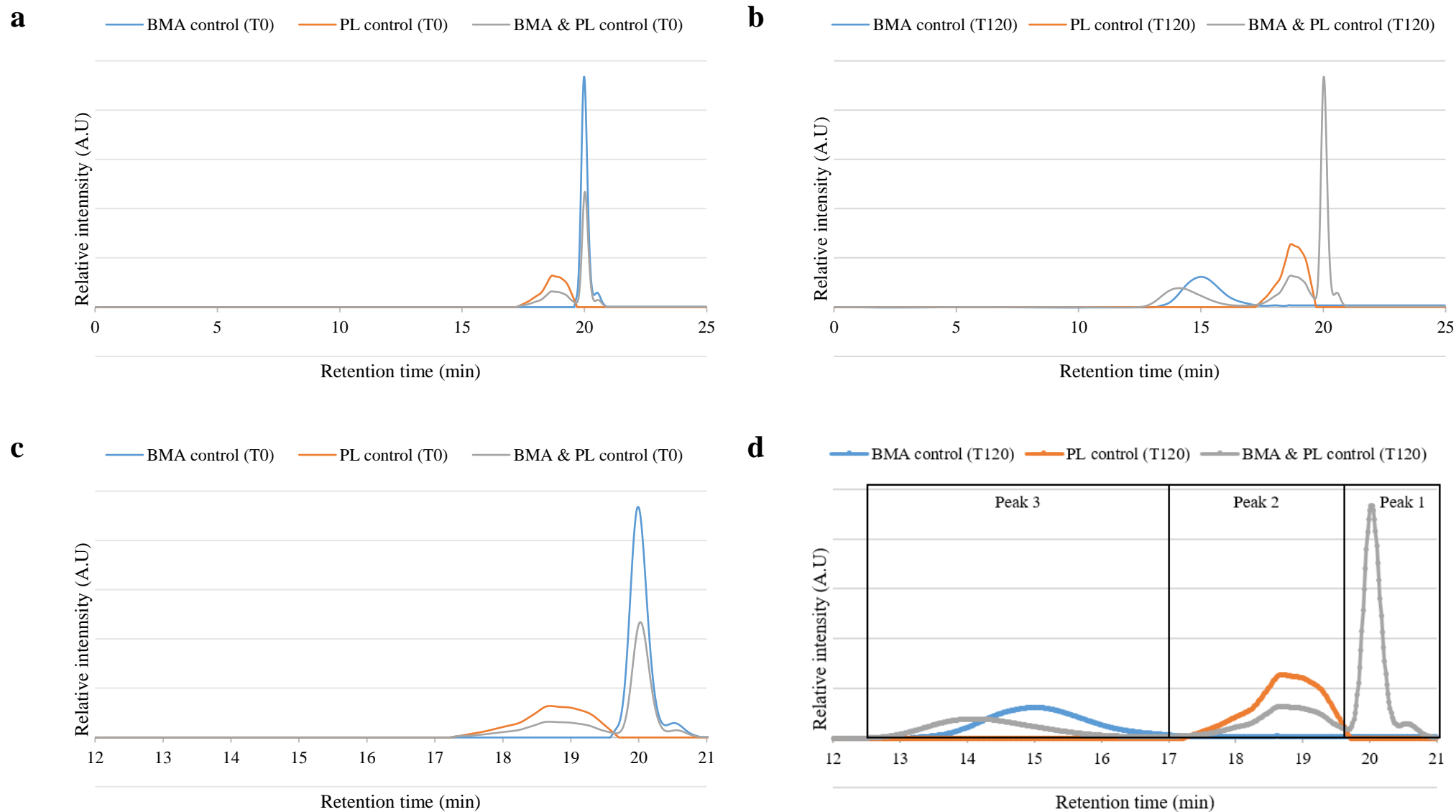
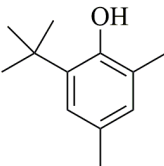
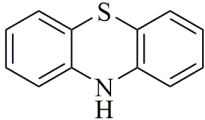
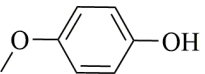
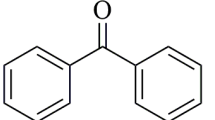
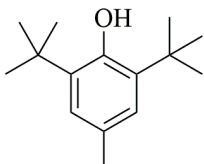
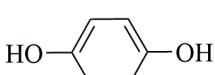


Figure 33 Size exclusion chromatogram of control BMA, Pyrolysis liquid and BMA/ Pyrolysis liquid transesterifications before (a) and after (b) temperature increase with magnified SEC's before (c) and after (d) temperature increase for 120 minutes.

3.2.3 Inhibitor addition to transesterification

In order to prevent this suspected radical polymerisation during the transesterification step, different types of radical inhibitor were added to the transesterification reaction. There are different inhibitors for radical polymerisations compared with other types of polymerisations, as well as some that only work in the presence of oxygen (aerobic) inhibitors.^{143,144} Despite the fact that transesterification took place under argon, there was no specific degassing step prior to transesterification so these aerobic inhibitors were included. There are a range of potential inhibitors, effective in methacrylate stabilisation, shown in Table 8.

Table 8 Radical inhibitors considered for transesterification

Chemical name	Structure	I/M adduct (t_0)	I/M adduct (t_{240})	Colour changes
2, tertbutyl 4-6— dimethyl phenol (Topanol A)		0.03	0.05	Yellow to orange
Phenothiazine (PTz)		Insoluble in BMA	Insoluble in BMA	Solution colourless, no change (yellow solid)
Mequinol (MEHQ)		0.01	0.08	Colourless to red
Benzophenone		0.18	0.18	Yellow, no change
Butylated hydroxytoluene (BHT)		0.05	0.12	Colourless to Pale yellow
Hydroquinone		0.07	0.40	Colourless, no change

Inhibitors interact with monomers to form complexes visible in the ^1H -NMR spectra as separate peaks. These adduct peaks are neither present in the spectra of the neat inhibitor nor monomer, hence the presence of an adduct means that both the monomer and inhibitor molecule are not available for reaction which may lead to lower yields. An example ^1H -NMR spectrum is shown in Figure 34.

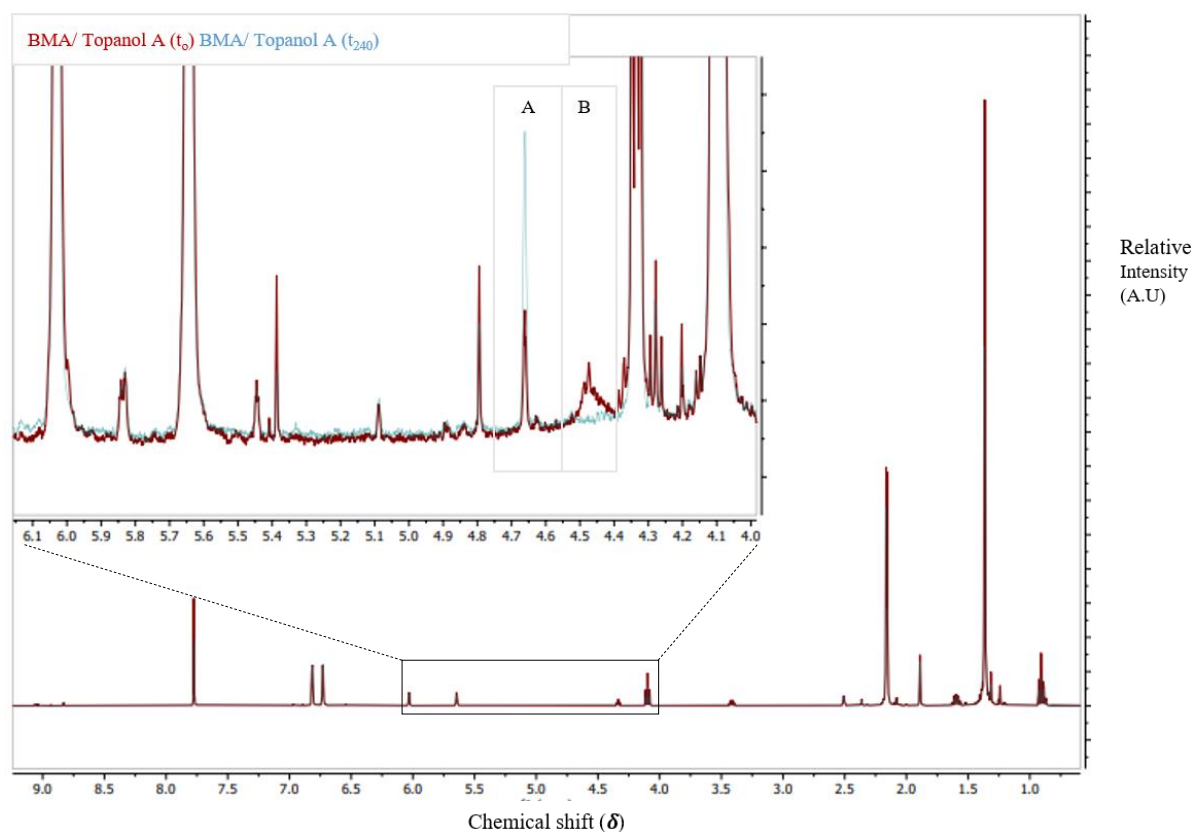


Figure 34 ^1H -NMR spectra of BMA/Topanol before (red) and after (blue) a simulated transesterification (160 °C, 4 hours). Showing a decrease in the peak at 4.5 ppm and an increase at 4.7 ppm.

Adducts in this experiment were deliberately generated using a 1:1 mass ratio of inhibitor to monomer and heating in a sealed vial at 160 °C for four hours to simulate the transesterification conditions. These concentrations far exceed those typically used in reaction, ~200 ppm; the higher concentrations were used to exaggerate the presence of adducts. The ratio of the ^1H -NMR adduct peak to the monomer peak protons was used to approximate concentration. Adducts displayed different chemical shifts dependant on the inhibitor structure. ^1H -NMR spectra recorded after initial mixing show the presence of adduct in all cases, suggesting that the adduct formation can occur very quickly. Peak A in Figure 34 seems to increase over the period of the transesterification where B seems to disappear, this suggests that there is a change in the nature of the interaction between inhibitor and monomer over time at increased temperature. An increase in adduct concentration after 240 minutes was seen in all but one sample. This suggests that the reaction conditions can have an effect on adduct formation, as the ^1H -NMR spectra look different before and after reaction and therefore reaction temperature should be considered when selecting an inhibitor. Colour changes also occurred, typically moving from colourless to yellow to orange to red, indicating an increase in the frequency of light being absorbed by the chromophore as the observed frequency of light was of lower frequency. These colour changes would indicate that there is a bigger difference between LUMO and

HOMO in the aromatic system indicative in a decrease in the number of electrons in the delocalised system of the molecular chromophore.¹⁴⁵ This observation is consistent with the mechanism of action of these anaerobic and aerobic inhibitors, shown in Figure 35 and Figure 36 respectively.

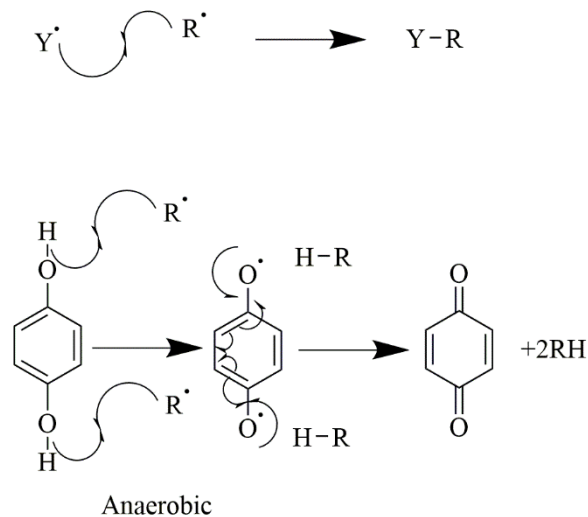


Figure 35 Mechanism of anaerobic radical inhibition. With general scheme shown above where Y= anaerobic inhibitor.

More detailed mechanism for quinone shown in the lower scheme.^{144,146}

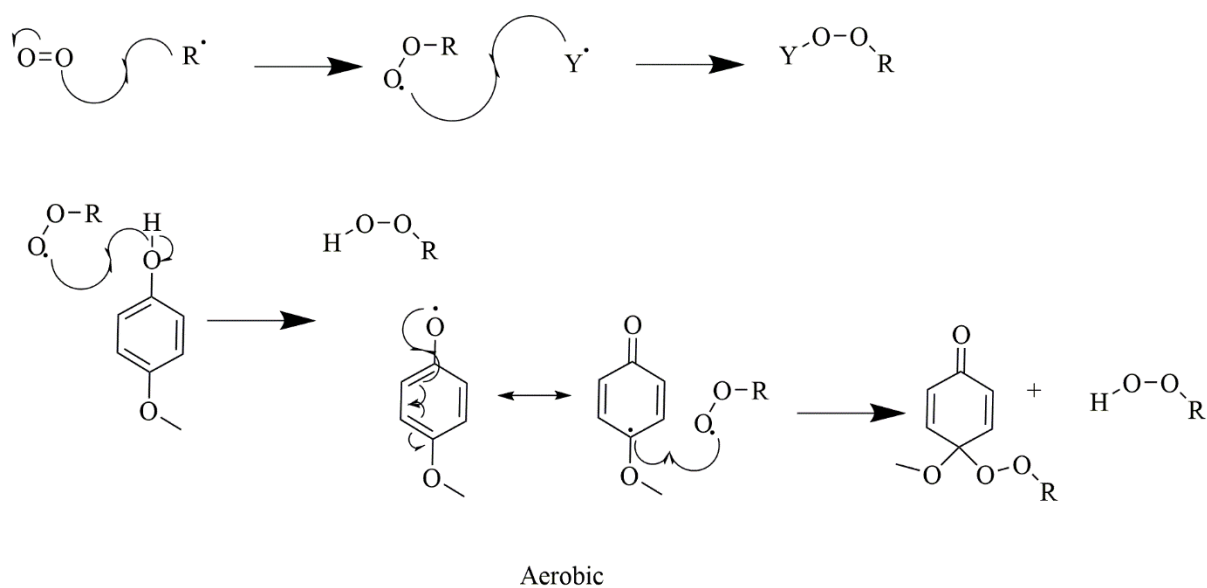


Figure 36 Mechanism of aerobic radical inhibition. With general scheme shown above where Y= aerobic inhibitor. More detailed mechanism for mequinone shown in the lower scheme.^{144,146}

This suggested that where a colour change is observed, radicals are being created and quenched by inhibitors. A lack of colour change does not necessarily mean there is no active inhibition, as the change may be outside the range of visible light and could be further investigated by UV spectroscopy, though the UV absorbance of pyrolysis liquid itself may hinder this investigation. The presence of radicals could be confirmed further through the use of in-situ electron parametric resonance (EPR) spectroscopy.¹⁴⁷ Further investigation into this phenomena and direct confirmation and quantification of the effectiveness of each radical inhibitor in the context of methacrylate transesterification is a potential area for future investigations.

From the results in Table 8, it is clear that for use in this experiment with BMA, topanol A is the most appropriate inhibitor as there is the lowest difference between initial adduct concentration and final adduct concentration. This has the caveat that these “control transesterifications” were under an argon atmosphere potentially reducing the effectiveness of the aerobic inhibitors. If considering inhibitors for reactions, such as the manufacture of methacrylic acid, which typically include the presence of oxygen, then this may have an effect on adduct formation and an aerobic inhibitor may prove more effective.

From a process perspective, the addition of an inhibitor is not an ideal solution to polymerisation during transesterification, as although inhibitors are commonly added in a low concentration, they can be expensive and add extra process units for addition and removal post transesterification as well as quality control analysis as residual inhibitor will negatively impact subsequent polymerisation.

3.2.4 Water Effects

Titanium butoxide is water sensitive and degraded to the less catalytically active titanium dioxide on contact with water. Pyrolysis liquid as received was 29wt% water, by Karl fischer (KF) titration. There were two possible solutions, either a less water sensitive transesterification catalyst is used, or the water is removed prior to TNBT addition. Zr, Sn and Zn based catalysts were considered in combination with topanol A inhibitor, shown in Table 9.

Table 9 Transesterification catalyst screening with the addition of Topanol A to prevent onset of polymerisation.

Catalyst	Pre-TE [OH] (mmol/g)	Post TE [OH] (mmol/g)
None	35	32
Sn(Oct) ₂	35	24
ZrOAc ₂	35	25
ZnOAc ₂	35	31
TNBT	35	28

The fundamentals of the transesterification reaction require removal of the alcohol reaction product during the reaction, to drive the position of equilibrium to the product. Ideally the reaction temperature should be below the boiling point of reactants, and above the boiling point of any by-product, in order to drive off the by-products and retain the product and reactants in the reaction vessel. The chemical origin of this is down to the competing forward and backward transesterification mechanisms shown in Figure 37.

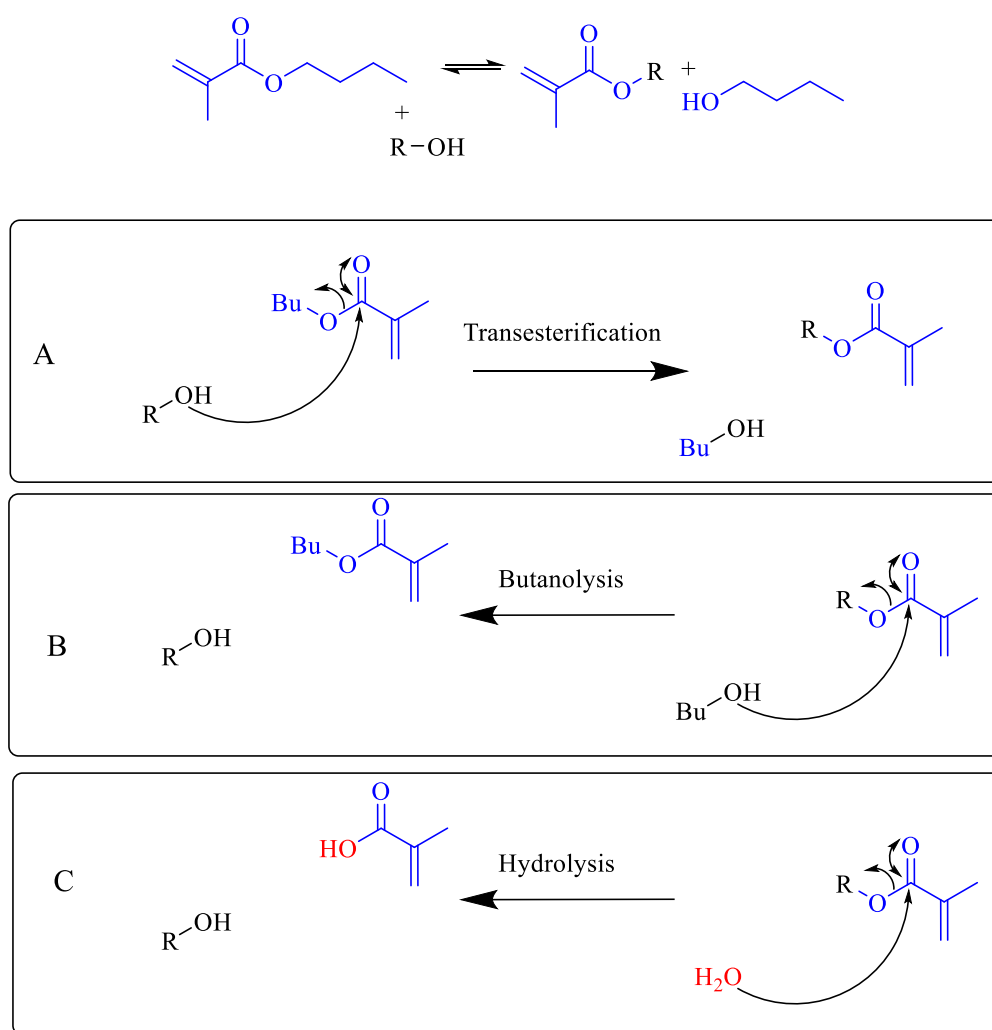


Figure 37 General transesterification reaction with mechanisms for forward transesterification (A) and backward hydrolysis reactions with butanol (B) and water (C). Where $R-OH$ represents an alcohol species

Reaction C in Figure 37, shows that water will eventually have to be removed from the reaction, regardless of catalyst choice, in order to fully drive the equilibrium to the products. This accounts for the reduced effectiveness of the Zr and Zn based catalysts when compared to the dried TNBT transesterification, despite their lack of water sensitivity. For this reason, the removal of water prior to catalyst addition was considered a superior approach.

It was proposed that if water was removed prior to transesterification, there would be reduced deactivation of Titanium catalyst and the reaction would give higher yields as there would be a reduced amount of the backward hydrolysis reaction.

3.2.5 Temperature Reduction

Prior to transesterification, water and volatile pyrolysis liquid components were removed by vacuum distillation (145 °C, 100 mbar, 30 minutes). When a preliminary transesterification was conducted with distilled pyrolysis liquid at 160 °C, a significant quantity of brown, insoluble solid was produced during the reaction. The low OH content from ³¹P-NMR indicated that either the transesterification reaction was successful, or that alcohols were incorporated into the solid and hence unavailable for dissolution, functionalisation and so were not observed by ³¹P-NMR. The insolubility of the products suggest that crosslinking has occurred, due to the addition of multiple methacrylate groups to one molecule. Previous literature report using massive excess of acyl chloride achieved similar products and suggested that this crosslinking is due to complete methacrylation of OH groups in the pyrolysis liquid,¹²² see Figure 38 .

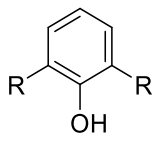
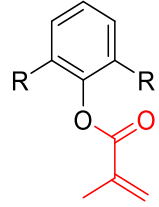
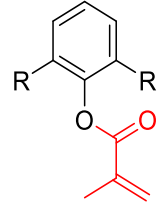
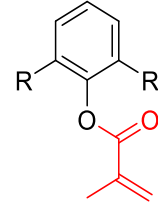
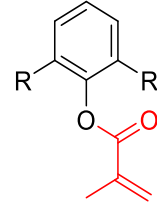
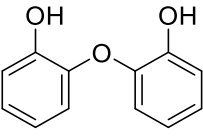
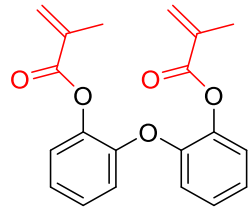
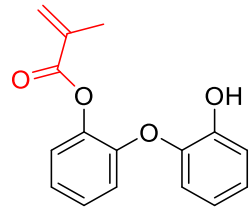
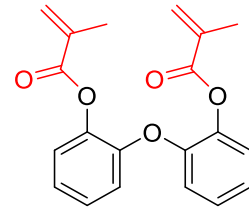
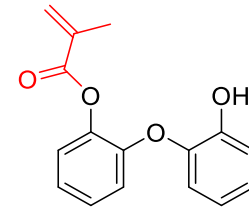
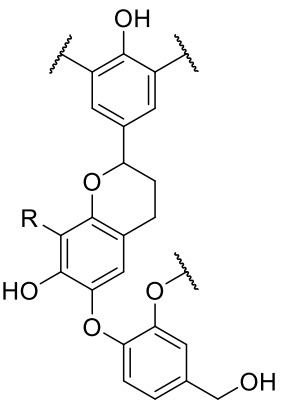
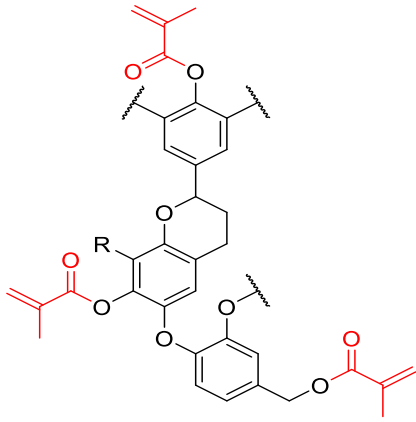
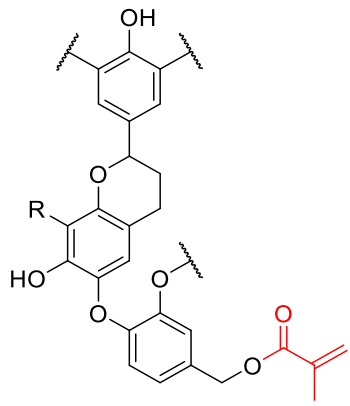
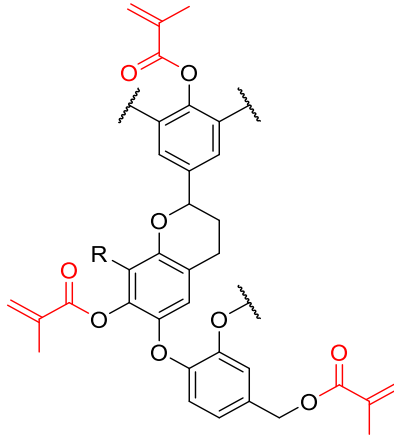
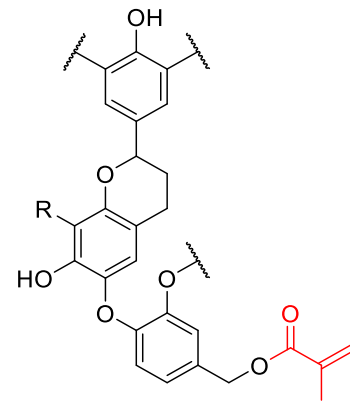
Number of OH groups per feed molecule, with representative diagram		Reaction Methacryloyl chloride to OH ratio (Room temperature, overnight, Dichloromethane (DCM))		Transesterification [1.2 BMA:OH], TNBT temperature (30 mins)	
		3.04:1	1:1	160 °C	145 °C
1	 $R=H, Me, OMe$				
2					
3					

Figure 38 Effect of stoichiometric excess of acyl chloride reagents on methacrylate content of products, adapted from¹²². Showing that an excess of acyl chloride can fully methacrylate all OH positions, as can increased temperature (160°C) transesterification. 1:1 acyl chloride gave similar degree of methacrylation as lower (145°C) transesterification.

It was suggested that reducing the degree of esterification could avoid this crosslinking; this was achieved with acyl chloride by reducing the stoichiometric excess.¹²⁵ It was hypothesised that a similar effect could be achieved in the transesterification through temperature reduction. A series of reactions was then performed to optimise the temperature at which the transesterification was conducted. It was demonstrated that by reducing the temperature, the amount of residual OH groups could be increased hence the degree of transesterification achieved was reduced.

Table 10 Comparison of established methacrylate transesterification temperatures for [OH] from ³¹P-NMR and observed time taken for sample to turn solid in minutes.

Temperature (°C)	Crosslink onset (minutes)	[OH] (mmol·g ⁻¹)		Degree of transesterification (%)
		t ₀	t ₁₂₀	
160	8	28.0	0	100
155	14	28.0	0.8	97
150	20	28.0	1.2	96
145	*	28.0	5.8	79

**denotes no solid onset observed.*

Table 10 shows that at lower reaction temperatures, as well as with a reduction in the degree of transesterification, the crosslink onset was delayed and at a reaction temperature of 145 °C this was avoided. Kinetic experiments, shown in Figure 39 show that there is no further decrease in OH content after 30 minutes. The reason why this reaction seems to stall at around 5 mmol is suspected to be due to large sterically hindered (tertiary) and unreactive alcohol groups. These are difficult to quantify by ³¹P-NMR as distinguishing 1°/2°/3° alcohols using this method done by empirical measurement of standards.

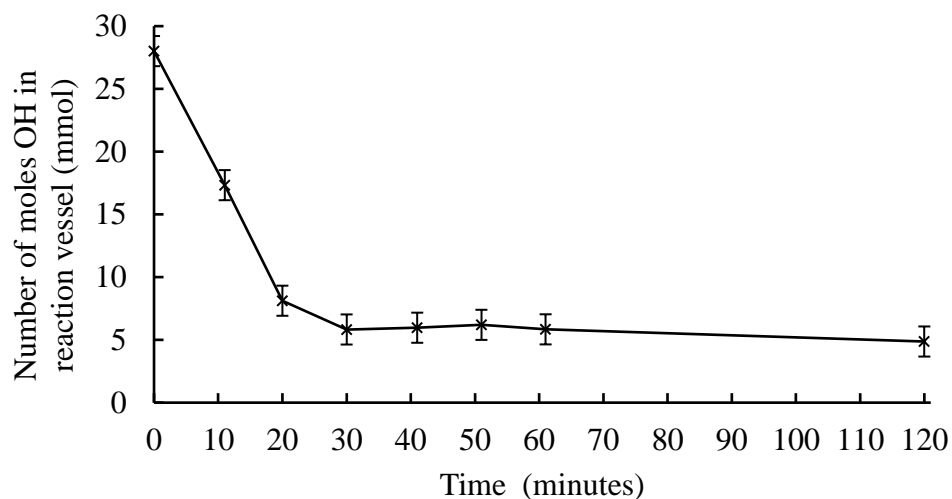


Figure 39 Decrease in hydroxyl content in the distilled pyrolysis liquid during the transesterification reaction at 145 °C along with transesterification reaction shown in the insert.

The concentration of alcohol was measured in the reaction vessel by ^{31}P -NMR along with the mass of Butanol (BuOH) by-product being removed by distillation throughout the reaction. Control reactions of distilled pyrolysis liquid and BMA with TNBT confirm that this decrease in $[\text{OH}]$ is due to transesterification reaction. Consequently, as conversion is less than 100% and an excess of BMA was added, there is unreacted BMA blended with functionalised pyrolysis liquid. This means that any polymer produced was likely a copolymer of BMA and pyrolysis liquid methacrylate monomers.

3.2.6 Catalyst screening

To confirm that Titanium butoxide (TNBT) was the optimum catalyst with the addition of pyrolysis liquid drying step, preliminary catalyst screening of some common transesterification catalysts was undertaken with results in Table 11.

Table 11 Effect of different catalysts on 145 °C transesterification of pyrolysis liquid. Note that the pyrolysis liquid was dried in one batch at 80 °C, 100 mbar, 30 mins and separated for the different experiments.

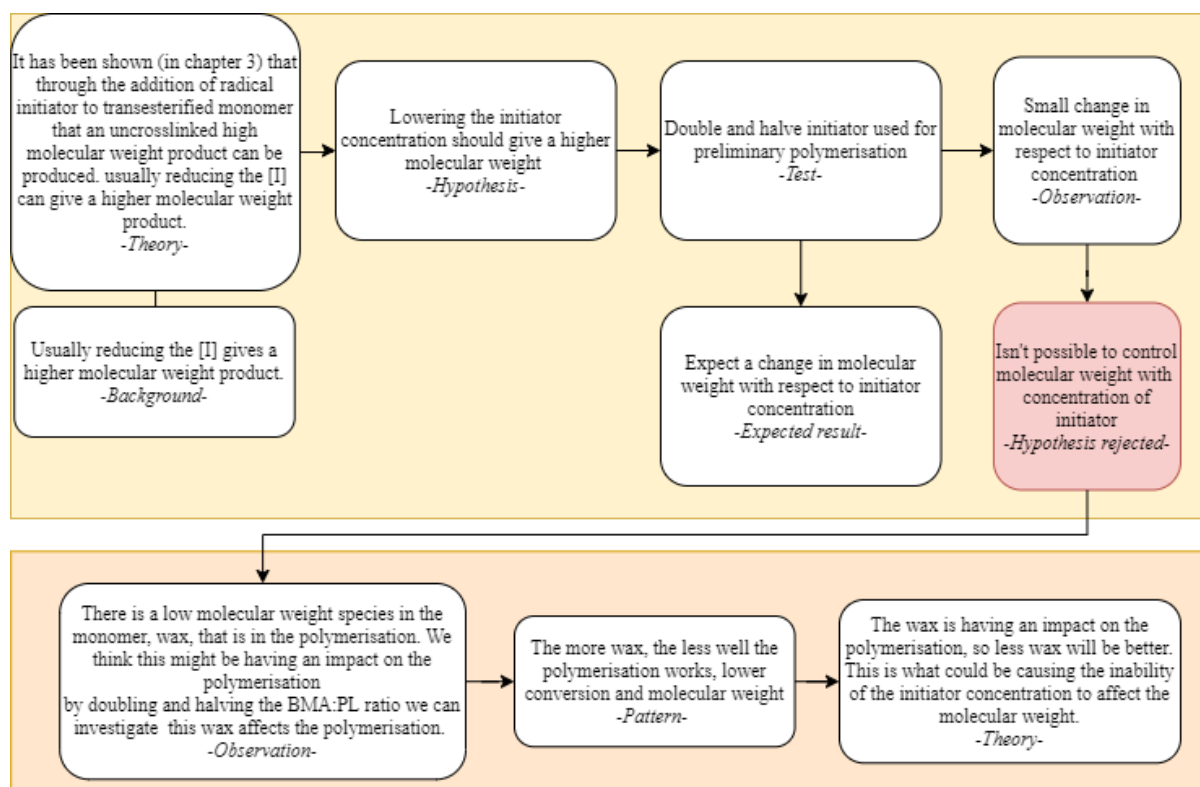
Catalyst	Pre-TE [OH]	Post TE [OH]	Degree of transesterification (%)
None	28.0	28.0	0
Sn(Oct) ₂	28.0	13.4	52
ZrOAc ₂	28.0	15.8	44
ZnOAc ₂	28.0	25.6	9
TNBT	28.0	5.8	79

The greatest difference in [OH] was observed when TNBT was used as a catalyst. This suggests that this is the most effective transesterification catalyst in this system when the pyrolysis liquid is dried. It is suggested that the Zinc based catalyst is a particularly ineffective catalyst in this system with a performance barely above control, probably due to the ZnOAc₂ only being sparingly soluble in the BMA/ Pyrolysis liquid mixture. This is observed as a light brown powder coating the inside of the round bottomed flask (RBF). There is still further potential for optimisation through the use of more specialist bespoke catalysts effective when pyrolysis liquid is wet and optimisation of the temperature for each of these potential catalysts however, this is a broad and promising area for future work.

This preliminary investigation shows that a drying step is necessary prior to transesterification in order to drive the reaction to completion and avoid catalyst deactivation. Different transition metal catalysts were screened with the most promising candidate identified. Temperature of the transesterification was reduced to avoid the early onset of polymerisation and this had the added benefit of reducing the degree of transesterification which avoids a crosslinked polymeric product.

3.3 Polymerisation of functionalised pyrolysis liquid

Below is a brief executive summary of the thought process from hypothesis to test and results rationale for the method development of the polymerisation of transesterified pyrolysis liquid. At this point in the process higher molecular weight is desirable, as such different approaches to find the root cause of unexpected behaviour with respect to initiator concentration were identified and mitigated.^{8,9,118,125,148} Where expected results are presented, this is an expected result if the original hypothesis was correct. Where “unexpected results” are seen this is where something that challenges the hypothesis were observed – typically followed by a revised hypothesis.



3.3.1 Initiator concentration

Since an optimised catalyst and reaction system for transesterification of pyrolysis liquid had been identified, investigation into the subsequent polymerisation of the transesterified pyrolysis liquid was undertaken with the functionalised pyrolysis liquid being used as the starting material for a free radical polymerisation. Typically with azo-based thermal initiators 1 mole of initiator will give rise to 2 moles of radicals. Since each radical is capable of initiating and propagating the polymerisation of a polymer chain the more initiator added to a reaction, the more radical chains will be formed. Hence, in a closed system each of those chains will contain a smaller fraction of monomer and will be shorter, the expectation is that as initiator concentration increases, the average chain length will be shorter and hence the molecular weight lower. The reason solvent is added to polymerisation is generally to lower the overall viscosity at higher conversion, the initial rate can be slower due to dilution but at higher conversion the rate should be higher and hence, usually, overall reaction yield will be higher. A secondary reason for the addition of solvent is to allow for better temperature control of the exothermic radical polymerisation, on larger scale this can lead to thermal runaway as the increased viscosity at higher conversions slows the dissipation of heat. The reaction scheme is outlined in Figure 40.

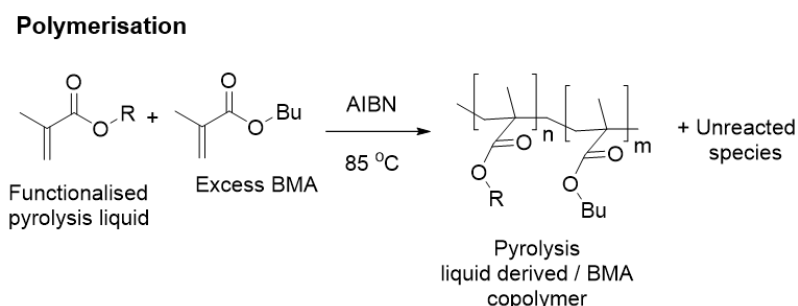


Figure 40 Polymerisation reaction scheme for radical polymerisation of a combination of functionalised pyrolysis liquid and unreacted excess BMA at 85°C using AIBN as a thermal radical initiator.

Concentration of radical initiator and presence of solvent (1:1%v/v) were varied. Conversion, M_p and polydispersity (\mathcal{D}) were compared, this data is shown in Table 12.

Table 12: Effect of initiator concentration and solvent on molecular weight of transesterified pyrolysis liquid polymer. Molecular weight determined by SEC and conversion by $^1\text{H-NMR}$.

Entry number	[AIBN] (wt%)	Reaction Type	Conversion	M_p (kDa)	M_n (kDa)	M_w (kDa)	\bar{D}
1	0.1	Bulk	71.6%	22.9	15.5	27.7	1.6
2	0.2	Bulk	77.3%	29.2	18.0	34.7	1.8
3	0.4	Bulk	85.7%	35.4	18.6	37.9	1.8
4	0.1	Toluene	nil	*	*	*	*
5	0.2	Toluene	30.6%	21.2	17.4	27.7	1.5
6	0.4	Toluene	77.9%	32.5	18.4	34.5	1.7

* indicates that no increase in molecular weight was observed relative to the control

Light scattering was used to calculate molecular weights and the refractive index increment (d_n/d_c) used was that of a BMA homopolymer, $0.087 \text{ mL}\cdot\text{g}^{-1}$. This assumption means that the generated molecular weights are likely only relatively correct as the structure of the pyrolysis polymer may not be a BMA homopolymer and so may have differing d_n/d_c values. The differences in polymer structure and molecular weight distribution likely affects M_n and M_w . As such, M_p was used in this comparison because of its lack of dependence on the distribution of the molecular weights in the sample. Increasing the initiator concentration was shown to result in an increase in conversion and peak molecular weight. For bulk polymerisations, M_p varied from 22.9-35.4 kDa and very low \bar{D} values were observed (*i.e.* below 2). Meanwhile, in toluene, the conversion and M_p were lower for the equivalent concentrations of initiator that had been used in the bulk reactions. However, very similar M_p and \bar{D} values were achieved when higher initiator concentrations were used. Lower conversions in solvent polymerisations compared to bulk reactions is not unexpected, however, the increase in molecular weight with respect to initiator concentration is unexpected. Representative Size Exclusion Chromatography (SEC) chromatograms for these materials are shown in Figure 41.

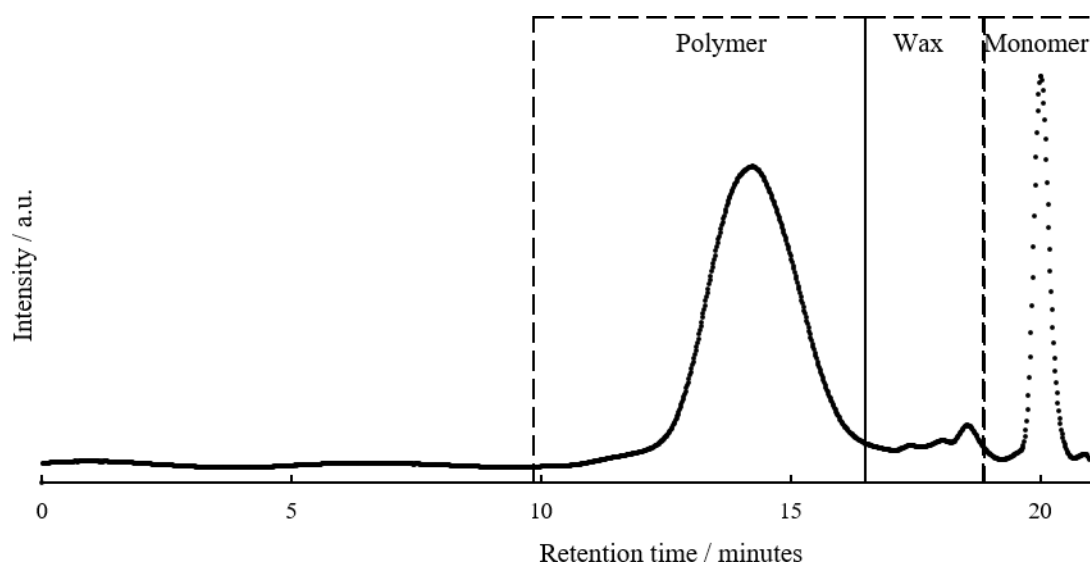


Figure 41 Size exclusion chromatograph of upgraded pyrolysis liquid prior to purification including annotation for pyrolysis polymer, wax and monomer peaks from left to right.

The pyrolysis liquid polymer number 3 was selected for further analysis owing to the highest conversion, molecular weight and T_g . The SEC chromatograms show that an additional molecular weight species is present in the polymer sample. A kinetic study of the evolution of the polymer peaks given in Figure 42 demonstrated that this material was present from the outset and did not increase during reaction.

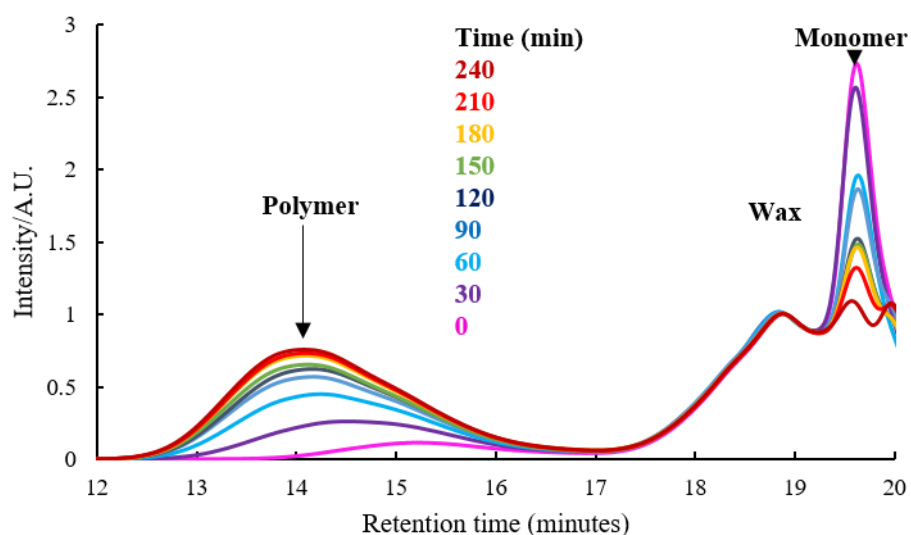


Figure 42 Time resolved size exclusion chromatography of pyrolysis liquid derived polymer polymerisation showing an increase in polymer peak, reduction in monomer and no change to the “wax” peak.

The only peaks noted to change during the reaction are the depletion of the monomer peak and the increase of a monomodal polymer peak. Thus, it is proposed that this additional peak may be an unreactive wax. The molecular weight of this wax, 0.5-2 kDa is similar to that of pyrolytic lignin. Additionally, the mono-modal nature of the polymer peak was unexpected. There is such a wide variety of alcohols present in the pyrolysis liquid that it was anticipated that their transesterification would have produced a wide range of different monomers with disparate levels of reactivity. A range of different polymers formed at different rates and resulting in different molecular weight products would give rise to a multi-modal size exclusion chromatogram, indeed looking at the molecular weight diagram, shown in Figure 43 there are several higher molecular weight species.

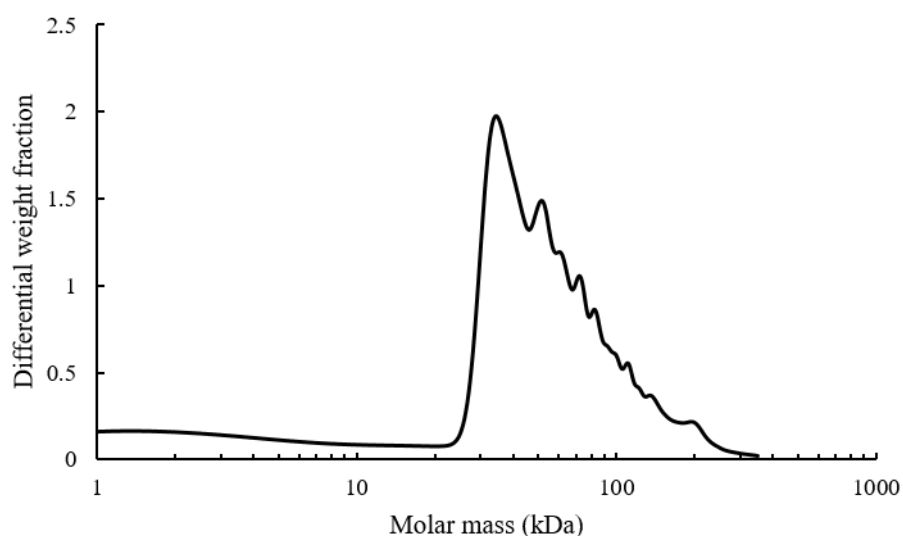


Figure 43 Molecular weight analysis of pyrolysis polymers using light scattering, d_n/d_c value of 0.087. Showing a minimum molar mass of 35 kDa with several higher molecular weight peaks up to 130 kDa

The effect of pyrolysis liquid concentration on the polymerisation was investigated further by varying the molar amount of BMA added to the pyrolysis liquid prior to transesterification. The stoichiometry and nomenclature used is provided in Table 13.

Table 13 Outline molar ratio calculations, the concentration of OH in pyrolysis liquid is 13.7 mmol g⁻¹ and molar mass BMA is 142.198 g mol⁻¹

BMA: pyrolysis liquid OH ratio	Mass of pyrolysis liquid added (g)	# moles OH	Mass of BMA added (g)	#moles BMA added	Mass BuOH distilled (g)	# moles BuOH distilled	# moles reacted from ³¹ P-NMR	Molar ratio BMA/ Pyrolysis liquid monomer (by BuOH)	Molar ratio BMA/ Pyrolysis liquid monomer (by ³¹ P-NMR)
0.6	19.53	0.27	22.83	0.16	4.68	0.063	0.230	2.54	0.70
1.2	18.6	0.25	43.48	0.31	7.15	0.096	0.213	3.17	1.44
2.4	20.29	0.28	94.87	0.67	9.08	0.123	0.238	5.45	2.80

By increasing the amount of residual BMA present in the transesterification step the effect of the pyrolysis liquid monomers on the polymerisation was effectively “diluted” however this “dilution” is key to understanding the effect of the wax.

3.3.2 “Wax” polymerisation effects

It was not possible to define the exact BMA:pyrolysis liquid monomer ratio in the transesterification product via ¹H-NMR analysis due to the overlap of coincidental peaks in the spectra. Instead, the mass of butanol condensate distilled out of the reaction vessel in the transesterification step was used as a measure of the amount of pyrolysis monomer formed. This value could then be compared to the amount of BMA in the feed to give an indicative measure of the BMA:pyrolysis liquid monomer ratio. The data used for this calculation is included in Table 13 and shows that this method of estimating the BMA:pyrolysis liquid monomer ratio underestimates the concentration of BMA in the monomer mixture compared with the ³¹P-NMR.

Table 14: Effect of initiator concentration and BMA ratio on conversion, M_p and \bar{D} of the produced polymers

Entry #	Ratio of BMA:pyrolysis liquid	[AIBN] (wt%)	Conversion (%)	M_p (kDa)	M_n (kDa)	M_w (kDa)	\bar{D}
Control	0.6:1	0	*	*	*	*	*
1	0.6:1	0.01	*	*	*	*	*
2	0.6:1	0.11	*	*	*	*	*
3	0.6:1	0.98	79	22.9	16.1	28.4	1.8
Control	1.2:1	0	*	*	*	*	*
4	1.2:1	0.02	8	29.8	6.99	35.7	5.1
5	1.2:1	0.17	11	27.4	9.86	33.4	3.4
6	1.2:1	0.80	82	24.6	15.8	29.5	1.9
7	1.2:1	1.00	85	22.9	20.9	34.3	1.6
Control	2.4:1	0	*	*	*	*	*
8	2.4:1	0.02	7	36.9	19.0	40.1	2.1
9	2.4:1	0.10	27	32.2	21.7	41.3	1.9
10	2.4:1	0.62	87	13.4	6.57	15.5	1.7

* indicates that no increase in molecular weight was observed relative to the control.

Table 14 shows increasing initiator concentration in the polymerisations resulted in a decrease in M_p , increased conversion and lower \bar{D} . When comparing the initiator concentrations, the effects of different BMA:pyrolysis liquid ratios are most apparent in their effect on M_p . In all cases, when initiator concentration was increased, the expected decrease in M_p was observed. The differences are more pronounced at higher BMA:pyrolysis liquid ratios. For example, comparing **5** with **7**, a 5.9 fold increase in initiator concentration decreased M_p by 17% where in the case of **9** and **10**, a 6.2 factor increase in initiator concentration reduced M_p by approximately 40%. For the same examples, the effect on dispersity is even more pronounced, with entries **5** & **7** showing a 52% decrease and **9** & **10** showing only a 13% decrease. Comparing samples with comparable initiator concentrations, entries **4** & **8**, similar conversions were found but entry **8** had higher molecular weight and lower dispersity. This suggests that the wide variety of monomers in the functionalised pyrolysis liquid decrease the conversion and molecular weight and increase polydispersity.

3.4 Pyrolysis liquid Transesterification and polymerisation developed method

The optimum developed experimental setup used is outlined in Figure 44 for drying and Figure 45 for transesterification¹²⁷ and functionalised pyrolysis liquid polymerisation¹⁴⁹.

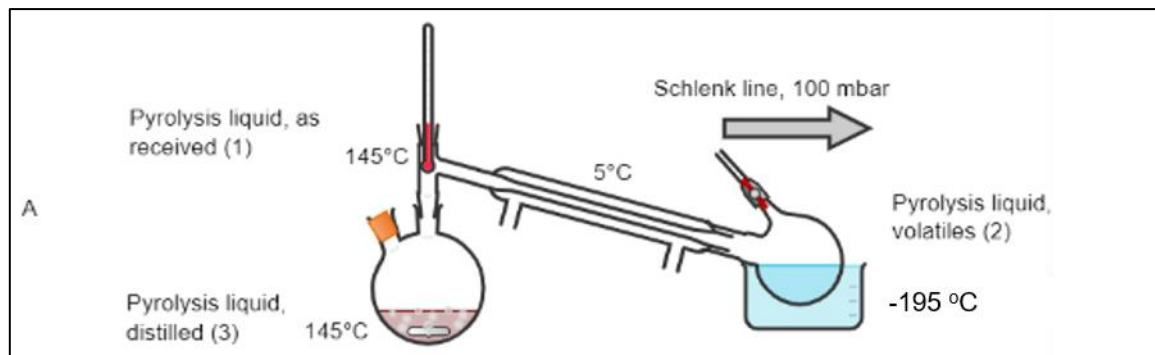


Figure 44 Experimental setup for the drying of pyrolysis liquid prior to transesterification. Note that liquid N₂ was used to achieve -195°C temperature and membrane pump was used to control pressure at 100 mbar.

A) Round bottom flask (RBF) in a Drysyn heating mantle at 145 °C. This was attached to a vacuum distillation head and trap, which was cooled to -195 °C to condense all vapours. Pressure was reduced to 100 mbar over a period of 20 minutes via a Schlenk line vacuum pump. Temperature was monitored in the Drysyn and still head. Aliquots of this distilled pyrolysis liquid and the distillate were set aside for subsequent analysis. Water content was confirmed by Karl Fischer (KF) analysis prior to transesterification, and the drying step was repeated if more than 0.5% water was detected. Concentration of OH in the distilled pyrolysis liquid, was determined by ³¹P-NMR, before addition of BMA. Ratios of 0.6, 1.2 and 2.4 were used in this work, as outlined previously in Table 14

Transesterification

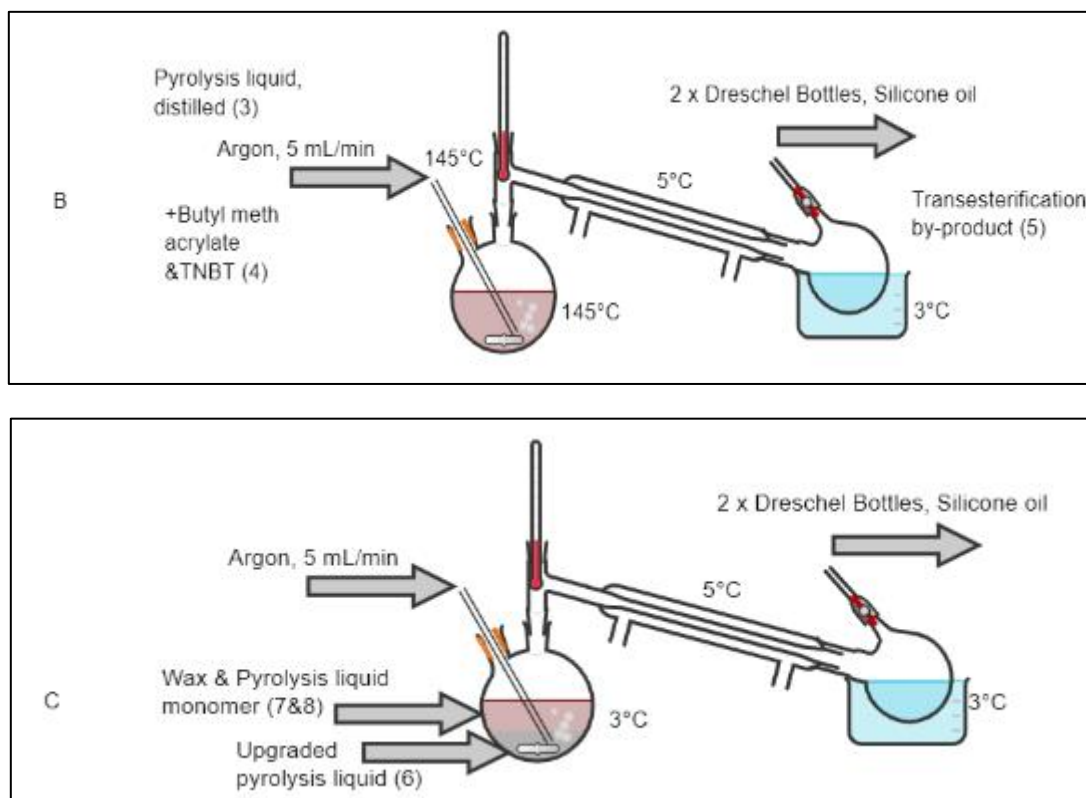
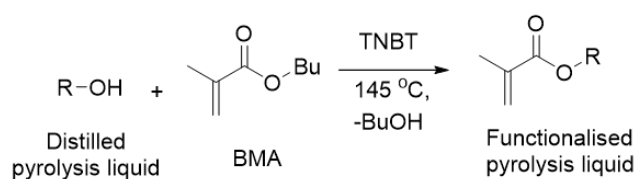


Figure 45 Transesterification reaction mechanism for the production of functionalised pyrolysis liquid and B) initial pyrolysis liquid transesterification experimental setup C) final experimental setup after transesterification.

B) The experimental setup, consisted of a two-neck round bottom flask with Suba seal and vacuum distillation head, followed by dreschel bottles, to prevent gas backflow. Stirring and Argon sparge, 5mL/min were begun 5 minutes prior to temperature increase. Temperature was measured in the oil bath, reaction vessel and still head. Addition of TNBT (0.6 mg, 0.0026 mmol) was treated as reaction start time (T_0). After reaction, the argon sparge and agitation were stopped and the mixture was then cooled to 3 °C for one hour, where $T=145$ °C, phase separation was observed shown in C). The upper, clear brown liquid monomer was separated, into a vial, from the lower, highly viscous opaque brown, upgraded pyrolysis liquid.

C) In this study, AIBN (0.2 wt%) was added to the transesterified pyrolysis liquid products (1.78g,) in a sealed vial. The sample was degassed via “freeze pump thaw” three times and backfilled with Argon. The temperature was subsequently raised to 85 °C in an oil bath and held for four hours with constant agitation. The reaction mixture was then allowed to cool to room temperature before the crude polymer was dissolved in approximately 5 mL acetone and precipitated into 600 mL of petroleum ether held at 0 °C. The precipitation solvent was separated from the polymer by decanting it from the light brown solid, which was the polymer product. The resulting polymer was then dried under vacuum at 50 °C.

3.5 Conclusions

In this chapter the focus was on developing a method to produce high molecular weight products from biomass pyrolysis liquid. Investigation into pyrolysis liquid transesterification showed that under standard conditions, polymerisation of methacrylate is initiated. Addition of inhibitor and reduction of reaction temperature are both presented as possible solutions. Temperature reduction was favoured due to reduced energy cost, process complexity, as well as no need to purchase, separate and then dispose of ancilliary reagents. Kinetic investigation of reduced temperature transesterification showed that reaction is complete after 30 minutes which, when compared to the standard two hours, represents an energy and time saving. Water was shown to have a significant effect on the transesterification reaction. It was shown that less water sensitive catalysts did not perform the transesterification in the presence of water, suggesting that water removal is needed to drive the transesterification to completion. Experimentally, this removal of water was carried out prior to addition of catalyst, *via* vacuum distillation, however this represents an extra process step that is undesirable, though could be achieved using similar equipment to the transesterification. Further catalyst screening and process development could combine the water removal and distillation steps in the functionalisation of the pyrolysis liquid.

The functionalised pyrolysis liquid was used as the starting material for a free radical polymerisation. Radical initiator concentration and solvent were treated as variables. Increasing the initiator concentration was shown to result in an increase in conversion and peak molecular weight and solvent was shown to have a negative effect on the polymerisation. A candidate pyrolysis liquid polymer was selected for further analysis owing to the highest conversion, molecular weight and T_g . The SEC chromatograms show that an additional molecular weight species is present in the polymer sample. A kinetic study demonstrated that this material was present from the outset and did not increase during reaction. The molecular weight of this wax, 0.5-2 kDa is similar to that of pyrolytic lignin. By varying the amount of residual BMA present in the transesterification step the effect of the pyrolysis liquid monomers on the polymerisation was investigated. By effectively changing the concentrations it was shown that these pyrolysis liquid monomers can reduce both the polymerisation conversion and molecular weight when in high concentration. Condensation polymerisation remains an opportunity for further investigation.

Chapter 4. Effect of pyrolysis liquid composition on polymer properties

4.1 Setting the Scene

There is a wide range of different acrylates with different physical and chemical properties. Within the wide range of acrylate applications, from adhesive binders to solid Perspex resin, there are uses for most of them. However, understanding how to manipulate these properties for a given application is pivotal to unlocking the value of an acrylate polymer.

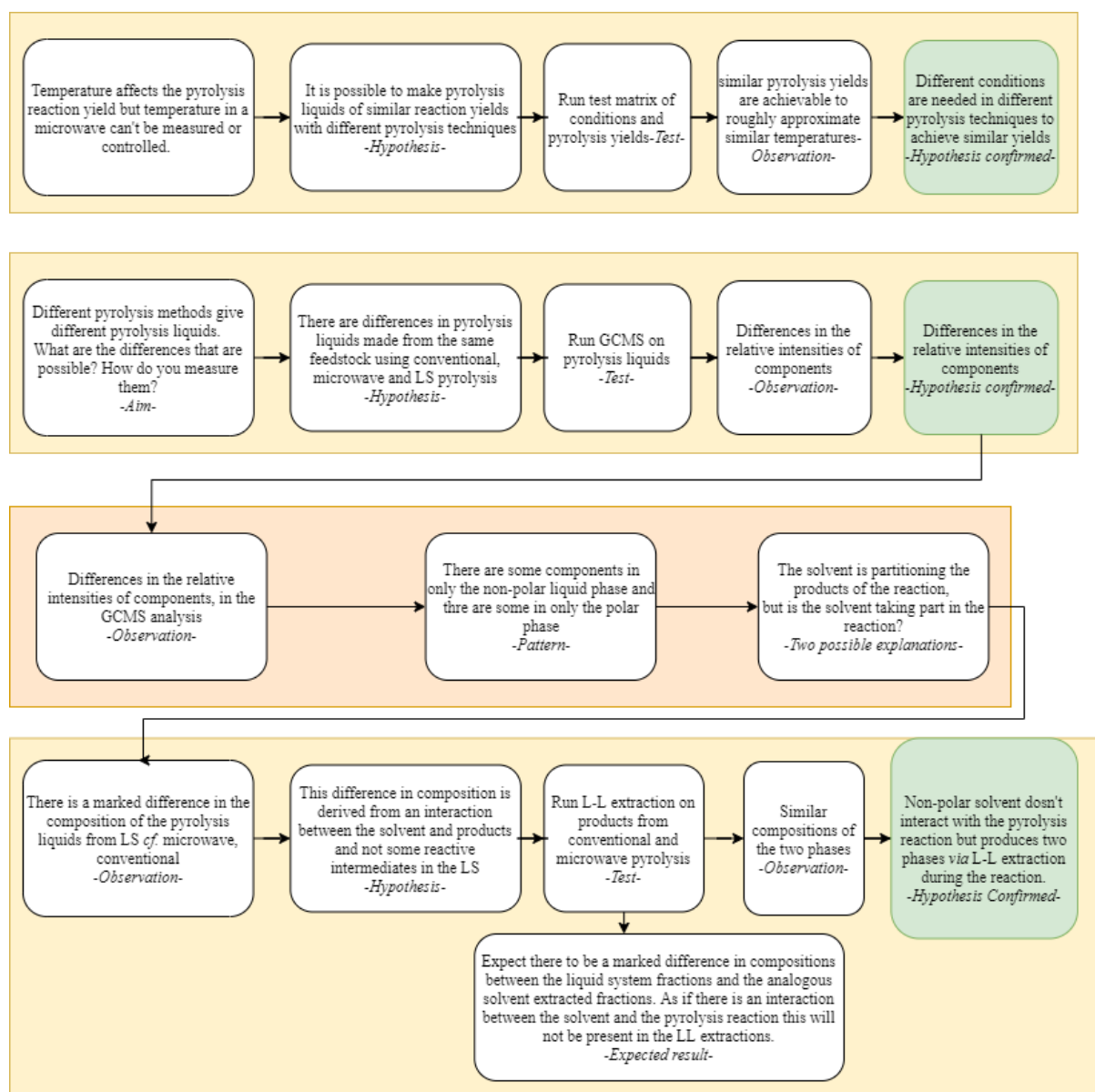
In the previous chapter it has been shown that the amount of pyrolytic lignin, or wax, left over in the pyrolysis liquid monomer has an effect on the polymerisation chemistry. The aim of this chapter is to investigate how:

1. The composition of pyrolysis liquid can be appropriately measured in the context of transesterification.
2. The heating method and solvent extractions affect pyrolysis liquid composition
3. The composition of the pyrolysis liquid subsequently affects polymer chemistry and properties.

These investigations go toward the end goal of understanding and manipulating the properties of pyrolysis liquid derived monomer so they can be exploited further in applications.

4.2 Pyrolysis liquid composition effects

Below is a brief executive summary of the thought process from hypothesis to test and results rationale for the production of different pyrolysis liquid *via* pyrolysis process. Where expected results are presented, this is an expected result if the original hypothesis was correct, although in this investigation there was not the change of hypothesis there are additional variables that were not previously anticipated – mainly the changes in GCMS component intensities were not the same changes originally anticipated, resulting in the addition of more subsequent hypotheses to explain these through fractionation.



Different pyrolysis methods have been shown to produce varied pyrolysis liquids from the same feedstock, whether by differences in mass and heat transfer due to different reactor conformation or by application of

different heating methods.^{44,50,150} The origin of some of these observed differences have been explained in previous work outlined in the introduction. It is widely accepted that the primary pyrolysis mechanisms remain similar with respect to temperature though the secondary reactions between the pyrolysis products also affect product distribution. It is thought that the pyrolysis temperature and sample residence time affect the type and duration of the secondary pyrolysis. The secondary pyrolysis reactions at higher temperatures cause the pyrolysis products to undergo pseudo “cracking” reactions into smaller gas molecules which exit the reaction system giving a high gas yield. At lower secondary pyrolysis temperatures secondary pyrolysis tends to combine into higher molecular weight species, hence char forms resulting in higher solid yield. If a liquid product is desired then these secondary pyrolysis reactions that lead to solid and gas products need to be limited. However, a direct comparison of the pyrolysis liquid yield and composition from gas inerted conventional, gas inerted microwave and the liquid inerted microwave pyrolysis, with identical feedstock and comparable reactor conformations has yet to be undertaken.

The objectives of this investigation are to address the following questions.

- What differences do we observe in pyrolysis liquids from gas inerted conventional and microwave pyrolysis and how can these liquids best be compared to the liquid inerted microwave pyrolysis liquids? What are the potential root causes of these differences?

4.2.1 Pyrolysis reaction temperature control

A main obstacle in pyrolysis research is that a consistent method to measure pyrolysis temperature across a range of heating methods does not exist. Temperature can be easily measured using either a thermocouple probe or an IR thermometer. These measure temperature in different ways, a thermocouple will measure the temperature at the tip of the probe through electromagnetic resistance changes due to temperature. This is applicable for measuring the core or surface temperature of a biomass sample. However these probes will need to be inserted into a sample and the presence of any probe or antenna has been shown to affect the magnetic fields in microwave cavities and hence potentially disrupt the sample heating.^{127,151,152} The other option is to use an IR thermometer which will give an indication of sample surface temperature through emitted radiation. This for microwave pyrolysis presents a new challenge as this requires line of sight to the sample from outside the cavity and as microwaves tend to heat from the core of a sample, it is not a direct measure of reaction temperature.

As such, in the current experimental setup temperature in a microwave is not directly measurable. This presents a challenge for this work as in order to fully control for the effect of temperature in pyrolysis it needs to be measured. However, the pyrolysis liquid yield is measurable. Therefore, provided the fundamental thermodynamics of the pyrolysis reactions remains constant across different heating modes, then if the yield of pyrolysis liquid is commensurate then the temperature of pyrolysis should also be comparable. Experimental conditions were identified such that commensurate pyrolysis liquid yields were observed, and these conditions and corresponding pyrolysis liquid yields are shown in Table 15.

Table 15 Power, time and particle sizes used for experiments.

Run	Heating mode	Heating method	Sample size (mm)	Mass loss (g)	Mass loss to liquid (%)	Standard deviation in mass loss to liquid
1	Gas inerted Conventional	450 °C, 600 seconds	25×5×5	5.20	54	1.7
2		1.5 kW, 5s		5.20	51	2.9
3		1.5 kW, 15s		7.39	49	8.4
4	Gas inerted	1.5 kW, 30s	25×15×15	13.30	36	21.5
5	Microwave	1.5 kW, 45s		12.35	31	21.8
6		1.5 kW, 60s		2.02	31	3.7
7		1.5 kW, 5s		-	-	-
8		1.5 kW, 15s		3.86	48	9.2
9		1.5 kW, 30s		6.93	49	5.2
10	Liquid inerted	1.5 kW, 45s	25×15×15	11.67	43	9.3
11	Microwave	1.5 kW, 60s		16.02	33	6.9
12	(Cyclohexane)	3 kW, 5s		-	-	-
13		3 kW, 10s		5.43	49	1.9
14		3 kW, 30s		15.47	36	7.9
	Liquid inerted					
15	Microwave	3 kW, 10s	25×15×15	6.09	50.99	1.9
	(Isopropanol)					
	Liquid inerted					
16	Microwave	3 kW, 10s	25×15×15	5.05	11.91	1.1
	(Water)					

The ratio of gas and liquid products/sample mass loss was used as a measure of reaction yield in Table 15. This is because due to the volumetric heating, absolute pyrolysis of the biomass in the microwave experiments was not possible under the experimental conditions. Therefore, the mass of unreacted starting material needed to be accounted for in mass loss calculations. The approach to this is highlighted in Table 16.

Table 16 Outline impacts of different pyrolysis mass loss calculations

Sample mass (g)	Degree of pyrolysis (%)	Mass of sample pyrolysed (g)	Product mass (g)			Yield (%)			Mass loss to Liquid (%)	Mass loss to Gas (%)
			Liquid	Gas	Solid	Liquid	Gas	Solid		
5	100	5	1	2	2	20	40	40	33	67
5	50	2.5	0.5	1	3.5	10	20	70	33	67
5	25	1.25	0.25	0.5	4.25	5	10	85	33	67

In Table 16 there is no difference in "yield" of liquid and gas product from pyrolysis: the ratio of liquid: gas: solid products remain the same. However, if you use experimental values for liquid, gas and solid product masses there appears to be a difference between experiments and this difference carries over to the yield (%) values. The best way to account for the difference in degree of pyrolysis is to calculate liquid and gas yields with respect to solid mass loss. The limitation of this method is the assumption that the same amount of solid residue is produced in each pyrolysis reaction *i.e.*, we don't quantify how much of the solid product is unreacted and how much is char.

From the conditions in Table 15 commensurate mass loss to liquid (%) and standard deviation were used to select the most comparable conditions to those of the gas inerted conventional pyrolysis liquid. Therefore, for the gas inerted microwave 1.5 kW, 5s was used and in the cyclohexane inerted microwave 3 kW, 10s was used. To keep a consistent method, the same conditions were used across a range of solvents. This resulted in consistent yields of pyrolysis liquid with respect to mass loss, however the overall mass of pyrolysis liquid isolated was much lower in the case of water. This is likely because water has a high dielectric constant and loss tangent and is also very effective at absorbing microwaves, potentially reducing the amount of power that reached the sample.

It has been shown that the overall yield of pyrolysis liquid with respect to temperature, is a bell curve, shown in Figure 46.

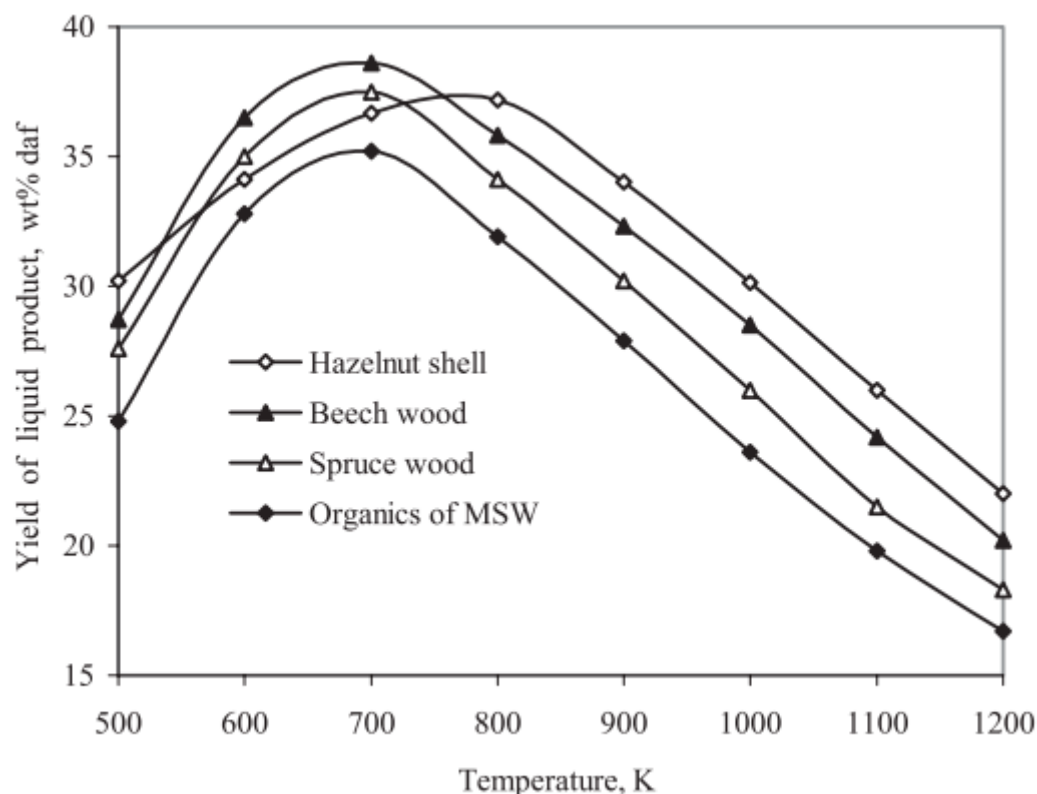


Figure 46 Effect of temperature on absolute pyrolysis liquid yields of different feedstock, taken from Demirbas et al.⁴⁰ Showing that different feedstock have different peak pyrolysis temperatures.

The work of Demirbas was originally focussed on the production of high HHV char, which is why the investigated temperatures are higher than those of this work however, Figure 46 shows that there are in places significant temperature differences between commensurate pyrolysis liquid yields. If this is interrogated for spruce wood, a similar pyrolysis liquid yield is observed at 500 K (227 °C) and at 1000 K (727 °C), however the difference between liquid yields for spruce wood at 600 K (327 °C) and 800 K (527 °C) is much smaller so there are limits to this approach. It should be noted that the pyrolysis liquid yield with respect to mass loss is around 46% (liquid 29%, solid 38%, gas 33%) is similar to the values generated in the experiments of Demirbas however there is a different feedstock, sample size, reaction time and reactor conformation which could explain the difference.

Solvent Partition Effects

In the liquid inerted fixed bed microwave pyrolysis there is a different thermal profile in the sample, due to the simultaneous microwave heating and solvent cooling of the sample. In addition, the reaction results in two pyrolysis liquid “fractions”: one soluble and the other insoluble in the selected solvent.¹⁰³ Pyrolysis liquid is commonly fractionated with toxic solvents, in order to remove polar molecules prior to upgrading or application, with endemic use of dichloromethane (DCM) in particular.^{124–126,153,154} This presents a plethora of sustainability

advantages for the liquid system as cyclohexane is far more sustainable, both in terms of production “footprint”, toxicity and long term environmental impact after use than DCM.¹⁵⁵ As this liquid-liquid separation occurs *in-situ*, liquid inerted fixed bed microwave pyrolysis eliminates process steps further reducing waste materials, plant footprint and equipment time.

Direct comparison of these liquid system pyrolysis liquids fractions with the crude pyrolysis liquids from fixed bed conventional or microwave pyrolysis is therefore not entirely fair. Figure 47 outlines the approach toward a direct compositional comparison.

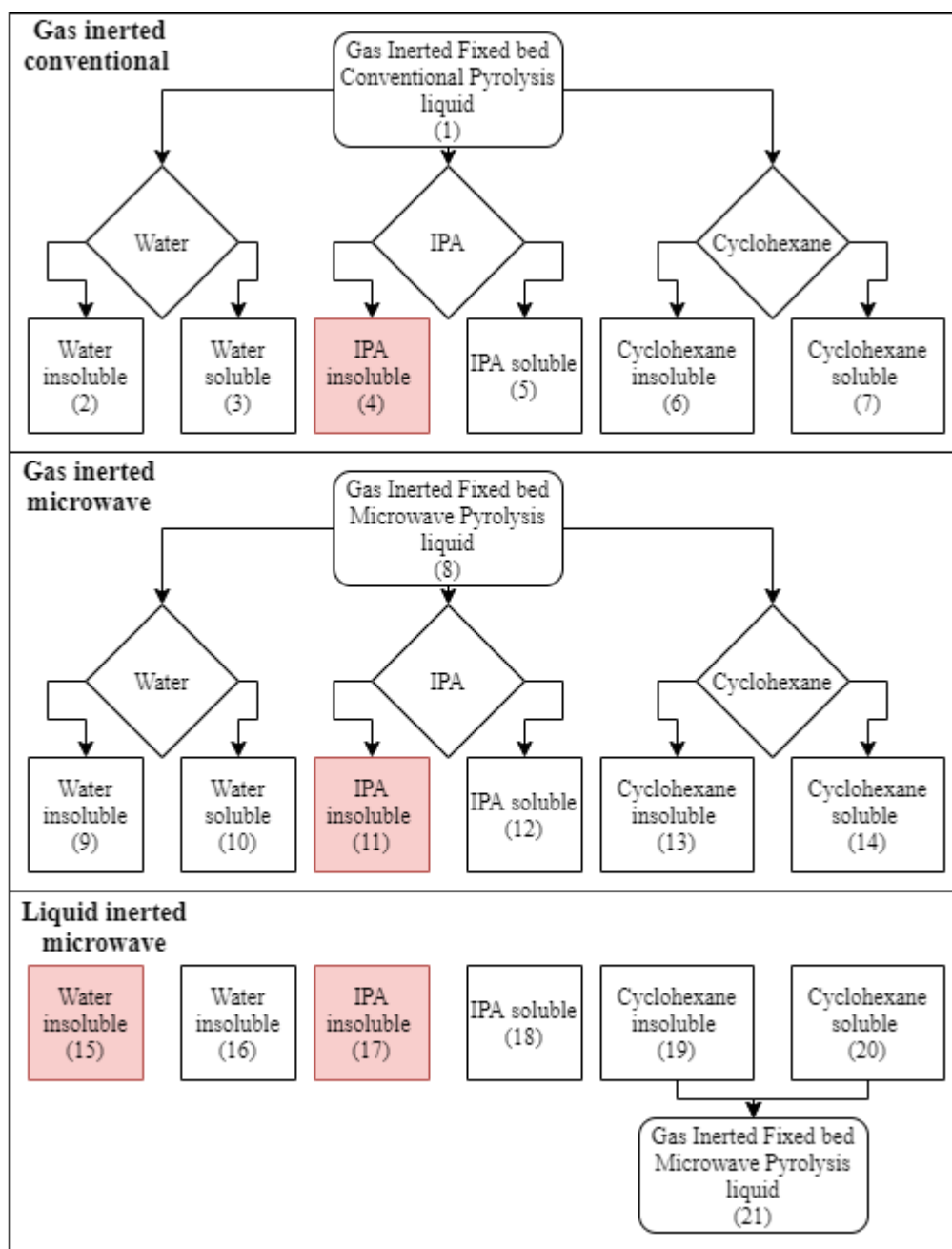


Figure 47 Schematic of liquid partitioning experiments of pyrolysis liquid with water, isopropanol and cyclohexane and the resulting fractions which have been numbered for ease of reference. Fractions coloured red were not experimentally isolated but included in the diagram for completeness.

In brief, the most straightforward analysis approach is to combine the solvent soluble and insoluble fraction to give a “crude” liquid inerted microwave pyrolysis liquid, box 21 in Figure 47. However, this method will not control any non-pyrolysis related interactions between pyrolysis liquid and solvent. The aim of this investigation is to shed light on whether the compositional differences are due to the solvent partition effects, an interaction between the solvent and pyrolysis reaction or some combination of both. For this reason, both approaches, namely

combination of the liquid system fractions into a single “liquid system crude” and liquid liquid separation of other crude pyrolysis liquids are included in this study.

In the interest of a fair test, both the conventional and microwave gas inerted fixed bed pyrolysis liquids were extracted, using three different solvents with a range of different relative polarities; water ($\delta_{\text{water}} = 1.000$), 2-propanol ($\delta_{2\text{-propanol}} = 0.546$) and Cyclohexane ($\delta_{\text{cyclohexane}} = 0.009$) to create, streams 2-7 and 9-14 for analysis.^{156,157} This should enable investigation into how to polarity of the solvent affects the ratio of soluble and insoluble products. The mass fraction of each stream is shown in Table 17.

Table 17 Stream mass fraction outline. Note that fractions 4,11 & 17 were not observed as the pyrolysis liquid appeared fully soluble in IPA. Note that fraction 15 was not observed experimentally as all pyrolysis liquid isolated was soluble in water. Fraction 21 is an “artificial crude” made by combining samples 19+20.

	#	Fraction		Crude mass added (g)	Isolated fraction mass (g)	Mass Fraction
Gas inerted Fixed bed furnace	1	Crude		-		1
	2	Water	Insoluble	5.84	0.6764	0.13
	3	Water	Soluble		5.55	0.95
	4	Isopropyl alcohol	Insoluble	5.46	NOT OBSERVED	0
	5	Isopropyl alcohol	Soluble		3.11	0.57
	6	Cyclohexane	Insoluble	5.21	3.7002	0.71
	7	Cyclohexane	Soluble		0.512	0.10
Gas inerted Fixed bed Microwave	8	Crude				1
	9	Water	Insoluble	1.43	0.8375	0.13
	10	Water	Soluble		1.32	0.93
	11	Isopropyl alcohol	Insoluble	4.22	NOT OBSERVED	0
	12	Isopropyl alcohol	Soluble		3.9249	0.93
	13	Cyclohexane	Insoluble	5.60	4.3137	0.77
	14	Cyclohexane	Soluble		0.6134	0.12
Liquid inerted fixed bed microwave	15	Water	Insoluble		NOT OBSERVED	0
	16	Water	Soluble	-	2.9576	1
	17	Isopropyl alcohol	Insoluble		NOT OBSERVED	0
	18	Isopropyl alcohol	Soluble	-	15.47	1
	19	Cyclohexane	Insoluble		10.35	0.80
	20	Cyclohexane	Soluble	-	2.5815	0.20
	21	“Artificial” Crude (19+20)		-		1

The first point to note is the lack of some fractions, IPA insoluble (4, 11 and 17). This is not surprising since pyrolysis liquid is usually completely miscible with IPA, however the lack of water insoluble fraction (15) in the

liquid inerted system is unexpected. It is commonly observed that fractionation of pyrolysis liquid occurs in pyrolysis liquid, when the water content is increased beyond 30%.^{158–160} The absence of this fraction in the liquid system is most likely not because the compounds did not form, but because they remain adhered to the biomass as opposed to precipitating out of solution as a separate liquid. The biomass could be further extracted with acetone post-pyrolysis in order to obtain this fraction however this would add a further level of complexity and is not within the scope of the current investigation. These fraction compositions are outlined in completeness in SI-3 and the fractions were grouped by solvent and presented in Table 18. The details of how these values are generated are presented in the experimental section and the collated peak area and assignments are provided in the appendices.

Table 18 Outline of liquid-liquid extraction effect on functional groups observed in GC-MS analysis of pyrolysis liquid. Note that this analysis on crude pyrolysis liquid is discussed in Table 20. These values were calculated from the absolute chromatogram peak area values relative to the total of the identified peak areas in the sample. The error is $\pm 0.5\%$. <1% show identified peaks at negligible concentration “-” are where no known peaks were identified.

Pyrolysis method	Extraction solvent	Acid	Ester	Alcohol	Aldehyde	Ketone	Furans	Sugars
Gas inerted furnace	Water insoluble	-	-	30%	2 %	<1%	15%	31%
	Water soluble	-	-	81%	5%	4%	2%	5%
Gas inerted microwave	Water insoluble	-	9%	44%	<1%	3%	1%	31%
	Water soluble	-	-	74%	5%		6%	13%
Liquid system	Water soluble	-	-	84%	4 %	3%	3 %	6%
Gas inerted furnace	Isopropyl alcohol	-	1%	69%	1%	5%	11 %	1%
Gas inerted microwave	Isopropyl alcohol	-	2%	49%	1%	4%	8%	14%
Liquid system	Isopropyl alcohol	-	2%	61%	<1%	5%	7%	12%
Gas inerted furnace	Cyclohexane insoluble	-	1%	45%	1%	12%	11%	9%
	Cyclohexane soluble	-	9%	56%	<1%	9%	14%	10%
Gas inerted microwave	Cyclohexane insoluble	-	3%	74%	1%	1%	10%	5%
	Cyclohexane soluble	-	10%	57%	1%	11%	5%	16%
Liquid system	Cyclohexane insoluble	-	<1%	55%	5%	4%	15%	7%
	Cyclohexane soluble	-	2%	72%		4%	2%	17%

Table 18 shows the differences in composition of initial alcohol products and secondary degradation products with different pyrolysis techniques and solvent extractions measured by gas chromatography. The most striking

observation from Table 18 is a positive correlation between the solvent polarity and the concentration of alcohols observed in the gas chromatogram. This is of interest because the crude pyrolysis liquids range from 42-63% alcohol before liquid-liquid extraction, and 74-84% after, regardless of whether pyrolysis took place in the liquid inerted microwave pyrolysis system or not. This could be explained by an interaction between the solvent and the keto-enol initial pyrolysis product with the position being pushed towards the enol (alcohol) causing a reduction in the observed ketones in the product. This effect is independent of the pyrolysis method used and can also explain the increase in the aldehyde concentration as the de-hydroxylation reaction is pushed to completion by an increased concentration of hydroxyl groups.

These results are of interest as despite the fact that these fractions are derived from the crude pyrolysis liquids, which have been observed to contain acid molecules, after fractionation no acid molecules are observed. The fact that these types of acids had been observed in the analogous crude pyrolysis liquids is key here. This MS analysis was done in positive mode, hence only positive ions are observed, where acids form much more stable negative ions than positive, this would explain the low/no acid concentration as an artefact of the analysis method. Since there were observed acid molecules (see Table 20) that are ostensibly no longer present in the fractionation this is indicative of a difference in acid concentration and not just a measurement limitation. This change in acid concentration could be due to co-removal of acids when the solvent is removed, either by rotary evaporation in the case of IPA and cyclohexane or by freeze-drying in the case of water. This could also be due to further reactions with the solvent, this does not seem an intuitive explanation in terms of water and cyclohexane though in the case of IPA it is certainly possible that there could be a reaction between acids and alcohol to form a greater concentration of esters. This begs another question of whether the difference in composition is due to the addition of solvent, the sample post-reaction conditions or due to the conditions required to remove the solvent. This could be further probed by quantifying pyrolysis liquid compositions before and after solvent removal and before and after storage. A comparison of the chromatograms before and after solvent removal is provided in Figure 48.

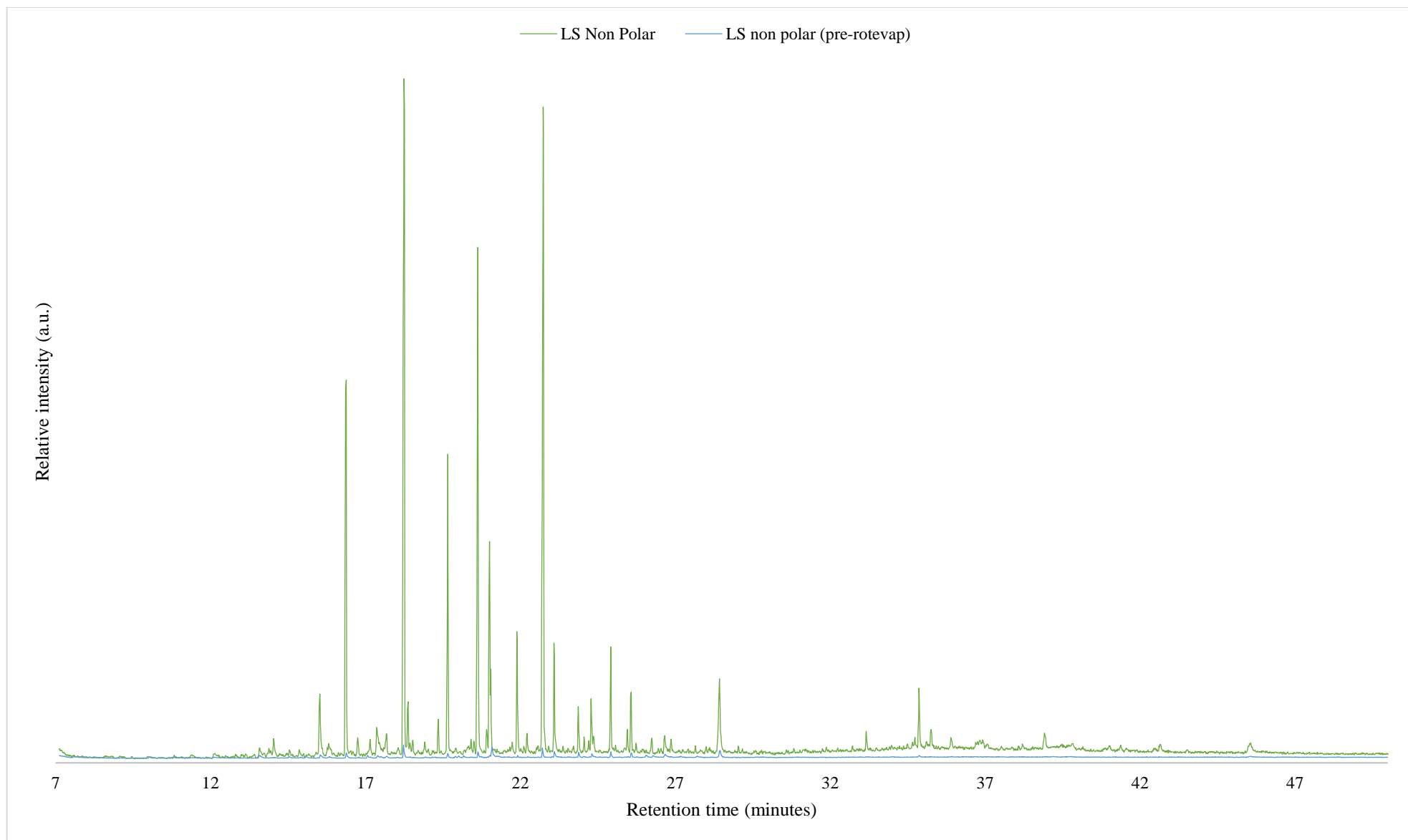


Figure 48 Chromatograms of Liquid system (LS) non-polar fractions (cyclohexane soluble) before and after solvent removal by rotary evaporation showing the increase in sample concentration following rotary evaporation – resulting in increased visibility of some low level components and a change in the relative concentration of some components.

From Figure 48 it is difficult to distinguish sample signal from background noise in the sample before solvent is removed as the concentration of pyrolysis liquid in the cyclohexane is so low. This is because there is approximately 5 g of sample dissolved in 1000 cm³ of solvent, this in turn is diluted to 1 mg·mL⁻¹ in DCM prior to injection. A potential solution to this would be to inject the cyclohexane/pyrolysis liquid neat into the GC-MS to maximise the concentration. However this approach, even when mitigated by only activating the detector after the elution of cyclohexane, is severely damaging to the components of the mass spectrometer, particularly the detector, column and sample injection needle. The effect of injection of a sample of too high a concentration can saturate the column meaning that sample that would ordinarily be slowed by the column will not be slowed down as there are no “free sites” for interaction, resulting in compounds eluting faster than they should.

The GC-MS analysis as presented is suitable to conclude that there are compositional differences between both the different heating methods and the products of the different solvent fractionation methods. The question around the applicability of the way GCMS has been applied, through the use of NIST assignment and molecular “categorisation”, remains pertinent. There is an element of human error in both the peak area assignment, as computational macros need occasional adjustment, the same is true of molecular assignment where this is a little of a “black box” to the user. An alternative approach would have been to pick individual compounds of interest, and focus only on these handful of peaks as indicative of wider changes in the pyrolysis liquid composition. This approach has been widely validated through various peer-review publications, though leaves the vast majority of pyrolysis liquid uncharacterised and leaves the question open for what else is going on outside the field of view of methanol, acetic acid, levoglucosan and the monolignol derivatives.

4.2.2 Pyrolysis method effect on liquid composition

From the original test matrix in Table 15 runs 1, 2, 13, 15 and 16 repeated in Table 19, show a difference in liquid and gas products yields under these conditions is less than 6%, excluding the liquid inerted water pyrolysis liquid.

Table 19 Selected comparable runs from initial test matrix

Heating mode	Heating method	Sample size (mm)	Mass loss to liquid (%)	Standard deviation in mass loss to liquid
Gas inerted conventional	450 °C, 600 seconds	25×5×5	54	1.7
Gas inerted microwave	1.5 kW, 5s	25×15×15	51	2.9
Liquid inerted microwave (cyclohexane)	3 kW, 10s	25×15×15	49	1.9
Liquid inerted microwave (Isopropanol)	3 kW, 10s	25×15×15	51	1.9
Liquid inerted microwave (Water)	3 kW, 10s	25×15×15	12	1.1

The closeness of the mass losses to liquid in the runs in Table 19 indicate that this approach to temperature control results in a similar product distribution, including unexpectedly when a more polar solvent is used. The notable exception to this is in the water inerted microwave. The cause for this is likely due to the high dielectric constant and loss tangent of water relative to the pine samples. This suggests that water selectively absorbs microwave energy instead of the sample, therefore much less microwave energy reaches the sample as the surrounding solvent is heated preferentially and will likely need more time to undergo pyrolysis to reach a similar yield to the other solvent experiments. To that end, the composition of liquid products from both gas inerted pyrolysis and both fractions from the cyclohexane inerted microwave pyrolysis experiments were investigated by GC-MS, the chromatograms are shown in Figure 49.

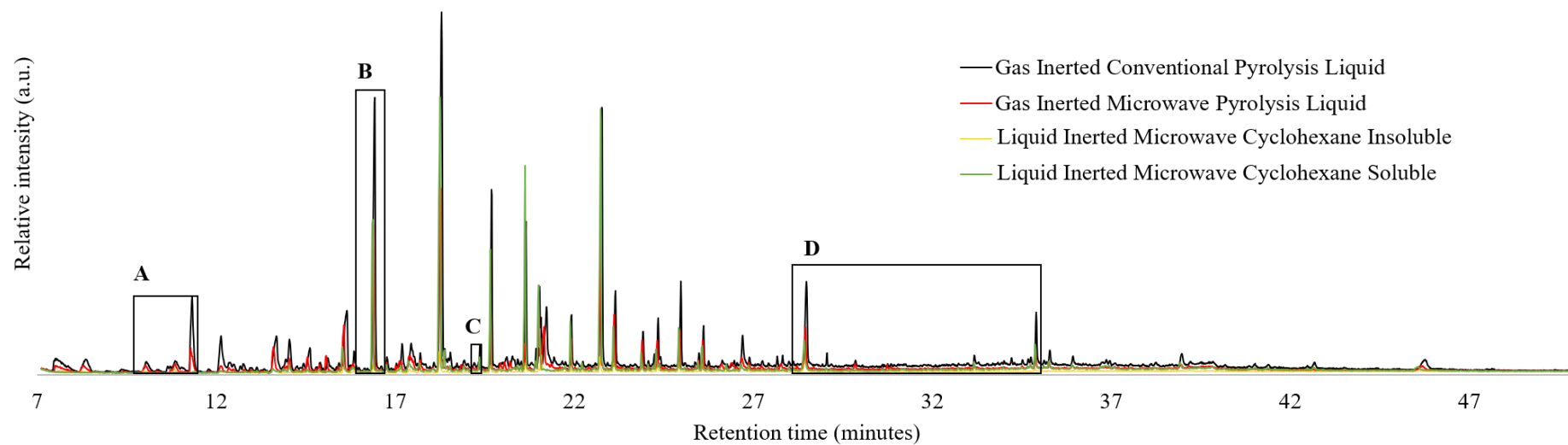


Figure 49 Chromatograms with the crude pyrolysis liquids from the gas inerted conventional and microwave pyrolysis experiments, along with the partitioned fractions from the liquid inerted microwave, including annotated interesting peaks A-D.

Figure 49 shows that despite similar yields between pyrolysis techniques, the fractions from the liquid inerted microwave show some distinct differences.

For instance in Peak A at 8 minutes retention time, there is 2-aminoacetamide present in all liquids apart from the liquid inerted cyclohexane soluble fraction, shown in Figure 50.

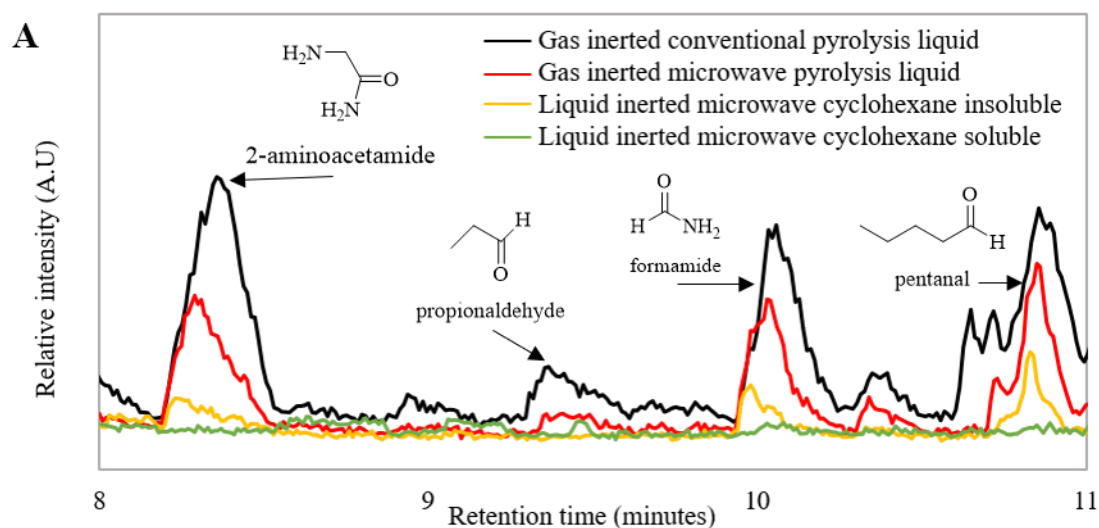


Figure 50 Magnified chromatogram from 8 to 11 minutes retention time (Peak A).

Conversely, in peaks B at 16.5 minutes and C at 18.5 minutes, the liquid inerted cyclohexane soluble fraction contains 2-methoxy phenol (B) and 4-ethyl 2-methoxy phenol (C) which are present in the other liquids, where in this case it is the cyclohexane insoluble fraction that does not, shown in Figure 51.

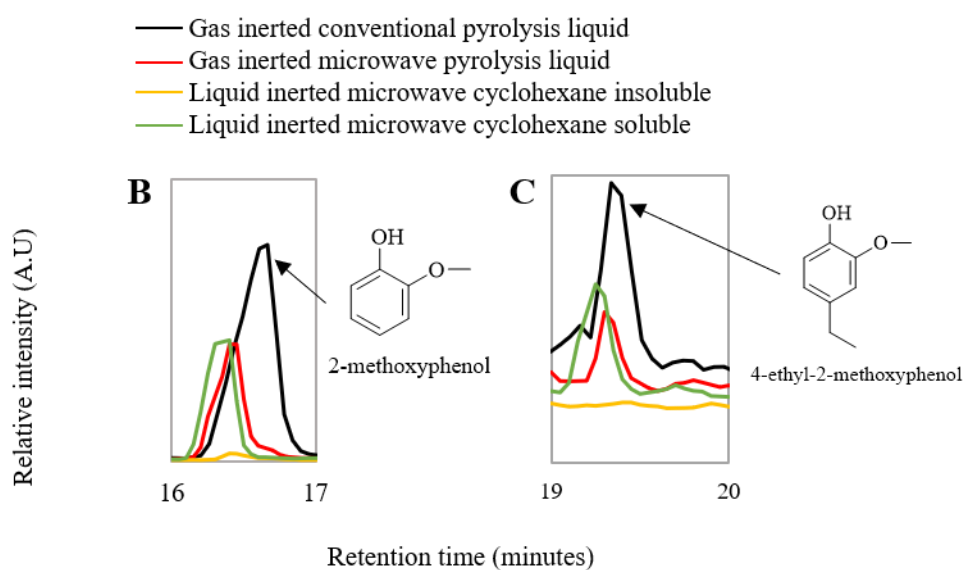


Figure 51 Magnified chromatogram from retention times 16 to 17 minutes (Peak B) and from 19 to 20 minutes (Peak C).

Interestingly, there is coniferyl aldehyde observed in the gas inerted pyrolysis liquids that are not observed in either of the liquid inerted fractions, shown in Figure 52.

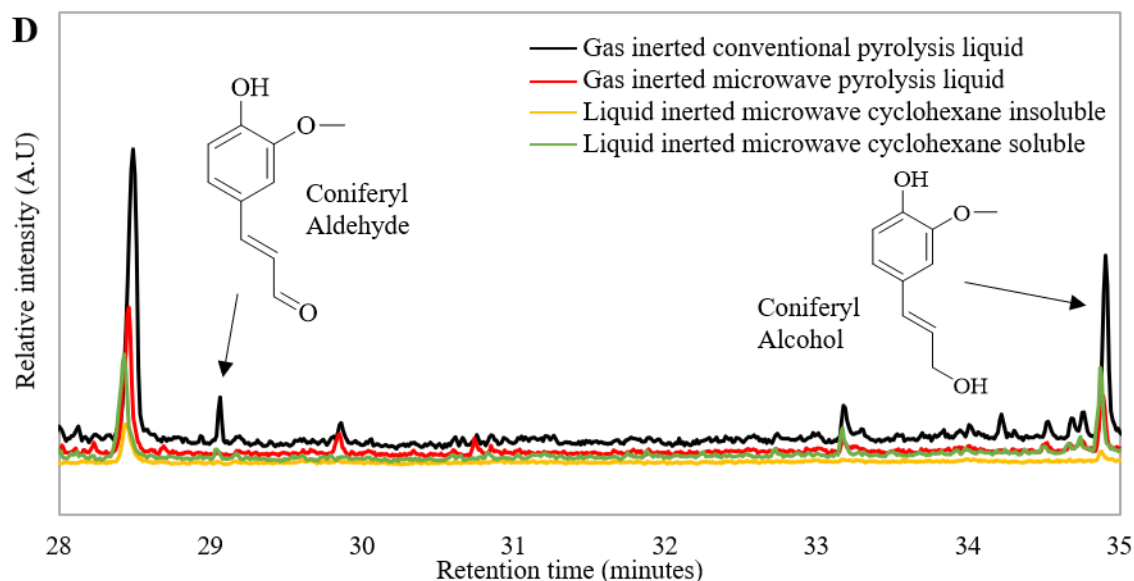


Figure 52 Magnified chromatogram from 28 to 35 minutes retention time (Peak D).

These differences in peak behaviour indicate that while some molecules partition into the solvent, some do not. This observation raises an additional question of how much compositional differences are due to the simultaneous heating and cooling unique to the liquid inerted microwave and how much are they down to the change in this partitioning.

Combined liquid system data

In Figure 53, the two liquid inerted microwave samples were combined (cyclohexane soluble and insoluble) prior to analysis, and comparisons are shown.

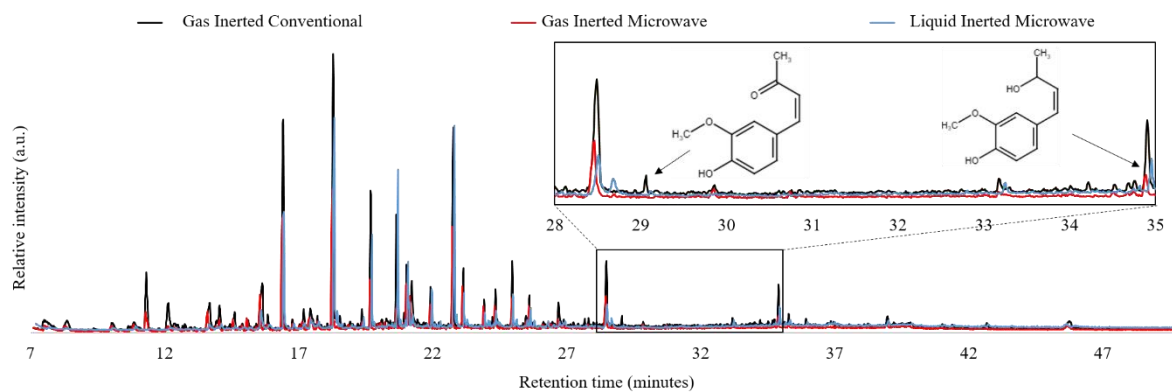


Figure 53 Gas Chromatograms of pyrolysis liquid from Gas Inerted Conventional, Gas inerted Microwave and liquid inerted microwave.

Few differences are apparent from the chromatograph, shown in Figure 53, apart from the extra peak at 29 minutes seen in the conventional pyrolysis liquid. This peak, identified as Coniferyl aldehyde through comparison with the NIST database, is a secondary decomposition product of lignin. However, the corresponding alcohol, seen at retention time of 35 minutes, is found in all pyrolysis liquids. The key question here is how much of this difference in composition is due to the heating method and how much is due to the reaction temperature. The fact that in Table 19 there are liquid product yields of 54, 51 and 49% with respect to mass loss, indicate that there were roughly similar temperatures of pyrolysis, if this was not the case then there would be different yields observed. A brief summary of the compositional differences observed is provided in Table 20.

Table 20 Summary of GCMS peak area ratios in fixed bed conventional and microwave pyrolysis along with combined liquid system pyrolysis liquid and industrial (BTL) pyrolysis liquid. pH was measured by probe. GC peak areas were integrated and all peaks >0.1% were identified and categorised by predominant functional group as a function of the total peak area.

	Acid	Alcohol	Ketone	Aldehyde	Amine	Furans	Sugars	pH
Industrial pyrolysis liquid	6%	29%	-	4%	-	26%	-	2.0
Gas inerted fixed bed furnace	0.5%	42%	12%	4%	7%	20%	1%	2.3
Gas inerted fixed bed microwave	0.2%	45%	7%	3%	0.2%	14%	14 %	2.8
Liquid inerted fixed bed microwave	-	63%	4%	3%	1%	9%	12%	3.5

The first observation from Table 20 is that the acid containing molecules are lower in concentration in the microwave pyrolysis techniques and there are no acid containing molecules observed in the GC-MS data of the liquid inerted microwave pyrolysis system. This is corroborated by the pH, which was measured immediately after pyrolysis. Acid content is considered the key indicator of the “aging” process of pyrolysis liquids, with a high acid content indicating that aging has occurred.¹⁶¹ The lack of acids observed in the Liquid inerted fixed bed microwave is consistent with ideas presented by Shepherd *et al*,¹⁰³ and Taqi *et al*¹⁰⁶ that less aging reactions are observed in the liquid inerted microwave pyrolysis system. However with reference to Table 18 it would seem that these acid fractions are not observed in the solvent extracted fractions, so leads to the question of whether the solvent removal is co-removing acid, there is also a systematic question around the MS analysis run in positive mode, this will only detect positive ions and it is more difficult to create a positive ion from an acid molecule hence potentially why less are observed.

This observation of acid content from Table 20 builds into two additional and seemingly different effects; firstly, an increase in alcohol concentration moving from Gas inerted fixed bed furnace pyrolysis to Gas inerted fixed bed microwave pyrolysis to the Liquid inerted fixed bed microwave and; secondly, a decrease in ketone concentration. This increase in alcohol concentration in the microwave systems is likely the product of more than one effect; an increase in the tautomerisation of ketone moieties to phenols due to the less acidic pH; a reduction in the degradation and oxidation of alcohols to the corresponding aldehyde and acid moieties; or more alcohols

being created in the primary pyrolysis reaction. In the most extreme case, comparing gas inerted fixed bed furnace to liquid inerted fixed bed microwave, this ketone to alcohol tautomerisation, by stoichiometry of the change in ketone concentration, only accounts for a 7.3% increase in alcohol, assuming 100% selectivity for the alcohol product. The lower concentration of aldehydes, formed from alcohols, observed in the liquid inerted microwave only accounts for a further 0.8%, again assuming a 100% selectivity. This leaves a 12.9% increase in alcohol unaccounted for when comparing gas inerted fixed bed furnace to liquid inerted fixed bed microwave. Since there is no evidence of “the microwave effect” altering the thermodynamics of pyrolysis, the remaining difference in alcohol concentration could be due to some other effect. The different post-pyrolysis sample morphology in the liquid inerted fixed bed microwave (B), when compared to the gas inerted fixed bed microwave (A) shown in Figure 54 lends credence to the high internal cell pressure proposed by Taqi *et al.*¹⁰⁶

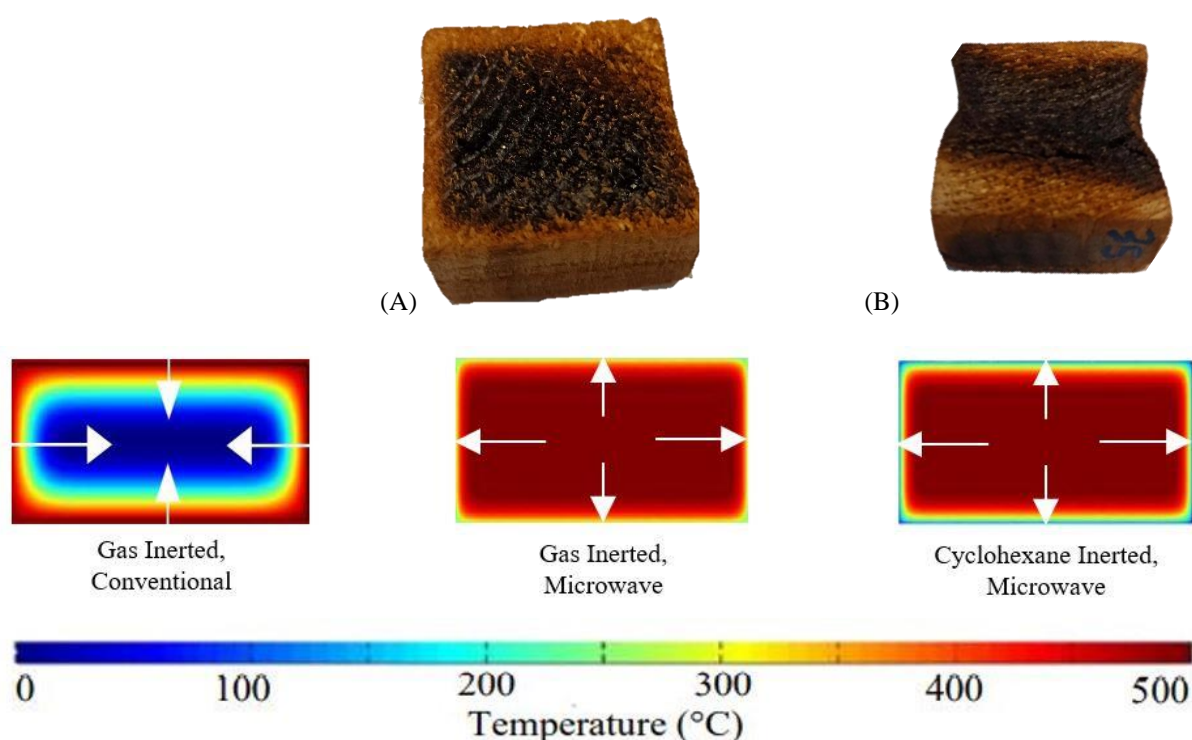


Figure 54 Post-pyrolysis sample morphology of gas inerted fixed bed microwave pyrolysis (A) and liquid inerted fixed bed microwave (B) alongside 2D COMSOL thermal models

The marked difference in appearance of A and B indicates a change in the interaction between the electromagnetic field and the sample when solvent is involved (B), it is likely that as this is a multi-modal system the distribution of energy across the sample is not as homogeneous as in the simpler gas inerted system. There is however still a larger area of the sample (B) that remains un-pyrolysed compared to (A) so there is some experimental agreement with modelling. There seems to be a difference in the appearance of the samples A/C with a wider area of non

pyrolysis than the modelling would suggest, perhaps the changes in dielectric constant are more pronounced in a bulk sample than would otherwise be predicted, hence a greater hot spotting effect as the hotter samples become more microwave absorbent which has not been accounted for in the model as this model is based on thermal dielectric data and heat transfer data from much smaller samples..

The Gas inerted fixed bed furnace pyrolysis liquid shows an increased amount of furan containing compounds, these are further indication of secondary degradation of lignin pyrolysis at elevated temperature, however furans are also primary pyrolysis products of hemi-cellulose and sugars; this would explain why more sugar and less furans are seen in microwave pyrolysis liquids.^{150,162,163} The increase in amine concentration could potentially be explained through the gaseous nitrogen and reactive pyrolysis species, which has been observed elsewhere.¹⁶⁴ This could further explain why there are less amines in the gas inerted fixed bed microwave as these reactive pyrolysis species are separated from the gaseous nitrogen by the outer biomass block.

4.2.3 Origins of distinct pyrolysis liquid compositions

The mechanism for formation of aldehydes from lignin was first proposed by Jarvis *et al*¹⁶⁵ and later confirmed and applied by Choi *et al*¹⁶⁶. Suggests, that following the β -O-4 bond cleavage of lignin, Enol (a) and phenone (b) moieties form first followed by subsequent reactions, shown in Figure 55. The caveat to this work is that this was based on lignin model compounds and not lignin itself so this is a potential explanation but there is a gap in the literature with regards to lignin itself.

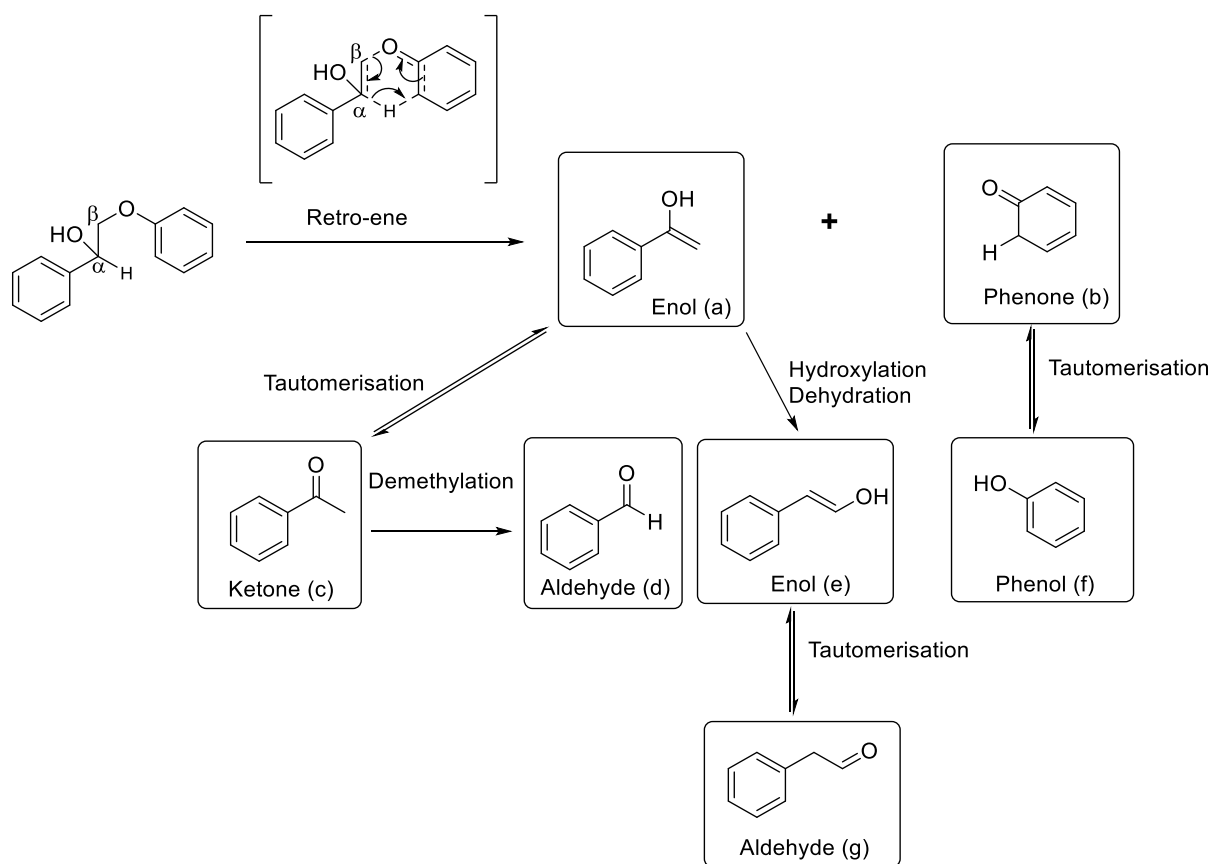


Figure 55 Primary and secondary pyrolysis reaction for lignin model compound 2-phenoxyphenylethanol (PPE: $\text{PhCHOHCH}_2\text{OPh}$) scheme adapted from original articles.^{165,166} Showing that despite a narrow input molecule, a wide range of products can be observed and explained, representing a significant challenge in the deconvolution of multiple pyrolysis liquid compounds.

Typically, following formation the phenone (b) will tautomerise to the phenol (f), this is an equilibrium so both products will be seen in pyrolysis liquid. The Enol (a) will, over time, undergo hydroxylation/dehydration to in essence “move” the OH group to the more stable chain end position enol (e) and subsequent tautomerisation will

give the aldehyde (g). Another route to aldehydes in pyrolysis liquid is tautomerisation of the enol (a) to the ketone (c) and subsequent demethylation/oxidation to aldehyde (d).

The formation of aldehyde is temperature dependant as it proceeds by an energetically unfavoured route. Lower aldehyde concentration in microwave pyrolysis *cf.* conventional pyrolysis is consistent with the work of Robinson *et al.* who found lesser secondary degradation of pyrolysis products in gas inerted fixed bed microwave heating.⁸⁴ Preservation of these enol functionalities in the pyrolysis liquid implies a better control of the operating conditions as they are prone to elimination in the earlier stages of pyrolysis. Moreover, it is expected that the higher the number of electron donating substituents on the phenolic unit, present in real lignin, the greater will be its reactivity towards side reactions shown in Figure 55, explaining the observed difference in concentrations of monophenols. This is because these differently substituted monophenols will undergo these forward and backward reactions at different rates; they will have different equilibrium constants so the position of equilibrium will vary for each individual monophenol differently depending on different conditions. It is thought that although the initial pyrolysis reaction forming alcohols and ketones from lignin will occur at the same rate in the different pyrolysis techniques, the varied feedstock and temperature profile in the sample will result in different secondary degradation products; aldehydes and phenols. Initial FT-IR of the difference between gas inerted fixed bed conventional pyrolysis liquid and gas inerted fixed bed microwave is shown in Figure 56.

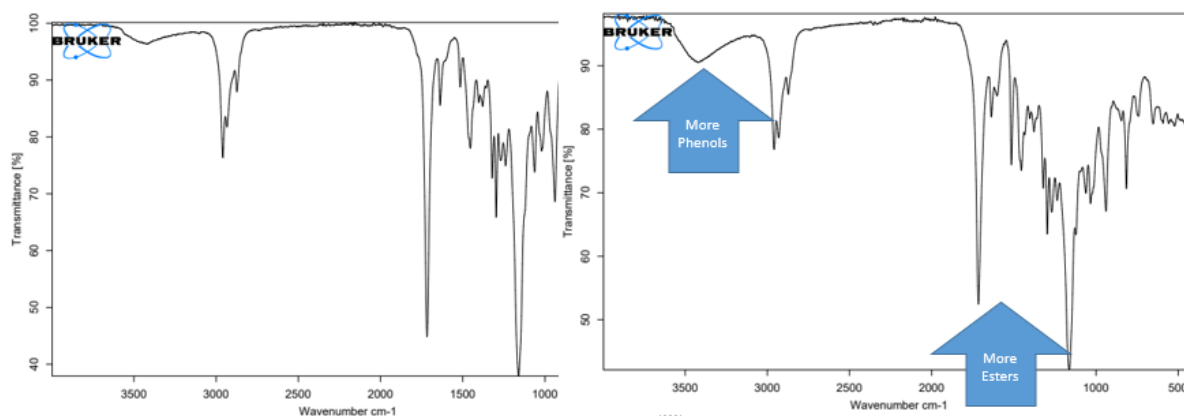


Figure 56 FT-IR of gas inerted conventional pyrolysis liquid on the left and gas inerted microwave on the right. Showing the increase in ester and phenol type compounds in the gas inerted microwave pyrolysis experiments

The data in Figure 56 shows a general increase in the phenol (3500 cm^{-1}) and ester (1600 cm^{-1}) compounds in the gas inerted fixed bed microwave pyrolysis liquid compared to the conventional pyrolysis liquid. This indicates that there is less decomposition of these species into IR inactive compounds. This increase in phenol content could be exploited as pyrolysis liquids have been used to replace phenol in resins and high value polymer materials.^{142,167}

Typically, a high ester content is desirable in a pyrolysis liquid as it improves storage stability, heating value, and overall quality for use as a fuel.¹⁶⁸

4.2.4 Summary

A challenge with the investigation of pyrolysis is the number of variables that need to be simultaneously controlled while one variable is altered, namely feedstock, temperature, reaction time, inerted medium and heating technique. Feedstock was kept constant and, as temperature across different pyrolysis techniques cannot be consistently measured, it was decided to investigate different pyrolysis inerting conditions and heating techniques that gave similar yields of pyrolysis liquid as an approximation of equivalent temperatures. Where applicable, solvent was removed from samples under reduced pressure, this presented issues in the GC-MS analysis as without solvent removal concentration was too low. However, some compounds were removed with the solvent which affects the absolute applicability of this analysis.

Pyrolysis liquid samples were interpreted in relation to less volatile primary and secondary decomposition reactions of model compound pyrolysis. The results showed that although there are not new molecules produced from biomass in the liquid inerted microwave, there were differences in the distribution of products observed. Differences between heating methods were noted with more furans observed in conventional pyrolysis liquids, consistent with literature elsewhere attributing this to a reduction in secondary pyrolysis reactions. A 15-20% increase in the alcohol concentration of the liquid inerted microwave pyrolysis system was comparable to the gas inerted microwave pyrolysis concentration. This was initially attributed to a pressure differential as a result of the solvent, consistent with literature elsewhere, and the physical changes in the sample, indicating that there could be some effect beyond just the solvent partition effect in the liquid inerted microwave pyrolysis system.¹⁰⁶ There were similar changes in the compositions of the liquid inerted microwave liquids, when compared to those from gas inerted microwave pyrolysis liquids that were extracted with solvent, across a range of solvent polarities. This similarity across pyrolysis methods could be attributed to an interaction between the pyrolysis liquid and the solvent with no evidence of the more reactive species surviving through to the analysis stage. As gas chromatography is a time averaged analysis technique, in situ –IR and EPR measurements will be needed to confirm the existence of more reactive molecules along with a way of preventing the solvent based decomposition of products in any subsequent liquid inerted microwave pyrolysis system.

The aim of this investigation was to understand how the composition of pyrolysis liquid can be appropriately measured in the context of transesterification. Gas chromatography and IR measurements showed that there are some observable compositional differences in the fractions however, this investigation highlighted that the solvent removal also effects the observed composition and therefore presents a significant challenge to the approach. This

means that in terms of the aim of understanding how the heating method and solvent extractions affect pyrolysis liquid composition these techniques require further refinement and full characterisation in the context of transesterification which could be useful but is not straightforward.

Full and absolute characterisation of the pyrolysis liquid was not needed for the transesterification investigation. Therefore, it was decided to push ahead with investigating how the composition of the pyrolysis liquid subsequently affects polymer chemistry and properties as a measure of alcohol concentration, which could be obtained through the literature published ^{31}P -NMR method.⁶⁵

4.3 Pyrolysis liquid composition effects on transesterification

In order to investigate how the composition of the pyrolysis liquid affects the properties of the polymer, first it was necessary to run a transesterification on the different pyrolysis liquids introduced as part of the investigation into solvent partition effects, in Figure 47. The aim of this part of the investigation is to establish whether the composition of the pyrolysis liquid has any effect on the transesterification chemistry. At the outset, it was thought that the major factor affecting the transesterification would be the concentration and type of alcohols in the pyrolysis liquid as fundamentally these are the molecules taking part in the reaction. Therefore, the initial hypothesis was that concentration and type of alcohol would therefore be the underlying cause of any correlations between fraction, the chemical origin of these fractions was thought to be less important. In the method development chapter, concentration of alcohol was kept constant through the use of the same, industrial scale, pyrolysis liquid. It was expected that a lower concentration of alcohol, would result in a lower yield in transesterification reaction.

The reason for this hypothesis is that the low alcohol concentration would effectively be diluted by everything else in the pyrolysis liquid ostensibly not taking part in the reaction. The pyrolysis liquids generated from different pyrolysis methods and liquid liquid fractionation underwent a transesterification reaction as optimised for the industrial pyrolysis liquid in the previous chapter. As part of this method, the solvent was first removed, alongside water under reduced pressure, as part of the drying step. During the transesterification reaction, the mass of butanol by-product distilled was used as a measure of reaction coordinate and hence reaction yield with respect to initial alcohol concentration. All reactions were conducted for 40 minutes which was determined to be the optimum reaction time for industrial pyrolysis liquid transesterification. The effect of different alcohol concentration on the transesterification is shown in Figure 57.

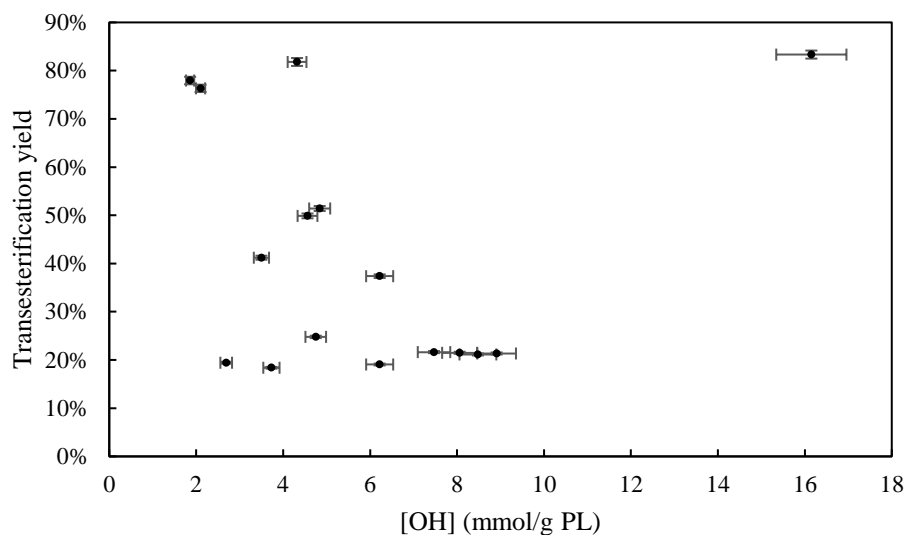


Figure 57 Effect of pyrolysis liquid alcohol concentration on the transesterification reaction yield.

The data in Figure 57 shows no conclusive correlation. However, if the data is grouped by the solvent fraction, as shown in

	Pyrolysis method	Solvent Fraction	Dry Pyrolysis liquid mass (g)	[OH] (mmol/g)	Initial moles OH (mmol)	Mass BuOH (g)	BuOH (mmol)	yield (%)
1	Gas inerted fixed bed furnace	Crude	7.56	4.32	32.66	1.98	26.71	81.79
8	Gas inerted fixed bed microwave	Crude	6.17	16.15	99.65	6.15	82.97	83.33
2	Gas inerted fixed bed furnace	Water Insoluble	0.67	2.1	1.41	0.08	1.08	76.32
9	Gas inerted fixed bed microwave	Water Insoluble	0.84	1.86	1.56	0.09	1.21	77.95
3	Gas inerted fixed bed furnace	Water Soluble	1.58	8.48	13.40	0.21	2.83	21.15
10	Gas inerted fixed bed microwave	Water Soluble	0.91	7.47	6.80	0.11	1.48	21.63
16	Liquid system	Water Soluble	1.04	8.91	9.27	0.15	2.02	21.34
5	Gas inerted fixed bed furnace	IPA Soluble	2.12	4.75	10.07	0.19	2.56	24.79
12	Gas inerted fixed bed microwave	IPA Soluble	2.94	8.06	23.70	0.38	5.13	21.49
18	Liquid system	IPA Soluble	15.47	6.22	96.22	0.14	18.34	19.06
6	Gas inerted fixed bed furnace	Cyclohexane Insoluble	3.48	3.5	12.18	0.37	4.99	41.21
13	Gas inerted fixed bed microwave	Cyclohexane Insoluble	3.88	6.22	24.13	0.67	9.04	37.37

19	Liquid system	Cyclohexane Insoluble	10.35	3.73	38.61	0.53	7.15	18.39
7	Gas inerted fixed bed furnace	Cyclohexane Soluble	0.28	4.56	1.28	0.05	0.67	49.88
14	Gas inerted fixed bed microwave	Cyclohexane Soluble	0.45	4.84	2.18	0.08	1.08	51.41
20	Liquid system	Cyclohexane Soluble	2.58	2.69	6.94	0.10	1.35	19.43

Table 21, then some interesting patterns in transesterification yield can be observed.

Table 21 Summary of effect of pyrolysis liquid composition on transesterification yield, measured by mass of distilled BuOH by-product.

	Pyrolysis method	Solvent Fraction	Dry Pyrolysis liquid mass (g)	[OH] (mmol/g)	Initial moles OH (mmol)	Mass BuOH (g)	BuOH (mmol)	yield (%)
1	Gas inerted fixed bed furnace	Crude	7.56	4.32	32.66	1.98	26.71	81.79
8	Gas inerted fixed bed microwave	Crude	6.17	16.15	99.65	6.15	82.97	83.33
2	Gas inerted fixed bed furnace	Water Insoluble	0.67	2.1	1.41	0.08	1.08	76.32
9	Gas inerted fixed bed microwave	Water Insoluble	0.84	1.86	1.56	0.09	1.21	77.95
3	Gas inerted fixed bed furnace	Water Soluble	1.58	8.48	13.40	0.21	2.83	21.15
10	Gas inerted fixed bed microwave	Water Soluble	0.91	7.47	6.80	0.11	1.48	21.63
16	Liquid system	Water Soluble	1.04	8.91	9.27	0.15	2.02	21.34
5	Gas inerted fixed bed furnace	IPA Soluble	2.12	4.75	10.07	0.19	2.56	24.79
12	Gas inerted fixed bed microwave	IPA Soluble	2.94	8.06	23.70	0.38	5.13	21.49
18	Liquid system	IPA Soluble	15.47	6.22	96.22	0.14	18.34	19.06
6	Gas inerted fixed bed furnace	Cyclohexane Insoluble	3.48	3.5	12.18	0.37	4.99	41.21
13	Gas inerted fixed bed microwave	Cyclohexane Insoluble	3.88	6.22	24.13	0.67	9.04	37.37
19	Liquid system	Cyclohexane Insoluble	10.35	3.73	38.61	0.53	7.15	18.39
7	Gas inerted fixed bed furnace	Cyclohexane Soluble	0.28	4.56	1.28	0.05	0.67	49.88
14	Gas inerted fixed bed microwave	Cyclohexane Soluble	0.45	4.84	2.18	0.08	1.08	51.41
20	Liquid system	Cyclohexane Soluble	2.58	2.69	6.94	0.10	1.35	19.43

From Table 21, there is a consistency of transesterification yield across similar pyrolysis liquid fractions. The water insoluble fractions (2 & 9) give moderate yields of 76-78% with alcohol concentrations of 1.86-2.10 mmol/g and the water soluble fractions (3, 10 & 16) gave much lower yields at 21% with concentrations of alcohol between 7.47-8.91 mmol/g. This is the opposite of the expected trend with respect to the concentration of alcohol.

The IPA soluble fractions (5, 12 & 18) are of particular interest as the crude pyrolysis liquids were entirely soluble in IPA so there was no fractionation. There is however a marked difference between transesterification yields (19-24%) when compared to the crude (81-83%). The origin of this chemical difference could be explained by an interaction, other than solubility, between the solvent and some molecules involved in the transesterification. Alternatively, as IPA was removed from the samples by rotary evaporation under reduced pressure, it is likely

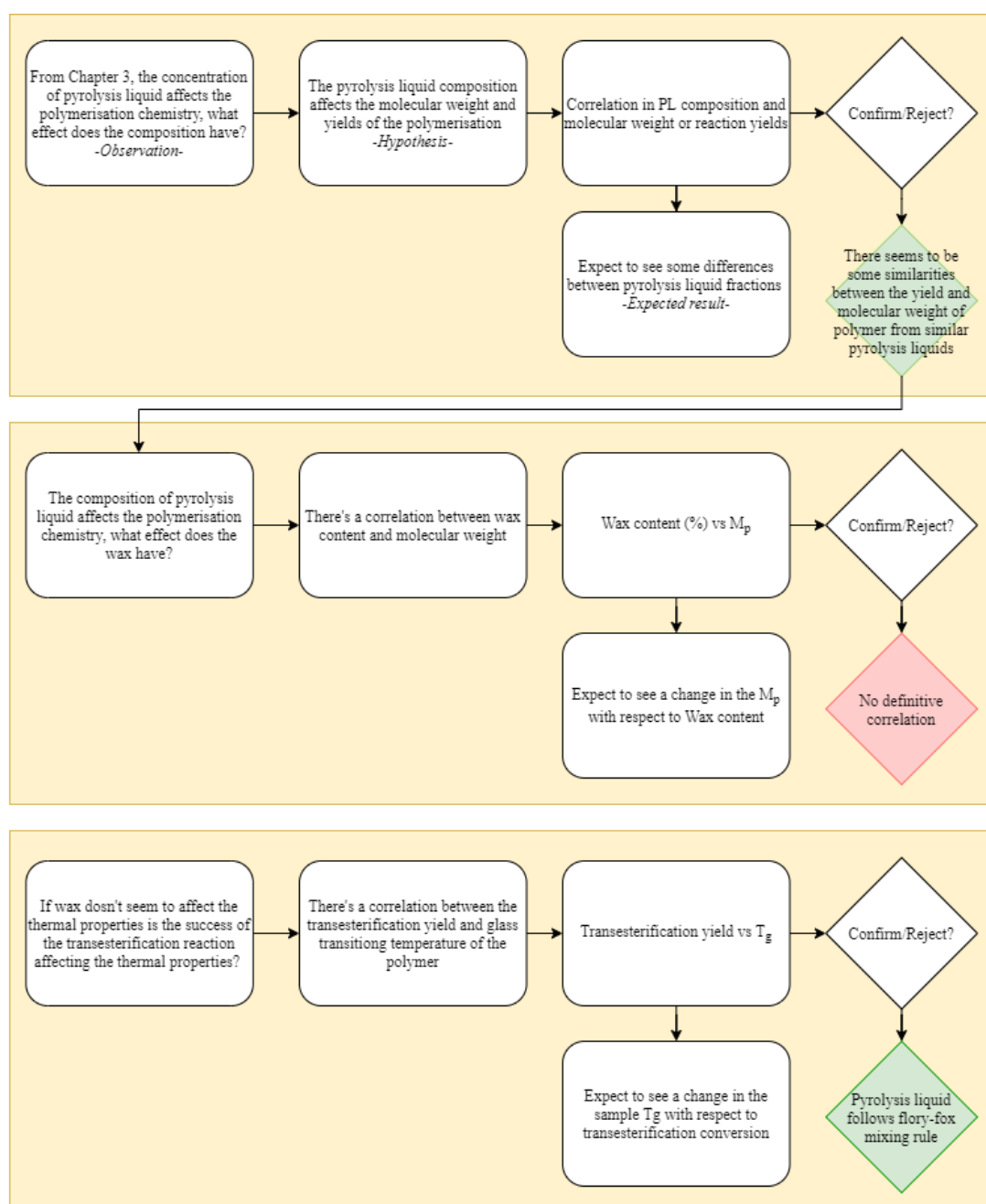
that there was co-removal of alcohols with a high vapour pressure. This would make sense as the most reactive would likely be those attached to the least steric bulk and coincidentally also the most volatile. This also raises further the questions of differences in alcohol reactivity with respect to transesterification, would primary, secondary and tertiary alcohols react at different rates?

Where in the commensurate water fractions there was little difference between the gas and liquid inerted pyrolysis systems, in terms of TE completion (*cf.* **2&9** vs. **3&10**). The liquid system cyclohexane insoluble fraction (**19**) has a lower yield, 18%, when compared to yields of 41-37% in the gas inerted systems (**6&13**). This trend is consistent across the Cyclohexane soluble fraction (20) where yields are as low as 19% when compared to the gas inerted system yields (**7&14**) at 49-51%.

This investigation shows that, despite consolidation of variables, the yields of both transesterification and polymerisation on different pyrolysis liquids remain inconsistent and therefore the composition and chemistry of pyrolysis liquid remains variable. The method developed for industrial pyrolysis liquid can be applied to other crude pyrolysis liquids from different methods and give similar yields however, solvent fractionation can have an enormous effect on the chemistry. It is not clear that the concentration of alcohols has an effect on the transesterification however, there are similarities between the transesterifications of different pyrolysis liquid fractions, despite different heating methods and concentrations of alcohol. It is clear from this investigation that a single drag and drop method for transesterification of pyrolysis liquid fractions is not feasible and further yield optimisation is needed for different fractions however, such optimisation was not necessary in this investigation and the unoptimised method used provided enough product to continue to polymerisation for characterisation.

4.4 Pyrolysis liquid composition effects on polymer properties

Below is a brief executive summary of the thought process from hypothesis to test and results rationale for the production of different pyrolysis liquid polymers from the various pyrolysis liquids which were produced in the previous investigation. Where expected results are presented, this is an expected result if the original hypothesis was correct. In this investigation there was not really a revision of hypothesis more a complete change in thinking from the correlation between wax content and molecular weight to the degree of transesterification determining the thermal properties. This hypothesis in hindsight fits better with the flory-fox mixing theory as an intrinsic explanation.^{169–171}



During the method development for the functionalisation of the industrial pyrolysis liquid, in chapter 3, it was noticed that there was an unreactive wax species present in the transesterified pyrolysis liquid. This wax was shown to affect the chemistry of the polymerisation and/or the material properties of the final product. These observations also raised questions as to whether there are other effects, that the inclusion of the wax produced, which had not been recognised as being due to the presence of this material. For example, its presence may be the origin of the changes to the transesterification chemistry. To try and define the full extent of the influence of this wax material, polymers were made, following the method developed in this work, from the different pyrolysis liquids and the fractions that they contain, introduced in Figure 47 are reproduced in Figure 58 for ease of reference.

The reason for this fractioning of the pyrolysis liquid is that in the liquid inerted fixed bed microwave pyrolysis the reaction results in two pyrolysis liquid “fractions”: one soluble and the other insoluble in the selected solvent.¹⁰³ Direct comparison of these liquid system pyrolysis liquids fractions with the crude pyrolysis liquids from fixed bed conventional or microwave pyrolysis is therefore not entirely fair. Figure 58 outlines the approach toward a direct compositional comparison. In the interest of a fair test, both the conventional and microwave gas inerted fixed bed pyrolysis liquids were extracted, using three different solvents with a range of different relative polarities; water ($\delta_{\text{water}} = 1.000$), 2-propanol ($\delta_{\text{2-propanol}} = 0.546$) and Cyclohexane ($\delta_{\text{cyclohexane}} = 0.009$) to create, streams 2-7 and 9-14 for comparison with streams 15-20 generated in the liquid inerted microwave pyrolysis system.^{156,157}

Full characterisation was conducted on a subset of five representative polymers produced from analogous fractions for the different reaction types conducted. This strategy was adopted to maximise the conclusions that could be drawn from these investigations. Polymers **1** and **2** were chosen to outline the difference between conventional and microwave pyrolysis. Polymers **11** and **12** allow for further comparison between conventional and microwave pyrolysis where solvent fractionation with cyclohexane is introduced as a variable. Polymer **16** was included for reference of higher wax content.

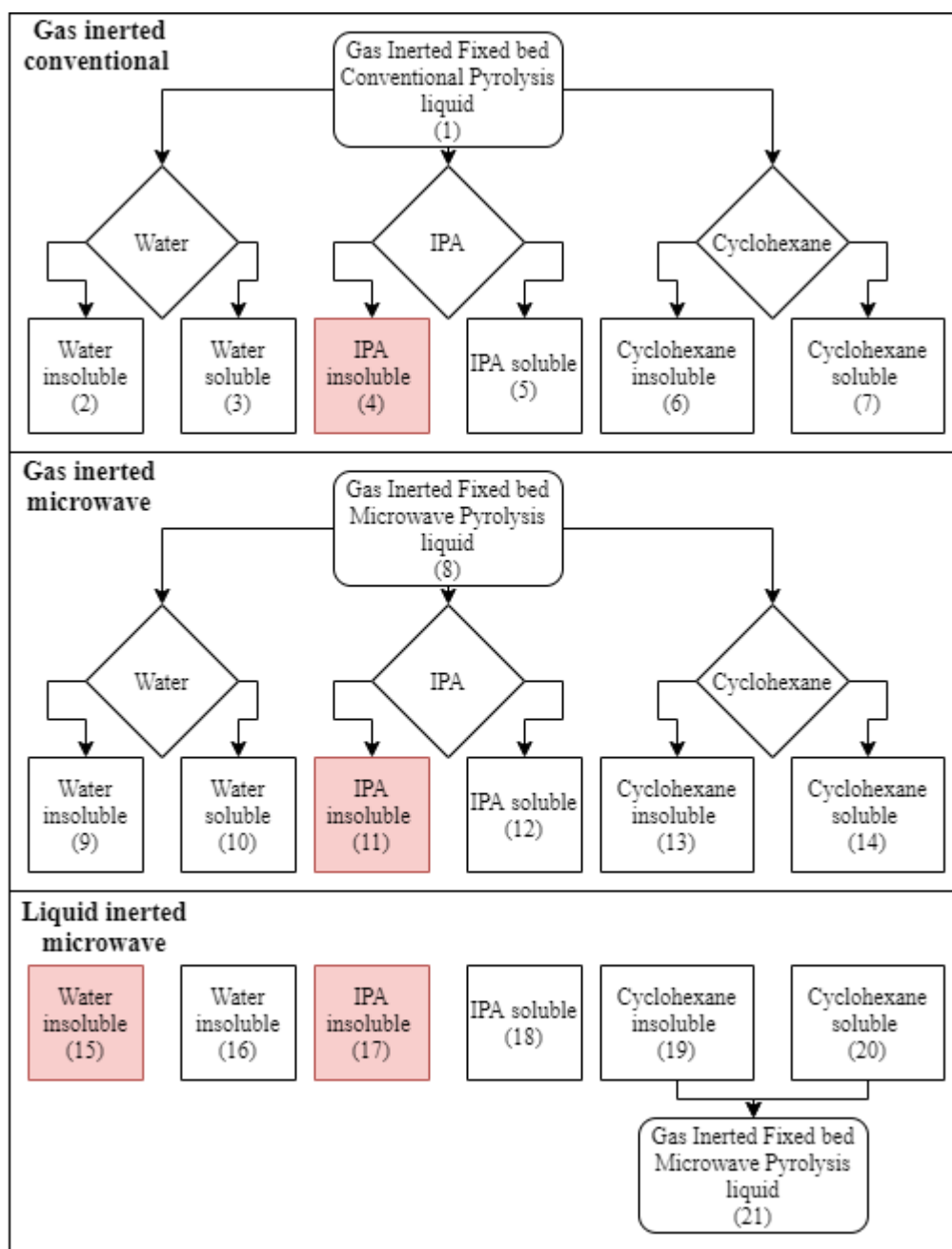


Figure 58 Schematic of liquid partitioning experiments and resulting fractions of pyrolysis liquid with water, isopropanol and cyclohexane and the resulting fractions which have been numbered for ease of reference. Fractions coloured red did not exist but included for completeness.

4.4.1 Pyrolysis liquid effect on molecular weight and yield

Since, in Figure 57 there was no clear correlation between the effect of the pyrolysis liquid composition and the chemistry of transesterification, it was prudent to see if there were effects on the radical polymerisation chemistry.

The molecular weights, and polymerisation yields are shown in Table 22.

Table 22 Summary of effect of pyrolysis liquid composition on molecular weight, conversion.

Entry #	Pyrolysis method	Solvent Fraction	M _n (kDa)	M _p (kDa)	M _w (kDa)	Polydispersity (M _w /M _n)	Polymer yield
1	Gas inerted conventional	Crude	42.2	46.3	56.3	1.33	54.75%
2		Water Insoluble	6.6*	4.6	36.7	5.56	82.05%
3		Water Soluble	28.3	29.5	31.1	1.10	82.49%
5		Isopropyl alcohol Soluble	3.50	4.3	16.8	4.80	76.02%
6		Cyclohexane Insoluble	41.1	55.8	59.9	1.46	79.21%
7		Cyclohexane Soluble	3.3*	2.2	13.2	4.00	79.21%
8	Gas inerted microwave	Crude	9.2	13.8	24.6	2.67	60.16%
9		Water Insoluble	16.4*	7.8	56.1	3.42	75.96%
10		Water Soluble	20.0*	10.3	66.8	3.34	74.75%
12		Isopropyl alcohol Soluble	21.3*	10.7	68.5	3.22	78.02%
13		Cyclohexane Insoluble	49	76.6	79.9	1.63	71.01%
14		Cyclohexane Soluble	2.8*	1.8	10.4	3.71	84.42%
16		Water Soluble	30*	15.4	108.5	3.62	77.32%
18	Liquid inerted microwave	Isopropyl alcohol Soluble	5.7	4.0	20.8	3.65	78.54%
19		Cyclohexane Insoluble	24.6*	15.6	49.4	2.01	81.48%
20		Cyclohexane Soluble	25.9	30.4	34.8	1.34	92.85%

Values marked * are suspected of being artificially higher due to coincident peaks. Polymer yield was calculated by comparison of ¹H-NMR monomer and polymer methacrylate peaks

Obvious from Table 22 was that there were a large range of molecular weights exhibited by the different polymers isolated from different sections of the process, as well as some of the differences between M_w , M_p and M_n .

The molecular weights of the wax peaks in these pyrolysis liquids were notably similar to that observed in the method development chapter *i.e.*, defined as material in the 1.5-2 kDa region. In some cases, the molecular weight of the polymer was much lower, hence there was no baseline separation between some of the peaks, as shown in Figure 59.

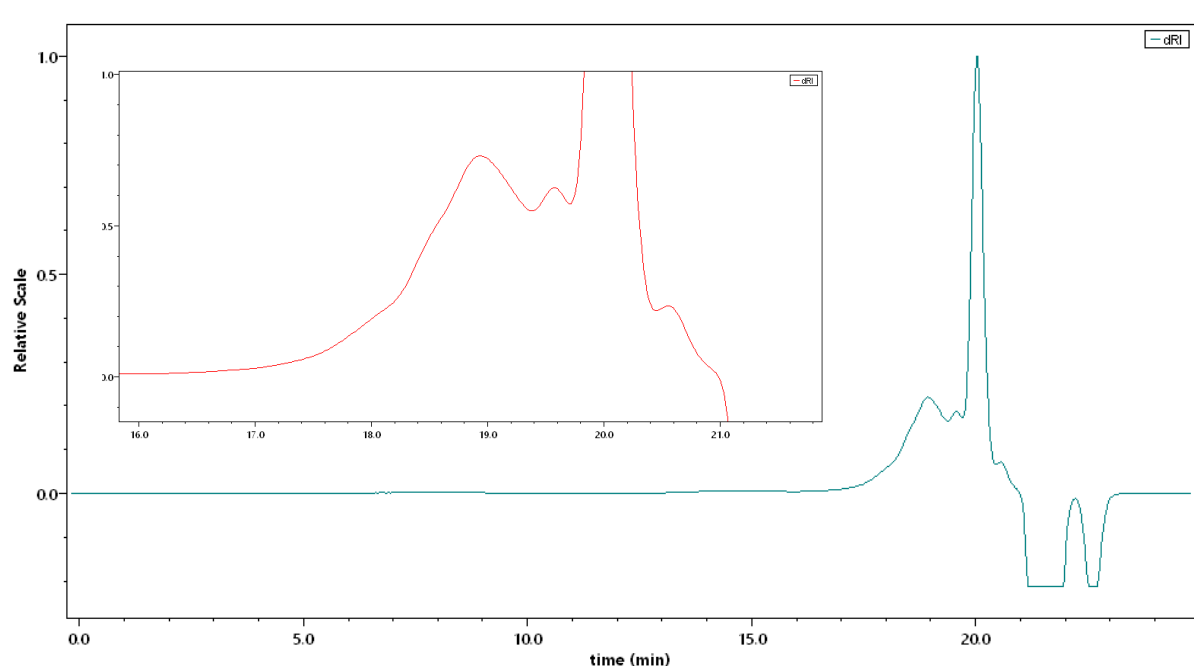


Figure 59 SEC chromatogram of polymer number 7 derived from gas inerted conventional pyrolysis liquid. Showing no clear baseline resolution between monomer, wax and polymer peaks.

As such the M_n , M_w and PDI data in Table 22 are not easily interpreted. This is because the lower molecular weight polymers were coincident with the wax, artificially inflating the concentration of the wax peak and also increasing the polymer M_n and M_w due to the exclusion of lower molecular weight species in the data analysis. This, in practice meant that in some cases M_n is artificially higher than M_p due to the cropping of the distribution. As a result, M_p was used for discussion in this work, as it is independent of the influence of molecular weight distribution and so gave a better estimation of changes in the material spectrum as a result of process changes

It should be noted that the polymer:wax ratio presented in Table 23 is calculated from the light scattering data assuming a constant refractive index increment (d_n/d_c). It is likely that;

- the wax is made up of many different molecules with different individual d_n/d_c values

- the concentration of these molecules will vary between pyrolysis liquids
- the d_n/d_c of the wax will be different to that of the polymer

These could be investigated by preparative scale GPC to isolate the wax and polymer fractions for further analysis.

Consequently, the M_p values were used as the primary indicator of molecular weight to define trends in the data for the reasons listed above, and so compare similar pyrolysis liquid fractions such that the patterns in the data became clear, as shown in Table 23.

Table 23 Summary of effect of pyrolysis liquid composition on peak molecular mass of polymer product, same data as Table 22 but grouped by solvent fraction as opposed to pyrolysis method. Transesterification yield was calculated by comparison of starting concentration of alcohol with moles of butanol distilled. Polymer yield was calculated by comparison of ¹H-NMR monomer and polymer methacrylate peaks. Note that the molecular weight data from Table 22 has been included for reference and values marked * are suspected of being artificially higher due to coincident polymer/wax GPC peaks.

Entry	Pyrolysis method	Solvent Fraction	Trans esterification yield (%)	Polymer yield (%)	Process efficiency (TE x PZN) (%)	M _p (kDa)	Polydispersity (M _w /M _n)	Polymer wax content
1	Gas inerted conventional	Crude	81.79	54.75	44.78	46.3	1.33	12.33%*
2	Gas inerted microwave	Crude	83.33	60.16	50.13	13.8	2.67	40.00%*
3	Gas inerted conventional	Water Insoluble	76.32	82.05	62.62	4.6	5.57	78.59%*
4	Gas inerted microwave	Water Insoluble	77.95	75.96	59.21	7.8	3.42	54.08%
5	Gas inerted conventional	Water Soluble	21.15	82.49	17.45	29.5	1.10	72.53%*
6	Gas inerted microwave	Water Soluble	21.63	74.75	16.17	10.3	3.34	2.09%
7	Liquid inerted microwave	Water Soluble	21.34	77.32	16.50	15.4	3.62	1.96%
8	Gas inerted conventional	IPA Soluble	24.79	76.02	18.85	4.3	4.80	98.49%*
9	Gas inerted microwave	IPA Soluble	21.49	78.02	16.77	10.7	3.22	2.90%
10	Liquid inerted microwave	IPA Soluble	19.06	78.54	14.97	4.0	3.65	77.62%*
11	Gas inerted conventional	Cyclohexane Insoluble	41.21	79.21	32.64	55.8	1.46	2.32%*
12	Gas inerted microwave	Cyclohexane Insoluble	37.37	71.01	26.54	76.6	1.63	3.28%*
13	Liquid inerted microwave	Cyclohexane Insoluble	18.39	81.48	14.98	15.6	2.01	77.16%*
14	Gas inerted conventional	Cyclohexane Soluble	49.88	79.21	44.78	2.2	4.00	2.33%
15	Gas inerted microwave	Cyclohexane Soluble	51.41	84.42	50.13	1.8	3.71	4.25%
16	Liquid inerted microwave	Cyclohexane Soluble	19.43	92.85	62.62	30.4	1.34	43.90%

From this data, all polymerisation gave at least 50% yield by $^1\text{H-NMR}$. It was noticeable that the two polymerisations of the functionalised crude pyrolysis liquids, polymers **1** and **2**, gave the lowest polymerisation yields. This is in contrast to the chemistry of transesterification where these fractions gave the highest yields. Conversely fractions **5–10** show transesterification yields of only 19-25% but polymerisation yields are consistently above 75%. These results would appear to show that where the transesterification yield is higher and hence more “pyrolysis monomer” was produced, the polymerisation yield was lower with the inverse also holding true to the trend. This leads to the potential hypothesis that the reactivity ratio of the methacrylated pyrolysis monomer is lower than that of the residual BMA, hence when the transesterification yield is higher and the concentration of pyrolysis monomer is greater, the polymerisation yield is lower. An estimation of the overall process efficiency was calculated via multiplication of the yields of transesterification and polymerisation steps.

Now, the process efficiency measurement is only a preliminary assessment of how well the conversion of pyrolysis liquid into pyrolysis polymer may proceed. It is important to note that this value did not consider the yields from the pyrolysis process nor does it include any losses due to the solvent fractioning of pyrolysis liquid. Since the crude pyrolysis liquids (**1&2**) did not undergo fractionation, and hence involve one less process step, these would likely have the overall highest process efficiency. If fractionation is desired, then a process that combines both pyrolysis and liquid fractionation is ideal and the process yield of the cyclohexane inerted microwave pyrolysis polymer (**16**) would seem to not only offer one less process step but the process efficiency from pyrolysis liquid to polymer would seem to be greater than separate fractionation steps.

This calculation revealed that in fact the water insoluble fractions of gas inerted pyrolysis (**3 & 4**) and cyclohexane soluble fraction from the liquid inerted (**16**) showed the greatest overall process efficiencies. Comparing the M_p values of fraction **3**, **4** and **16** it is clear that fraction **16** shows the highest molecular weight material.

4.4.2 Wax effect on polymerisation

Looking at the peak molecular weight (M_p) and polydispersity of all polymers, there are considerable differences between similar pyrolysis liquids. Fraction **11**, **12** and **13** exemplify this where with roughly similar polymerisation yields 70-80% show a range of M_p values from 15 – 76 kDa and dispersity values from 1.4-2.0. Indicating, that while the polymerisation reaction chemistry may be similar, in similar pyrolysis fractions there may be differences in the products.

Building on the findings from the earlier chapter where an unreactive wax was identified, this same peak was identified and quantified using the light scattering peak area relative to the polymer peak. The wax content of the

polymers and compared to M_p are presented in Figure 60, individual data points are labelled with fraction numbers.

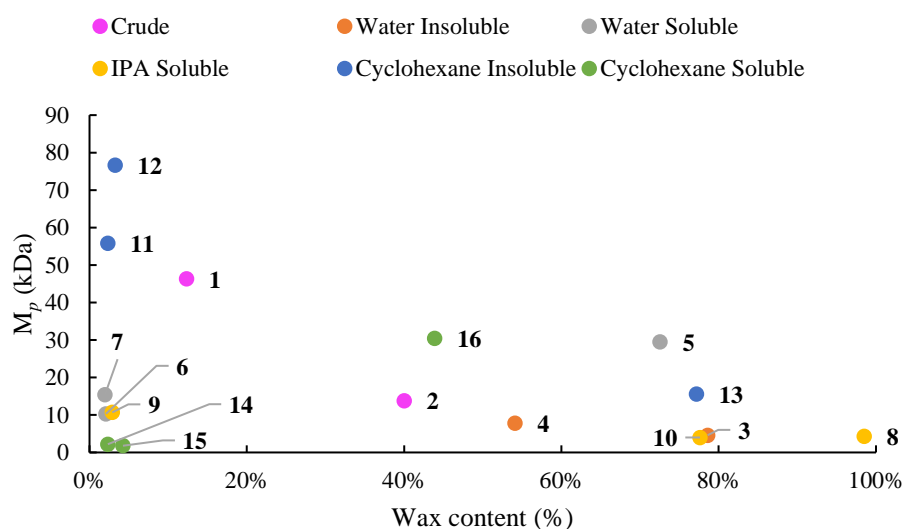


Figure 60 The effect of wax content of polymer on the peak molecular weight of polymer produced by radical polymerisation of the functionalised pyrolysis liquids. With fractions numbered for ease of reference.

From Figure 60 it appears to be a non-linear but negative correlation between wax content and molecular weight.

However, there were some notable exceptions where there was low wax content and low molecular weight. These were runs **7**, **10**, **12**, **14** and **16** in Table 23, including the water-soluble fractions (grey), isopropyl alcohol soluble fractions (yellow) and cyclohexane soluble fractions (green). These results were interrogated separately and the only water-soluble fraction result that seemed to follow the trend was from the gas inerted conventional pyrolysis liquid (**5**) where in the cyclohexane soluble fraction the result that seemed to fit the trend would be in the liquid inerted microwave (**16**). Both the seemingly acceptable results were of higher molecular weight than other results of similar wax contents and as such were not deemed reliable.

It is interesting to note that for the isopropanol soluble fractions (**8-10**) there were low molecular weights despite reasonable polymerisation yields across a range of wax contents. Due to the low molecular weight and high conversion, a greater number of radicals could have formed during the polymerisation which then limited the molecular weight. Alternatively, a molecule was present only in this fraction and acted as a pseudo “chain transfer” agent and hence limiting the molecular weight in this manner – this is less likely due to broad dispersity observed. Though the GPC, as a measure of polydispersity in this case, is hampered by the coelution of polymer and wax

peaks. This phenomenon is potentially of interest for further investigation as it is consistent across all three fractions.

The crude (magenta) and water insoluble fractions (orange) showed a decrease in molecular weight with respect to wax content however the water insoluble fraction had a higher overall wax contents and also showed less significant differences in molecular weight, suggesting that the effect wax content on molecular weight is more apparent at lower overall wax concentration.

4.4.3 Thermal properties

The OH content of the starting pyrolysis liquid, molecular weight data, wax content, glass transition temperature and decomposition temperature are reported in Table 24.

Table 24 Preliminary thermal analysis of pyrolysis polymer materials, with pyrolysis liquid alcohol concentration data from Table 21 and transesterification yield, M_p , and wax data from Table 23 included for ease of reference.

Sample #	Pyrolysis	Fraction	[OH] (mmol/g Pyrolysis liquid)	Trans esterification yield (%)	M_p	Polymer wax content	T_g	T_{deg}
1	Gas inerted conventional	Crude (1)	4.32	81.79	46.3	12.33%	-6.09	145
2		Cyclohexane insoluble (11)	3.50	41.21	55.8	2.32%	8.38	148
3	Gas inerted Microwave	Crude (2)	16.15	83.33	13.8	40.00%	-5.93	83
4		Cyclohexane insoluble (12)	6.22	37.37	76.6	3.28%	2.23	132
5	Liquid system	Cyclohexane insoluble (13)	3.73	18.39	15.6	77.16%	17.3	80

Initially there are a few patterns that emerge from this data, where the molecular weight of the polymer is higher, in samples **1**, **2** and **4** the decomposition temperature is higher however, in the samples with lower molecular weight, **3** and **5**, the decomposition temperature is lower. This could indicate that the decomposition is due to the chain ends as where molecular weight is lower, the chain end density is higher and so consequently decomposition begins at a lower temperature. It has been shown elsewhere that methacrylate chain ends can be capped to further increase thermal stability of methacrylate polymers and this kind of investigation could prove a promising way to further improve the thermal stability of the polymer in future work.¹⁷²

If the T_g values are compared with the transesterification yield values, there should be a pattern as a lower transesterification conversion should mean that there is a greater amount of unreacted BMA in the “transesterified

monomer” fraction. Now bearing in mind the Flory-fox mixing rule for methacrylate polymers, that should mean that the lower the transesterification completion, the closer the T_g should be to that of the BMA feed. This data is presented in Figure 61.

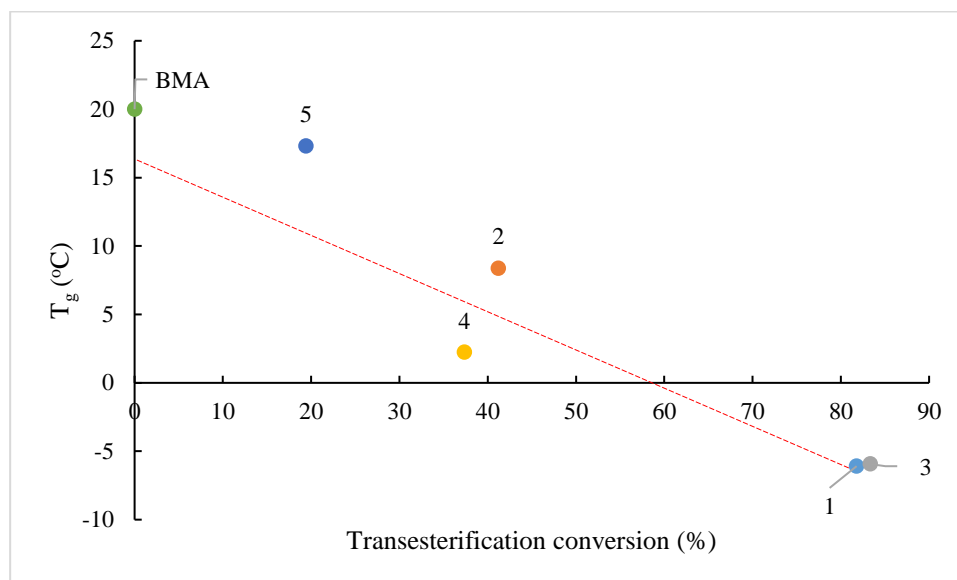


Figure 61 Glass transition temperature vs transesterification completion for five targeted pyrolysis polymers with T_g of BMA included for reference. Note that line of best fit excludes point number 5 and continues beyond data points.

From Figure 61, it is clear that there seems to be a linear negative correlation between transesterification conversion and glass transition temperature, a line of best fit can be fitted with the equation $y = -0.3236x + 20.174$ and with the $R^2 = 0.9224$ indicating a good fit. The implications of this in terms of the Flory fox mixing diagram for where x, the conversion, is 100% and this would be representing, hypothetically where any unreacted BMA is removed would mean that the T_g would be in the region of -12 °C. This ostensibly would mean that despite the difference in pyrolysis method, wax content and pyrolysis liquid alcohol content, the glass transition temperature could be tuned through control of the transesterification conversion. The differences in transesterification conversion observed under the same conditions, raise further questions about whether there is a difference in reactivities of the alcohols in the pyrolysis liquid and hence this limits which alcohols are being converted into monomer and hence form a part of the polymer. This is discussed further in the future work section.

4.4.4 Summary

Pyrolysis liquids from a range of different pyrolysis methods using a consistent feedstock and equivalent pyrolysis temperatures were transesterified using a developed method and subsequently polymerised in this investigation. Despite some difficulties in discerning peak molecular weights of polymer-due to coelution of wax and low

molecular weight species-data on the molecular weight, dispersity, wax content and yields of methacrylate polymers from various pyrolysis liquid fractions were presented.

In terms of the yields of the different reaction steps, there are many ways to interrogate this and the reader is invited to use the data presented here for their own interpretation but there seems to be similarities between the yields of similar pyrolysis liquid fractions, further indicating a broad compositional similarity. The isopropanol soluble fraction of pyrolysis liquids exhibited a consistently low molecular weight polymer.

A strong trend in the transesterification conversion effect on the glass transition temperature of the polymer was observed. From this data a T_g of -12 °C for the pyrolysis liquid monomer was quantified. This observation could allow for control over the thermal properties of the pyrolysis polymer through control of transesterification reaction coordinate.

4.5 Preliminary Application specific testing

The following section presents data, results and interpretation of work undertaken by Matthew Elsmore and included in this section with his permission and will be subject to publication elsewhere at a later date.

The main effort of this work was to investigate pyrolysis and the effect on the physical properties of the polymer in order for screening of potential applications. The challenge with identifying applications for completely novel polymers is that in order to comprehensively conclude that an application is appropriate, then an intensive and specific regime of testing is necessary; The original end goal of this work was to identify one or two potential applications and generate data to investigate whether this material was appropriate. A further challenge is that applications are not mutually exclusive; the same product can be used for more than one application and there may be overlaps in the testing required for different applications but the approach of the authors was to treat each application differently. These challenges proved to be too ambitious a goal for a PhD finishing in 2020. However, the testing rationale and “roadmap” for application testing are included below;

Based on experience during manual handling of the novel polymer generated from pyrolytic lignin, it was found that the material exhibited highly tacky behaviour and bonded to a wide range of laboratory apparatuses manufactured from steel (spatulas and tweezers), wood (work benches), glass (vials), plastics (bottle lids) and protective rubber gloves. This behaviour indicated potential application as a hot melt adhesive (HMA). Originally, the scope was to include testing with both HMA and pressure sensitive adhesives (PSA) as potential target applications. This was later expanded to include bitumen binder type materials.

where the ability to adhere to substrates of varying chemistry is highly beneficial, whilst also offering the option of re-use and recyclability via application of heat. However, the presence of T_g slightly below ambient conditions poses problems regarding creep under loading, whereby the polymer dissipates applied stresses through viscous relaxation. The result of such behaviour would cause gradual separation of the adhesive bond and eventual failure. In an effort to overcome this, copolymerisation with MMA was carried out at varying concentrations, providing an increase in T_g . To confirm the viability of such an application, this requires vigorous characterisation of adhesive strength and processing performance in order to establish suitable conditions for bond formation in comparison with a commercial benchmark for validation.

A further industrial application for this novel family of polymers is in road surfacing, where a necessity for renewable asphalt and bitumen binders has been expressed in the relevant literature.^{173–178} Conversely to HMA, bitumen binders typically exhibit sub-zero degrees Celsius glass transition temperatures and very low viscosities at ambient conditions. The ability to adhere well to aggregate materials is imperative to ensure the structural integrity of road surfacing, which in addition to the widely available and sustainable nature of biomass feedstock indicates methacrylate polymers from pyrolysed wood to be a suitable candidate in this field. Through variation of the waxy oligomeric content of the lignin-derived polymer, it was found that T_g and viscosity could be greatly influenced as discussed in this thesis. Through further investigation into the relationship between molecular weight properties, wax concentration and thermorheological performance, it will likely be possible to establish optimal polymer compositions for use in this application.

4.5.1 Preliminary Adhesive testing

During polymer characterisation it was noted the extreme affinity for metallic surfaces. It was proposed that the pyrolysis polymer would be suitable for use in HMA applications due to the melt flow and adhesive properties empirically observed. Preliminary data was generated to quantify this, shown in Figure 62.

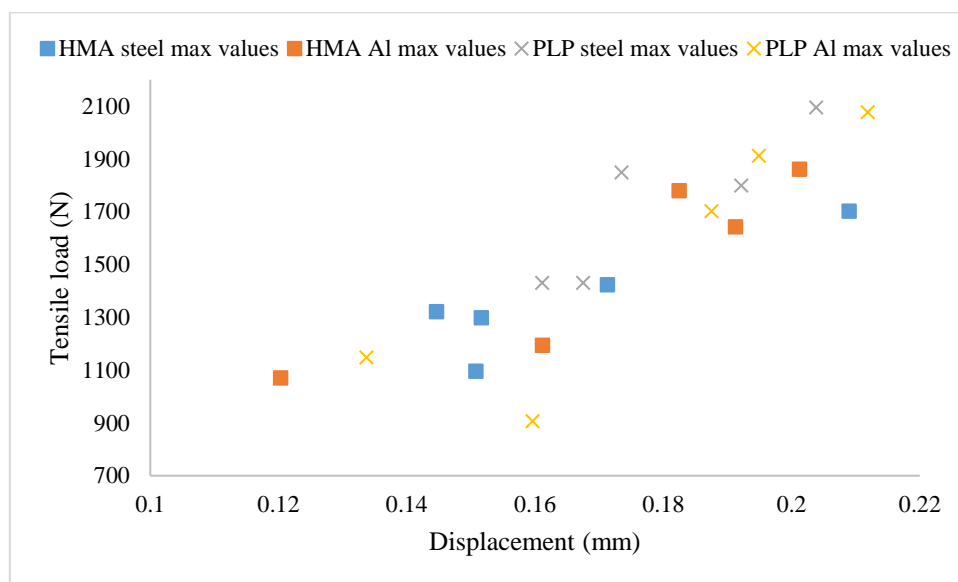


Figure 62 Tensile load as a function of displacement for the pyrolysis liquid polymer (X) and an industrial hot melt adhesive (square) across both stainless steel and aluminium fixtures.

Figure 62 shows that the ratio of displacement to tensile load for the industrial HMA and the pyrolymer of similar magnitude and the failure load of the pyrolymer is slightly higher which implies a similar if not slightly improved adhesive behaviour, should be noted that the pyrolymer failed cohesively. Additional adhesive testing on copolymerised polymer is underway. Please note this experimental work was carried out by Matthew Elsmore.

4.5.2 Tuning Polymer Properties through copolymerisation

In order to meet the performance requirement of different applications, it would be desirable to alter the physical and chemical properties of any pyrolysis derived polymeric product. The addition of a second monomer in the polymerisation will typically affect the T_g of the product in line with the Flory-Fox equation.^{170,179–182} The level of chain entanglement can also affect the brittleness exhibited by the copolymer. Therefore, Di(ethylene glycol) methyl ether methacrylate (DEGMA) and Methyl Methacrylate (MMA) were chosen in the hope that they would lower and raise the T_g and decrease and increase the amount of chain iteration and entanglement of the resulting pyrolymer respectively. The copolymers synthesized within this study are detailed in Table 25.

Table 25 Physical and molecular properties of Transesterified pyrolysis liquid polymer containing copolymers synthesised by free radical polymerisation.

Monomer(s)	Feed ratio (%)	Copolymer ratio (%) [*]	Conv. (%)	\bar{D}	M_n (g·mol ⁻¹)	T_g (°C) obs
1 MMA	100	-	-	2.1	117300	105
2 DEGMA	100	-	-	1.6	116200	-36
3 Transesterified industrial pyrolysis liquid	100	-	77	1.8	20400	14.8
4	77/23	74/26	55	2.2	26400	-5.60
5 Transesterified industrial pyrolysis	58/42	63/37	61	2.7	38300	-16.83
6 liquid /DEGMA	50/50	47/53	58	2.1	80000	-20.06
7	39/61	37/63	57	3.1	111300	-20.86
8	20/80	23/77	53	3.8	140000	-22.13
9	78/22	90/10	65	1.9	20300	14.66
10 Transesterified industrial pyrolysis	59/41	79/21	76	1.9	27400	17.82
11 liquid / MMA	48/52	69/31	83	2.5	26400	17.94
12	39/61	59/41	84	1.9	32500	26.17
13	19/81	13/87	79	2.3	44300	73.5

^{*}Defined by ¹H-NMR analysis of methacrylate peaks

To investigate the ability to tune the T_g of the resultant copolymer, five representative feed ratios for two different comonomers were used and the resulting copolymers were subjected to spectroscopic analysis to define composition. NMR spectroscopic analysis of the copolymers showed that the final compositions were typically close to the target levels (Table 25). These results defined that the reactivity ratios of the monomer used were sufficiently alike that the polymerization process was robust enough for commercial manufacture of the target coating materials with an acceptable level of batch to batch reproducibility. The T_g s of the resultant copolymers were then measured experimentally and plotted against the values predicted by the Flory-Fox equation (see Figure

64) and were found to be in good agreement showing a linear trend ($R^2 = 0.96$). Deviation from the predicted value is likely due to residual high boiling point of the monomer within the copolymer material.

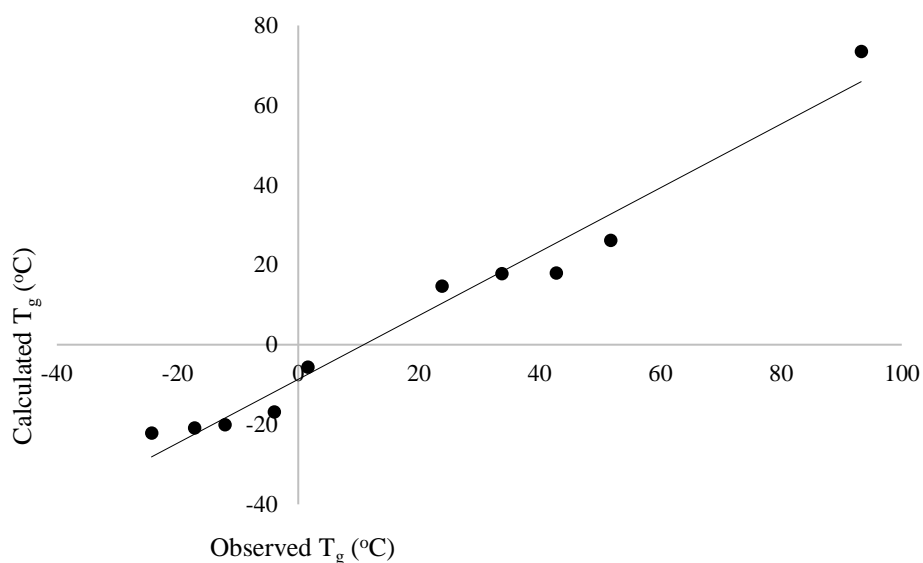


Figure 63 Flory fox plot to outline the relationship between predicted values shown by line and observed T_g values for copolymers

The linear trend in the data confirmed that this polymerization technique could be used to predictably deliver a copolymer with a target T_g by measuring that of the “hit” homopolymers and that these systems are robust enough to allow the fine tuning of the thermal and potentially the consequent mechanical properties. Subsequent experiments will investigate the adhesive properties of the polymer initially focussing on the level of DEGMA incorporation. The data in Table 25 shows that of the polymers synthesised, only the 60 and 80wt% of MMA copolymer exhibited a T_g that was below room temperature and thus likely to produce a flexible adhesive. Hence these combinations were selected for further study. The molecular weights of the resulting polymers were shown to typically increase as the comonomer concentration increased, with this effect being more pronounced in the DEGMA than the MMA copolymers.

Since the copolymerisations have been conducted in bulk without control agent, it is hypothesised that there is a species in the pyrolysis liquid that is acting as a control agent and when there is less pyrolysis liquid, there is less of this species. The increase in DEGMA concentration led to a reduction in the system viscosity because the reaction temperature employed is $\sim 70^\circ\text{C}$ above DEGMA’s T_g but is closer to, or below that, of the transesterified pyrolysis liquid and MMA copolymers. Thus any diffusion limitations that radicals encounter are reduced as the

lower T_g monomer concentration is increased, and therefore they operate more efficiently resulting in a higher molecular weight product.

The pyrolysis polymer was taken forward for adhesive testing and 80:20 mol% ratios were highlighted as a candidate to be taken forward for adhesive testing because the lower T_g and higher molecular weight are likely to make a more flexible and cohesive hence more usable adhesive. Nevertheless, the effect of varying DEGMA concentration on the molecular weights of the final polymers requires further investigation to confirm these proposed hypotheses.

The preliminary conclusion from this work is that for HMA, the focus should be on improving the usability (operating window), colour and smell. Formulation/copolymerisation could go a long way to realising these aims and it has been shown that copolymerisation can have a drastic effect on the physical properties.

4.5.3 Thermal and rheological properties of pyrolysis polymer and p(BMA)

The following is reproduced from published work elsewhere based on the work of Matthew Elsmore.¹⁸³

Following from the previous section where potential was seen for this pyrolymer material in use as a hot melt adhesive, the rheological behaviour and hence the rough operating window could be outlined along with any potential differences in behaviour relative to BMA across potential use temperatures.

The elastic storage modulus G' and viscous loss modulus G'' responses measured in thermal ramps at constant 1 Hz frequency are shown in Figure 64 for the pyrolysis polymer and the p(BMA). In order to account for the slightly different T_g , the ordinate axis is offset by T_g . The elastic and viscous parts of the responses of both materials are similar across a broad range of temperature, with only some deviation noted at higher temperature.

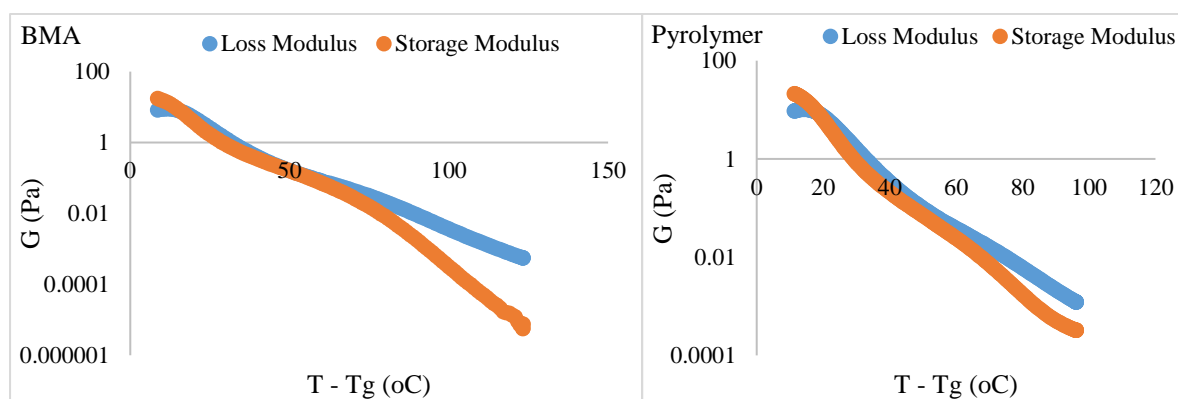


Figure 64 Thermal scan conducted at a cooling rate of $2\text{ }^{\circ}\text{C}\cdot\text{min}^{-1}$ shows G' (a) and G'' (b) response for the pyrolysis polymer and p(BMA). Close agreement between the two materials is noted for temperatures around T_g , however deviation at higher temperatures is observed.

In order to study this in more detail, isothermal frequency sweeps were carried out at temperature intervals of 30, 35, 40, 45, 55, 65, 80, 100 °C for the pyrolysis polymer and 40, 50, 60, 80, 95, 125 °C for p(BMA), to provide sufficient overlap of individual data curves to form mastercurves. Temperature intervals were predicted using the Williams–Landel–Ferry equation and universal C_1 and C_2 constants aiming for an overlap of 0.5 decades of frequency.^{184,185} The individual isothermal curves were manually shifted in frequency to produce the T_g -normalised frequency mastercurves of G' and G'' shown in Figure 65.

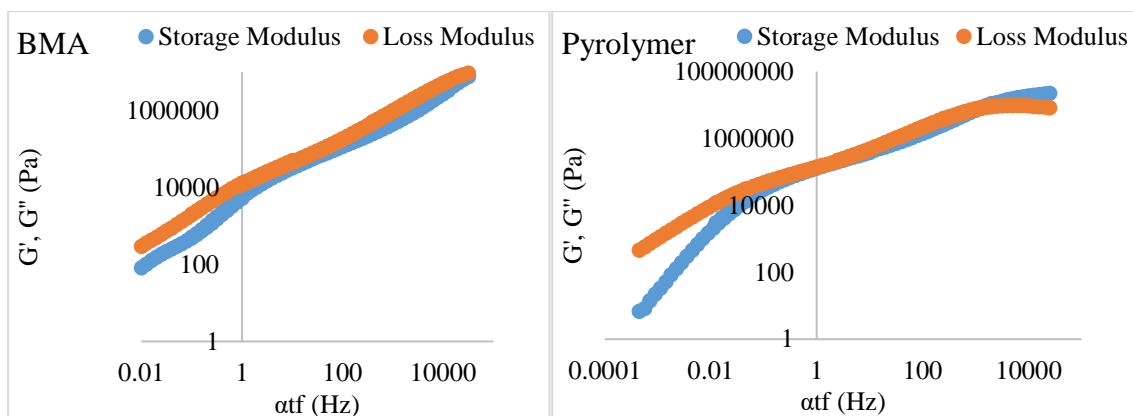


Figure 65 Frequency mastercurves for (a) the pyrolysis polymer and (b) p(BMA) at $T_{ref} = T_g + 50$ °C. G' , G'' .

Although the behaviour is similar, there are two important differences. Firstly, the pyrolysis polymer exhibits lower moduli by approximately an order of magnitude across the temperature range. Secondly, in the low frequency flow region, the p(BMA) exhibits the expected power-law behaviours with gradients very close to 2 and 1 in G' and G'' respectively, but the pyrolysis polymer does not, particularly in G' .¹⁸⁶ These differences point to the role of the wax component in reducing the elasticity and the viscosity and preventing a clear entanglement plateau. In addition, structural changes are apparent at high temperatures in the pyrolysis polymer in processes related to those that eventually lead to char formation. The key point is the region of $T-T_g$ around the operating window, since this for most applications would be around room temperature, the region 10-60 °C is most important and is where good similarity between pyrolysis polymer and BMA lies in both Figure 64 and Figure 65.

4.5.4 Thermal instability

The low molecular weight pyrolysis polymers exhibit a low thermal degradation temperature, this in some cases is coupled with a high melt flow temperature often with a melt flow region of only 20-30 °C. This is not a big processing window. Routes to improving this depend on the method of decomposition at these elevated temperatures. Often the polymer chain end groups determine the thermal decomposition. Polymers where chain ends that are more thermally stable than the chain itself will not degrade preferentially at the chain ends. A study into the thermal decomposition pathway of the polymer would fit well with the bio-degradability work along with studies into decomposition products of both routes. This investigation would shed light on approaches to increasing the melt flow region by increasing the thermal degradation temperature. It would tie the pyrolysis polymers work together and close the life cycle loop if there were a way to thermally recover monomer from the polymer product. This could be applicable in various other fields where polyacrylates are used as these are currently not widely recyclable.

4.5.5 Bitumen binder

During the preliminary rheological investigation it was noticed that the rheological profile of the pyrolysis liquid polymer was similar to that of other synthetic bitumen binders developed by Airey *et al.*^{173–175,177,178,187,188} This led to a further potential application. The testing regime for this is similar to that of HMA and so the investigations could be conducted in parallel. The specific test required would be very dependent on the rheological profile, as well as thermal stability and moisture sensitivity. A brief summary of the testing that could form the foundation of an investigation into the use of pyrolysis liquid polymers as bitumen binders would include;

- Moisture sensitivity work/leaching.
- Water contact angle testing at different temperatures.
- Rheology and further adhesive testing.
- Formulation and additive testing.
- Toxicity/ cytotoxicity testing.
- Leaching, aging and oxidation testing.
- Accelerated aging testing (Temperature, moisture, UV effects on mechanical and rheological properties).

4.6 Conclusions

A direct comparison of the pyrolysis liquid composition from gas inerted conventional, gas inerted microwave and the liquid inerted microwave pyrolysis, with identical feedstock and comparable reactor conformations has been undertaken. Temperature was a key variable in pyrolysis reactions and can affect both the composition and yield of pyrolysis. Pyrolysis liquid yield with respect to mass loss was within 6% so reaction temperature was assumed not to be the cause of compositional differences. This study showed that there are significant compositional differences by GC-MS in the liquid inerted microwave pyrolysis system. The broad compositional differences in the liquid inerted microwave pyrolysis system showed a reduction in the acid content, indicating less secondary pyrolysis with a correspondingly higher alcohol content as these molecules are usually consumed in the reaction. This trend was exemplified in the specific differences in the Coumaryl alcohol and Coumaryl aldehyde concentrations. These observations lend further weight to pyrolysis reaction mechanisms proposed elsewhere.

An investigation into the solvent partition effects showed that while there is a partition effect that could account for some of the differences in the acid and alcohol concentrations, there are 15-20% that are not explained by the partition and could be due to a difference in the system where liquid inerting is used in place of gas.

The transesterification method developed for industrial pyrolysis liquid can be applied to other crude pyrolysis liquids from different methods and give similar yields however, solvent fractionation can have an enormous effect on the chemistry. It is not clear if the concentration of alcohols has an effect on the transesterification however, there are similarities in the yields the transesterifications of different pyrolysis liquid fractions, despite different heating methods and concentrations of alcohol.

Transesterified pyrolysis liquid was subsequently polymerised in this investigation. All polymerisations went to at least 50% conversion, it is noticeable that the two polymerisations of the functionalised crude pyrolysis liquids, gave the lowest polymerisation conversions, this is in contrast to the chemistry of transesterification where these were the most successful fractions.

A strong trend in the transesterification conversion effect on the glass transition temperature of the polymer was observed. From this data a T_g of $-12\text{ }^{\circ}\text{C}$ for the pyrolysis liquid monomer was quantified. It was shown that the T_g could further be altered through copolymerisation with DEGMA and MMA. This observation could allow for control over the thermal properties of the pyrolysis polymer through either control of transesterification reaction

coordinate or through copolymerisation. Preliminary analysis shows that there is potential to make use of these tunable properties in hot melt adhesive or in bitumen binder applications.

Chapter 5. Conclusions, future work and recommendations

5.1 Conclusions

The first chapter of this Thesis focussed on developing a method to produce high molecular weight products from biomass pyrolysis liquid. Investigation into pyrolysis liquid transesterification showed that under standard conditions, polymerisation of methacrylate was initiated during transesterification. Addition of radical inhibitor and reduction of reaction temperature were both presented as possible solutions. Temperature reduction was favoured due to reduced energy cost, process complexity, as well as no need to purchase, separate and then dispose of ancilliary reagents. Kinetic investigation of reduced temperature transesterification showed that the transesterification reaction is complete after 30 minutes which, when compared to the standard two hours, represents a further energy and time saving. Water was shown to have a significant effect on the transesterification reaction. It was shown that less water sensitive catalysts did not perform the transesterification in the presence of water, suggesting that water removal is needed to drive the transesterification to completion. Experimentally, this removal of water was carried out prior to addition of catalyst, via vacuum distillation. However, this represents an extra process step which is undesirable. On a lab scale, this step could be achieved using similar equipment to the transesterification however, it is unclear if the same could be said for larger scale production. Further catalyst screening and process development could combine the water removal and distillation steps in the functionalisation of the pyrolysis liquid in processes of increasing scale.

The functionalised pyrolysis liquid was used as the starting material for a free radical polymerisation. Radical initiator concentration and solvent were treated as variables. Increasing the initiator concentration has shown to result in an increase in conversion and peak molecular weight and solvent has shown to have a negative effect on the polymerisation, both in terms of conversion and on peak molecular weight. A candidate pyrolysis liquid polymer was selected for further analysis owing to the highest conversion, molecular weight and T_g . The SEC chromatograms show that an additional molecular weight species is present in the polymer sample. A kinetic study demonstrated that this material was present from the outset and did not increase during reaction. The molecular weight of this wax, 0.5-2 kDa is similar to that of pyrolytic lignin. By varying the amount of residual BMA present in the transesterification step, the effect of the pyrolysis liquid monomers on the polymerisation was investigated.

Through effectively changing the concentrations, it was shown that these pyrolysis liquid monomers reduce both the polymerisation conversion and molecular weight when in high concentration.

In the second chapter experimental conditions, to compare pyrolysis heating methods with equivalent yields, were generated. These were empirically confirmed through the small variation in liquid yields observed between methods. These pyrolysis liquids were interpreted in relation to the primary and secondary decomposition reactions of model compound pyrolysis. The results showed that although there were no new molecules in the liquid inerted microwave pyrolysis liquid, there were differences in the distribution of products. Differences between heating methods were noted with more furans observed in conventional pyrolysis liquids, consistent with literature elsewhere. A 15-20% increase in the alcohol concentration of the liquid inerted microwave pyrolysis system was identified compared to the gas inerted microwave pyrolysis. This difference in composition of the liquid inerted microwave, when compared to gas inerted microwave pyrolysis liquids extracted with solvent, show consistency across a range of solvent polarities. This similarity across pyrolysis methods could be attributed in part to an interaction between the pyrolysis liquid and the solvent with no evidence of the more reactive species surviving through to the ex-situ analysis stage, though a direct comparison of gas inerted and liquid inerted pyrolysis is not possible and such a comparison would be needed for a definitive conclusion.

The subsequent investigation into applying the industrial pyrolysis liquid transesterification method to these different pyrolysis liquids showed mixed results, with yields from 40-80% in both transesterification and polymerisation steps. This reinforces that, despite the best efforts of the author to rationalise variables, the composition and chemistry of pyrolysis liquid remains varied and unpredictable as one transesterification method, although consistent when applied to similar pyrolysis liquids is not consistent across a range of different pyrolysis liquids. The method developed for industrial pyrolysis liquid can be applied to other crude pyrolysis liquids from different methods and give similar yields however, solvent fractionation can have an enormous effect on the chemistry. It is not clear whether the concentration of alcohols have an effect on the transesterification however there are similarities between the transesterifications of different pyrolysis liquid fractions, despite different heating methods and concentrations of alcohol. It is clear from this investigation that transesterification of pyrolysis liquid fractions is feasible and though yields were in some cases low, they were consistent across similar pyrolysis liquids and this method provided enough monomer to continue to polymerisation for characterisation.

The polymerisation reaction data across the board looked positive, with all polymerisations, bar those of the crude pyrolysis liquids, going to at least 70% yield.

There seemed to be similarities between the yields of transesterification of similar pyrolysis liquid fractions but differences between fractions, for instance water insoluble fractions of conventional and microwave gas inerted pyrolysis give transesterification yields of 76.32 and 77.95% where the corresponding water soluble fractions give 21.15 and 21.63% respectively. An apparent negative correlation between wax content and M_p was observed but further investigation would be needed to conclude if there is causality. Five of the synthesised polymers were characterised further.

An apparent negative correlation between wax content and M_p was observed but further investigation would be needed to conclude there is a causality, this had a knock-on effects as the polymers with high wax content had lower molecular weight and hence also lower thermal decomposition temperatures.

A strong trend in the transesterification conversion effect on the glass transition temperature of the polymer was observed. From this data a T_g of -12 °C for the pyrolysis liquid monomer was quantified. This observation could allow for control over the thermal properties of the pyrolysis polymer through control of transesterification reaction coordinate.

5.2 General Future work

The future work from this thesis is tied to its weaknesses. There are several negative properties of the pyrolysis liquid derived polymer and any future work should, in the opinion of the author, focus on mitigating these.

5.2.1 Pyrolysis analysis

In this study, there was a similarity across pyrolysis methods that could be attributed to an interaction between the pyrolysis liquid and the solvent with no evidence of the more reactive species surviving through to the analysis stage. As gas chromatography is a time averaged analysis technique, in situ IR and EPR measurements will be needed to confirm the existence of more reactive molecules along with a way of preventing the solvent-based decomposition of products in any subsequent liquid inerted microwave pyrolysis system – to further probe whether these more reactive species exist and are degrading before ex-situ analysis can be conducted.

5.2.2 Further transesterification and polymerisation method development

One of the main conclusions from this work is that one single method cannot be applied to different pyrolysis liquids with the same results. In this work enough material was generated using unoptimized methods to generate some physical property data.

There is an unproven hypothesis that the reactivity of pyrolysis alcohols should follow from the general reactivity of alcohols ($1^\circ > 2^\circ > 3^\circ$) with respect to their transesterification, this has been proven to be the case for the transesterification of terpenols in unpublished work. This could be validated by applying this kind of approach to transesterifications of butyl methacrylate with model compounds from pyrolysis liquid, of the vanillin type. If this investigation was coupled with further analysis of the alcohols on pyrolysis liquid, with a particular focus into the distribution of 1° , 2° and 3° alcohols, this could go some way towards further accounting for the variation in reactivity of different pyrolysis liquids with respect to transesterification.

Now, this raises the question of how these could be effectively quantified, in light of the difficulty of separating and resolving individual pyrolysis liquid components by chromatography. Traditionally this type of classification is done where some reagent, namely an oxidising agent like acidified potassium dichromate(VI) solution, oxidises alcohols and the concentration of the aldehydes is measured through colorimetric reaction with an indicator. This is sometimes done as a secondary school science experiment by bubbling vapours through Schiff's reagent, for example, shown in Figure 66.

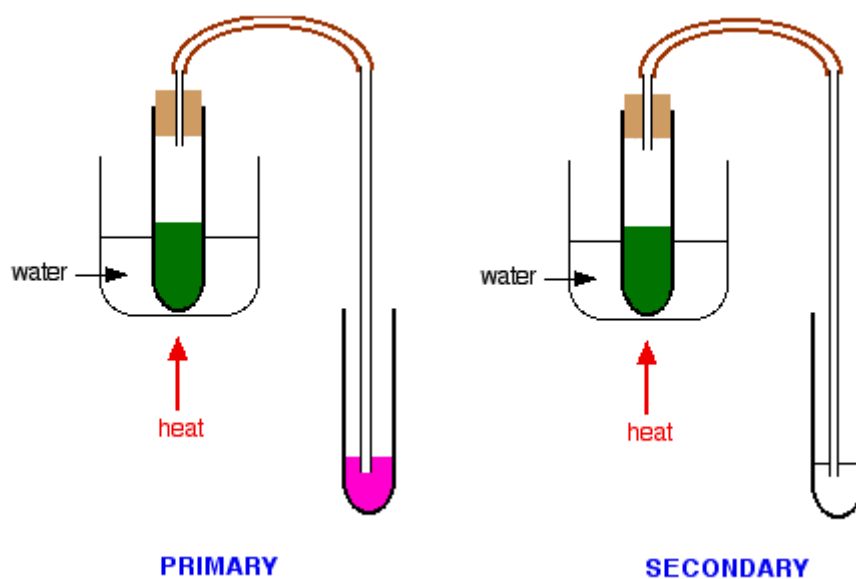


Figure 66 Outline of experimental set up for traditional quantitative colorimetric measurement of alcohol concentration

This kind of colorimetric approach is not applicable, even when using UV measurement and calibration curves, to pyrolysis liquid because it is highly pigmented, with other species that can migrate into the indicator solution confusing results as well as volatile ketones and acid species that can react in place of those generated by the oxidation reaction.

It is anticipated, that instead of a colorimetric analysis, that through reactive titration, a relative analysis of alcohol distribution could be derived. It is proposed to use a series of more reactive acetylating reagents, followed by an acid value titration. This would mainly work through selectively reacting the 1° 2° and 3° alcohols giving a starting acid value for the pyrolysis liquid, a value post acetylation of 1°, post acetylation of 1° and 2°, and post acetylation of 1°, 2° and 3° alcohols, in order to characterise the different pyrolysis liquid fractions.

It would be proposed not to approach all of the pyrolysis liquids in this study but potentially the 5 fractions taken forward for further analysis.

The outcome of this investigation and analysis could shed further light on the composition of pyrolysis liquids and distribution of alcohols in the pyrolysis liquid fractions.

5.2.3 Liquid microwave pyrolysis and transesterification optimisation

The main purpose of this investigation was to outline if two, seemingly distinct processes, biomass pyrolysis and transesterification could be linked. It would seem from this study that that is the case. The drawback to the approach taken in this work was that each process was considered largely in isolation with respect to the other. A main drawback to this separation of steps is that in order for the transesterification to occur, solvent removal is required prior to transesterification as the solvent boiling points were all below reaction temperature (80-100 °C *cf.* 145 °C) hence solvents were distilled off prior to reaction. Moving forward, it will be necessary to look for solvents that are both compatible with the microwave pyrolysis system in terms of polarity and viscosity but also have boiling points high enough such that there is no need to remove them prior to the transesterification and polymerisation steps. This will also mean that they do not contain groups likely to become involved in the chemistry, unsaturated double bonds (Michael reaction), OH groups, and acid groups for instance and have a boiling point at least above 145 °C. This future investigation will probably include a further kinetic study, similar to the one presented in chapter 3 however with the added variable of solvent, as well as amount of solvent included as further variables. The good news is that this type of constraint really narrows the playing field, the solvents used in this study, along with some constraints and future suggestions are included in Table 26.

Table 26 Outline of solvents used in this study, some constraints and potentially useful solvents for future investigations.¹⁸⁹

Solvent	Boiling point (°C)	Polarity	Dynamic viscosity at 298 K (mPa·s)	Comment
Cyclohexane	80.75	0.009	0.86	These are the solvents used in this study
Water	100	0.546	0.89	
Isopropanol	82.5	1.000	2.37	
Constraint	>145	<0.500		This is included for reference
Kerosene	150-275	0.01-0.1	1.64	Potential future solvents for combined pyrolysis/transesterification system
Cyclohexanone	155	0.281	0.99	
Aniline	184.4	0.420	4.47	

The solvent options were briefly explored as part of the initial pyrolysis investigations and high boiling point solvents were deliberately excluded from subsequent experiments on the grounds that would be difficult to remove prior to transesterification. Some liquid-liquid separations by water, acetone, methanol and acetonitrile of pyrolysis liquid in kerosene were attempted and acetonitrile was able to extract the most mass of dissolved pyrolysis liquid. Water extracted very little and acetone was miscible with kerosene. This route of investigation was discontinued on the grounds that instead of removing a solvent distillation step an additional liquid liquid extraction step prior to solvent removal step was being added. Now, at the time of this investigation, the idea of leaving the pyrolysis liquid dissolved in solvent for the transesterification reaction did not occur to the authors at the time, had this investigation been followed through, then this disadvantage would probably have become an advantage. It should also be noted that viscosity of the solvent has an impact on the liquid system, since kerosene is a much more viscous liquid than water for example. Effectively the bubble formation and removal from the biomass sample was much slower in kerosene and, a pseudo-leidenfrost effect was observed on the particle surface at high temperatures where a critical heat flux was reached and no more thermal energy could be absorbed from the sample by the solvent. It is unclear if this is desirable and would be worth considering as part of any subsequent investigation, for this reason cyclohexanone could be one such solvent that could potentially satisfy all these constraints.

5.2.4 Condensation polymerisation

Condensation polymerisation of pyrolysis liquid remains an opportunity for further investigation. The initial investigation in this work was based on the assumption that there are diol and diacid species in the pyrolysis liquid that are capable of reacting further to produce higher molecular weight polymer. It is suggested that the presence

of these species is robustly confirmed with multiple different analysis techniques before continuing with any investigation into condensation polymerisation of pyrolysis liquid.

5.2.5 Polymer identification

Full identification of the polymer from pyrolysis liquid requires characterisation of the transesterified pyrolysis monomers and the low molecular weight wax species. Investigation into how these species behave over time and at increased temperatures is of interest. The work of holmberg *et al*¹¹² has laid the groundwork for this investigation however, this will need to be supplemented with species observed in the pyrolysis polymer that were not included in that work.

It should be noted that the polymer:wax ratio used for this work was calculated from the light scattering data assuming a constant refractive index increment (d_n/d_c) of 0.087 mL/g. It is likely that;

- the wax is made up of many different molecules with different individual d_n/d_c values
- the concentration of these molecules will vary between pyrolysis liquids
- the d_n/d_c of the wax will be different to that of the polymer

As part of this work, preparative scale GPC would allow for separation, identification and characterisation of low molecular weight waxes in the pyrolysis polymer to allow further conclusions to be drawn about the affect of the pyrolysis liquid composition on the properties of the polymer.

5.2.6 End of use, biodegradability and biocompatibility

Inherent to the methacrylate polymer, is the strong carbon backbone that provides structural stability. This, while useful in applications, becomes a crutch after use as there is so little opportunity for this backbone to break in nature. The lack of recyclability will force disposal to recover the energy through combustion. A possible route to more biodegradable version of the pyrolysis polymer would be to replace this strong backbone with a slightly weaker, an ester or amide for example. These are much more available for hydrolysis and subsequently more likely to be biodegradable. This increased backbone flexibility will likely change the physical properties and hence the target application.

This will potentially involve a change in the type of polymerisation, from addition to condensation and this presents further options for comparison as the degradation products of this hydrolysis reaction may have, different positive and negative consequences for the environment. The question then becomes around running the

transesterification on a monomer that will polymerise to give a polymer with an ester, ether or amide backbone, or a combination of methacrylate with other condensation polymerisation compatible monomers.

In turn this will raise the question of biodegradability and what the decomposition products will look like. The products of common biodegradable polymers, poly-lactic acid (PLA) for example likely degrade into lactic acid which exists in nature. However, the degradation products of any pyrolysis polymer will have potentially surprising decomposition products, which ideally should be investigated prior to widespread use. The biocompatibility of the monomer, polymer and post-use degradation products should be identified as part of the LCA of the pyrolymers. With these tests it is important to distinguish what is achievable from what is technically feasible.

5.2.7 Regulatory concerns

COSHH, REACH are there for a reason. There is a common exception from the requirement to produce a pre-manufacture notice -the “polymer exemption” this is fundamentally to do with the idea that, if a molecule is larger than 10 kDa and made from benign monomers, then it is considered too large to interact with the body and may therefore be considered safe if the manufacture consists of non-toxic materials. As per the pre-requisite testing for a CAS number, pyrolysis liquid is primarily considered a fuel and is as such not expected to come into contact with humans so toxicity testing for regulatory purposes is not applicable. This means that formally no toxicity testing has been conducted on pyrolysis liquid. The fact that pyrolysis liquid is an “unknown or variable composition, complex reaction products or of biological materials” (UVCB) mixture further complicates matters as not all pyrolysis liquids are the same. It is unclear exactly what testing will be required, as this will be application specific, but it is likely that in order to access higher value materials from pyrolysis liquid, in applications involving human exposure, then further testing is needed.

Chapter 6. References

1. MacArthur, D. E. Beyond plastic waste. *Science* (80-.). **358**, 843 (2017).
2. Zheng, J. & Suh, S. Strategies to reduce the global carbon footprint of plastics. *Nat. Clim. Chang.* **9**, 374–378 (2019).
3. Ignatyev, I. A., Thielemans, W. & Vander Beke, B. Recycling of polymers: A review. *ChemSusChem* **7**, 1579–1593 (2014).
4. Sardon, H. & Li, Z.-C. Introduction to plastics in a circular economy. *Polym. Chem.* **11**, 4828–4829 (2020).
5. Stern, N. *Stern Review final report*. (2007).
6. York, R. Do alternative energy sources displace fossil fuels? *Nat. Clim. Chang.* **2**, 441–443 (2012).
7. Perkins, S. What are polymers? <https://www.sciencenewsforstudents.org/article/explainer-what-are-polymers>.
8. Hart, D. J. Free-Radical Carbon-Carbon Bond Formation in rganic Synthesis. *Science* (80-.). **223**, 883–888 (1984).
9. Walling, C. Some properties of radical reactions important in synthesis. *Tetrahedron* **41**, 3887–3900 (1985).
10. Tedder, J. M. & Walton, J. C. The importance of polarity and steric effects in determining the rate and orientation of free radical addition to olefins: Rules for determining the rate and preferred orientation. *Tetrahedron* **36**, 701–707 (1980).
11. Clive, D. L. J., Pham, M. P. & Subedi, R. Carbocyclization by radical closure onto O-trityl oximes: Dramatic effect of diphenyl diselenide. *J. Am. Chem. Soc.* **129**, 2713–2717 (2007).
12. Witczak, Z. J. & Li, Y. New stereoselective approach to (-)- δ -multistriatin1. *Tetrahedron Lett.* **36**, 2595–2598 (1995).
13. Matsugi, M. *et al.* Highly stereoselective synthesis of carbocycles via a radical addition reaction using 2,2'-azobis(2,4-dimethyl-4-methoxyvaleronitrile) [V-70L]. *J. Org. Chem.* **64**, 6928–6930 (1999).

14. Kita, Y. *et al.* Practical radical additions under mild conditions using 2,2'-azobis(2,4-dimethyl-4-methoxyvaleronitrile) [V-70] as an initiator. *Org. Process Res. Dev.* **2**, 250–254 (1998).
15. Gotandaa, K. *et al.* Efficient Stereoselective Synthesis of α -C-Glycopyranosides Using. *Tetrahedron* **55**, 10315–10324 (1999).
16. Wakabayashi, T., Shiozaki, M. & Kurakata, S. I. Practical stereoselective synthesis of α -linked C-glucosamine propionic acid esters: Conversion to GLA-60 derivatives. *Carbohydr. Res.* **337**, 97–104 (2002).
17. Plastics pact. [https://wrap.org.uk/taking-action/plastic-packaging/the-uk-plastics-pact#:~:text=The UK Plastics Pact is,a circular economy for plastics.&text=The Pact will stimulate innovative,total amount of plastic packaging](https://wrap.org.uk/taking-action/plastic-packaging/the-uk-plastics-pact#:~:text=The%20UK%20Plastics%20Pact%20is,a%20circular%20economy%20for%20plastics.&text=The%20Pact%20will%20stimulate%20innovative,total%20amount%20of%20plastic%20packaging).
18. Nagai, K. New developments in the production of methyl methacrylate. *Appl. Catal. A Gen.* **221**, 367–377 (2001).
19. Eastham, Graham Ronald (Wilton, Redcar, G., Disley, Zoe Bethany Clare (Nottingham, G., Johnson, David William (Wilton, Redcar, G., Stephens, Gill (Nottingham, G. & Waugh, Mark (Wilton, Redcar, G. PROCESS FOR THE PRODUCTION OF METHYL METHACRYLATE. (2019).
20. Poly, I. P. B. & Nanocomposites, G. Thermal Decomposition Kinetics and Mechanism of. 9–11.
21. Pellis, A. *et al.* Enzymatic synthesis of lignin derivable pyridine based polyesters for the substitution of petroleum derived plastics. *Nat. Commun.* **10**, (2019).
22. BASF. Ecoflex. https://plastics-rubber.basf.com/global/en/performance_polymers/products/ecoflex.html.
23. Geyer, R., Jambeck, J. R. & Law, K. L. Production, use, and fate of all plastics ever made - Supplementary Information. *Sci. Adv.* **3**, 19–24 (2017).
24. Kelloggs. Pringles. <https://www.pringles.com/uk/recycle.html>.
25. Suarez, C. A., Edmonds, M. & Jones, A. P. Earth Catastrophes and their Impact on the Carbon Cycle. 301–306 (2019) doi:10.2138/gselements.15.5.301.
26. Isikgor, F. H. & Becer, C. R. Lignocellulosic biomass: a sustainable platform for the production of bio-based chemicals and polymers. *Polym. Chem.* **6**, 4497–4559 (2015).

27. Hannon, M., Gimpel, J., Tran, M., Rasala, B. & Mayfield, S. Biofuels from algae: challenges and potential Importance & challenges of algal biofuels. *Biofuels* **1**, 763–784 (2010).
28. Pignolet, O., Jubeau, S., Vaca-Garcia, C. & Michaud, P. Highly valuable microalgae: Biochemical and topological aspects. *J. Ind. Microbiol. Biotechnol.* **40**, 781–796 (2013).
29. Kostas, E. T. *et al.* Microwave pyrolysis of *Laminaria digitata* to produce unique seaweed-derived bio-oils. *Biomass and Bioenergy* **125**, 41–49 (2019).
30. Williams, C. L., Westover, T. L., Emerson, R. M., Tumuluru, J. S. & Li, C. Sources of Biomass Feedstock Variability and the Potential Impact on Biofuels Production. *Bioenergy Res.* **9**, 1–14 (2016).
31. Huber, G. W., Iborra, S. & Corma, A. Synthesis of transportation fuels from biomass: Chemistry, catalysts, and engineering. *Chem. Rev.* **106**, 4044–4098 (2006).
32. Kenney, K. L., Smith, W. A., Gresham, G. L. & Westover, T. L. Understanding biomass feedstock variability. *Biofuels* **4**, 111–127 (2013).
33. Tumuluru, J. S., Hess, J. R., Boardman, R. D., Wright, C. T. & Westover, T. L. Formulation, pretreatment, and densification options to improve biomass specifications for Co-firing high percentages with coal. *Ind. Biotechnol.* **8**, 113–132 (2012).
34. Darr, M. J. & Shah, A. Biomass storage: An update on industrial solutions for baled biomass feedstocks. *Biofuels* **3**, 321–332 (2012).
35. Bridgwater, A. V. Principles and practice of biomass fast pyrolysis processes for liquids. *J. Anal. Appl. Pyrolysis* **51**, 3–22 (1999).
36. Carpenter, D., Westover, T. L., Czernik, S. & Jablonski, W. Biomass feedstocks for renewable fuel production: A review of the impacts of feedstock and pretreatment on the yield and product distribution of fast pyrolysis bio-oils and vapors. *Green Chem.* **16**, 384–406 (2014).
37. Dibble, C. J., Shatova, T. A., Jorgenson, J. L. & Stickel, J. J. Particle morphology characterization and manipulation in biomass slurries and the effect on rheological properties and enzymatic conversion. *Biotechnol. Prog.* **27**, 1751–1759 (2011).
38. Van Walsum, G. P. *et al.* Conversion of lignocellulosics pretreated with liquid hot water to ethanol. *Appl. Biochem. Biotechnol. - Part A Enzym. Eng. Biotechnol.* **57–58**, 157–170 (1996).

39. Demirbas, A. Effects of temperature and particle size on bio-char yield from pyrolysis of agricultural residues. *J. Anal. Appl. Pyrolysis* **72**, 243–248 (2004).
40. Demirbas, A. Effect of temperature on pyrolysis products from biomass. *Energy Sources, Part A Recover. Util. Environ. Eff.* **29**, 329–336 (2007).
41. Fahmi, R., Bridgwater, A. V., Donnison, I., Yates, N. & Jones, J. M. The effect of lignin and inorganic species in biomass on pyrolysis oil yields, quality and stability. *Fuel* **87**, 1230–1240 (2008).
42. Reza, M. T., Emerson, R., Uddin, M. H., Gresham, G. & Coronella, C. J. Ash reduction of corn stover by mild hydrothermal preprocessing. *Biomass Convers. Biorefinery* **5**, 21–31 (2015).
43. Shao, Y., Wang, J., Preto, F., Zhu, J. & Xu, C. Ash deposition in biomass combustion or co-firing for power/heat generation. *Energies* **5**, 5171–5189 (2012).
44. Bridgwater, A. V. Review of fast pyrolysis of biomass and product upgrading. *Biomass and Bioenergy* **38**, 68–94 (2012).
45. Wang, M., Liu, C., Li, Q. & Xu, X. Theoretical insight into the conversion of xylose to furfural in the gas phase and water. *J. Mol. Model.* **21**, (2015).
46. Alonso, D. M., Wettstein, S. G. & Dumesic, J. A. Bimetallic catalysts for upgrading of biomass to fuels and chemicals. *Chem. Soc. Rev.* **41**, 8075–8098 (2012).
47. Li, Y. *et al.* An “ ideal lignin ” facilitates full biomass utilization. (2018).
48. Oasmaa, A., Fonts, I., Pelaez-Samaniego, M. R., Garcia-Perez, M. E. & Garcia-Perez, M. *Pyrolysis Oil Multiphase Behavior and Phase Stability: A Review. Energy and Fuels* vol. 30 (2016).
49. Olarte, M. V *et al.* Standardization of chemical analytical techniques for pyrolysis bio-oil : history , challenges ,. 496–507 (2016) doi:10.1002/bbb.
50. Elliott, D. C., Meier, D., Oasmaa, A., Beld, B. Van De & Bridgwater, A. V. Results of the International Energy Agency Round Robin on Fast Pyrolysis Bio-oil Production. *Energy & Fuels* **31**, 5111–5119 (2017).
51. Dugaard, D. E. & Brown, R. C. Enthalpy for pyrolysis for several types of biomass. *Energy and Fuels* **17**, 934–939 (2003).

52. He, F., Yi, W. & Bai, X. Investigation on caloric requirement of biomass pyrolysis using TG-DSC analyzer. *Energy Convers. Manag.* **47**, 2461–2469 (2006).
53. Van de Velden, M., Baeyens, J., Brems, A., Janssens, B. & Dewil, R. Fundamentals, kinetics and endothermicity of the biomass pyrolysis reaction. *Renew. Energy* **35**, 232–242 (2010).
54. Yang, H. *et al.* Estimation of enthalpy of bio-oil vapor and heat required for pyrolysis of biomass. *Energy and Fuels* **27**, 2675–2686 (2013).
55. Chen, Q. *et al.* Investigation of heat of biomass pyrolysis and secondary reactions by simultaneous thermogravimetry and differential scanning calorimetry. *Fuel* **134**, 467–476 (2014).
56. Atsonios, K., Panopoulos, K. D., Bridgwater, A. V. & Kakaras, E. Biomass fast pyrolysis energy balance of a 1kg/h test rig. *Int. J. Thermodyn.* **18**, 267–275 (2015).
57. Stas, M., Chudoba, J. & Kubic, D. Petroleomic Characterization of Pyrolysis Bio-oils : A Review. 10283–10299 (2017) doi:10.1021/acs.energyfuels.7b00826.
58. Staš, M., Kubička, D., Chudoba, J. & Pospíšil, M. Overview of analytical methods used for chemical characterization of pyrolysis bio-oil. *Energy and Fuels* **28**, 385–402 (2014).
59. Lu, Y., Li, G. S., Lu, Y. C., Fan, X. & Wei, X. Y. Analytical Strategies Involved in the Detailed Componential Characterization of Biooil Produced from Lignocellulosic Biomass. *Int. J. Anal. Chem.* **2017**, (2017).
60. Staš, M. *et al.* Quantitative analysis of pyrolysis bio-oils: A review. *TrAC - Trends Anal. Chem.* **126**, (2020).
61. Bernal, E. Limit of Detection and Limit of Quantification Determination in Gas Chromatography. *Adv. Gas Chromatogr.* (2014) doi:10.5772/57341.
62. Long, G. L. & Winefordner, J. D. Limit of Detection: A Closer Look at the IUPAC Definition. *Anal. Chem.* **55**, 713A-724A (1983).
63. Marathe, P. S., Juan, A., Hu, X., Westerhof, R. J. M. & Kersten, S. R. A. Evaluating quantitative determination of levoglucosan and hydroxyacetaldehyde in bio-oils by gas and liquid chromatography. *J. Anal. Appl. Pyrolysis* **139**, 233–238 (2019).

64. Lensink, C., Markuszewski, R., Verkade, J. G. & Wroblewski, A. E. ³¹P NMR Spectroscopic Analysis of Coal Pyrolysis Condensates and Extracts for Heteroatom Functionalities Possessing Labile Hydrogen. *Energy and Fuels* **2**, 765–774 (1988).
65. Olarte, M. V *et al.* Determination of Hydroxyl Groups in Pyrolysis Bio-oils using ³¹P-NMR Laboratory Analytical Procedure (LAP). 1–9 (2016) doi:NREL/TP-5100-65887.
66. Hao, N., Ben, H., Yoo, C. G., Adhikari, S. & Ragauskas, A. J. Review of NMR Characterization of Pyrolysis Oils. (2016) doi:10.1021/acs.energyfuels.6b01002.
67. Ben, H. & Ferrell, J. R. Supplementary information In-Depth Investigation on Quantitative Characterization of Pyrolysis Oil by ³¹P NMR. 1–6 (2016).
68. Ringer, M., Putsche, V. & Scahill, J. Large-Scale Pyrolysis Oil Production: A Technology Assessment and Economic Analysis. (2006) doi:10.2172/894989.
69. Fouilland, T., Grace, J. R. & Ellis, N. Recent advances in fluidized bed technology in biomass processes. *Biofuels* **1**, 409–433 (2010).
70. Naimi, L. J. *et al.* The Canadian Society for Bioengineering Cost and Performance of Woody Biomass Size Reduction for Energy Production. *CSBE/SCGAB 2006 Annu. Conf.* (2006).
71. Wright, M. M., Satrio, J. A., Brown, R. C., Dugaard, D. E. & Hsu, D. D. Techno-economic analysis of biomass fast pyrolysis to transportation fuels. Technical Report NREL/TP-6A20-46586. *Nrel* **89**, 463–469 (2010).
72. Sokhansanj, S., Kumar, A. & Turhollow, A. F. Development and implementation of integrated biomass supply analysis and logistics model (IBSAL). *Biomass and Bioenergy* **30**, 838–847 (2006).
73. Bridgwater, A. V. & Peacocke, G. V. C. Fast pyrolysis processes for biomass. *Renew. Sustain. energy Rev.* **4**, 1–73 (2000).
74. Scott, D. S., Majerski, P., Piskorz, J. & Radlein, D. Second look at fast pyrolysis of biomass - the RTI process. *J. Anal. Appl. Pyrolysis* **51**, 23–37 (1999).
75. Scott, D. S. & Piskorz, J. The flash pyrolysis of aspen-poplar wood. *Can. J. Chem. Eng.* **60**, 666–674 (1982).

76. Scott, D. S. & Piskorz, J. The continuous flash pyrolysis of biomass. *Can. J. Chem. Eng.* **62**, 404–412 (1984).
77. Scott, D. S., Plskorz, J. & Radleln, D. Liquid Products from the Continuous Flash Pyrolysis of Biomass. *Ind. Eng. Chem. Process Des. Dev.* **24**, 581–588 (1985).
78. Oasmaa, A., Van De Beld, B., Saari, P., Elliott, D. C. & Solantausta, Y. Norms, standards, and legislation for fast pyrolysis bio-oils from lignocellulosic biomass. *Energy and Fuels* **29**, 2471–2484 (2015).
79. BTL-BTG. BTG-BTL pyrolysis process. 2019 <https://www.btg-btl.com/en/technology>.
80. Auersvald, M., Macek, T., Schulzke, T., Staš, M. & Šimáček, P. Influence of biomass type on the composition of bio-oils from ablative fast pyrolysis. *J. Anal. Appl. Pyrolysis* **150**, 104838 (2020).
81. Dahmen, N. *et al.* State of the Art of the BioliqÖ Process for Synthetic Biofuels Production. *Environ. Prog. Sustain. Energy* **31**, 176–181 (2012).
82. Santos, J., Ouadi, M., Jahangiri, H. & Hornung, A. Valorisation of lignocellulosic biomass investigating different pyrolysis temperatures. *J. Energy Inst.* **93**, 1960–1969 (2020).
83. Meredith, R. *Engineers' Handbook of Industrial Microwave Heating*. (IET, 1998).
84. Robinson, J. *et al.* Microwave Pyrolysis of Biomass: Control of Process Parameters for High Pyrolysis Oil Yields and Enhanced Oil Quality. *Energy & Fuels* **29**, 1701–1709 (2015).
85. Dundas, A. A. *et al.* Methodology for the synthesis of methacrylate monomers using designed single mode microwave applicators. *React. Chem. Eng.* **4**, 1472–1476 (2019).
86. Adam, M. Understanding Microwave Pyrolysis of Biomass Materials. (University of Nottingham, 2017).
87. Jones, D. A., Lelyveld, T. P., Mavrofidis, S. D., Kingman, S. W. & Miles, N. J. Microwave heating applications in environmental engineering - A review. *Resour. Conserv. Recycl.* **34**, 75–90 (2002).
88. Metaxas, A. C. & Meredith, R. *Industrial microwave heating*. (Peter Peregrinus Ltd, 1983).
89. Clark, D. E. Microwave Processing. *Annu. Rev. Mater. Sci* **26**, 299–331 (1996).
90. Reader, H. C. Understanding microwave heating systems: A perspective on state-of-the-art. *Adv. Microw. Radio Freq. Process. - Rep. from 8th Int. Conf. Microw. High Freq. Heat.* 3–14 (2006) doi:10.1007/978-

91. Bykov, Y. V., Rybakov, K. I. & Semenov, V. E. High-temperature microwave processing of materials. *J. Phys. D. Appl. Phys.* **34**, R55–R75 (2001).
92. Kitchen, H. J. *et al.* Modern microwave methods in solid-state inorganic materials chemistry: From fundamentals to manufacturing. *Chem. Rev.* **114**, 1170–1206 (2014).
93. Remya, N. & Lin, J. G. Current status of microwave application in wastewater treatment-A review. *Chem. Eng. J.* **166**, 797–813 (2011).
94. Robinson, J. P., Kingman, S. W., Baranco, R., Snape, C. E. & Al-Sayegh, H. Microwave pyrolysis of wood pellets. *Ind. Eng. Chem. Res.* **49**, 459–463 (2010).
95. Clark, J. H., Luque, R. & Matharu, A. S. Green chemistry, biofuels, and biorefinery. *Annu. Rev. Chem. Biomol. Eng.* **3**, 183–207 (2012).
96. Yin, C. Microwave-assisted pyrolysis of biomass for liquid biofuels production. *Bioresour. Technol.* **120**, 273–284 (2012).
97. Motasemi, F. & Afzal, M. T. A review on the microwave-assisted pyrolysis technique. *Renew. Sustain. Energy Rev.* **28**, 317–330 (2013).
98. Huang, Y., Chiu, P. & Lo, S. Mini review A review on microwave pyrolysis of lignocellulosic biomass. *Sustain. Environ. Res.* **26**, 103–109 (2016).
99. Axelsson, L. *et al.* Perspective: Jatropha cultivation in southern India: Assessing farmers' experiences. *Biofuels, Bioprod. Biorefining* **6**, 246–256 (2012).
100. Miura, M., Kaga, H., Sakurai, A., Kakuchi, T. & Takahashi, K. Rapid pyrolysis of wood block by microwave heating. *J. Anal. Appl. Pyrolysis* **71**, 187–199 (2004).
101. Ellison, C., McKeown, M. S., Trabelsi, S. & Boldor, D. Dielectric properties of biomass/biochar mixtures at microwave frequencies. *Energies* **10**, 1–11 (2017).
102. Shepherd, B. J. Development of a Liquid Inerted Microwave Pyrolysis Process. (University of Nottingham).
103. Shepherd, B. J. *et al.* Microwave pyrolysis of biomass within a liquid medium. *J. Anal. Appl. Pyrolysis*

- 134**, 381–388 (2018).
104. Shang, H., Lu, R. R., Shang, L. & Zhang, W. H. Effect of additives on the microwave-assisted pyrolysis of sawdust. *Fuel Process. Technol.* **131**, 167–174 (2015).
 105. Robinson, J. *et al.* Electromagnetic simulations of microwave heating experiments using reaction vessels made out of silicon carbide. *Phys. Chem. Chem. Phys.* **12**, 10793–10800 (2010).
 106. Taqi, A., Farcot, E., Robinson, J. P. & Binner, E. R. Understanding microwave heating in biomass-solvent systems. *Chem. Eng. J.* **393**, 124741 (2020).
 107. Kostas, E. T., Beneroso, D. & Robinson, J. P. The application of microwave heating in bioenergy: A review on the microwave pre-treatment and upgrading technologies for biomass. *Renew. Sustain. Energy Rev.* **77**, 12–27 (2017).
 108. Omar, S., Alsamaq, S., Yang, Y. & Wang, J. Production of renewable fuels by blending bio-oil with alcohols and upgrading under supercritical conditions. *Front. Chem. Sci. Eng.* **13**, 702–717 (2019).
 109. Holmberg, A. L., Stanzione, J. F., Wool, R. P. & Epps, T. H. A Facile Method for Generating Designer Block Copolymers from Functionalized Lignin Model Compounds. *ACS Sustain. Chem. Eng.* **2**, 569–573 (2014).
 110. Holmberg, A. L., Karavolias, M. G. & Epps, T. H. RAFT polymerization and associated reactivity ratios of methacrylate-functionalized mixed bio-oil constituents[†]. *Polym. Chem.* **6**, 5728–5739 (2015).
 111. Holmberg, A. L., Reno, K. H., Nguyen, N. A., Wool, R. P. & Epps, T. H. Syringyl Methacrylate, a Hardwood Lignin-Based Monomer for High-Tg Polymeric Materials. *ACS Macro Lett.* **5**, 574–578 (2016).
 112. Holmberg, A. L. *et al.* Softwood Lignin-Based Methacrylate Polymers with Tunable Thermal and Viscoelastic Properties. *Macromolecules* **49**, 1286–1295 (2016).
 113. Llevot, A., Grau, E., Carlotti, S., Grelier, S. & Cramail, H. From Lignin-derived Aromatic Compounds to Novel Biobased Polymers. *Macromol. Rapid Commun.* **37**, 9–28 (2016).
 114. methacrylates: chemical safety. <https://www.chemicalsafetyfacts.org/methacrylates/>.
 115. Stanzione, J. F., Giangiulio, P. A., Sadler, J. M., Scala, J. J. La & Wool, R. P. Lignin-Based Bio-Oil Mimic

- as Biobased Resin for Composite Applications. *ACS Sustain. Chem. Eng.* **1**, 419–426 (2013).
116. Stanzione, J. F., Sadler, J. M., La Scala, J. J., Reno, K. H. & Wool, R. P. Vanillin-based resin for use in composite applications. *Green Chem.* **14**, 2346–2352 (2012).
 117. Wang, S., Bassett, A. W., Wieber, G. V., Stanzione, J. F. & Epps, T. H. Effect of methoxy substituent position on thermal properties and solvent resistance of lignin-inspired poly(dimethoxyphenyl methacrylate)s. *ACS Macro Lett.* **6**, 802–807 (2017).
 118. Qazi, S. S., Li, D., Briens, C., Berruti, F. & Abou-zaid, M. M. Antioxidant Activity of the Lignins Derived from. (2017) doi:10.3390/molecules22030372.
 119. Holmberg, A. L., Karavolias, M. G. & Epps, T. H. Polymer Chemistry. 5728–5739 (2015) doi:10.1039/c5py00291e.
 120. Hatton, F. L. Recent advances in RAFT polymerization of monomers derived from renewable resources. *Polym. Chem.* **11**, 220–229 (2020).
 121. Sullivan, J. A. & Burnham, S. The selective oxidation of glycerol over model Au/TiO₂ catalysts - The influence of glycerol purity on conversion and product selectivity. *Catal. Commun.* **56**, 72–75 (2014).
 122. Bai, X. Controlled Radical Polymerization of Crude Lignin Bio-oil Containing Multihydroxyl Molecules for Methacrylate Polymers and the Potential Applications. *ACS Sustain. Chem. Eng.* **7**, 9050–9060 (2019).
 123. Wang, S., Shuai, L., Saha, B., Vlachos, D. G. & Epps, T. H. From Tree to Tape: Direct Synthesis of Pressure Sensitive Adhesives from Depolymerized Raw Lignocellulosic Biomass. *ACS Cent. Sci.* **4**, 701–708 (2018).
 124. Rover, M. R. *et al.* Repolymerization of pyrolytic lignin for producing carbon fiber with improved properties Biomass and Bioenergy Repolymerization of pyrolytic lignin for producing carbon fiber with improved properties. *Biomass and Bioenergy* **95**, 19–26 (2016).
 125. Qu, W. *et al.* Controlled Radical Polymerization of Crude Lignin Bio-oil Containing Multihydroxyl Molecules for Methacrylate Polymers and the Potential Applications. *ACS Sustain. Chem. Eng.* **7**, 9050–9060 (2019).
 126. Kim, K. H., Bai, X., Cady, S., Gable, P. & Brown, R. C. Quantitative Investigation of Free Radicals in Bio-Oil and their Potential Role in Condensed-Phase Polymerization. *ChemSusChem* **8**, 894–900 (2015).

127. Dundas, A. A., Hook, A. L., Alexander, M. R., Kingman, S. W. & Irvine, D. J. Methodology for the synthesis of methacrylate monomers using designed single mode microwave applicators. *React. Chem. Eng.* 1472–1476 (2019) doi:10.1039/c9re00173e.
128. Monomer Technologies. 2019 <https://www.luciteinternational.com/monomers-emea-manufacturing-monomer-technologies-18/>.
129. Zhu, L., Li, K., Zhang, Y. & Zhu, X. Upgrading the Storage Properties of Bio-oil by Adding a Compound Additive. *Energy and Fuels* **31**, 6221–6227 (2017).
130. Moldoveanu, S. C. *Pyrolysis of Alcohols and Phenols. Pyrolysis of Organic Molecules* (2019). doi:10.1016/b978-0-444-64000-0.00004-4.
131. Westmoreland, P. R. & Fahey, P. J. Dehydration and dehydrogenation kinetics of OH groups in biomass pyrolysis. *Chem. Eng. Trans.* **50**, 73–78 (2016).
132. Boucher, M. E., Chaala, A., Pakdel, H. & Roy, C. Bio-oils obtained by vacuum pyrolysis of softwood bark as a liquid fuel for gas turbines. Part II: Stability and ageing of bio-oil and its blends with methanol and a pyrolytic aqueous phase. *Biomass and Bioenergy* **19**, 351–361 (2000).
133. Painter, P. C. & Coleman, M. M. *Fundamentals of Polymer science*. (Technomic, 1997).
134. Stevens, M. P. *Polymer chemistry and introduction*. (Oxford university press, 1990).
135. Young, R. J. & Lovell, P. A. *Introduction to polymers*. (Chapman and Hall, 1991).
136. Agilent Technologies Inc. An Introduction to Gel Permeation Chromatography and Size Exclusion Chromatography. *Primer* 1–32 (2015).
137. Nam, K. H. & Jo, W. H. The effect of molecular weight and polydispersity of polystyrene on the interfacial tension between polystyrene and polybutadiene. *Polymer (Guildf)*. **36**, 3727–3731 (1995).
138. Gaborieau, M. & Castignolles, P. Size-exclusion chromatography (SEC) of branched polymers and polysaccharides. 1413–1423 (2011) doi:10.1007/s00216-010-4221-7.
139. Smith, A. D. *et al.* Dielectric properties of free-radical polymerizations: Molecularly symmetrical initiators during thermal decomposition. *Ind. Eng. Chem. Res.* **49**, 1703–1710 (2010).
140. Kostas, E. T., Cooper, M., Shepherd, B. J. & Robinson, J. P. Identification of Bio-oil Compound Utilizing

- Yeasts Through Phenotypic Microarray Screening. *Waste and Biomass Valorization* **11**, 2507–2519 (2020).
141. Gramlich, W. M., Theryo, G. & Hillmyer, M. A. Copolymerization of isoprene and hydroxyl containing monomers by controlled radical and emulsion methods. *Polym. Chem.* **3**, 1510–1516 (2012).
 142. Ryan, J. *et al.* Solvent-free manufacture of methacrylate polymers from biomass pyrolysis products. *React. Chem. Eng.* (2021) doi:10.1039/d0re00419g.
 143. Lartigue-Peyrou, F. The use of phenolic compounds as free-radical polymerization inhibitors. *Ind. Chem. Libr.* **8**, 489–505 (1996).
 144. Becker, H. & Vogel, H. The role of hydroquinone monomethyl ether in the stabilization of acrylic acid. *Chem. Eng. Technol.* **29**, 1227–1231 (2006).
 145. Abou-Hatab, S., Spata, V. A. & Matsika, S. Substituent Effects on the Absorption and Fluorescence Properties of Anthracene. *J. Phys. Chem. A* **121**, 1213–1222 (2017).
 146. Pospíšil, J., Nešpůrek, S. & Zweifel, H. The role of quinone methides in thermostabilization of hydrocarbon polymers - I. Formation and reactivity of quinone methides. *Polym. Degrad. Stab.* **54**, 7–14 (1996).
 147. Davies, M. J. Detection and characterisation of radicals using electron paramagnetic resonance (EPR) spin trapping and related methods. *Methods* **109**, 21–30 (2016).
 148. Rajan Babu, T. V. Stereochemistry of Intramolecular Free-Radical Cyclization Reactions. *Acc. Chem. Res.* **24**, 139–145 (1991).
 149. Barner-Kowollik, C. & Perrier, S. The Future of Reversible Addition Fragmentation Chain Transfer Polymerization. *J. Polym. Sci. Part A Polym. Chem.* **46**, 5715–5723 (2008).
 150. Elliott, D. C. Analysis and comparison of biomass pyrolysis/gasification condensates: Final report. *Other Inf. Portions this Doc. are illegible Microfich. Prod. Orig. copy available until Stock is exhausted* Medium: ED; Size: Pages: 100 (1986).
 151. Bartoli, M., Frediani, M., Briens, C., Berruti, F. & Rosi, L. An overview of temperature issues in microwave-assisted pyrolysis. *Processes* **7**, 1–14 (2019).

152. Leclerc, P. Dépolymérisation du Polystyrène par Pyrolyse Micro-onde. (2018).
153. Qu, W., Xue, Y., Gao, Y., Rover, M. & Bai, X. Repolymerization of pyrolytic lignin for producing carbon fiber with improved properties. *Biomass and Bioenergy* **95**, 19–26 (2016).
154. Davis, K. M. *et al.* Recovery and utilization of lignin monomers as part of the biorefinery approach. *Energies* **9**, 1–28 (2016).
155. Alder, C. M. *et al.* Updating and further expanding GSK's solvent sustainability guide. *Green Chem.* **18**, 3879–3890 (2016).
156. Reichardt, C. & Welton, T. *Solvents and Solvent Effects in Organic Chemistry, Fourth edition.* (2010).
157. Murov, S. Properties of Organic Solvents. 04/10/10 <https://sites.google.com/site/miller00828/in/solvent-polarity-table> (2010).
158. Joseph, J. *et al.* Compositional Changes to Low Water Content Bio-oils during Aging: An NMR, GC/MS, and LC/MS Study. *Energy and Fuels* **30**, 4825–4840 (2016).
159. Kantarelis, E., Yang, W. & Blasiak, W. Production of liquid feedstock from biomass via steam pyrolysis in a fluidized bed reactor. *Energy and Fuels* **27**, 4748–4759 (2013).
160. Garcia-Perez, M., Chaala, A., Pakdel, H., Kretschmer, D. & Roy, C. Characterization of bio-oils in chemical families. *Biomass and Bioenergy* **31**, 222–242 (2007).
161. Black, S. & Ferrell, J. R. Accelerated aging of fast pyrolysis bio-oil: A new method based on carbonyl titration. *RSC Adv.* **10**, 10046–10054 (2020).
162. Alén, R., Kuoppala, E. & Oesch, P. Formation of the main degradation compound groups from wood and its components during pyrolysis. *J. Anal. Appl. Pyrolysis* **36**, 137–148 (1996).
163. Elliott, D. C. Relation of reaction time and temperature to chemical composition of pyrolysis oils. *ACS Symp. Ser.* 55–65 (1988) doi:10.1021/bk-1988-0376.ch006.
164. Terrell, E. & Garcia-Perez, M. Application of nitrogen-based blowing agents as an additive in pyrolysis of cellulose. *J. Anal. Appl. Pyrolysis* **137**, 203–211 (2019).
165. Jarvis, M. W. *et al.* Direct detection of products from the pyrolysis of 2-phenethyl phenyl ether. *J. Phys. Chem. A* **115**, 428–438 (2011).

166. Choi, Y. S. *et al.* Pyrolysis reaction networks for lignin model compounds: Unraveling thermal deconstruction of β -O-4 and α -O-4 compounds. *Green Chem.* **18**, 1762–1773 (2016).
167. Barde, M., Adhikari, S., Via, B. K. & Auad, M. L. Synthesis and characterization of epoxy resins from fast pyrolysis bio-oil. *Green Mater.* **6**, 76–84 (2018).
168. Hilten, R. N., Bibens, B. P., Kastner, J. R. & Das, K. C. In-line esterification of pyrolysis vapor with ethanol improves Bio-oil quality. *Energy and Fuels* **24**, 673–682 (2010).
169. Pfister, D., Storti, G., Tancini, F., Costa, L. I. & Morbidelli, M. Synthesis and Ring-Opening Polymerization of Cyclic Butylene 2,5-Furandicarboxylate. *Macromol. Chem. Phys.* **216**, 2141–2146 (2015).
170. Fox, T. G. Influence of diluent and of copolymer composition on the glass transition temperature of a polymer system. *Bull. Am. Phys. Soc.* (1956).
171. Wu, L., Mincheva, R., Xu, Y., Raquez, J. M. & Dubois, P. High molecular weight poly(butylene succinate-co-butylene furandicarboxylate) copolyesters: From catalyzed polycondensation reaction to thermomechanical properties. *Biomacromolecules* **13**, 2973–2981 (2012).
172. Tang, J. & Chen, E. Y. X. Effects of Chain Ends on Thermal and Mechanical Properties and Recyclability of Poly(γ -butyrolactone). *J. Polym. Sci. Part A Polym. Chem.* **56**, 2271–2279 (2018).
173. Airey, G. D. & Mohammed, M. H. Rheological properties of polyacrylates used as synthetic road binders. *Rheol Acta* 751–763 (2008) doi:10.1007/s00397-007-0250-3.
174. Airey, G. D. *et al.* Rheology of polyacrylate binders produced via catalytic chain transfer polymerization as an alternative to bitumen in road pavement materials. *Eur. Polym. J.* **47**, 1300–1314 (2011).
175. Zhang, J. *et al.* Moisture damage evaluation of aggregate – bitumen bonds with the respect of moisture absorption , tensile strength and failure surface. **0629**, (2017).
176. Airey, G. *et al.* Linear Viscoelastic Behaviour of Polyacrylate Binders and Bitumen Blends Linear Viscoelastic Behaviour of Polyacrylate Binders and Bitumen Blends. **0629**, (2011).
177. Airey, G. D., Mohammed, M. H. & Fichter, C. Rheological characteristics of synthetic road binders. *Fuel* **87**, 1763–1775 (2008).

178. Zhang, J. *et al.* Moisture sensitivity examination of asphalt mixtures using thermodynamic , direct adhesion peel and compacted mixture mechanical tests. **0629**, (2018).
179. Cypcar, C. C., Camelio, P., Lazzeri, V., Mathias, L. J. & Waegell, B. Prediction of the Glass Transition Temperature of Multicyclic and Bulky Substituted Acrylate and Methacrylate Polymers Using the Energy , Volume , Mass (EVM) QSPR Model. **1**, 8954–8959 (1996).
180. Krause, S., Gormley, J. J., Shetter, J. A. & Warren, H. Glass Temperatures of Some Acrylic Polymers. **3**, 3573–3586.
181. Lu, Y. & Hsu, C. Preparation of Poly (2 , 5-thienyleneethylene) and Poly (2 , 5-furyleneethylene) by Vapor Phase Pyrolysis of (5-Methyl-2-thienyl) methyl Benzoate and (5-Methyl-2-furyl) methyl Benzoate. **9297**, 5546–5550 (1996).
182. Adlington, K. *et al.* Application of Targeted Molecular and Material Property Optimization to Bacterial Attachment-Resistant (Meth) acrylate Polymers Application of Targeted Molecular and Material Property Optimization to Bacterial Attachment-Resistant (Meth) acrylate Poly. (2016) doi:10.1021/acs.biomac.6b00615.
183. Ryan, J. *et al.* Solvent-free manufacture of methacrylate polymers from biomass pyrolysis products. *React. Chem. Eng.* **6**, 335–344 (2021).
184. Williams, M. L., Landel, R. F. & Ferry, J. D. The Temperature Dependence of Relaxation Mechanisms in Amorphous Polymers and Other Glass-forming Liquids. *J. Am. Chem. Soc.* **77**, 3701–3707 (1955).
185. Dudowicz, J., Douglas, J. F. & Freed, K. F. The meaning of the “ universal ” WLF parameters of glass-forming polymer liquids. *J. Chem. Phys.* **014905**, 1–7 (2017).
186. Rubinstein, M. & Cloby, R. H. *Polymer Physics*. (OUP Oxford, 2003).
187. Zhang, J., Airey, G. D., Grenfell, J., Apeagyei, A. K. & Barrett, M. International Journal of Adhesion & Adhesives Development of a composite substrate peel test to assess moisture sensitivity of aggregate – bitumen bonds. *Int. J. Adhes. Adhes.* **68**, 133–141 (2016).
188. Airey, G. D., Grenfell, J. R. A., Apeagyei, A., Subhy, A. & Presti, D. Lo. Time dependent viscoelastic rheological response of pure ., *Mech Time-Depend Mater* 455–480 (2016) doi:10.1007/s11043-016-9295-y.

189. Dean, J. A. *Lange's Handbook of Chemistry*. (1999).

Chapter 7. Appendix

		Fraction*	Mass Fraction	Acid	Alcohol	Aldehyde	Amine	Aromatic	Ester	Furans	Ketone	Sugars	Water
Industrial pyrolysis liquid		Crude	1	6	29	4	-	3	1	26	-	-	29
Gas inerted Fixed bed furnace	Crude		1	0.50%	41.99%	3.61%	7.01%	0.28%	0.35%	20.25%	11.54%	0.78%	13.70%
	Water	I/S	0.13	0.97%	30.48%	2.39%		0.34%		14.74%	0.44%	30.89%	
	Water	Sol	0.95		81.38%	4.88%	2.35%	0.25%		1.70%	4.07%	5.19%	
	IPA	Sol	0.57		68.64%	0.99%	0.23%	0.84%	1.49%	11.40%	5.43%	9.61%	1.37%
	Cycohexane	I/S	0.71		44.72%	1.11%	5.87%		1.06%	10.72%	11.51%	9.31%	15.70%
	Cycohexane	Sol	0.1		56.28%	0.43%	0.12%	0.45%	8.95%	13.84%	9.43%	10.27%	0.22%
Gas inerted Fixed bed Microwave	Crude		1	0.18%	45.37%	3.14%	2.08%		1.34%	13.84%	6.96%	14.11%	12.98%
	Water	I/S	0.13		43.51%	0.32%			9.06%	0.80%	3.29%	31.14%	
	Water	Sol	0.93		74.00%	4.72%	0.54%			5.57%		12.98%	
	IPA	Sol	0.93		48.58%	0.73%	0.23%		1.53%	7.98%	3.86%	36.15%	0.95%
	Cycohexane	I/S	0.77		74.41%	0.54%	5.94%		2.71%	9.76%	1.07%	4.84%	0.73%
	Cycohexane	Sol	0.12		56.70%	0.84%	0.14%		9.70%	5.45%	10.88%	16.04%	0.26%
Liquid inerted fixed bed microwave	Crude		1		63.01%	2.77%	1.42%		1.15%	8.99%	4.25%	11.56%	6.86%
	Water	sol	1		83.96%	3.83%			0.00%	3.32%	2.68%	5.65%	
	IPA	Sol	1		61.21%	0.30%	0.90%		1.81%	7.43%	5.05%	16.43%	6.89%
	Cycohexane	I/S	0.80		54.89%	5.21%	1.85%		0.00%	14.79%	4.05%	6.90%	12.32%
	Cycohexane	Sol	0.20		71.69%		0.92%		2.44%	2.40%	4.44%	16.71%	1.40%

SI-3 Table to show mass balance, water content and functional group concentrations present in pyrolysis liquids from different pyrolysis methods on Pinewood feedstock with liquid liquid

extractions, note that KF analysis was not conducted on water fractions.

*sol=soluble I/S = insoluble

1. Gas inerted conventional pyrolysis liquid – “crude”				
RT (min)	Area	Name	Area Percent	Category
7.52	2.1E+09	Urea	4.52%	Amine
8.368	1.43E+09	Acetamide, 2-amino-	3.09%	Amine
9.392	1.93E+08	Boronic acid, ethyl-	0.42%	Acid
10.073	1.11E+09	Propanal	2.40%	Aldehyde
10.359	2.37E+08	Formamide, N-(cyanomethyl)-	0.51%	Amine
10.889	8.26E+08	Pentanal, 2-methyl-	1.78%	Aldehyde
11.338	2.15E+09	Furfural	4.63%	Furans
12.147	2.15E+09	2-Furanmethanol	4.63%	Furans
12.686	1.48E+08	3-Carene	0.32%	Aromatic
13.265	72752935	trans-2-Pentenoic acid	0.16%	Acid
13.706	2.15E+09	1,2-Cyclopentanedione	4.63%	Ketone
13.973	3.53E+08	2,3-Pentanedione	0.76%	Ketone
14.066	1.55E+09	2-Furancarboxaldehyde, 5-methyl-	3.35%	Furans
14.468	2.21E+08	1-Propanone, 1-(2-furanyl)-	0.48%	Furans
14.642	1.55E+09	2(5H)-Furanone	3.35%	Ketone
15.129	7.17E+08	Oxazolidine, 2,2-diethyl-3-methyl-	1.55%	Furans
15.671	2.15E+09	3-Methylcyclopentane-1,2-dione	4.63%	Ketone
16.442	2.15E+09	Phenol, 2-methoxy-	4.63%	Alcohol
17.053	2.27E+08	Furyl hydroxymethyl ketone	0.49%	Furans
17.216	9.74E+08	2-Cyclopenten-1-one, 3-ethyl-2-hydroxy-	2.10%	Alcohol
17.458	1.25E+09	Furyl hydroxymethyl ketone	2.69%	Furans
17.723	3.39E+08	Phenol, 4-methoxy-3-methyl-	0.73%	Alcohol
18.104	1.7E+08	Creosol	0.37%	Alcohol
18.312	2.15E+09	Creosol	4.63%	Alcohol
18.962	1.88E+08	butanedioic acid, mono(3,4-dimethylphenyl) ester	0.40%	Ester
19.71	2.15E+09	Phenol, 4-ethyl-2-methoxy-	4.63%	Alcohol
19.942	70087641	2-Methoxy-5-methylphenol	0.15%	Alcohol
20.289	4.21E+08	1,4:3,6-Dianhydro-.alpha.-d-glucopyranose	0.91%	Sugars
20.544	97341606	5-Hydroxymethylfurfural	0.21%	Furans
20.672	2.15E+09	2-Methoxy-4-vinylphenol	4.63%	Alcohol
20.961	3.82E+08	5-Acetoxyethyl-2-furaldehyde	0.82%	Furans
21.249	2.15E+09	5-Hydroxymethylfurfural	4.63%	Furans
21.937	9.83E+08	Phenol, 2-methoxy-4-(1-propenyl)-	2.12%	Alcohol
22.799	2.15E+09	Levoglucosan	4.63%	Sugars
23.169	1.92E+09	Benzaldehyde, 3-hydroxy-4-methoxy-	4.13%	Alcohol
23.946	6.99E+08	Phenol, 2-methoxy-4-propyl-	1.51%	Alcohol
24.994	1.71E+09	2-Propanone, 1-(4-hydroxy-3-methoxyphenyl)-	3.68%	Alcohol
25.505	3.32E+08	benzoic acid, 4-hydroxy-3-propyl-	0.72%	Alcohol
26.398	1.65E+08	Vanillin	0.35%	Alcohol
26.712	1.06E+09	Benzenepropanol, 4-hydroxy-3-methoxy-	2.29%	Alcohol
27.686	1.56E+08	2-Propanone, 1-(4-hydroxy-3-methoxyphenyl)-	0.34%	Alcohol
28.506	2.15E+09	Coniferyl aldehyde	4.63%	Alcohol
29.064	2.11E+08	4-(1-Hydroxyallyl)-2-methoxyphenol	0.45%	Alcohol
34.91	8.38E+08	phenol, 4,4'-[dithiobis(methylene)]bis[2-methoxy-	1.81%	Alcohol
36.854	68132604	Coniferyl alcohol	0.15%	Alcohol

2. Gas inerted conventional pyrolysis liquid – “water insoluble”				
RT (min)	Area	Name	Area Percent	Category
9.925	14018822	Propanal	2.97%	Aldehyde
11.352	5738067	Furfural	1.22%	Furans
12.015	7973341	2-Furanmethanol	1.69%	Furans
12.663	1980201	3-Carene	0.42%	Aromatic
12.78	11708927	2-Furanmethanol	2.48%	Furans
13.248	5720462	trans-2-Pentenoic acid	1.21%	Acid
13.664	2598736	3-Methylcyclopentane-1,2-dione	0.55%	Ketone
14.502	3575877	1-Propanone, 1-(2-furanyl)-	0.76%	Furans
16.087	5571497	Phenol, 2-methoxy-	1.18%	Alcohol
17.425	3906301	Furyl hydroxymethyl ketone	0.83%	Furans
17.799	2141975	Phenol, 4-methoxy-3-methyl-	0.45%	Alcohol
18.467	16936600	Creosol	3.59%	Alcohol
19.757	4779382	Phenol, 4-ethyl-2-methoxy-	1.01%	Alcohol
19.851	25901239	2-Methoxy-5-methylphenol	5.50%	Alcohol
20.5	9238506	5-Hydroxymethylfurfural	1.96%	Furans
21.172	44405876	5-Acetoxymethyl-2-furaldehyde	9.42%	Furans
21.547	8920557	Vanillin	1.89%	Alcohol
22.854	1.58E+08	Levogluconan	33.49%	Sugars
23.528	6123145	Phenol, 2-methoxy-4-(1-propenyl)-	1.30%	Alcohol
23.892	10001772	Phenol, 2-methoxy-4-propyl-	2.12%	Alcohol
25.508	4869955	benzoic acid, 4-hydroxy-3-propyl-	1.03%	Alcohol
26.305	2480811	Vanillin	0.53%	Alcohol
27.637	3158623	2-Propanone, 1-(4-hydroxy-3-methoxyphenyl)-	0.67%	Alcohol
28.692	23601699	D-Allose	5.01%	Sugars
29.085	22016991	4-(1-Hydroxyallyl)-2-methoxyphenol	4.67%	Alcohol
29.63	15085009	2-Propanone, 1-(4-hydroxy-3-methoxyphenyl)-	3.20%	Alcohol
34.907	21801144	phenol, 4,4'-[dithiobis(methylene)]bis[2-methoxy-	4.63%	Alcohol
36.945	29205749	Coniferyl alcohol	6.20%	Alcohol

3. Gas inerted conventional pyrolysis liquid – “water soluble”

RT (min)	Area	Name	Area Percent	Category
8.274	5094545	Acetamide, 2-amino-	0.12%	Amine
9.996	63432907	Propanal	1.53%	Aldehyde
10.851	1.4E+08	Propanal	3.36%	Aldehyde
11.869	4489407	Formaldehyde, dipropylhydrazone	0.11%	Amine
12.421	23148467	Formaldehyde, dipropylhydrazone	0.56%	Amine
12.686	10426492	3-Carene	0.25%	Aromatic
13.62	1.58E+08	2(5H)-Furanone	3.81%	Ketone
13.955	7997598	2,3-Pentanedione	0.19%	Ketone
15.113	65285225	N-Butyl-tert-butylamine	1.57%	Amine
15.494	3443692	2(5H)-Furanone, 3-methyl-	0.08%	Ketone
15.575	1.56E+08	2-Cyclopenten-1-one, 2-hydroxy-3-methyl-	3.76%	Alcohol
16.215	4968619	2-Cyclopenten-1-one, 3-ethyl-2-hydroxy-	0.12%	Alcohol
16.411	2.85E+08	Phenol, 2-methoxy-	6.85%	Alcohol
17.102	85386967	Creosol	2.05%	Alcohol
17.438	30947820	Furyl hydroxymethyl ketone	0.74%	Furans
18.244	6.07E+08	2-Cyclopenten-1-one, 3-ethyl-2-hydroxy-	14.61%	Alcohol
19.217	15564565	2-Methoxy-6-methylphenol	0.37%	Alcohol
19.702	1.39E+08	Phenol, 4-ethyl-2-methoxy-	3.35%	Alcohol
19.923	37133410	2-Methoxy-5-methylphenol	0.89%	Alcohol
20.193	30521911	5-Acetoxyethyl-2-furaldehyde	0.73%	Furans
20.708	78239863	2-Cyclopenten-1-one, 4-hydroxy-3-methyl-2-(2-propenyl)-	1.88%	Alcohol
21.838	17501093	Phenol, 4-ethyl-2-methoxy-	0.42%	Alcohol
21.943	48678355	Phenol, 2-methoxy-4-(1-propenyl)-	1.17%	Alcohol
22.199	12219351	3,4-Anhydro-d-galactosan	0.29%	Sugars
22.743	1.98E+08	1,4:3,6-Dianhydro-.alpha.-d-glucopyranose	4.75%	Sugars
22.987	7846266	2-Methoxy-4-vinylphenol	0.19%	Alcohol
23.477	9311447	5-Acetoxyethyl-2-furaldehyde	0.22%	Furans
23.92	1.41E+08	Phenol, 2-methoxy-4-(1-propenyl)-	3.40%	Alcohol
24.355	92943717	2-Methoxy-4-vinylphenol	2.24%	Alcohol
24.894	6074737	Phenol, 2-methoxy-4-(1-propenyl)-	0.15%	Alcohol
25.61	1.22E+08	1-(2-Hydroxy-4-methoxyphenyl)propan-1-one	2.93%	Alcohol
26.078	74681527	Phenol, 2-methoxy-4-(1-propenyl)-	1.80%	Alcohol
26.395	1.13E+09	Vanillin	27.26%	Alcohol
26.7	1.04E+08	Benzenepropanol, 4-hydroxy-3-methoxy-	2.51%	Alcohol
27.729	52490764	Phenol, 2-methoxy-4-propyl-	1.26%	Alcohol
28.52	1.29E+08	Apocynin	3.11%	Alcohol
29.623	14898394	2-Propanone, 1-(4-hydroxy-3-methoxyphenyl)-	0.36%	Alcohol
32.464	11028756	(E)-4-(3-Hydroxyprop-1-en-1-yl)-2-methoxyphenol	0.27%	Alcohol
33.868	6462751	3,4-Altrosan	0.16%	Sugars
36.621	11982378	Coniferyl alcohol	0.29%	Alcohol
36.727	6665023	Coniferyl alcohol	0.16%	Alcohol
44.272	4615523	phenol, 4,4'-[dithiobis(methylene)]bis[2-methoxy-	0.11%	Alcohol

5. Gas inerted conventional pyrolysis liquid – “isopropyl alcohol soluble”				
RT (min)	Area	Name	Area Percent	Category
8.268	67756721	Acetamide, 2-amino-	0.23%	Amine
9.855	1.44E+08	Propanal	0.50%	Aldehyde
10.789	1.45E+08	Propanal	0.50%	Aldehyde
11.045	1.43E+08	Furfural	0.49%	Furans
12.102	1.54E+09	2-Furanmethanol	5.32%	Furans
12.649	2.46E+08	3-Carene	0.85%	Aromatic
14.062	1.71E+09	3-Furanmethanol	5.90%	Alcohol
14.362	24219159	2-Propen-1-ol, 2-methyl-, acetate	0.08%	Ester
14.571	5.59E+08	1-Propanone, 1-(2-furanyl)-	1.93%	Furans
14.78	1.27E+09	1,2-Cyclopentanedione	4.38%	Ketone
15.09	3.26E+08	2(5H)-Furanone	1.13%	Ketone
15.588	1.83E+09	2-Cyclopenten-1-one, 2-hydroxy-3-methyl-	6.32%	Alcohol
16.406	2.15E+09	Phenol, 2-methoxy-	7.42%	Alcohol
17.045	66316484	Furyl hydroxymethyl ketone	0.23%	Furans
17.173	2.44E+08	Creosol	0.84%	Alcohol
17.429	2.38E+08	Furyl hydroxymethyl ketone	0.82%	Furans
17.71	1.66E+08	Phenol, 4-methoxy-3-methyl-	0.57%	Alcohol
18.086	75826397	Creosol	0.26%	Alcohol
18.273	2.15E+09	2-Cyclopenten-1-one, 3-ethyl-2-hydroxy-	7.42%	Alcohol
19.683	1.98E+09	1,4:3,6-Dianhydro-.alpha.-d-glucopyranose	6.84%	Sugars
19.93	35623457	2-Methoxy-5-methylphenol	0.12%	Alcohol
20.106	3.3E+08	5-Acetoxymethyl-2-furaldehyde	1.14%	Furans
20.258	4.71E+08	5-Hydroxymethylfurfural	1.63%	Furans
20.646	1.6E+09	2-Methoxy-4-vinylphenol	5.52%	Alcohol
21.022	1.17E+09	2-Methoxy-4-vinylphenol	4.06%	Alcohol
21.41	2.51E+08	Vanillin	0.87%	Alcohol
21.924	5.25E+08	Phenol, 2-methoxy-4-(1-propenyl)-	1.82%	Alcohol
22.251	75188113	Phenol, 2-methoxy-4-propyl-	0.26%	Alcohol
22.752	2.15E+09	Levogluconan	7.42%	Sugars
23.137	7.21E+08	2-Propanone, 1-(4-hydroxy-3-methoxyphenyl)-	2.49%	Alcohol
23.924	4.45E+08	Phenol, 2-methoxy-4-propyl-	1.54%	Alcohol
24.336	4.26E+08	2-Methoxy-4-vinylphenol	1.47%	Alcohol
24.97	9.56E+08	Benzenepropanol, 4-hydroxy-3-methoxy-	3.30%	Alcohol
25.606	5.67E+08	benzoic acid, 4-hydroxy-3-propyl-	1.96%	Alcohol
26.183	5.97E+08	4-Hydroxy-2-methoxycinnamaldehyde	2.06%	Alcohol
26.712	2.15E+09	Benzenepropanol, 4-hydroxy-3-methoxy-	7.42%	Alcohol
27.602	26665654	2-Propanone, 1-(4-hydroxy-3-methoxyphenyl)-	0.09%	Alcohol
28.478	8.39E+08	3,4-Altrosan	2.90%	Sugars
29.061	73509530	4-(1-Hydroxyallyl)-2-methoxyphenol	0.25%	Alcohol
34.889	4.13E+08	Phthalic acid, di(2-propylpentyl) ester	1.43%	Ester
36.717	19375350	Coniferyl alcohol	0.07%	Alcohol
36.847	33241823	Coniferyl alcohol	0.11%	Alcohol

6. Gas inerted conventional pyrolysis liquid – “Cyclohexane insoluble”

RT (min)	Area	Name	Area Percent	Category
8.278	3.82E+08	Acetamide, 2-amino-	6.27%	Amine
9.991	78950219	Propanal	1.30%	Aldehyde
10.846	2.95E+08	1,2-Cyclopentanedione	4.86%	Ketone
11.361	2.09E+08	Furfural	3.43%	Furans
11.875	23009985	2-Furancarboxaldehyde, 5-methyl-	0.38%	Furans
12.08	1.72E+08	2-Furanmethanol	2.82%	Furans
13.283	8008737	Oxazolidine, 2,2-diethyl-3-methyl-	0.13%	Furans
13.57	5.26E+08	1,2-Cyclopentanedione	8.65%	Ketone
14.534	2.05E+08	2-Cyclopenten-1-one, 2-hydroxy-3-methyl-	3.37%	Alcohol
14.785	20152940	2-Cyclopenten-1-one, 3-ethyl-2-hydroxy-	0.33%	Alcohol
15.365	9634140	Phenol, 2-methoxy-	0.16%	Alcohol
15.836	5481499	2-Cyclopenten-1-one, 3-ethyl-2-hydroxy-	0.09%	Alcohol
16.339	14870910	Phenol, 2-methoxy-	0.24%	Alcohol
16.772	10972158	2-Methoxy-5-methylphenol	0.18%	Alcohol
17.092	1.64E+08	Furyl hydroxymethyl ketone	2.70%	Furans
17.425	47778552	Furyl hydroxymethyl ketone	0.79%	Furans
17.529	1.06E+08	Creosol	1.75%	Alcohol
17.701	1.56E+08	Phenol, 4-methoxy-3-methyl-	2.56%	Alcohol
17.941	11956729	Phenol, 4-ethyl-	0.20%	Alcohol
18.27	4.64E+08	2-Cyclopenten-1-one, 3-ethyl-2-hydroxy-	7.63%	Alcohol
19.191	40217640	Adrenalone	0.66%	Amine
19.704	45718617	Phenol, 4-ethyl-2-methoxy-	0.75%	Alcohol
19.922	93887682	2-Methoxy-5-methylphenol	1.54%	Alcohol
20.185	1.24E+08	5-Acetoxyethyl-2-furaldehyde	2.04%	Furans
20.746	89486526	2-Cyclopenten-1-one, 4-hydroxy-3-methyl-2-(2-propenyl)-	1.47%	Alcohol
21.096	5.49E+08	2-Methoxy-4-vinylphenol	9.03%	Alcohol
21.727	24315215	5-Acetoxyethyl-2-furaldehyde	0.40%	Furans
22.262	10073167	Phenol, 2-methoxy-3-(2-propenyl)-	0.17%	Alcohol
22.78	66964387	Levogluconan	1.10%	Sugars
23.127	2.72E+08	Phenol, 2-methoxy-4-(1-propenyl)-	4.48%	Alcohol
23.911	1.6E+08	Phenol, 2-methoxy-4-(1-propenyl)-, (Z)-	2.63%	Alcohol
24.256	14157127	Benzaldehyde, 3-(chloroacetoxy)-4-methoxy-	0.23%	Ester
24.337	2.18E+08	2-Methoxy-4-vinylphenol	3.58%	Alcohol
24.938	3.1E+08	2-Propanone, 1-(4-hydroxy-3-methoxyphenyl)-	5.09%	Alcohol
25.4	23316160	Phenol, 2-methoxy-4-propyl-	0.38%	Alcohol
26.09	1.63E+08	Phenol, 2-methoxy-4-(1-propenyl)-	2.67%	Alcohol
26.307	61335577	2-Propanone, 1-(4-hydroxy-3-methoxyphenyl)-	1.01%	Alcohol
26.684	1.76E+08	4-(1-Hydroxyallyl)-2-methoxyphenol	2.90%	Alcohol
27.678	15465618	2-Propanone, 1-(4-hydroxy-3-methoxyphenyl)-	0.25%	Alcohol
28.456	6.03E+08	3,4-Altrosan	9.91%	Sugars
29.191	7301515	ethanone, 1-(2H-1-benzopyran-3-yl)-	0.12%	Ketone
31.02	2944518	Coniferyl aldehyde	0.05%	Alcohol
31.227	5117170	Hexadeca-2,6,10,14-tetraen-1-ol, 3,7,11,16-tetramethyl-	0.08%	Impurity
33.715	1930314	Hexanedioic acid, bis(2-ethylhexyl) ester	0.03%	Impurity
34.7	16396130	phenol, 4,4'-[dithiobis(methylene)]bis[2-methoxy-	0.27%	Alcohol
34.897	60696098	Phthalic acid, di(2-propylpentyl) ester	1.00%	Ester
36.751	16289460	Coniferyl alcohol	0.27%	Alcohol
39.058	3490570	benzene, 1,1'-(1,2-ethynediyl)bis[2,4-dimethoxy-	0.06%	Impurity

7. Gas inerted conventional pyrolysis liquid – “Cyclohexane soluble”				
RT (min)	Area	Name	Area Percent	Category
10.638	1.51E+08	Propanal	0.43%	Aldehyde
11.297	1.24E+09	Furfural	3.52%	Furans
12.099	1.12E+09	2-Furanmethanol	3.19%	Furans
12.677	1.6E+08	3-Carene	0.46%	Aromatic
13.596	8.36E+08	1,2-Cyclopentanedione	2.37%	Ketone
13.919	2.04E+08	1-Butanone, 1-(2-furanyl)-	0.58%	Furans
14.035	1.1E+09	2-Furancarboxaldehyde, 5-methyl-	3.13%	Furans
14.425	2.23E+08	1,2-Cyclopentanedione	0.63%	Ketone
14.781	62523660	2(5H)-Furanone	0.18%	Ketone
15.08	59213229	2(5H)-Furanone	0.17%	Ketone
15.416	43255132	N-Butyl-tert-butylamine	0.12%	Amine
15.602	2.15E+09	2(5H)-Furanone, 3-methyl-	6.10%	Ketone
15.832	3.73E+08	2-Cyclopenten-1-one, 2-hydroxy-3-methyl-	1.06%	Alcohol
16.428	2.15E+09	Phenol, 2-methoxy-	6.10%	Alcohol
17.188	5.68E+08	Creosol	1.61%	Alcohol
17.442	8.55E+08	Furyl hydroxymethyl ketone	2.43%	Furans
17.695	2.91E+08	2-Methoxy-5-methylphenol	0.83%	Alcohol
18.084	1.38E+08	Creosol	0.39%	Alcohol
18.302	2.15E+09	4H-Pyran-4-one, 3,5-dihydroxy-2-methyl-	6.10%	Alcohol
18.67	32061857	2-Norpinanol, 3,6,6-trimethyl-	0.09%	Alcohol
18.936	1.6E+08	Phenol, 4-ethyl-2-methoxy-	0.45%	Alcohol
19.702	2.15E+09	1,4:3,6-Dianhydro-.alpha.-d-glucopyranose	6.10%	Sugars
19.936	2.6E+08	2-Methoxy-5-methylphenol	0.74%	Alcohol
20.225	1.78E+08	2-Methoxy-4-vinylphenol	0.51%	Alcohol
20.34	1.24E+08	5-Acetoxymethyl-2-furaldehyde	0.35%	Furans
20.525	2.37E+08	5-Hydroxymethylfurfural	0.67%	Furans
20.673	2.15E+09	Phenol, 2-methoxy-4-(1-propenyl)-	6.10%	Alcohol
20.948	4.08E+08	Phenol, 4-(2-propenyl)-	1.16%	Alcohol
21.04	2.15E+09	Phenol, 2-methoxy-4-(1-propenyl)-	6.10%	Alcohol
21.502	1.21E+08	Vanillin	0.34%	Alcohol
21.922	1.6E+09	Phenol, 2-methoxy-4-(1-propenyl)-	4.55%	Alcohol
22.133	74969670	Phenol, 2-methoxy-4-propyl-	0.21%	Alcohol
22.79	2.15E+09	Levogluconan	6.10%	Sugars
23.119	9.79E+08	2-Propanone, 1-(4-hydroxy-3-methoxyphenyl)-	2.78%	Alcohol
23.901	3.05E+08	4-(1-Hydroxyallyl)-2-methoxyphenol	0.87%	Alcohol
24.953	1.12E+09	Benzenepropanol, 4-hydroxy-3-methoxy-	3.19%	Alcohol
25.587	3.75E+08	benzoic acid, 4-hydroxy-3-propyl-	1.06%	Alcohol
26.085	93037643	Coniferyl aldehyde	0.26%	Alcohol
26.444	1.07E+09	3,4-Altrosan	3.04%	Sugars
26.664	4.07E+08	D-Allose	1.16%	Sugars
27.825	2.03E+08	Phenol, 2-methoxy-4-propyl-	0.58%	Alcohol
28.454	1.41E+09	3-(3-Hydroxy-4-methoxyphenyl)-l-alanine	4.01%	Alcohol
29.059	2.94E+08	4-(1-Hydroxyallyl)-2-methoxyphenol	0.84%	Alcohol
34.898	1.01E+09	Phthalic acid, di(2-propylpentyl) ester	2.87%	Ester
35.19	2.15E+09	Phthalic acid, di(2-propylpentyl) ester	6.10%	Ester
36.846	1.32E+08	Coniferyl alcohol	0.38%	Alcohol

8. Gas inerted microwave – “Crude”				
RT (min)	Area	Name	Area Percent	Category
8.286	5.82E+08	Acetamide, 2-amino-	2.40%	Amine
10.033	5.13E+08	Propanal	2.11%	Aldehyde
10.848	3.64E+08	Propanal	1.50%	Aldehyde
11.29	1.08E+09	Furfural	4.44%	Furans
12.134	3.9E+08	2-Furanmethanol	1.60%	Furans
13.26	49432014	trans-2-Pentenoic acid	0.20%	Acid
13.603	1.11E+09	Phenol, 2-methoxy-	4.55%	Alcohol
14.551	4.94E+08	1-Propanone, 1-(2-furanyl)-	2.03%	Ketone
15.074	6.01E+08	Oxazolidine, 2,2-diethyl-3-methyl-	2.48%	Furans
15.567	1.45E+09	3-Methylcyclopentane-1,2-dione	5.96%	Ketone
16.39	2.15E+09	Phenol, 2-methoxy-	8.85%	Alcohol
17.119	1.71E+08	Creosol	0.70%	Alcohol
17.42	5.6E+08	Furyl hydroxymethyl ketone	2.31%	Furans
17.699	3.36E+08	Phenol, 4-methoxy-3-methyl-	1.38%	Alcohol
18.035	1.43E+08	Creosol	0.59%	Alcohol
18.258	2.15E+09	2-Cyclopenten-1-one, 3-ethyl-2-hydroxy-	8.85%	Alcohol
19.186	1.01E+08	Phenol, 2-methoxy-4-(1-propenyl)-	0.42%	Alcohol
19.66	1.22E+09	Phenol, 4-ethyl-2-methoxy-	5.02%	Alcohol
19.939	1.78E+08	Phenol, 2-methoxy-4-(1-propenyl)-, (Z)-	0.73%	Alcohol
20.629	5.78E+08	2-Methoxy-4-vinylphenol	2.38%	Alcohol
21.157	1.23E+09	5-Acetoxymethyl-2-furaldehyde	5.08%	Furans
21.904	6.14E+08	Phenol, 2-methoxy-4-(1-propenyl)-	2.53%	Alcohol
22.739	2.15E+09	Levoglucozan	8.85%	Sugars
23.122	1.29E+09	Benzaldehyde, 3-hydroxy-4-methoxy-	5.32%	Alcohol
23.905	5.87E+08	Phenol, 2-methoxy-4-propyl-	2.42%	Alcohol
24.948	7.71E+08	2-Propanone, 1-(4-hydroxy-3-methoxyphenyl)-	3.17%	Alcohol
25.593	5.86E+08	benzoic acid, 4-hydroxy-3-propyl-	2.41%	Alcohol
26.123	2.57E+08	Phenol, 2-methoxy-4-(1-propenyl)-	1.06%	Alcohol
26.392	3.38E+08	Vanillin	1.39%	Alcohol
26.685	3.91E+08	D-Allose	1.61%	Sugars
27.66	45804310	2-Propanone, 1-(4-hydroxy-3-methoxyphenyl)-	0.19%	Alcohol
28.459	1.4E+09	3,4-Altrosan	5.76%	Sugars
34.886	3.73E+08	Phthalic acid, di(2-propylpentyl) ester	1.54%	Ester
36.839	40845977	Coniferyl alcohol	0.17%	Alcohol

9. Gas inerted microwave – “Water insoluble”				
RT (min)	Area	Name	Area Percent	Category
10.269	5181875	Propanal	0.36%	Aldehyde
11.31	10010055	Furfural	0.70%	Furans
14.548	3117370	1-Propanone, 1-(2-furanyl)-	0.22%	Furans
16.55	53652148	1,2-Cyclopentanedione, 3-methyl-	3.73%	Ketone
17.493	8232810	Phenol, 2-methoxy-	0.57%	Alcohol
17.722	9181908	Phenol, 4-methoxy-3-methyl-	0.64%	Alcohol
18.309	1.85E+08	2-Cyclopenten-1-one, 3-ethyl-2-hydroxy-	12.87%	Alcohol
18.876	1949140	Creosol	0.14%	Alcohol
19.648	6692327	Phenol, 4-ethyl-2-methoxy-	0.47%	Alcohol
20.689	70481844	2-Methoxy-4-vinylphenol	4.90%	Alcohol
21.037	59415762	2-Methoxy-4-vinylphenol	4.13%	Alcohol
21.95	1.48E+08	Phenol, 2-methoxy-4-(1-propenyl)-, (Z)-	10.28%	Alcohol
22.349	10713755	Benzaldehyde, 3-hydroxy-4-methoxy-	0.75%	Alcohol
22.746	4.92E+08	Levogluconan	34.25%	Sugars
23.805	7925045	Phenol, 2-methoxy-4-propyl-	0.55%	Alcohol
24.792	13602901	2-Propanone, 1-(4-hydroxy-3-methoxyphenyl)-	0.95%	Alcohol
25.485	5338359	benzoic acid, 4-hydroxy-3-propyl-	0.37%	Alcohol
26.151	8617579	Phenol, 2-methoxy-4-(1-propenyl)-	0.60%	Alcohol
26.622	7414432	D-Allose	0.52%	Sugars
26.761	5723615	Benzenepropanol, 4-hydroxy-3-methoxy-	0.40%	Alcohol
27.685	7878406	2-Propanone, 1-(4-hydroxy-3-methoxyphenyl)-	0.55%	Alcohol
28.41	8164582	3,4-Altrosan	0.57%	Sugars
28.502	86500362	Coniferyl aldehyde	6.02%	Alcohol
29.052	15543095	4-(1-Hydroxyallyl)-2-methoxyphenol	1.08%	Alcohol
34.496	26535291	Phthalic acid, di(2-propylpentyl) ester	1.85%	Ester
34.88	1.21E+08	Phthalic acid, di(2-propylpentyl) ester	8.44%	Ester
36.721	24388685	Coniferyl alcohol	1.70%	Alcohol
36.838	34974288	Coniferyl alcohol	2.43%	Alcohol

10. Gas inerted microwave – “Water soluble”				
RT (min)	Area	Name	Area Percent	Category
8.278	21395715	Acetamide, 2-amino-	0.56%	Amine
9.979	44160413	Propanal	1.15%	Aldehyde
10.832	1.42E+08	Propanal	3.68%	Aldehyde
13.605	1.25E+08	Phenol, 2-methoxy-	3.24%	Alcohol
14.127	20527411	1,3-Dioxolane, 2-butyl-2-methyl-	0.53%	Furans
15.062	4586357	Oxazolidine, 2,2-diethyl-3-methyl-	0.12%	Furans
15.55	1.94E+08	Oxazolidine, 2,2-diethyl-3-methyl-	5.04%	Furans
16.382	2.59E+08	Phenol, 2-methoxy-	6.75%	Alcohol
17.425	35902648	Phenol, 2-methoxy-	0.93%	Alcohol
17.706	46580950	Phenol, 4-methoxy-3-methyl-	1.21%	Alcohol
18.222	6.9E+08	2-Cyclopenten-1-one, 3-ethyl-2-hydroxy-	17.93%	Alcohol
19.664	2.21E+08	Phenol, 4-ethyl-2-methoxy-	5.74%	Alcohol
20.562	12049321	Creosol	0.31%	Alcohol
22.722	3.45E+08	Levoglucozan	8.96%	Sugars
23.116	1.44E+08	Phenol, 4-ethyl-2-methoxy-	3.75%	Alcohol
23.896	1.08E+08	Phenol, 2-methoxy-4-propyl-	2.81%	Alcohol
24.328	1.03E+08	2-Methoxy-4-vinylphenol	2.67%	Alcohol
24.928	1.38E+08	Phenol, 2-methoxy-4-(1-propenyl)-, (Z)-	3.60%	Alcohol
25.491	17821334	Phenol, 2-methoxy-4-(1-propenyl)-	0.46%	Alcohol
26.066	74618555	Phenol, 2-methoxy-4-(1-propenyl)-	1.94%	Alcohol
26.361	8.69E+08	Vanillin	22.60%	Alcohol
26.678	34573904	Apocynin	0.90%	Alcohol
27.1	11843149	2-Propanone, 1-(4-hydroxy-3-methoxyphenyl)-	0.31%	Alcohol
28.466	1.4E+08	3,4-Altrosan	3.63%	Sugars
34.894	25845316	D-Allose	0.67%	Sugars
35.067	5961422	Benzenepropanol, 4-hydroxy-3-methoxy-	0.16%	Alcohol
36.777	12746654	Coniferyl alcohol	0.33%	Alcohol

12. Gas inerted microwave – “Isopropyl alcohol soluble”				
RT (min)	Area	Name	Area Percent	Category
9.986	31336360	Propanal	0.41%	Aldehyde
10.785	25125872	Propanal	0.33%	Aldehyde
11.392	43503851	Furfural	0.57%	Furans
12.112	24944505	2-Furanmethanol	0.33%	Furans
14.031	3.08E+08	2-Furancarboxaldehyde, 5-methyl-	4.03%	Furans
14.751	2.97E+08	2(5H)-Furanone	3.89%	Ketone
15.084	83857655	Oxazolidine, 2,2-diethyl-3-methyl-	1.10%	Furans
16.368	6.53E+08	Phenol, 2-methoxy-	8.55%	Alcohol
17.079	65631056	Furyl hydroxymethyl ketone	0.86%	Furans
17.413	89437151	Furyl hydroxymethyl ketone	1.17%	Furans
17.71	40087809	Phenol, 4-methoxy-3-methyl-	0.52%	Alcohol
18.039	49593986	Creosol	0.65%	Alcohol
18.221	1.16E+09	2-Cyclopenten-1-one, 3-ethyl-2-hydroxy-	15.17%	Alcohol
19.659	3.49E+08	Phenol, 4-ethyl-2-methoxy-	4.57%	Alcohol
20.627	4.31E+08	2-Methoxy-4-vinylphenol	5.65%	Alcohol
21.901	1.83E+08	Phenol, 2-methoxy-4-(1-propenyl)-	2.40%	Alcohol
22.713	1.04E+09	Levogluconan	13.65%	Sugars
23.024	1.17E+08	Vanillin	1.53%	Alcohol
23.893	1.57E+08	Phenol, 2-methoxy-4-propyl-	2.06%	Alcohol
24.309	1.63E+08	2-Methoxy-4-vinylphenol	2.13%	Alcohol
24.929	2.02E+08	2-Propanone, 1-(4-hydroxy-3-methoxyphenyl)-	2.64%	Alcohol
25.376	17418763	Benzeneamine, 3-ethyl-4-hydroxy-	0.23%	Amine
25.479	51767673	benzoic acid, 4-hydroxy-3-propyl-	0.68%	Alcohol
26.076	85696531	Phenol, 2-methoxy-4-(1-propenyl)-	1.12%	Alcohol
26.455	1.3E+09	3,4-Altrosan	17.07%	Sugars
26.674	1.36E+08	D-Allose	1.79%	Sugars
27.659	11712480	2-Propanone, 1-(4-hydroxy-3-methoxyphenyl)-	0.15%	Alcohol
28.447	3.05E+08	3,4-Altrosan	3.99%	Sugars
29.046	22526805	4-(1-Hydroxyallyl)-2-methoxyphenol	0.29%	Alcohol
34.881	1.18E+08	Phthalic acid, di(2-propylpentyl) ester	1.54%	Ester
34.998	42071905	phenol, 4,4'-[dithiobis(methylene)]bis[2-methoxy-	0.55%	Alcohol
36.718	28246004	Coniferyl alcohol	0.37%	Alcohol

13. Gas inerted microwave – “Cyclohexane insoluble”				
RT (min)	Area	Name	Area Percent	Category
7.643	16650255	Urea	0.99%	Amine
8.264	76536758	Acetamide, 2-amino-	4.54%	Amine
10.236	7488657	Propanal	0.44%	Aldehyde
11.398	35751865	Furfural	2.12%	Furans
12.196	9404520	2(5H)-Furanone, 3-methyl-	0.56%	Ketone
12.448	7104682	3-Methylcyclopentane-1,2-dione	0.42%	Ketone
13.14	6681413	Phenol	0.40%	Alcohol
13.638	55416882	Phenol, 2-methoxy-	3.28%	Alcohol
14.362	4412815	Phenol, 3-methyl-	0.26%	Alcohol
14.569	20163919	1-Propanone, 1-(2-furanyl)-	1.19%	Furans
14.936	11266159	2-Cyclopenten-1-one, 3-ethyl-2-hydroxy-	0.67%	Alcohol
15.143	59029246	Phenol, 3-methyl-	3.50%	Alcohol
15.635	80572966	Phenol, 4-methoxy-3-methyl-	4.77%	Alcohol
16.453	68250650	Phenol, 2-methoxy-	4.04%	Alcohol
17.118	13976330	Creosol	0.83%	Alcohol
17.464	3889668	Phenol, 3-ethyl-	0.23%	Alcohol
17.994	7049551	Adrenalone	0.42%	Amine
18.292	1.25E+08	Phenol, 4-ethyl-2-methoxy-	7.43%	Alcohol
19.918	24511442	2-Methoxy-5-methylphenol	1.45%	Alcohol
20.366	12459455	2-Methoxy-4-vinylphenol	0.74%	Alcohol
21.135	1.08E+08	5-Acetoxymethyl-2-furaldehyde	6.42%	Furans
21.895	3648418	Eugenol	0.22%	Alcohol
22.275	5638191	Phenol, 2-methoxy-4-(1-propenyl)-, (Z)-	0.33%	Alcohol
22.702	3179563	Phenol, 4-(2-propenyl)-, acetate	0.19%	Alcohol
22.818	80562315	Levogluconan	4.77%	Sugars
23.027	9114391	trans-Isoeugenol	0.54%	Alcohol
23.144	87129041	Vanillin	5.16%	Alcohol
23.854	4256022	Phenol, 2-methoxy-4-propyl-	0.25%	Alcohol
24.357	38947527	3-Hydroxy-4-methoxybenzoic acid, methyl ester	2.31%	Ester
24.951	67635079	Apocynin	4.01%	Alcohol
25.288	3840407	2-Propanone, 1-(4-hydroxy-3-methoxyphenyl)-	0.23%	Alcohol
25.612	50938355	1-(2-Hydroxy-4-methoxyphenyl)propan-1-one	3.02%	Alcohol
26.074	35470551	Phenol, 2-methoxy-4-(1-propenyl)-	2.10%	Alcohol
26.294	3.37E+08	2-Naphthalenol, 3-methoxy-	19.99%	Alcohol
27.627	4682939	Methyl 3-(4-hydroxy-3-methoxyphenyl)propanoate	0.28%	Alcohol
27.696	27364239	2-Propanone, 1-(4-hydroxy-3-methoxyphenyl)-	1.62%	Alcohol
28.513	1.06E+08	Coniferyl aldehyde	6.30%	Alcohol
28.858	18048750	Coniferyl aldehyde	1.07%	Alcohol
29.603	12298136	2-Propanone, 1-(4-hydroxy-3-methoxyphenyl)-	0.73%	Alcohol
32.291	10863431	Hexanedioic acid, bis(2-ethylhexyl) ester	0.64%	Impurity
32.953	11394508	phenol, 4,4'-[dithiobis(methylene)]bis[2-methoxy-	0.68%	Alcohol
33.922	5479816	Phthalic acid, di(2-propylpentyl) ester	0.32%	Ester
36.872	9283723	Coniferyl alcohol	0.55%	Alcohol

14. Gas inerted microwave – “Cyclohexane soluble”				
RT (min)	Area	Name	Area Percent	Category
8.241	46459425	Acetamide, 2-amino-	0.15%	Amine
10.83	2.69E+08	Propanal	0.84%	Aldehyde
13.591	1.13E+09	1,2-Cyclopentanedione	3.53%	Ketone
13.908	2.69E+08	2,3-Pentanedione	0.84%	Ketone
15.082	4.38E+08	Oxazolidine, 2,2-diethyl-3-methyl-	1.37%	Furans
15.606	2.09E+09	3-Methylcyclopentane-1,2-dione	6.53%	Ketone
16.407	2.15E+09	Phenol, 2-methoxy-	6.71%	Alcohol
17.03	1.15E+08	Furyl hydroxymethyl ketone	0.36%	Furans
17.182	4.31E+08	Creosol	1.35%	Alcohol
17.381	8.3E+08	Furyl hydroxymethyl ketone	2.59%	Furans
17.685	2.47E+08	Phenol, 4-methoxy-3-methyl-	0.77%	Alcohol
18.069	1.84E+08	Creosol	0.58%	Alcohol
18.302	2.15E+09	Creosol	6.71%	Alcohol
18.915	2.33E+08	Phenol, 2-methoxy-	0.73%	Alcohol
19.681	2.15E+09	Phenol, 4-ethyl-2-methoxy-	6.71%	Alcohol
19.939	1.48E+08	Creosol	0.46%	Alcohol
20.198	1.61E+08	5-Acetoxymethyl-2-furaldehyde	0.50%	Furans
20.515	2.03E+08	5-Hydroxymethylfurfural	0.63%	Furans
20.633	1.94E+09	2-Methoxy-4-vinylphenol	6.07%	Alcohol
21.032	2.15E+09	2-Methoxy-4-vinylphenol	6.71%	Alcohol
21.915	1.98E+09	Phenol, 2-methoxy-4-(1-propenyl)-	6.20%	Alcohol
22.583	2.57E+08	Phenol, 2-methoxy-4-(1-propenyl)-	0.80%	Alcohol
22.771	2.15E+09	Levogluconan	6.71%	Sugars
23.123	1.59E+09	Benzaldehyde, 3-hydroxy-4-methoxy-	4.98%	Alcohol
23.719	71676322	Phenol, 2-methoxy-4-propyl-	0.22%	Alcohol
23.894	5.09E+08	Phenol, 2-methoxy-4-propyl-	1.59%	Alcohol
24.221	1.25E+08	Phenol, 2-methoxy-4-propyl-	0.39%	Alcohol
24.314	8.09E+08	4-(1-Hydroxyallyl)-2-methoxyphenol	2.53%	Alcohol
24.945	1.23E+09	1,6-Anhydro-.beta.-d-talopyranose	3.86%	Sugars
25.462	3.72E+08	benzoic acid, 4-hydroxy-3-propyl-	1.16%	Alcohol
26.369	3.45E+08	Vanillin	1.08%	Alcohol
26.653	4.24E+08	D-Allose	1.32%	Sugars
27.66	1.16E+08	2-Propanone, 1-(4-hydroxy-3-methoxyphenyl)-	0.36%	Alcohol
28.444	1.34E+09	3,4-Altrosan	4.18%	Sugars
34.882	9.65E+08	Phthalic acid, di(2-propylpentyl) ester	3.01%	Ester
35.176	2.15E+09	Phthalic acid, di(2-propylpentyl) ester	6.71%	Ester
36.708	2.35E+08	Coniferyl alcohol	0.74%	Alcohol

15. Liquid inerted microwave – “Water insoluble”				
RT (min)	Area	Name	Area Percent	Category
10.007	43595584	Propanal	1.95%	Aldehyde
10.832	42717376	Propanal	1.91%	Aldehyde
11.271	13816496	Furfural	0.62%	Furans
12.396	25322077	Oxazolidine, 2,2-diethyl-3-methyl-	1.13%	Furans
13.616	60432429	3-Methylcyclopentane-1,2-dione	2.70%	Ketone
14.533	6073280	Phenol, 2-methoxy-	0.27%	Alcohol
15.104	35686536	Oxazolidine, 2,2-diethyl-3-methyl-	1.59%	Furans
15.488	16687075	2-Cyclopenten-1-one, 2-hydroxy-3-methyl-	0.75%	Alcohol
16.408	1.65E+08	Phenol, 2-methoxy-	7.36%	Alcohol
17.116	39347015	Creosol	1.76%	Alcohol
17.439	12397814	Creosol	0.55%	Alcohol
18.24	2.67E+08	2-Cyclopenten-1-one, 3-ethyl-2-hydroxy-	11.94%	Alcohol
19.689	74333239	Phenol, 4-ethyl-2-methoxy-	3.32%	Alcohol
19.92	29251701	2-Methoxy-5-methylphenol	1.31%	Alcohol
20.686	46400352	2-Methoxy-4-vinylphenol	2.07%	Alcohol
21.039	20617965	2-Methoxy-4-vinylphenol	0.92%	Alcohol
21.532	9880456	Phenol, 2-methoxy-4-(1-propenyl)-	0.44%	Alcohol
21.799	10931996	Phenol, 2-methoxy-4-(1-propenyl)-	0.49%	Alcohol
22.735	91894555	Levogluconan	4.10%	Sugars
23.139	1.09E+08	Benzaldehyde, 3-hydroxy-4-methoxy-	4.85%	Alcohol
23.418	7261105	Phenol, 2-methoxy-4-propyl-	0.32%	Alcohol
23.907	73064517	Phenol, 2-methoxy-4-propyl-	3.26%	Alcohol
24.14	2497050	2-Propanone, 1-(4-hydroxy-3-methoxyphenyl)-	0.11%	Alcohol
24.939	1.49E+08	2-Propanone, 1-(4-hydroxy-3-methoxyphenyl)-	6.68%	Alcohol
25.597	68157215	benzoic acid, 4-hydroxy-3-propyl-	3.04%	Alcohol
26.346	6.34E+08	Vanillin	28.30%	Alcohol
26.697	35405382	D-Allose	1.58%	Sugars
27.174	37098029	Benzenepropanol, 4-hydroxy-3-methoxy-	1.66%	Alcohol
27.718	18302498	Phenol, 2-methoxy-4-propyl-	0.82%	Alcohol
28.526	62456915	Coniferyl aldehyde	2.79%	Alcohol
34.918	31794284	phenol, 4,4'-[dithiobis(methylene)]bis[2-methoxy-	1.42%	Alcohol

18. Liquid inerted microwave – “Isopropyl alcohol soluble”				
RT (min)	Area	Name	Area Percent	Category
8.222	66023142	Acetamide, 2-amino-	0.96%	Amine
9.98	22174124	Propanal	0.32%	Aldehyde
11.336	1.74E+08	Furfural	2.53%	Furans
13.589	1.49E+08	1,2-Cyclopentanedione	2.17%	Ketone
14.039	99231512	2-Furancarboxaldehyde, 5-methyl-	1.45%	Furans
14.466	12578008	1-Propanone, 1-(2-furanyl)-	0.18%	Furans
15.089	81713490	Oxazolidine, 2,2-diethyl-3-methyl-	1.19%	Furans
15.531	2.23E+08	3-Methylcyclopentane-1,2-dione	3.24%	Ketone
16.362	6.68E+08	Phenol, 2-methoxy-	9.73%	Alcohol
17.081	59048700	Furyl hydroxymethyl ketone	0.86%	Furans
17.394	67654994	Furyl hydroxymethyl ketone	0.99%	Furans
17.707	55364816	Phenol, 4-methoxy-3-methyl-	0.81%	Alcohol
18.03	1.19E+08	Creosol	1.73%	Alcohol
18.226	1.23E+09	Creosol	17.93%	Alcohol
19.653	4.37E+08	Phenol, 4-ethyl-2-methoxy-	6.36%	Alcohol
19.91	36469541	2-Methoxy-5-methylphenol	0.53%	Alcohol
20.177	53642742	5-Acetoxymethyl-2-furaldehyde	0.78%	Furans
20.616	4.96E+08	2-Methoxy-4-vinylphenol	7.23%	Alcohol
21.909	1.78E+08	Phenol, 2-methoxy-4-(1-propenyl)-	2.60%	Alcohol
22.712	1.02E+09	Levogluconan	14.82%	Sugars
23.108	2.78E+08	Vanillin	4.06%	Alcohol
23.889	1.37E+08	Phenol, 2-methoxy-4-propyl-	2.00%	Alcohol
24.926	2.2E+08	2-Propanone, 1-(4-hydroxy-3-methoxyphenyl)-	3.21%	Alcohol
26.076	99047528	Phenol, 2-methoxy-4-(1-propenyl)-	1.44%	Alcohol
26.307	1.94E+08	D-Allose	2.82%	Sugars
26.677	1.6E+08	Benzenepropanol, 4-hydroxy-3-methoxy-	2.33%	Alcohol
28.444	3.41E+08	Coniferyl aldehyde	4.97%	Alcohol
29.052	32957720	4-(1-Hydroxyallyl)-2-methoxyphenol	0.48%	Alcohol
29.601	10847605	2-Propanone, 1-(4-hydroxy-3-methoxyphenyl)-	0.16%	Alcohol
34.876	1.33E+08	Phthalic acid, di(2-propylpentyl) ester	1.94%	Ester
36.751	12588042	Coniferyl alcohol	0.18%	Alcohol

19. Liquid inerted microwave – “Cyclohexane insoluble”				
RT (min)	Area	Name	Area Percent	Category
9.976	81347686	Propanal	1.68%	Aldehyde
10.828	2.06E+08	Propanal	4.26%	Aldehyde
11.368	7808240	Furfural	0.16%	Furans
13.576	1.63E+08	1,2-Cyclopentanedione	3.37%	Ketone
14.529	60464793	2(3H)-Furanone	1.25%	Ketone
15.071	1.02E+08	N-Butyl-tert-butylamine	2.11%	Amine
15.55	2.18E+08	2-Cyclopenten-1-one, 2-hydroxy-3-methyl-	4.50%	Alcohol
15.837	99270418	Phenol	2.05%	Alcohol
16.379	2.25E+08	Phenol, 2-methoxy-	4.65%	Alcohol
17.065	1.12E+08	Furyl hydroxymethyl ketone	2.32%	Furans
17.396	1.14E+08	Furyl hydroxymethyl ketone	2.36%	Furans
17.694	1.27E+08	2-Furanmethanol, tetrahydro-5-methyl-, trans-	2.61%	Furans
18.025	27476586	Creosol	0.57%	Alcohol
18.231	5.04E+08	Phenol, 4-methoxy-3-methyl-	10.41%	Alcohol
19.662	1.93E+08	Phenol, 4-ethyl-2-methoxy-	3.98%	Alcohol
19.915	56880323	2-Methoxy-5-methylphenol	1.17%	Alcohol
20.17	72973827	1,4:3,6-Dianhydro-.alpha.-d-glucopyranose	1.51%	Sugars
20.635	1.7E+08	2-Methoxy-4-vinylphenol	3.52%	Alcohol
21.087	4.56E+08	5-Hydroxymethylfurfural	9.41%	Furans
21.999	24139680	Phenol, 2-methoxy-4-(1-propenyl)-	0.50%	Alcohol
22.711	3.08E+08	Levogluconan	6.36%	Sugars
23.882	2.19E+08	Phenol, 2-methoxy-4-propyl-	4.52%	Alcohol
24.932	2.11E+08	2-Propanone, 1-(4-hydroxy-3-methoxyphenyl)-	4.36%	Alcohol
25.584	1.59E+08	4-(1-Hydroxyallyl)-2-methoxyphenol	3.29%	Alcohol
25.957	10296586	Phenol, 2-methoxy-4-(1-propenyl)-	0.21%	Alcohol
26.062	1.01E+08	Phenol, 2-methoxy-4-(1-propenyl)-	2.09%	Alcohol
26.295	1.13E+08	Vanillin	2.33%	Alcohol
26.667	1.67E+08	Benzenepropanol, 4-hydroxy-3-methoxy-	3.46%	Alcohol
27.708	81311837	Phenol, 2-methoxy-4-propyl-	1.68%	Alcohol
28.446	4.36E+08	Coniferyl aldehyde	9.01%	Alcohol
29.606	14623412	2-Propanone, 1-(4-hydroxy-3-methoxyphenyl)-	0.30%	Alcohol

20. Liquid inerted microwave – “Cyclohexane soluble”				
RT (min)	Area	Name	Area Percent	Category
12.14	87380964	2-Furanmethanol	0.41%	Furans
13.59	1.65E+08	1,2-Cyclopentanedione	0.77%	Ketone
14.037	2.22E+08	2-Furancarboxaldehyde, 5-methyl-	1.04%	Furans
15.525	7.46E+08	1,2-Cyclopentanedione	3.48%	Ketone
15.768	53243144	2(3H)-Furanone	0.25%	Ketone
16.376	2.15E+09	Phenol, 2-methoxy-	10.03%	Alcohol
17.151	1.99E+08	N-Butyl-tert-butylamine	0.93%	Amine
17.36	5.3E+08	2-Cyclopenten-1-one, 2-hydroxy-3-methyl-	2.48%	Alcohol
18.248	2.15E+09	Phenol	10.03%	Alcohol
18.92	1.44E+08	Phenol, 2-methoxy-	0.67%	Alcohol
19.659	2.14E+09	Phenol, 4-ethyl-2-methoxy-	9.99%	Alcohol
19.915	63369285	2-Methoxy-5-methylphenol	0.30%	Alcohol
20.41	1.29E+08	2-Furanmethanol, tetrahydro-5-methyl-, trans-	0.60%	Furans
20.631	2.15E+09	2-Methoxy-4-vinylphenol	10.03%	Alcohol
20.912	1.86E+08	Phenol, 4-methoxy-3-methyl-	0.87%	Alcohol
21.006	2.03E+09	2-Methoxy-4-vinylphenol	9.47%	Alcohol
21.892	9.42E+08	Phenol, 2-methoxy-4-(1-propenyl)-	4.40%	Alcohol
22.74	2.15E+09	Levogluconan	10.03%	Sugars
23.089	9.08E+08	Vanillin	4.24%	Alcohol
23.719	78926074	1,4:3,6-Dianhydro-.alpha.-d-glucopyranose	0.37%	Sugars
23.871	4.14E+08	Phenol, 2-methoxy-4-propyl-	1.93%	Alcohol
24.058	1.1E+08	2-Methoxy-4-vinylphenol	0.51%	Alcohol
24.211	82525255	5-Hydroxymethylfurfural	0.39%	Furans
24.917	7.33E+08	2-Propanone, 1-(4-hydroxy-3-methoxyphenyl)-	3.42%	Alcohol
25.576	4.87E+08	Phenol, 2-methoxy-4-(1-propenyl)-	2.27%	Alcohol
26.246	1.67E+08	Vanillin	0.78%	Alcohol
26.539	44275818	Phenol, 2-methoxy-4-propyl-	0.21%	Alcohol
26.656	2.55E+08	D-Allose	1.19%	Sugars
27.65	62139010	2-Propanone, 1-(4-hydroxy-3-methoxyphenyl)-	0.29%	Alcohol
28.429	1.15E+09	3,4-Altrosan	5.37%	Sugars
29.043	60628472	4-(1-Hydroxyallyl)-2-methoxyphenol	0.28%	Alcohol
31.882	29985602	Benzenepropanol, 4-hydroxy-3-methoxy-	0.14%	Alcohol
33.678	24152934	Coniferyl aldehyde	0.11%	Alcohol
34.868	5.31E+08	Phthalic acid, di(2-propylpentyl) ester	2.48%	Ester
36.703	56430485	Coniferyl alcohol	0.26%	Alcohol